TECHNICAL REPORT STANDARD TITLE PAGE

1. Report No. TX FHWA/TX 05/0-1700-8	2. Government Accession No.	3. Recipient's Catalog No.
4. Title and Subtitle Relating Seismic Modulus to Strength Parameters of Portland Cement Concrete		**5. Report Date** May 2005 **6. Performing Organization Code**
7. Authors D. Yuan, S. Nazarian, A. Perea and D. Zhang		**8. Performing Organization Report No.** Research Report 0-1700-8
9. Performing Organization Name and Address Center for Transportation Infrastructure Systems The University of Texas at El Paso, El Paso, Texas 79968-0516		**10. Work Unit No.** **11. Contract or Grant No.** Project No. 0-1700
12. Sponsoring Agency Name and Address Texas Department of Transportation Research and Technology Implementation Office P.O. Box 5080, Austin, Texas 78763-5080		**13. Type of Report and Period Covered** Tehnical Report 9/02– 8/04 **14. Sponsoring Agency Code**

15. Supplementary Notes
Research Performed in Cooperation with TxDOT and the Federal Highway Administration
Research Study Title: Improving Portland Cement Concrete Pavement Performance

16. Abstract
Impacts of mix design and curing regime on the development of strength and modulus parameters of portland cement concrete (PCC) were investigated. The feasibility of using seismic nondestructive testing techniques to monitor and predict the strength and modulus development of PCC was enhanced. . The seismic modulus can be related to the strength parameters and static modulus obtained from conventional testing on the molded specimens or drilled cores.

A database, containing results from about 1200 standard cylinders made from fifteen concrete mixes, has been developed. Preliminary relationships between the seismic modulus and the strength parameters and static modulus are proposed in the basis of the type of coarse aggregate. Unlike a strength-maturity relationship that is usually very specific to a particular mix under a particular curing condition, a seismic modulus-based relationship is mainly affected by the nature of coarse aggregate. The techniques used in this study have shown to be a rapid, simple and economic means for estimating the strength and modulus development of concrete and for determining the time required to open a repaired or newly constructed concrete pavement to traffic.

Findings from this study would be useful in the following two ways:

1. Improving Rigid Pavement Design: The developed relationships can be incorporated in the design codes such as CRCP-11 to improve the assumptions with regards to the relationships between the strength and modulus of the concrete in early ages. In that manner, the models that predict several distress types can yield more realistic results.
2. Construction Quality Management: It was found that the strength and the seismic modulus for laboratory-cured specimens are highly correlated. Furthermore, it was demonstrated that such relationships are not significantly impacted by the environmental-related and most material-related parameters. Also it was demonstrated that the seismic moduli obtained from field testing are well-related to the seismic moduli obtained from laboratory testing. Therefore, seismic nondestructive testing (NDT) devices can be utilized for quality control of in situ concrete to minimize coring.

17. Key Words	18. Distribution Statement
Portland Cement Concrete, Early Age, Opening, Seismic Nondestructive Testing, Maturity	No restrictions. This document is available to the public through the National Technical Information Service, 5285 Port Royal Road, Springfield, Virginia 22161, www.ntis.gov

19. Security Classified (of this report)	20. Security Classified (of this page)	21. No. of Pages	22. Price
Unclassified	Unclassified	142	

Form DOT F 1700.7 (8-69)

Relating Seismic Modulus to Strength Parameters of Portland Cement Concrete

by

Deren Yuan, Ph.D.
Soheil Nazarian, Ph.D., P.E.
Antonio Perea, BSCE, P.E.
and
Dong Zhang, MSCS

Research Project 0-1700
Project Title: Improving Portland Cement Concrete Pavement Performance

Conducted for
Texas Department of Transportation

Research Report 0-1700-8

May 2005

Performed in cooperation with the Texas Department of Transportation and the Federal Highway Administration

Center for Transportation Infrastructure Systems
The University of Texas at El Paso
El Paso, TX 79968-0516

Disclaimers

The contents of this report reflect the view of the authors who are responsible for the facts and the accuracy of the data presented herein. The contents do not necessarily reflect the official views or policies of the Texas Department of Transportation or the Federal Highway Administration. This report does not constitute a standard, a specification or a regulation.

The material contained in this report is experimental in nature and is published for informational purposes only. Any discrepancies with official views or policies of the Texas Department of Transportation or the Federal Highway Administration should be discussed with the appropriate Austin Division prior to implementation of the procedures or results.

NOT INTENDED FOR CONSTRUCTION, BIDDING, OR PERMIT PURPOSES

Deren Yuan. Ph.D.
Soheil Nazarian, Ph.D., P.E. (69263)
Antonio Perea, BSCE, P.E. (91940)
Dong Zhang, MSCS

Acknowledgments

The authors would like to express their sincere appreciation to the Project Management Committee of this project, especially George Lantz, Gerald Lankes, Moon Won, Andrew Wimmsatt and David Head, for their support. We would also like to thank Tomas Saenz of El Paso District and Jim Hunt of the Dallas District for their help in coordinating site access and any other assistance asked for. As usual the personnel of El Paso District Lab, especially Hector Chanez and Hector Zuniga, were always available to help.

Jobe Concrete of El Paso, Texas donated all the concrete mixes used in this study. Ned Finney and Steve Coiro spent their valuable time on preparing the concrete mixes. Jobe Concrete also provided the shipping truck that brought the limestone gravel from Austin to El Paso used in this study.

This is a collaborative study amongst UTEP Center for Transportation Infrastructure Systems, the Center for Transportation Research (CTR) and the Texas Transportation Institute (TTI). Dr. Frank McCullough of CTR is the Research Supervisor. We significantly benefited from the technical assistance of Dr. McCullough and other CTR staff. We also appreciate the collaboration with Dr. Dan Zollinger of TTI.

Executive Summary

Several Texas Department of Transportation (TxDOT) districts rely solely on portland cement concrete (PCC) pavements for heavily traveled highways and urban/suburban sections of the interstate. Results from previous TxDOT research efforts and other literature have demonstrated that there are significant differences between the development rate in modulus and that in either tensile or compressive strength with curing time. This is potentially problematic, as it leads to increased stresses in the concrete and may be an underlying cause of excessive horizontal cracking observed in some PCC pavements across the state.

To investigate this problem, an extensive laboratory experiment to characterize the development in both strength and modulus with time under controlled conditions was carried out. The measured parameters were splitting tensile strength, compressive strength and static modulus as well as seismic modulus. In all instances, the maturity of the concrete as a function of time and temperature (time-temperature factor) was measured.

The laboratory experiment consisted of two phases. In Phase I, standard cylinders were made from eight different mixes and cured in five different conditions. Preliminary relationships between the seismic modulus and the strength and static modulus are proposed in the basis of the type of coarse aggregates. The focus of the second phase of this study was toward the impact of chemical admixture and gradation on the relationships developed in Phase I.

Unlike a strength-maturity relationship that is usually very specific to a particular mix under a particular curing condition, a seismic modulus-based relationship is mainly affected by the nature of the coarse aggregate and, to a lesser extent, by other parameters such as curing condition, admixture, and water-cement ratio.

Findings from this study would be useful in the following two ways:

1. Improving Rigid Pavement Design: The developed relationships can be incorporated in the design codes such as CRCP-11 to improve the assumptions with regards to the relationships between the strength and modulus of the concrete in early ages. In that manner, the models that predict several distress types can yield more realistic results.

2. Construction Quality Management: It was found that the strength and the seismic modulus for laboratory-cured specimens are highly correlated. Also it was demonstrated that such relationships are not significantly impacted by the environmental-related and most material-related parameters. Furthermore, it was demonstrated that the seismic moduli obtained from field testing are well-related to the seismic moduli obtained from laboratory testing. Therefore, seismic nondestructive testing (NDT) devices can be utilized for quality control of in situ concrete to minimize coring.

Implementation Statement

This project, which is tailored towards developing procedures and equipment that can be immediately implemented, is an important missing link towards developing a rational criterion for quality control and opening of PCC roads to traffic. To implement the methods and the technology recommended by this research, the guidelines for proper use of these methods and technology has been established, which should be feasible for both TxDOT and contractor. In addition, comprehensive models that relate seismic modulus to strength parameters have been developed that are incorporated in the design software developed at the Center for Transportation Research under the current study.

Most of the laboratory and field equipment are already available for immediate limited implementation and evaluation.

Table of Contents

List of Figures

List of Tables

Chapter 1

Introduction

Objectives

Major mechanical properties of portland cement concrete (PCC) pavements, such as the compressive, flexural/split tensile strengths test and static modulus of elasticity, are measured through conventional testing on concrete cylinders, beams and cores. TxDOT and many other highway agencies have use these testing parameters as the basis for PCC pavement mix design and as the final acceptance criteria of concrete pavements. In recent years, the concept of concrete seismic modulus measured with stress-wave techniques have been investigated by TxDOT and other highway agencies because of its nondestructive nature, precision and speed of tests.

The compressive strength, flexural/split tensile strength and modulus affect the performance of rigid pavements in different ways. The compressive strength test is perhaps the most common measure of concrete quality, although compressive failure rarely occurs in PCC pavements. The compressive strength is affected by coarse aggregate characteristics, water to cement ratio, cement type and content, mineral additives and entrained air (Hansen et al., 2001). The tensile strength affects directly the performance of PCC pavements because it is well documented that concrete pavements fail in tension. Also, the initiation of transverse cracking and corner breaking on PCC pavements is essentially related to the tensile characteristics of concrete. The concrete modulus controls the overall PCC slab deformation from traffic loading to the slab curling stresses.

A first step towards investigating the above issues would be to perform a systematic laboratory experiment to examine the impact of different concrete pavement designs on the development of strength and modulus parameters with time under controlled conditions. The findings from such an experiment would be useful not only to improving pavement design but also to ongoing NDT work which typically estimates in situ strength from seismic modulus. This study involves performing the conventional compressive and split tensile tests, the static modulus tests, as well as the seismic tests on standard cylinders. The report contains results obtained from the experiment on 22 different concrete mixtures using either El Paso siliceous river gravel (SRG) or Central Texas limestone (LS) as coarse aggregates.

Organization

Chapter 2 contains a brief background on the previous work on the topics discussed above. Chapter 3 describes in detail the test methodologies used in this study, the test protocols for each methodology and typical results obtained. Chapter 4 contains the impact that different mix-related and environmental-related parameters have on the strength and stiffness parameters measured in this study. All correlations developed for this project between various strength and stiffness parameters and seismic modulus are described in Chapter 5. In Chapter 6, a field case study is provided to demonstrate the field use of the methods proposed. The report is summarized and the conclusions are drawn in Chapter 7. Several appendices supplement the methods used in this study and the results shown in the report.

Chapter 2

Background

A number of material and construction factors related to PCC slabs may have significant effects on the performance of a PCC pavement. Adequate slab thickness, effective concrete strength, effective consolidation, correct dowel alignment, proper application of the curing compound, and proper timing and location of the saw-cuts (to establish the joints) all contribute to achieving maximum performance. From a structural design standpoint, slab thickness and concrete strength are the two most important parameters and, thus, the critical components of any concrete pavement structural design methodology. Small deviations in the as-constructed values of these parameters (from their design specifications) may result in significant differences in pavement life.

Mixture characteristics are selected based on the intended use of the concrete. In the case of PCC pavements, in addition to compressive and flexural strengths, other characteristics such as environmental conditions will affect decisions regarding the design of the mixture. Most of the desirable properties of hardened concrete depend primarily upon the quality of the cementitious paste, and therefore, the water-cement ratio is the primary parameter in a mix design. Differences in concrete strength as related to mix design for a given water-cement ratio result from:

1. Changes in the aggregate size, grading, surface texture and shape
2. Differences in types and sources of cementing materials.
3. The entrained-air content.
4. The presence of admixtures.
5. The length of curing time.

Traditionally, the quality of in-place concrete is judged based on the strength of specimens that are cured under ideal conditions. As such, the quality of construction practices and the effectiveness of the curing method under the field environmental conditions are ignored. For decisions on the opening of roadway to traffic these parameters play critical roles. A more direct measurement of the in-place concrete strength is necessary to develop better acceptance criteria.

To a significant degree, pavement performance can be predicted based on the concrete material properties, the environmental conditions prevailing during placement and curing of pavement, and the pavement type. One of the primary findings of previous TxDOT studies by McCullough et al. (1995), Green et al. (1997) and McCullough et al. (1998) was that the concrete coarse aggregate type was a significant factor in pavement performance. A large part of the performance differences in concrete pavements could be directly attributed to the coarse aggregate type used. Although the early-age concrete strength is relatively low, the bond strength of concrete with LS aggregates is significantly greater when compared to concrete made with SRG aggregates.

Concrete strength has a significant impact on a PCC pavement performance. Generally, a concrete mix design is developed to satisfy minimum strength requirements corresponding to an accepted standard or specification. In construction, the control of strength is achieved through close control of the mix proportions (aggregate, cement and water) and placement operations (ambient temperature, consolidation and curing). The standard method for evaluating the strength of concrete in pavement applications is to test molded specimens for compressive, flexural or tensile strength. A disadvantage of this approach is that the strength of molded specimens does not reflect actual in situ strength. It is often necessary to directly determine in situ strength from drilled cores, which is an expensive, and time-consuming and, sometimes, difficult task (Ramaiah et al., 2001). Compressive strength is determined from cylindrical concrete specimens; however, the state of stress induced under this test method is not representative of the conditions under which PCC pavements typically deteriorate. Flexural strength is determined from concrete beams and is the current standard for expressing PCC pavement tensile strength because it characterizes the strength under the state of stress that the concrete experiences under typical field loading conditions. Splitting tensile strength is obtained from concrete cylinders of the same type used for compressive strength; however they are tested along their longitudinal axis. This is the preferable measure of tensile strength because the strength is reflective of the coarse aggregates ability to bond with the paste, which is one of the characteristics of excessive horizontal cracking.

Table 2.1 provides a list of feasible methods available for measuring PCC pavements strength. The direct methods shown refer to those tests in which the strength is measured directly according to a standard test method (e.g., ASTM). The indirect methods refer to those tests that rely on the measurement of one or more properties that are *indirectly* related (either mechanically or statistically correlated) with concrete strength.

There are limitations associated with each of the current test methods used for determining concrete strength. In general, these limitations are associated with the need to obtain samples in the field, transport them to the laboratory, and test them to failure. In the case of conventional concrete strength testing using beams, the samples must be fabricated in the field, which are relatively heavy and bulky to transport. Also it is difficult to obtain high quality beams from finished PCC pavements.

Table 2.1 – Test Methods for Concrete Strength

Method	Concrete Test
Direct	Compressive Strength Test Flexural Strength Test Split Tensile Strength Test (Indirect)
Indirect	Maturity Test Seismic Test Integrated Maturity/Seismic Method

Even though the quality of the concrete may be determined as early as 12 hours after placement, the slabs in a pavement are normally not accepted and the contractor is not compensated until the 28-day strength results are obtained. The level of effort required for these tests is significant and the time lag between pavement construction and getting the test result is problematic. Moreover, these conventional tests represent a limited sampling upon which major decisions are made regarding the acceptability of the as-constructed pavement. Clearly, improvements to the current methods use to assess in-place PCC pavement properties would benefit both contractors and owner agencies.

In the last 20 years, new and innovative technologies have evolved because of the need to address the limitations of conventional concrete test methods. The maturity method (ASTM C1074) is one major innovation that minimizes the need for field sampling and testing in order to monitor development of concrete strength. By conducting laboratory strength testing on the PCC specimens before construction and then using the results to establish a strength-maturity relationship, the strength gain of the in-situ concrete can be estimated by simply monitoring the in-situ concrete temperature with time after construction. There is an up-front cost associated with this method and a separate maturity relationship must be established whenever there is a change in mix design, but these limitations of this method are minimal.

In general, maturity method based on the Arrhenius function (practiced in Europe) employs the activation energy of concrete, which results in a nonlinear function. The maturity method based on the Saul's function, which is practiced in U.S., employs a datum temperature and assumes that the maturity function is linear (Ansari et al., 1999). In general, the linear function is not very accurate. However, for simplicity and ease of application during the construction process, it is appropriate to use the linear function (Carino et al., 1983). In this case, the datum temperature has to be determined for temperatures appropriate for the actual thermal experiences at the construction site. Mortar cube tests are performed for this activity for temperatures below as well as above the field climate (Ansari et al., 1999).

The seismic NDT methods also represent a recent major innovation in concrete pavement testing. Although the analytical processes associated with seismic technology have been around for a long time, the recent evolution of computer microchip technology has made it possible to develop equipment and software that can process the complex information in split seconds rather than hours. Pulse-velocity test equipment is commercially available. This equipment can measure the speed of ultrasonic waves that generate and travel along the surface of the slab and use them to estimate both the dynamic modulus and associated strength of the in-situ concrete.

The primary limitations of the pulse-velocity method are the effect of large size aggregate on the propagation of the waves and the need for good acoustic contact of the sensors with the pavement surface. The portable seismic pavement analyzer (PSPA) is another device that employs an impact load and measures the speed of lower-frequency and larger-amplitude surface waves to estimate concrete dynamic modulus and corresponding strength. The use of surface waves instead of direct arrivals of compression waves, as done with the pulse velocity test, minimizes many limitations of ultrasonic devices.

The integrated maturity-seismic method is an approach that represents a blend of the concrete maturity and seismic methods. The advantage of the maturity method is in estimating the strength of concrete in the field; however, it does not provide any information on the construction quality. On the other hand, the seismic method is quite sensitive to construction-related parameters. Under this combined approach, which was recently developed for PCC highway applications in Texas (Yuan et al., 2003), laboratory specimens are prepared for compressive and/or flexural strength testing in accordance with the typical maturity test method. However, before the specimens are subjected to the strength test, they are tested with the free-free resonant column (FFRC) method (ASTM C215) to determine the dynamic modulus and, if needed, the Poisson's ratio. The result is a database that can be used to establish relationships between seismic wave velocities or dynamic modulus and strengths. With these relationships, it then becomes possible to estimate concrete properties using the PSPA at numerous locations throughout the project. The only real limitations of this method are the cost associated with the up-front lab testing effort and the quality of the correlations between the PCC strengths and the wave velocities measured by the seismic equipment.

Strength Relationships

Extensive literature exists on the variation in flexural or tensile strength with compressive strength (ACI Committee 363, 1984; Tachibana et al., 1981). It is assumed that materials characteristics, in general, affect the tensile properties in a similar manner as the compressive strength. However, recent literature suggests that factors impacting the aggregate-matrix bond are more important to the tensile strength of concrete than compressive strength (McCullough et al., 1998); Forster, 1997; Mohamed and Hansen, 1999). Also, it has been assumed that the rate of increase in modulus is similar to the rate of increase in compressive strength. However, as indicated by McCullough et al. (1998) amongst others, the rate of increase in modulus with time is significantly different from that of either tensile or compressive strength of the same concrete at different ages. This is potentially problematic, as it would lead to increased stresses in the concrete and may be an underlying cause of excessive horizontal cracking observed in some thick PCC pavements.

The modulus of concrete is one of the most important mechanical properties of concrete since it impacts the serviceability and the structural performance of concrete structures. The elastic modulus of concrete is directly related to the properties of the cement paste, the stiffness of the aggregates, and also the method used in determining the modulus. Myers (1999) describes that the gain in modulus occurred more gradually at early-ages for higher coarse aggregate contents for a given cementitious content. This may be attributed to the larger coarse aggregate surface area present in a higher coarse aggregate factor (CAF) mix. In general, the larger the amount of

coarse aggregates with a high elastic modulus in a concrete mixture is, the greater the modulus of elasticity of concrete will be. Increasing the coarse aggregate content beyond 40 percent appeared to benefit the elastic modulus, but did not appear to benefit the compressive strength (Myers, 1999).

Many investigations have been conducted to develop accurate relationship between compressive and flexural or tensile strength. Though many investigations have been done, the results have been conflicting (Ramaiah et al., 2001). The most utilized relationship that is recommended by ACI is between the flexural and compressive strengths, where flexural strength is assumed to be 7.5 times the square root of the specified concrete compressive strength. Though this relationship is perceived to underestimate the strength, it continues to be used because it is conservative and simple to manipulate (Ramaiah et al., 2001). The relationship between the flexural and compressive strengths depends on the type of coarse aggregate used because the properties of aggregate, especially its shape and surface texture, affect the ultimate strength in compression very much less than the strength in tension of the cracking load in compression (Neville, 1996). As discussed previously, it has long been known that concrete pavements fail in tension, thus, using compressive tests to estimate flexural and then to estimate tensile strength is highly undesirable because this approach does not consider other important variables such aggregate bonding. The tensile strength of concrete is more sensitive to inadequate curing than the compressive strength, possibly because the effects of non-uniform shrinkage of flexural test beams are very serious. Thus, air cured concrete has a lower tensile to compression ratio than the concrete cured in water (Neville, 1996). Figure 2.1 shows examples of strength relationships from building codes used in various countries.

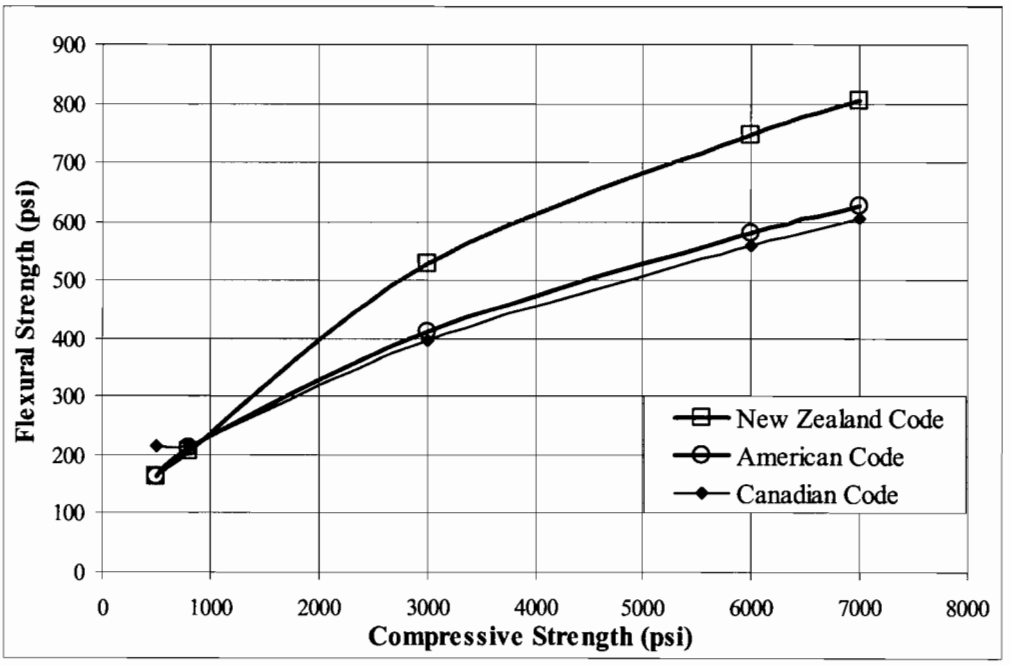

Figure 2.1 – Relationship between Flexural Strength and Compressive Strength for Different Building Codes

Though much research has been conducted in attempt to accurately model strength relationships, no model has been universally accepted. The accuracy of the strength prediction depends directly on the degree of correlation between the strength of the concrete and the quantity measured by the in-place test. Thus, the user of the in-place test should have an understanding of what quantity is measured by the test and how this quantity is related to the strength of the concrete. A key element of construction for quality control and quality assurance (QC/QA) processes in PCC pavements is the measurement of the as-constructed PCC strength. The accurate measurement of these parameters under a valid quality control program provides essential information to the contractor and owner agencies that can be used to correct materials and/or construction problems, improve process control, and limit the production of defective pavement. At the same time, the accurate measurement of the parameters as part of a valid quality assurance program provides the owner agency with a basis for acceptance and, if necessary, pay adjustments. To meet rapid construction schedules, form removal, application of post-tensioning, termination of curing and the removal of reshores must be carried out as early as is possible and safe. The determination of in-place strength to enable these operations to proceed safely at the earliest possible time requires the use of reliable in-place tests. Conversely, it is clear that some major recent construction failures would not have occurred had some measures been adopted (Lew, 1980; Carino et al., 1983).

Table 2.2 –Empirical Concrete Strength Relationships

Predict Parameters	Related Parameters	Relationship	R^2	Comments	Source
Compressive Strength (f_c, psi)	Water-Cement Ratio (w/c)	$\log f_c = 4.16 - 0.8586 w/c$	0.84	Normal augmentation	Popovics (1990)
		$\log f_c = 4.71 - 1.374 w/c - 0.00052 c$	0.93	Augmented by the cement content c	
		$\log f_c = 4.43 - 0.792 w/c - 0.00111 w$	0.93	Augmented by the water content w	
Dynamic Tensile Strength (f_{td}, any unit)	Static Tensile Strength (f_{to}, any unit)	$f_{td} = \left[1.95 - 3.32\left(\frac{1-\varepsilon^{1/8}}{2.2+3.2\varepsilon^{1/8}}\right)\right] f_{to}$		ε = strain-rate magnitude in strains per second (any consistent set of strength units)	Oh (1987)
Elastic Modulus (E_c, GPa))	Compressive Strength (f_c', MPa)	$E_c = 2.9\sqrt{f_c'}$		7 curing conditions: air 13 & 24C, polyethylene sheet 13 & 24C, moist 100% humidity 13C, water 13 & 24C. Unit weight: 1912-1978 kg/m3 and 1919-1979 kg/m3 for 7 and 28 days of curing, respectively.	Khaloo and Kim (1999)

Table 2.2 –Empirical Concrete Strength Relationships (Con't)

Predict Parameters	Related Parameters	Relationship	R^2	Comments	Source
Elastic Modulus (E_c, MPa)	Compressive Strength (f_c', MPa)	$E_c = 5050\sqrt{f_c'}$		12h – 28 days	Mesbah, et al. (2002)
Elastic Modulus (E_c, GPa)	Static Modulus (E_d, GPa)	$E_c = 9\times10^{-11}(65E_d + 1600)^{3.2}$		w/c: between 0.30-0.45	
Split Tensile Strength (f_{sp}, MPa)	Compressive Strength (f_c', MPa)	$f_{sp} = (0.00168f_c' + 0.53)\sqrt{f_c'}$		No-silica fume concretes.	Setunge et al. (1993)
		$f_{sp} = 0.614\sqrt{f_c'}$		Silica fume concretes. $60 \le f_c' \le 120$ MPa	
Tensile Strength (f_{ct}, psi)	Compressive Strength (f_c', psi)	$f_{ct} = 1.38(f_c')^{0.69}$	0.95		Oluokun (1991)

Table 2.2 –Empirical Concrete Strength Relationships (Con't)

Predict Parameters	Related Parameters	Relationship	R^2	Comments	Source
Tensile Strength (f_t, psi)	Compressive Strength (f_c', psi)	$f_t = 0.584\left[f_c'\right]^{0.79}$		Applicable to concrete at early ages (12 hr and over)	Oluokun et al. (1991).
		$f_t = 0.928\left(f_c'\right)^{0.6}$		Applicable to ages when compressive strength of concrete is less than or equal to 1000 psi	
Tensile Strength (f_{sp}, psi)	Compressive Strength (f_c', psi)	$f_{sp} = \alpha(t) f_c'^{0.666}$		$\alpha(t) = \gamma t^{-\psi}$ $\gamma = 0.36$ and $\psi = 0.07$ provide a lower bound curve to give $\alpha = 0.30$ at 14 days and 0.26 at 91 days	Rezansoff. and Corbett (1988)

Chapter 3

Test Program

On the basis of the general objectives of this project summarized in Chapter 1, the issues to be addressed and studied can be itemized in the following manner:

1. In terms of the gain rate, is the early-age strength of concrete normalized to 28-day strength, f/f_{28}, similar to the early-age modulus normalized to 28-day modulus, E/E_{28}? (
2. If not, can f/f_{28} be quantified with respect to E/E_{28}?
3. More generally, can strength be related to modulus?
4. More specifically, can seismic modulus, $E_{seismic}$, be used to predict strength?
5. What parameters impact strength-modulus relationship?

To address these issues, a test matrix was devised in conjunction with the Project Management Committee (PMC) of this project. The study was carried out in two phases. In phase I, the mix-related parameters considered were the coarse aggregate type (LS/SRG), aggregate condition (clean/dirty) and the use of mineral admixtures (FA/no FA). As shown in Table 3.1a, the matrix required eight concrete mixes: four with the LS aggregates and the other four with the SRG aggregates. Also, in Phase I of this study, five different curing conditions were applied to the specimens from each of the eight mixes. These conditions include water curing at temperatures of 70°F and 95°F with 100% relative humidity, room curing at temperatures of 70°F and 95°F with about 40% and 20% humidity levels, respectively, and field curing with variable temperature and variable humidity. As such, over 800 standard 6 in. by 12 in. cylinders were prepared and tested.

Based on the successful completion of the first phase of the study, the number of parameters to be considered was expanded in a second phase. In Phase II, the mix-related parameters that were considered included the coarse aggregate factor (low/high), the concentration of water reducer agents (low/high) and the use of the ground-granulated blast furnace slag instead of the fly ash (GGBFS/FA). In this phase, only clean El Paso SRG aggregates were used. Also, in Phase II, three different curing conditions were considered in the study for each of the seven mixtures. These curing conditions include water curing at temperatures of 70°F and 95°F with 100% relative humidity, and field curing with variable temperature and variable humidity. In Phase II, the dry

curing of the specimens was eliminated from the work plan because of the detrimental impact that this condition has on the quality of concrete. The test matrix for Phase II is shown in Table 3.1b. Seven mixes and about 400 standard cylinders were prepared and tested in this phase.

Table 3.1 – Mix Design Matrix and Curing Regimes for Experiment

a) Phase I

Aggregate Type			LS				SRG			
Aggregate Condition			Clean		Dirty		Clean		Dirty	
Fly Ash			Y	N	Y	N	Y	N	Y	N
Curing / Temperature	Field									
	Water	70°F								
		95°F								
	Room	70°F								
		95°F								

b) Phase II

Aggregate Type			SRG							
CAF			Low				High			
Water Reducer			Low		High		Low		High	
Fly Ash (FA) / GGBFS			GGBFS	FA	GGBFS		FA	GGBFS	FA	GGBFS
Curing / Temperature	Field									
	Water	70°F								
		95°F								

Mix Design

As stated earlier, fifteen mix designs were used in the study. The mix parameters are summarized in Table 3.2. All mixes were designed for a 7-day flexural strength of not less than 555 psi (3820 kPa) for specimens cured under ideal condition (water curing at 70°F).

Table 3.2 – Mix Design Summary for Phase I and Phase II

Phase	Aggregate Type	Aggregate Condition	CAF	Water Reducer	Mineral Admixtures	Mix Design Gradations in (lbs) for 1 yd^3				
						Coarse Aggregate	Fine Aggregate	Portland Cement	Water	Mineral Admixtures
I	LS	Clean	0.65	Low	FA	1775	1242	382	221	111
		Clean	0.65	Low	None	1775	1242	545	221	0
		Dirty	0.65	Low	FA	1775	1242	382	221	111
		Dirty	0.65	Low	None	1775	1242	545	221	0
	SRG	Clean	0.65	Low	FA	1775	1242	382	221	111
		Clean	0.65	Low	None	1775	1242	545	221	0
		Dirty	0.65	Low	FA	1775	1242	382	221	111
		Dirty	0.65	Low	None	1775	1242	545	221	0
II	SRG	Clean	0.65	Low	GGBFS	1775	1242	273	221	248
		Clean	0.65	High	GGBFS	1775	1242	273	221	248
		Clean	0.65	High	FA	1775	1242	382	221	111
		Clean	0.70	Low	GGBFS	1775	1242	273	221	248
		Clean	0.70	Low	FA	1775	1242	382	221	111
		Clean	0.70	High	GGBFS	1775	1242	273	221	248
		Clean	0.70	High	FA	1775	1242	382	221	111

In Phase I, four mixes were prepared with crushed LS aggregates and another four with SRG aggregates. From the four LS mixes, two were prepared with clean aggregates while the other two with dirty aggregates. The difference between the two clean and the two dirty mixes was the presence or absence of fly ash. In one mix, no fly ash was added while in the other 30% fly ash by volume was used. The same procedure was also applied to the four mixes made with LS aggregates. The water/cement ratios were 0.45 for the mixes with the fly ash and 0.41 for the mixes without the fly ash. In all mixes, the maximum aggregate size was 1 in. (25 mm) and the coarse aggregate factor (CAF) was 0.65.

In Phase II, seven mixes were prepared with the SRG aggregates from El Paso, Texas. Only clean aggregates were used. The variable parameters in Phase II were the CAF, the concentration of water reducer and the amount of GGBFS. Three mixes were prepared with a low CAF (0.65) and four mixes with a high CAF (0.70). From the three mixes with the low CAF's, one contained low concentration of water reducer while the other two contained high concentrations of water reducer. From the four mixes with high CAF's, two had low concentration of water reducer while the other two had high concentrations of water reducer. The difference between the two high and the two low water reducer mixes was the presence of either GGBFS or fly ash.

Aggregate Type

The appropriate selection of coarse aggregate type is of great importance to the concrete properties and the performance of concrete pavements. Coarse aggregate influences the magnitude of stress development due to the hydration process, the extent of transverse crack widths and the load transfer properties. In Phase I, siliceous river gravel from the El Paso, Texas area and crushed limestone from the Austin, Texas area were used. In Phase II only siliceous river gravel from the El Paso, Texas area was used

Aggregate Condition

In Phase I, two aggregate conditions were considered: "clean" and "dirty". The so-called clean aggregates were the standard materials used in the day-to-day operation of TxDOT. The decant values were about 0.5 and 0.9 for the SRG and LS aggregates, respectively.

To develop "dirty" aggregates, the "clean" aggregates were placed inside a concrete mixer along with adequate water to saturate them. Clay was then gradually added to the saturated aggregates while it was being agitated. This combination of the aggregates and clay was then dumped and allowed to dry for at least four days before it was used in a concrete mix. A reasonably thick film of clay was evident on the aggregates after drying. During sample preparation, some of the coated aggregates were separated and washed by trickling water on them. A coat of clay was still detectable on the aggregate. The decant values for both SRG and LS dirty aggregates were about 3.

Curing Condition

In Phase I, the cylinders prepared from each mix were divided into five groups. The first group was placed in a temperature control room of 70°F (21°C). The specimens in this group were considered as being room-cured under cool or standard condition. The second group was placed in a temperature control room of 95°F (35°C). The specimens in this group were considered as being room-cured under hot condition. The relative humidity of the 70°F and 95°F rooms was approximately 40% and 20% or less, respectively. The third group of specimens were cured in a water tank (wet-curing) placed in a temperature control room of 70°F (21°C), while the fourth was place in a water tank placed in a temperature control room of 95°F (35°C). The fifth group of specimens was buried in sand outside the building to cure under the natural condition for the duration of the experiment; this was called field curing. In Phase II, the dry curing was eliminated from the study since there is enough information for this type of curing from Phase I for evaluation. As such, only three groups of specimens were poured and tested, that is, the water-cured at 70°F and 95°F as well as the field-cured cured under the natural condition.

Coarse Aggregate Factor

The coarse aggregate factor is defined as a ratio of the weight of the coarse aggregates to the volume of the mix multiply by the dry rodded unit weight of the aggregates. In phase I of this study, the CAF was not a mix dependent variable, therefore the mix were designed with a standard CAF value of 0.65 for both the LS and SRG aggregates. The impact of different CAF's was study in Phase II. Two different CAF's were used, a low CAF of 0.65 and a high CAF of 0.70.

Mineral Admixtures

Fly ash (FA), ground-granulated blast furnace slag (GGBFS) and silica fume (SF) are just some of the industrial by-products now available for use as additives in the portland cement concrete mixes. Use of these particular additives, despite their economic or environmental consideration, is becoming popular because of the advantages in delaying the hydration process. In Phase I, fly ash was used in mixes with both types of aggregates. In Phase II, the admixtures used were FA and GGBFS.

Chemical Admixtures

The purpose of using water-reducing admixtures in concrete mixes is to obtain a reduction in water while retaining the desired workability. A Boral NR water reducing admixture was used in both Phase I and Phase II. The effects of adding water reducing agent to a concrete mix was set as a variable. Low range water reducers can reduce the water requirements on a mix from 5% to 10%. On the other hand, high range water reducers can achieve a reduction in water demand up to 20%.

Test Protocol

Specimens were tested at 1 day, 3 days, 7 days and 28 days after they were poured. TxDOT test method Tex-447-A (ASTM C192) was used to prepare the specimens. For each mix and each curing condition, at least one specimen was equipped with a thermocouple attached to a maturity meter. On each test day, five specimens were tested: two specimens were subjected to split tensile tests, and three to compressive strength/static modulus tests.

For each test day and each mix, the test protocol consisted of five phases: seismic modulus tests, compressive strength tests, static modulus tests, split tensile strength tests, maturity tests. Each is discussed below.

1. *Seismic Modulus Tests*: Shortly before a specimen was subjected to a mechanical test, the free-free resonant column test (ASTM C215) was carried out on the specimen. Since this test is nondestructive, this activity did not impact the results from the other tests.
2. *Compressive Strength Tests*: Standard compression tests (ASTM C39, Tex-418-A) were performed on three cylinders. The average compressive strength from the three tests was obtained.
3. *Static Modulus Tests*: After the compressive strength from the first cylinder in item 2 was determined, static modulus tests (ASTM C469) was performed on the other two cylinders before compressive strength tests. The average static modulus from the two tests was obtained.
4. *Split Tensile Strength Tests*: Standard split tensile tests (ASTM C496, Tex-421-A) was performed on two cylinders. An aligning jig was used to position the cylinder on its longitudinal axis. The average tensile strength from the two tests was obtained.
5. *Maturity Tests*: The specimens equipped with thermocouples were either connected to a maturity meter or a temperature data-logger. The temperature was continuously recorded for 28 days. The temperature history was converted to the time-temperature factor or to the equivalent age as per Test Method Tex-426-A (ASTM C1074).

Conventional testing on all cylinders for compressive strength, splitting tensile strength and static modulus was conducted using an Instron-Satec System with control software of Nu Vision Partner V5.1E (see Figures 3.1 through 3.3). Seismic testing on all cylinders was conduct using a free-free resonant column device shown in Figure 3.4, developed at UTEP. Appendix A contains a description of this method.

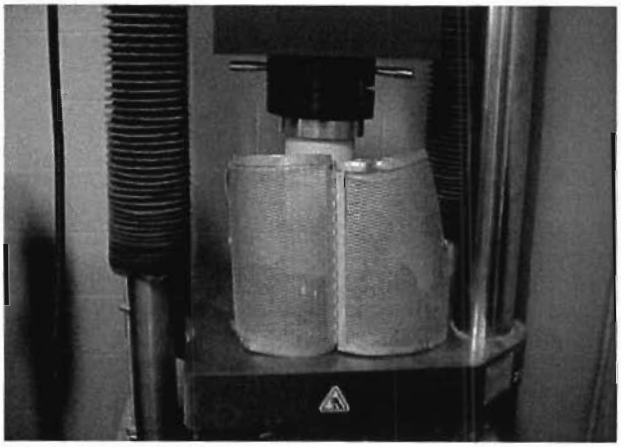

Figure 3.1 - Compressive Test in Progress

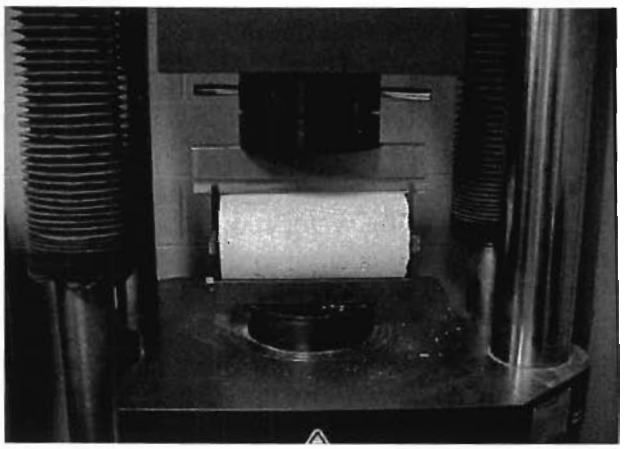

Figure 3.2 – Split Tensile Test in Progress

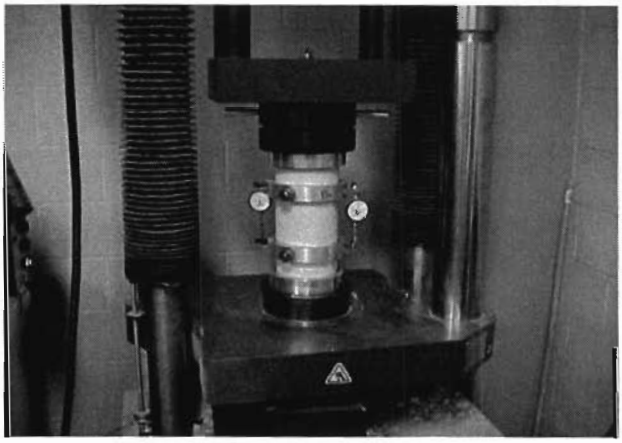

Figure 3.3 – Static Modulus Test in Progress

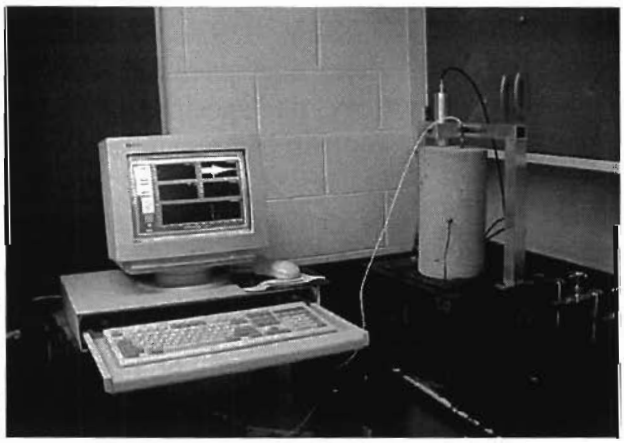

Figure 3.4 – Free-Free Resonant Column Test in Progress

Typical Results

Typical variations in compressive strength, tensile strength, static modulus and seismic modulus with time and maturity (time-temperature factor or TTF) for cylinders prepared from a mix with clean LS aggregates, with fly ash and cured in water of 70°F (21°C), also called the LS standard mix for this study, are shown in Figures 3.5 and 3.6, respectively. The variation patterns of all strength and modulus parameters with time are similar to those with maturity for a given mix cured at the same conditions. Furthermore, the gains in two modulus parameters are evidently slower than those in two strength parameters after the age of about 3 days. Similar features also exist for other mixes involved in this study.

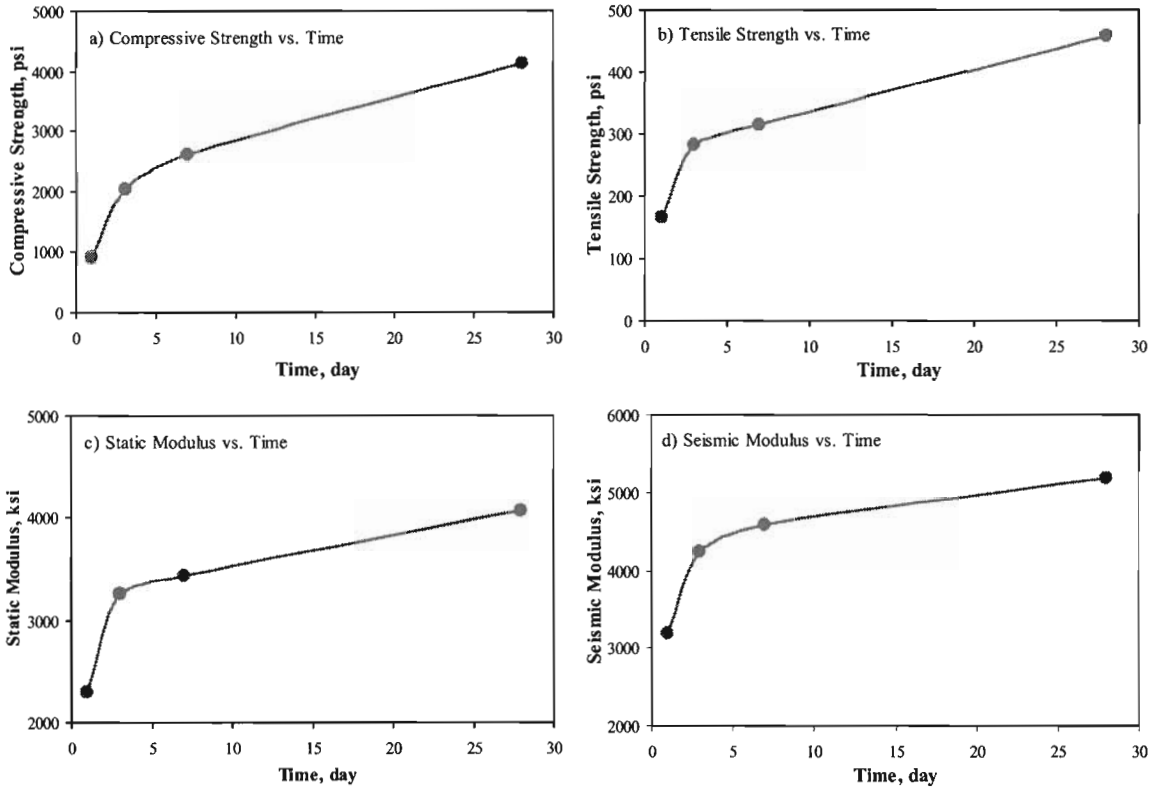

Figure 3.5 – Typical Variation in Strength and Modulus Parameters with Time

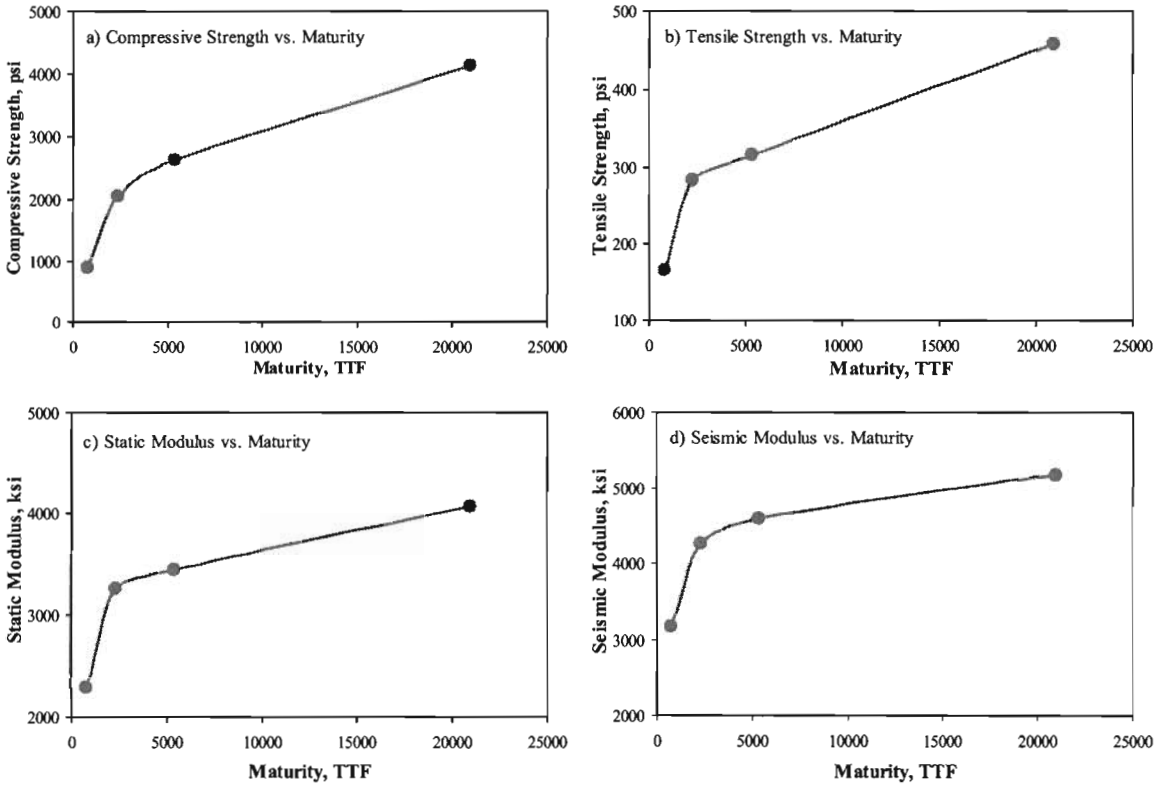

Figure 3.6 – Typical Variation in Strength and Modulus Parameters with Maturity

To have a clear picture of the development patterns of individual strength and modulus parameters with time, the values of each parameter at different ages are normalized to its value at the age of 28 days. Comparisons of such normalized parameters are shown in Figure 3.7. Several features can be observed from this figure:

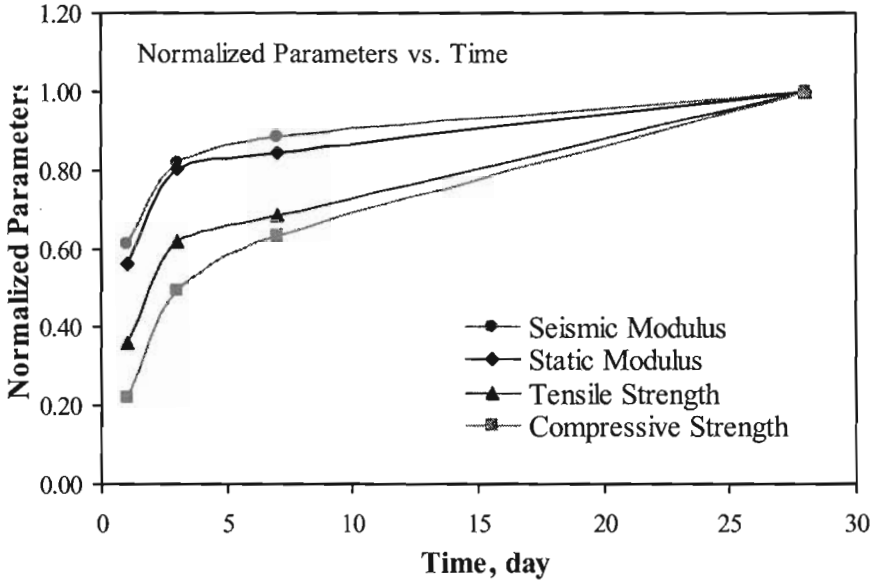

Figure 3.7 – Comparison of Typical Gain Patterns in Normalized Strength and Modulus Parameters with Time

1. The gain in strength parameters is evidently different from that of modulus parameters.
2. At early ages, from about 24 hours to about 3 days, the strength and modulus parameters exhibit similar patterns in terms of the gain rate.
3. After 3 to 7 days, the two strength parameters demonstrate higher gain rate as compared to the two modulus parameters.
4. The rate of increase in compressive strength is somewhat greater than that of the split tensile strength after the ages of about 3 to 7 days.
5. The rates of increase in static modulus and seismic modulus are almost identical. The small deviation between the two curves is, most likely, due to testing errors for static modulus.

After the strengths and moduli from 1-day through 28-day tests were obtained for a given mix, different parameters were correlated. First, the average compressive strengths and the average seismic moduli were correlated. As shown in Figure 3.8a, a power curve describes the data quite well. Similarly, the possibility of relating the average split tensile strengths and the average seismic moduli was studied. The results from this activity and the corresponding best fit curve are shown in Figure 3.8b. The data is well-described with a power curve as well. Finally, the average static and seismic moduli are related. As shown in Figure 3.8c, these two parameters also relate very well with a linear relationship.

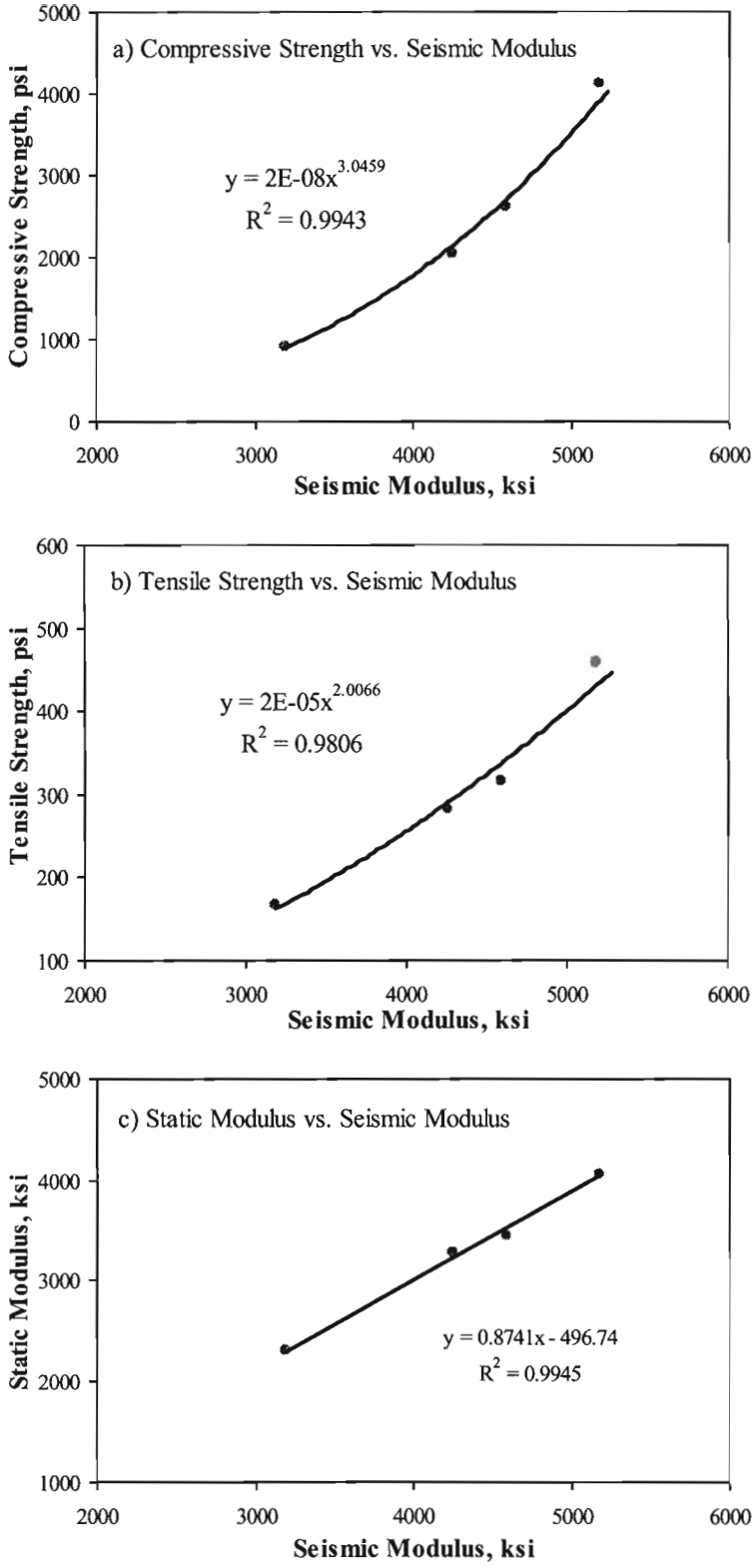

Figure 3.8 – Typical Relationships between Strength Parameters and Static Modulus to Seismic Modulus

Chapter 4

Parameters Affecting Strength and Modulus Gain

It is well documented that the modulus and different strength parameters affect the PCC pavement performance in different manners. In general, the parameters that impact the development of strength and modulus of concrete can be classified into the following three groups: mix-related, construction-related and environmental-related parameters. Within the limits of this study (laboratory experiments), only the mix-related and environment-related parameters were consider.

The compressive strength test of concrete is perhaps the most common measure of concrete quality, although compressive failure rarely occurs on PCC pavements. The flexural/splitting tensile strength directly affects the performance of PCC pavements. The initiation of transverse cracking and corner breaking of a PCC slab is also directly related to the PCC tensile characteristics.

The static modulus of a PCC controls the overall slab deformation from traffic loading and the slab curling stresses. The elastic modulus increases as the compressive strength increases. In general, the material characteristics affect the modulus in the same way as the compressive strength. However, as indicated by McCullough et al. (1998) and the results from our experiments, the increase in the modulus with time is significantly different from that of either the tensile or compressive strength of the same concrete. This is potentially problematic, as it would lead to increased stresses in the concrete, and may be an underlying cause of excessive horizontal cracking observed in some PCC pavements. Results from this study are included in this chapter, however due to a large number of alternatives in comparing the results, only typical examples are included in this chapter. Detailed results can be inspected in Appendices B and C.

Phase I - Mix-Related Parameters

The mix-related parameters studied in phase I were the type of coarse aggregate (LS/SRG), the amount of fly ash (with FA/without FA) and the clay coating of coarse aggregates (Clean/Dirty). For simplicity, only results related to specimens prepared with clean LS & SRG aggregates, with fly ash and cured in water at 70° F (21° C), also called "standard mix," are presented in this chapter.

Impact of Coarse Aggregate Type

The effects of using different types of coarse aggregates on concrete strength have been reported in several recent articles. The important characteristics of the coarse aggregates are their origin, texture and size. Zia et al. (1994) showed that the compressive strength and elastic modulus were significantly influenced by the mineralogical characteristics of the aggregates.

The variations in strength and modulus with respect to time for specimens prepared with LS and SRG aggregates are compared in Figure 4.1. At a given time, the strength and modulus for the mix with LS aggregates are greater as compared to the mix with SRG aggregates. The gain rates (slope) of both the compressive and the tensile strengths with time are also greater for the mix with the LS aggregates as compared to the SRG aggregates (Figures 4.1a and 4.1b). The increase in the static and seismic moduli with time can be assumed to be constant after 3 days according to Figures 4.1c and 4.1d. Moduli from the mix with the LS aggregates are greater than the SRG aggregates. The type of coarse aggregates mainly affects the magnitude of both strength and modulus and, to a lesser content, the development rate of these parameters, especially, after two or three days.

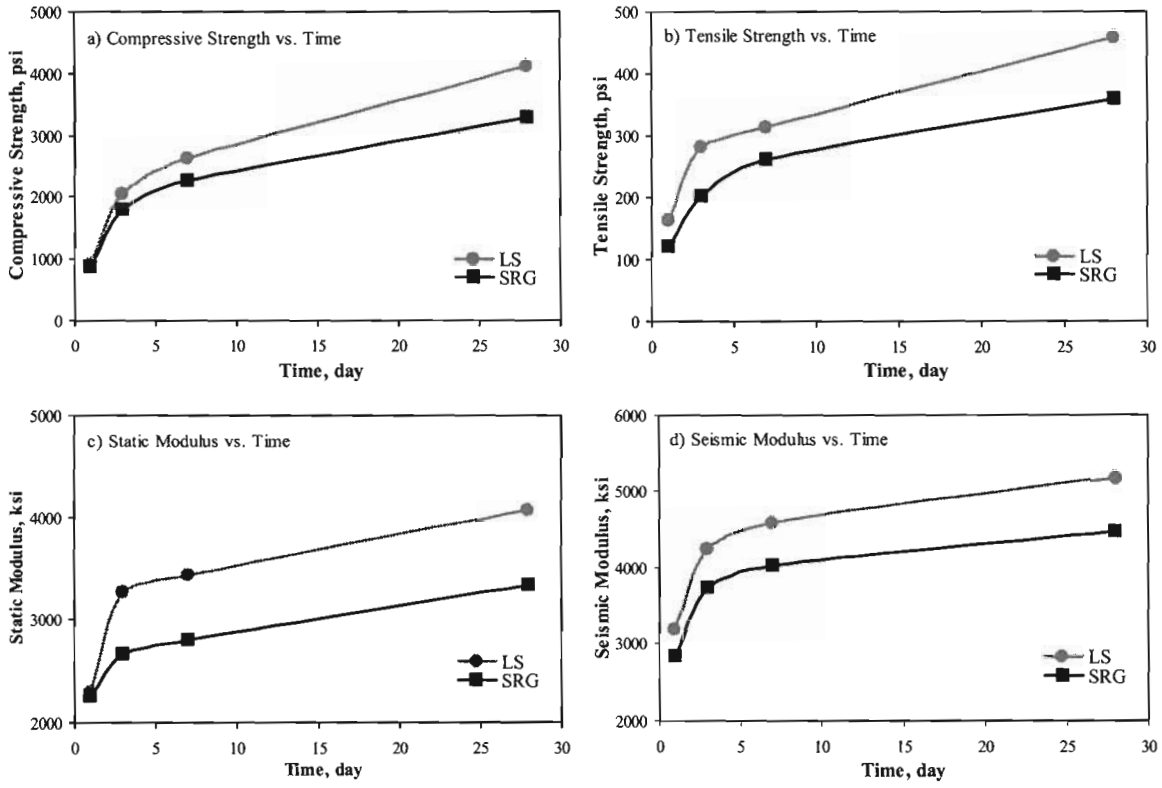

Figure 4.1 – Impact of Coarse Aggregate Type on Development of Strength and Modulus Parameters with Time

Various relationships have been widely used to estimate the tensile strength as well as the static modulus from the compressive strength tests (Oluokun, 1991; Mesbah et al., 2002). Figure 4.2 shows typical correlations between the tensile strength and the static modulus with the compressive strength. As shown in Figure 4.2a, if a relationship between the tensile and compressive strengths is

to be used, a specific equation that accounts for the type of coarse aggregate needs to be established instead of a general equation. The same patterns are evident in Figure 4.2b between the static modulus and compressive strength. However, as the compressive strength increases the gap between the relationships for the two aggregates increases.

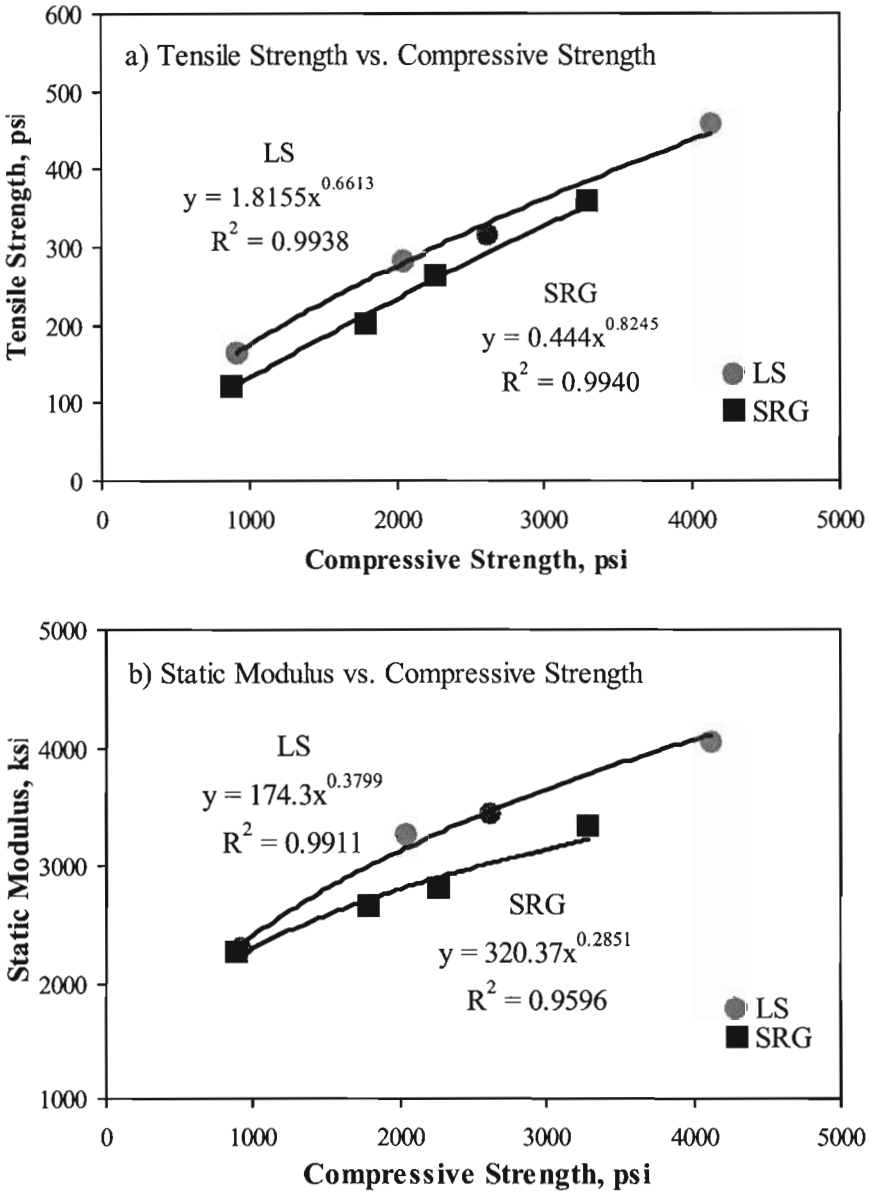

Figure 4.2 – Typical Correlations between Tensile Strength and Static Modulus to Compressive Strength

The relationships between compressive and tensile strengths and static modulus to seismic modulus are shown in Figure 4.3. All three relationships are well correlated. For the compressive strength relationship (Figure 4.3a), the two mixes yield different patterns. The tensile strength to seismic modulus (Figure 4.3b) and static modulus to seismic modulus (Figure 4.3c) relationships are closer to one another.

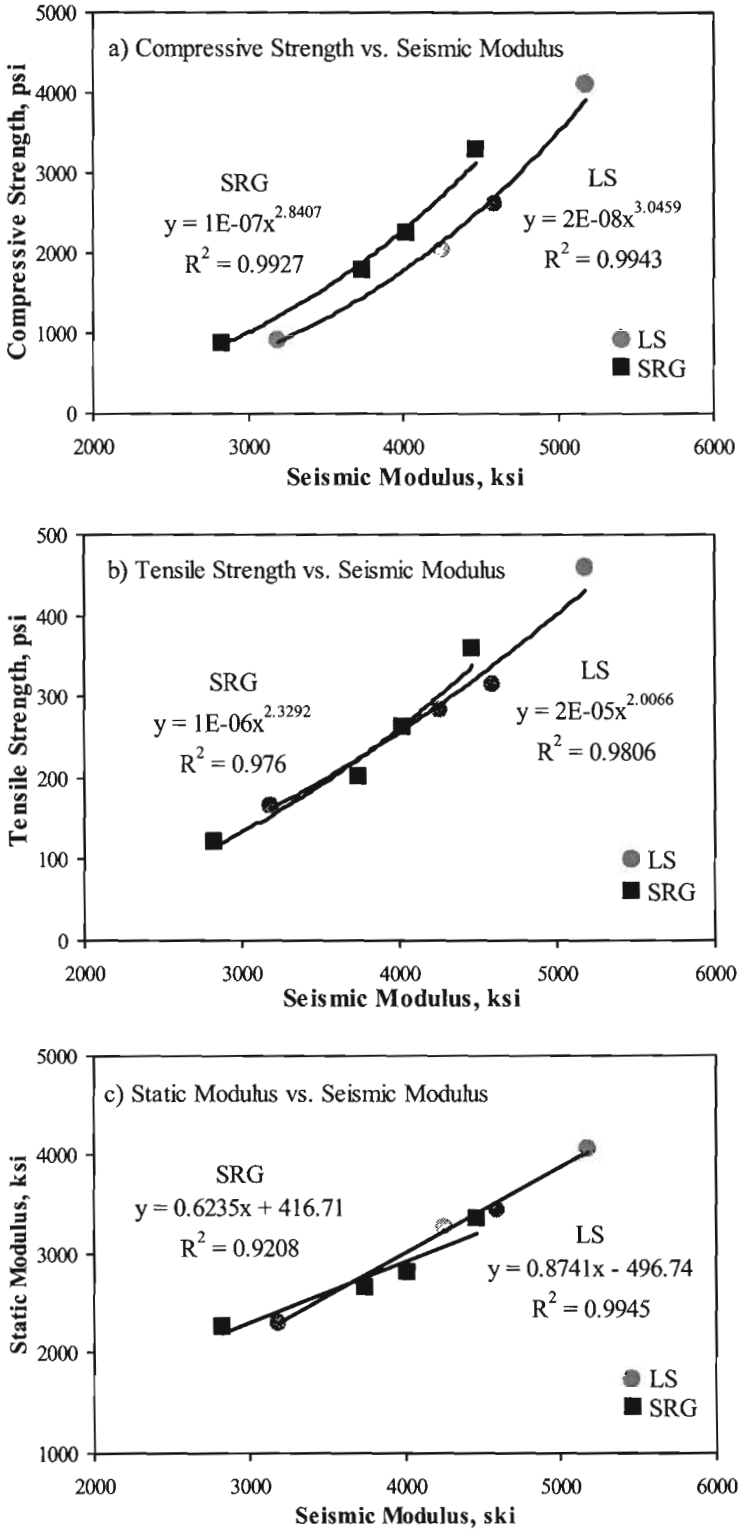

Figure 4.3 – Typical Relationships between Strength Parameters and Static Modulus to Seismic Modulus for Different Coarse Aggregate Types

The variations in compressive strength, tensile strength, static modulus and seismic modulus as a function of maturity for specimens prepared with both the LS and SRG aggregates are shown in Figure 4.4. Since maturity is a function of time (the temperature histories were about the same), the trends in Figure 4.4 are similar to those in Figure 4.1. The strengths and moduli at a given TTF for the mix with the LS aggregates are greater than the same parameters from the SRG aggregates.

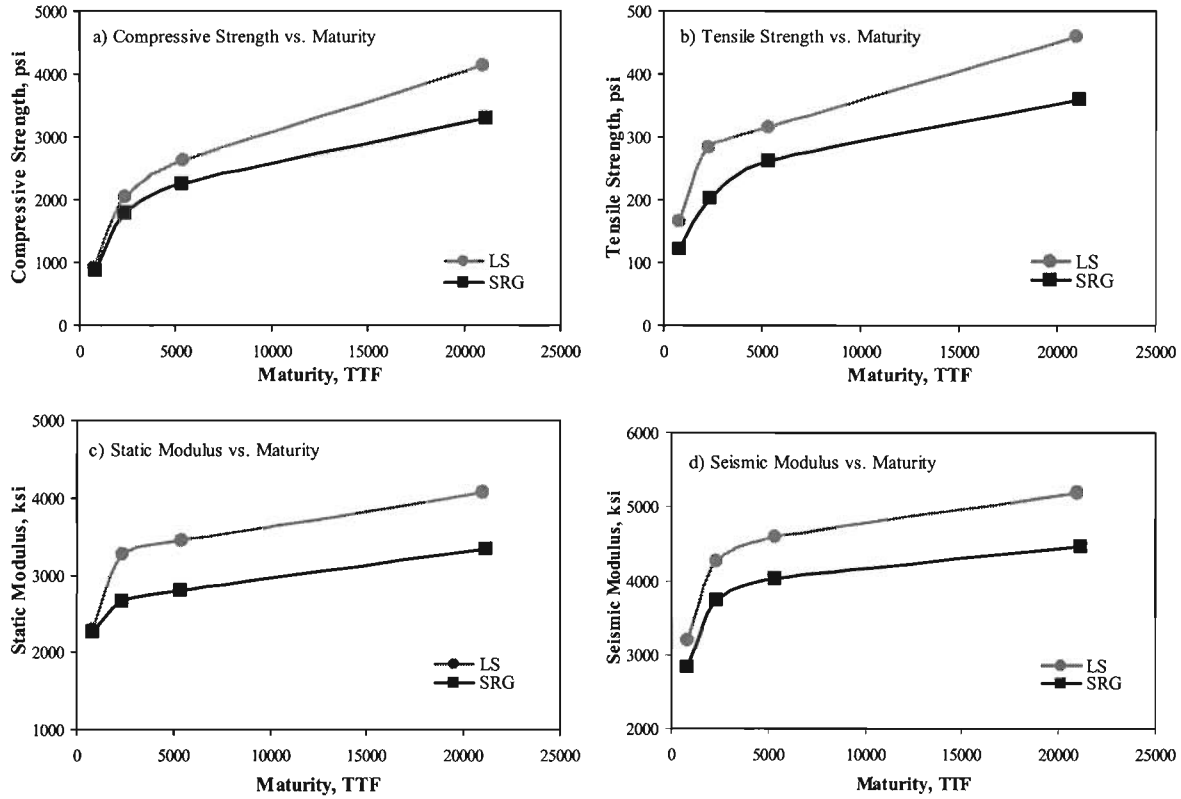

Figure 4.4 – Typical Impact of Coarse Aggregate Type on Strength and Modulus Parameters with Maturity

Impact of Fly Ash

The variations in strengths and moduli of the two standard mixes with and without fly ash are compared in Figure 4.5. As shown in Figure 4.5a, at a given time, the mixes with pure cement exhibit higher compressive strengths. The same behavior is observed in Figure 4.5b, where the mixes with pure cement exhibit higher tensile strengths. As shown in Figures 4.5c and 4.5d, the trends for the two moduli are similar to the strength parameters.

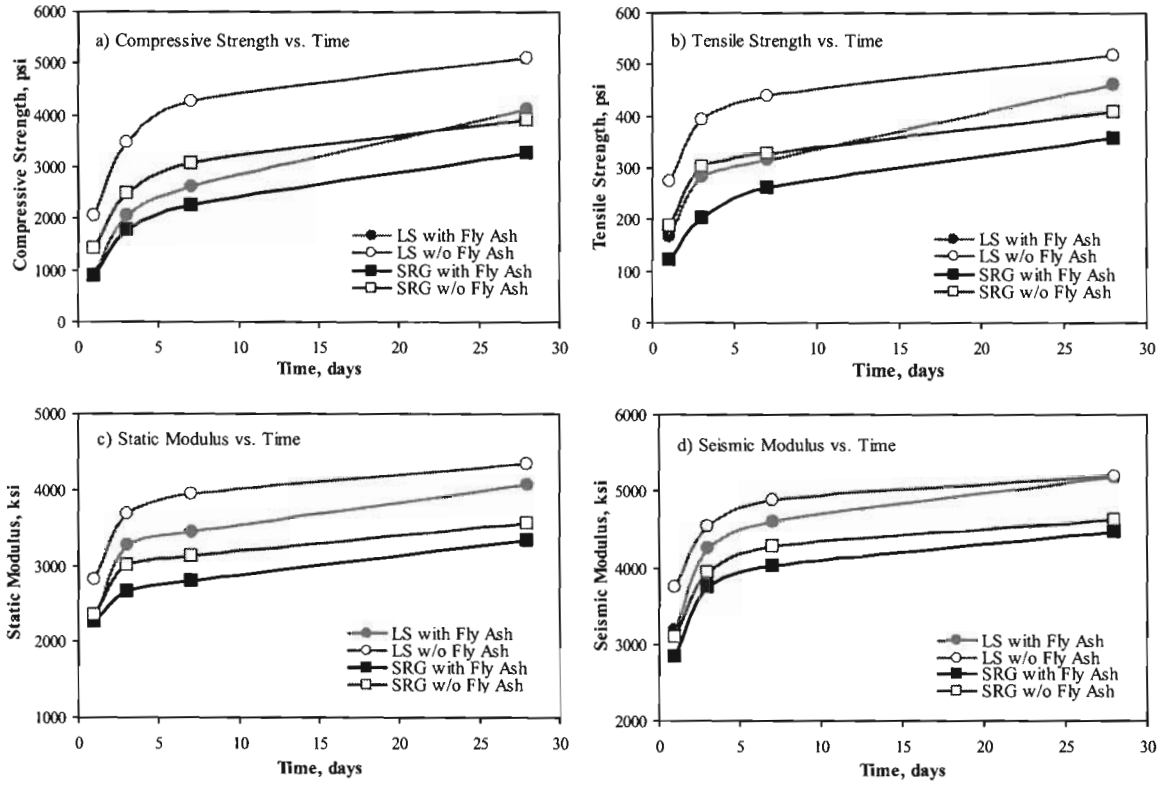

Figure 4.5 – Impact of Fly Ash on Strength and Modulus with Time

Impact of Clay Coating Coarse Aggregates

The variations of the two strengths and moduli with time for both standard mixtures (clean) are compared to those from similar mixtures prepared with clay-coated (dirty) aggregates in Figure 4.6. The clay coating of aggregates has similar effects on the mixes with LS and SRG coarse aggregates. A concrete mix with dirty aggregates exhibits a significant reduction in its strength and modulus, especially in tensile strength.

Phase II - Mix-Related Parameters

The mix-related parameters considered in Phase II were the coarse aggregate factor (low CAF/high CAF), the amount of water reducer agents (low WR/high WR) and the use of ground-granulated blast furnace slag (GGBFS). Only clean SRG aggregates from El Paso, Texas were used in Phase II. For simplicity, only results from specimens prepared with SRG aggregate, with fly ash and cured in water at 70° F (21° C), also called "standard mix" are presented in this section.

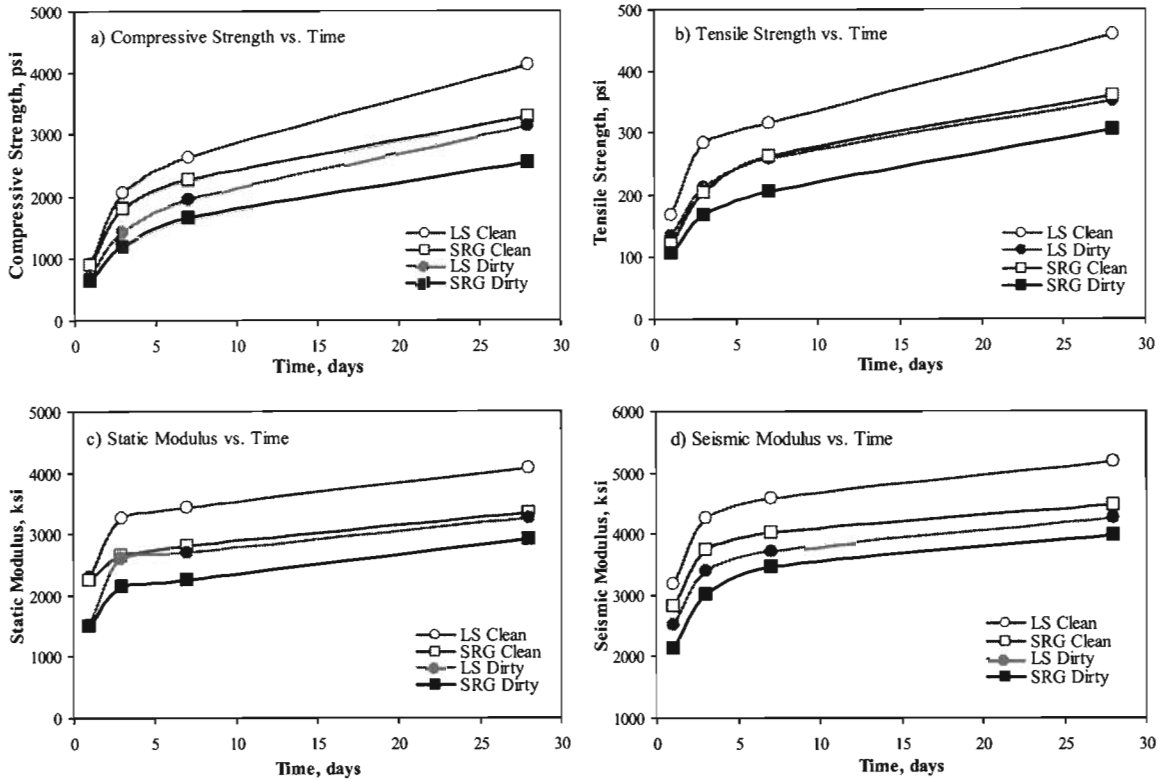

Figure 4.6 – Variations in Strength and Modulus Parameters with Time for Mixes with Clean and Dirty Coarse Aggregates

Impact of the Coarse Aggregate Factor

The coarse aggregate factor (CAF) is the ratio in percentage of the volume of coarse aggregates to the unit volume of the concrete mix. The CAF is an indicator of the relative coarseness of the mix. If the CAF is increased, the mix will become more under-sanded; while if it is decreased, the mix will become over-sanded. A value of 0.65 was used for the low CAF and a value of 0.70 for the high CAF.

Figure 4.7 illustrates the variations in strengths and moduli with respect to time for the mixes with the low and high CAF's. The compressive strengths are fairly similar. The tensile strengths are almost the same for the first 7 days, after which the mix with a low CAF exhibits a higher tensile strength. In terms of both static modulus (Figure 4.7c) and seismic modulus (Figure 4.7d), the mix with a low CAF always exhibits higher values.

Impact of Amounts of Water Reducer Agents

The amounts of water reducer used were about 5.0 oz/cwt and 15.0 oz/cwt for the low WR mix and the high WR mix, respectively. The impacts of the amount of water reducer on strength and modulus parameters are shown in Figure 4.8. As shown in Figure 4.8a, the mix with the high water reducer achieves higher compressive strength at any given time. However, the amount of water

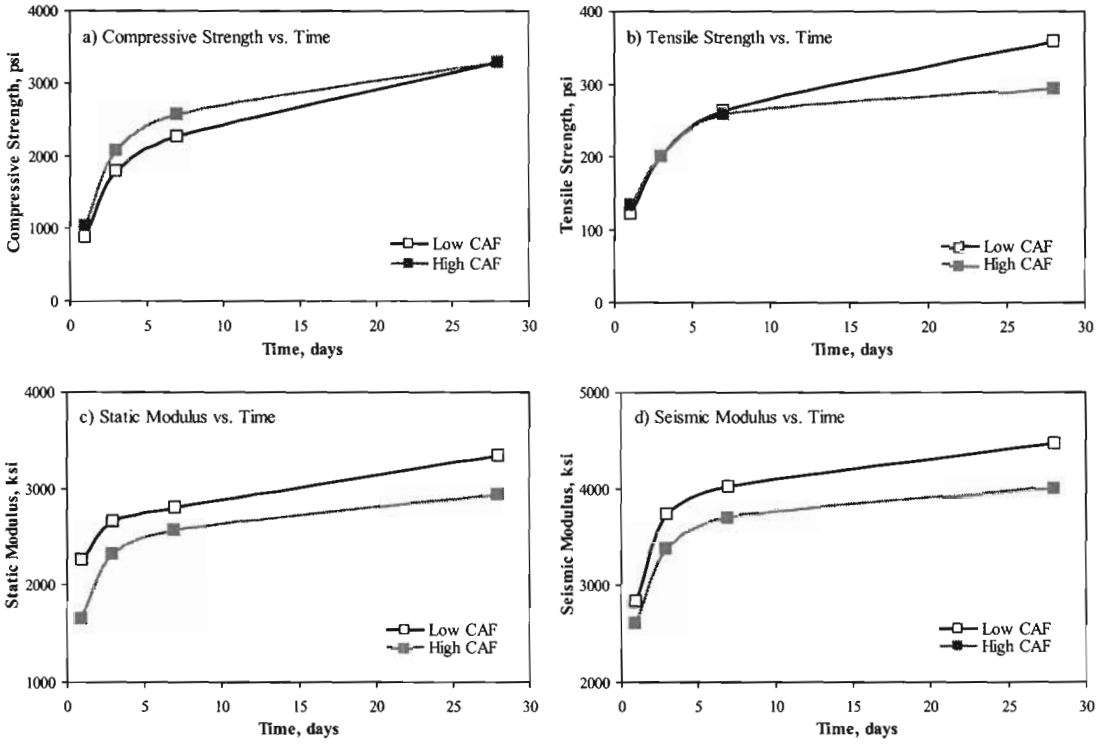

Figure 4.7 – Variations in Strength and Modulus Parameters with Time for Mixes with Different Coarse Aggregate Factors

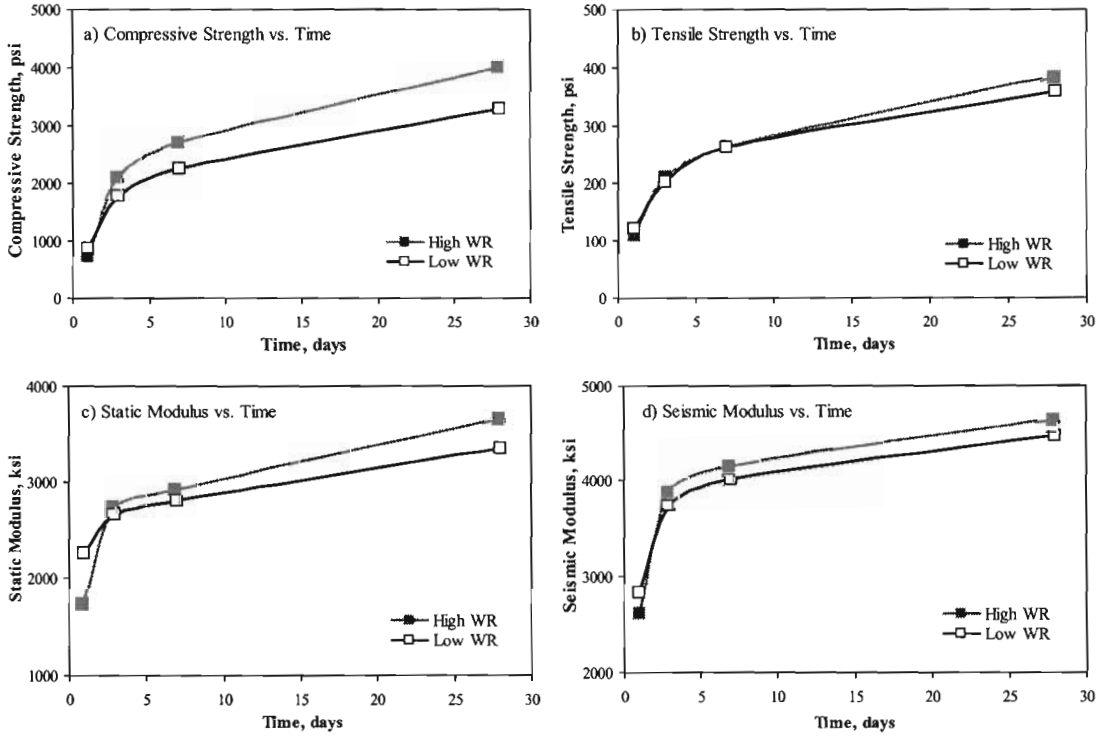

Figure 4.8 – Variations in Strength and Modulus Parameters with Time for Mixes with Different Amounts of Water Reducer

reducer does not seem to significantly impact the tensile strength (Figure 4.8b). The static and seismic moduli are similar as shown in Figures 4.8c and 4.8d.

Impact of Ground-Granulated Blast Furnace Slag

The variations in compressive strength, tensile strength, static modulus and seismic modulus with time for a mixture with the fly ash and similar mix with the ground-granulated blast furnace slag (GGBFS) are compared in Figure 4.9. From Figure 4.9a, the compressive strength of the mix with the GGBFS is greater than the mix with the fly ash. On the other hand, the tensile strengths from the two mixes are fairly similar (Figure 4.9b). As shown in Figure 4.9c, the static modulus from the GGBFS mix is generally greater when compared to the mix with the fly ash. The seismic moduli from the two mixtures are fairly similar (Figure 4.9d).

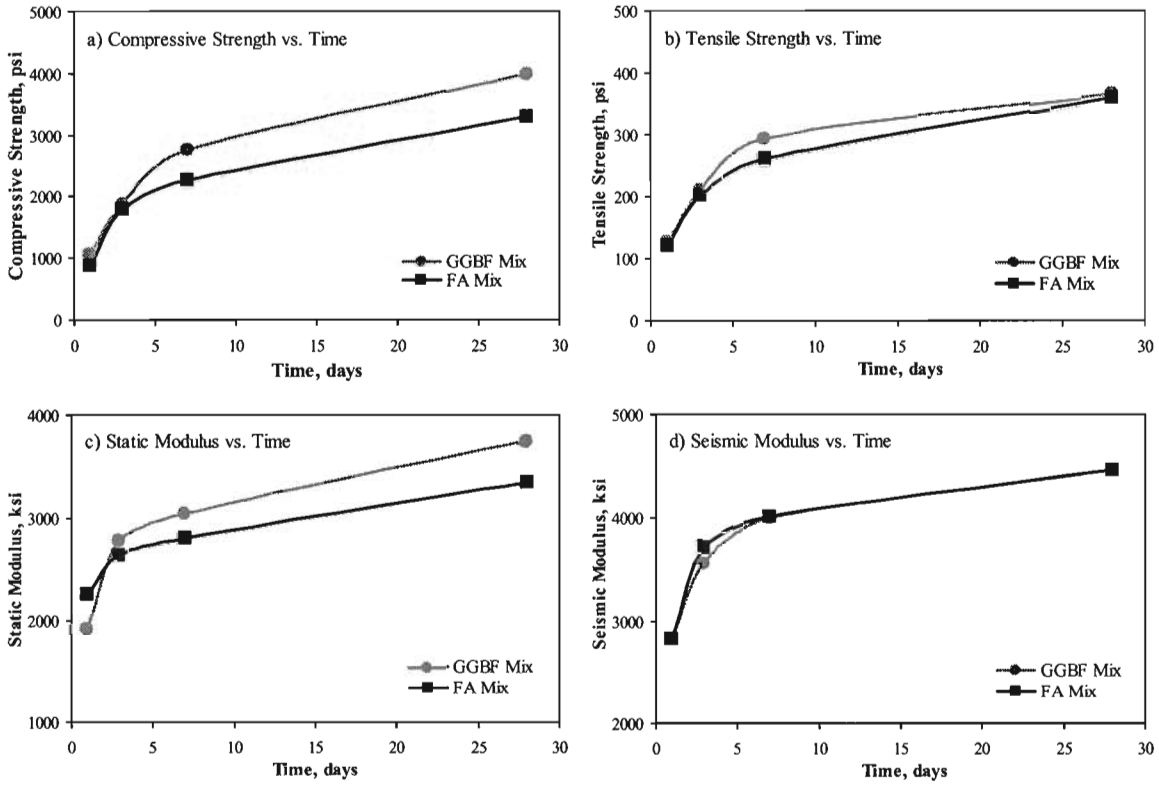

Figure 4.9 – Variations in Strength and Modulus Parameters with Time for Mixes with GGBFS and Fly Ash

Environmental Parameters

In this study, the environmental-related parameters that affect the development of strength and modulus of concrete are temperature and humidity. These two parameters considered in Phase I were water curing at temperatures of 70°F and 95°F with 100% relative humidity, room curing at temperatures of 70°F and 95°F with 40% to 20% relatively humidity, and field curing with variable temperature and humidity. Again, for simplicity, only the results from specimens prepared with fly ash and clean aggregates are presented below.

Impact of Curing at Different Temperatures

Water curing was carried out at temperatures of 70°F and 95°F. In both cases, a humidity of 100% was assumed because the specimens were always maintained in a water tank until their appropriate test times. Figure 4.10 demonstrates the strength and modulus developments for the two standard mixes at the different temperatures. The specimens from the LS mix cured at 95°F typically exhibit higher compressive and tensile strengths. The static moduli from specimens cured at 95°F are somewhat greater as well. However, the seismic moduli are fairly similar. For the SRG mix, the strengths and moduli are quite similar for both curing temperatures.

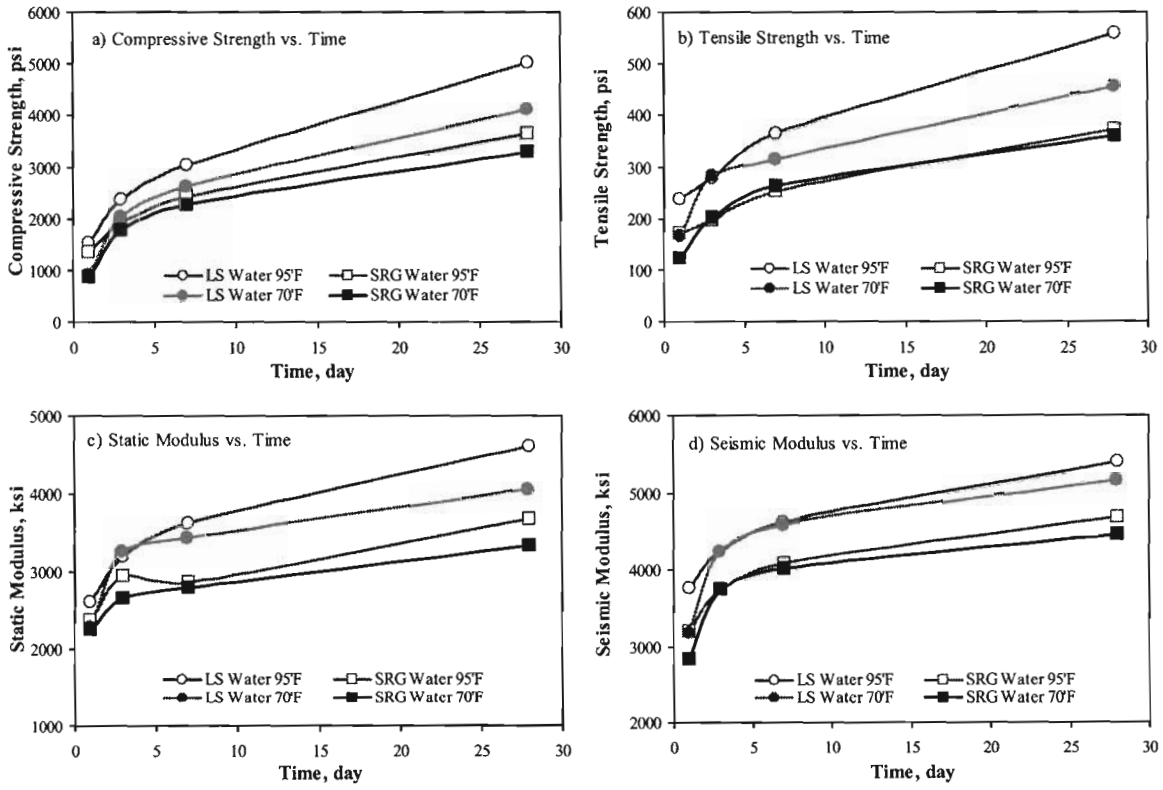

Figure 4.10 – Impact of Curing Temperature on Strengths and Moduli for Water-Cured Specimens

Figure 4.11 contains similar information to Figure 4.10 except that the curing was carried out outside a water tank. The relative humidity in the 70°F curing room was about 40% while for the 95°F curing room was about 20%. The variations in strength parameters with time are somewhat erratic at temperature of 95°F (see Figures 4.11a and 4.11b). The compressive strengths of specimens from the SRG mix cured at 95°F decrease after 7 days of curing, while the tensile strengths remain constant. Although the compressive strengths of the specimens from the LS mix cured at 95°F and 70°F are similar, the tensile strengths of the specimens cured at 95°F start to decrease after 7 days of curing. The static and seismic moduli are shown in Figures 4.11c and 4.11d, respectively. The static moduli are similar for both curing temperatures. Similar trends are apparent for the seismic moduli. However, the seismic moduli for specimens cured at 95°F are somewhat lower than those cured at 70°F.

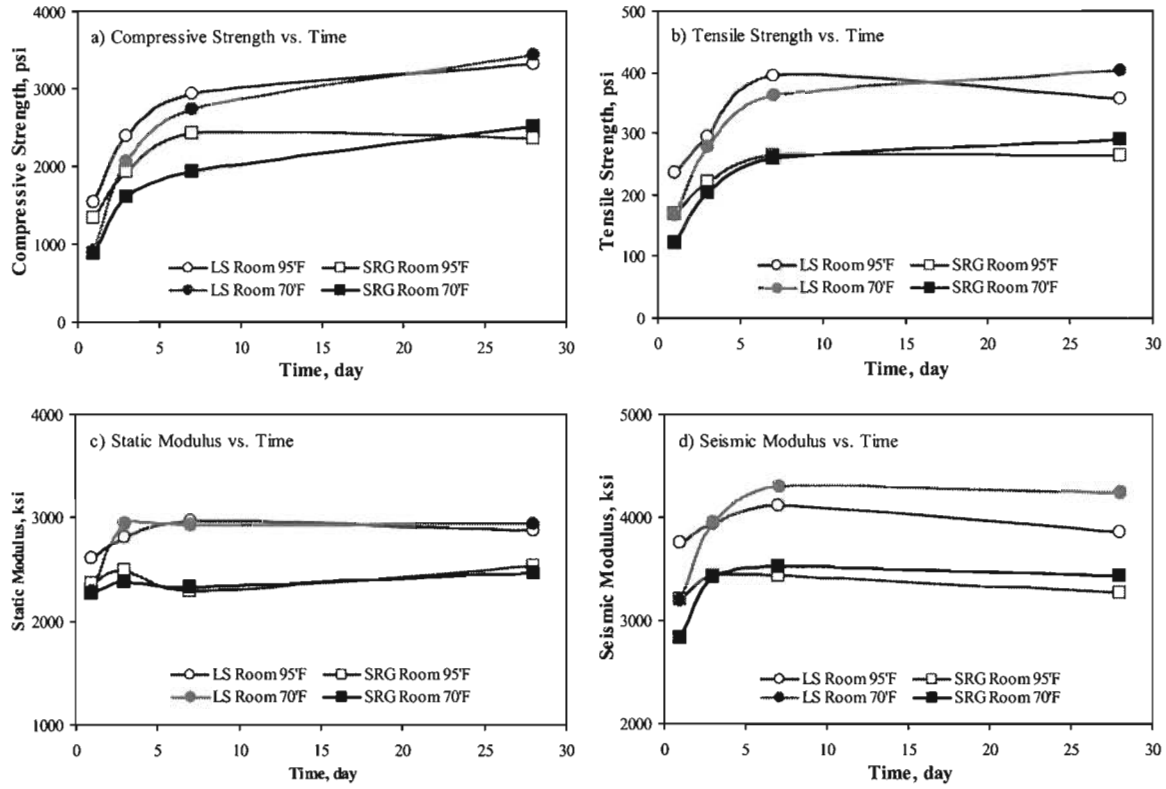

Figure 4.11 – Impact of Curing Temperature on Strengths and Moduli for Room-Cured Specimens

Impact of Curing at Different Humidity Levels

The variations in compressive strength, tensile strength, static modulus and seismic modulus of specimens cured at 70°F with time for the two types of aggregates when cured within and outside the water tank, which represents two relative humidity levels of 100% and 40%, respectively, are compared in Figure 4.12. For the LS aggregates, the compressive strengths are similar up to 7 days; however the 28-day strengths of the specimens cured in the tank are greater than those cured outside the tank. On the other hand, for the SRG aggregates, the compressive strengths are similar up to three days, after which, the specimens cured in water exhibit higher strength. In terms of tensile strength, again, the strengths are similar up to about 7 days. But the 28 day strengths of the water-cured specimens are greater than air-cured ones. It seems that the tensile strength seize to increase after 7 days for both mixtures. The seismic and static moduli of the water-cured specimens are significantly greater than the air-cured specimens for both aggregates.

Figure 4.13 contains the similar information as Figure 4.12 except that the curing temperature was 95°F and the relative humidity was 20% outside the water tank. Once again, up to about 7 days, the compressive strengths are similar for the water-cured and air-cured specimens for both types of aggregates. After 7 about days, the water-cured specimens are significantly stronger than the water-cured ones. The 28-day compressive strengths of air-cured specimens are somewhat lower than the 7-day strength as well. The tensile strengths follow the same patterns as the compressive strengths, as shown in Figure 4.13b. As for the specimens cured at 70°F, the static and seismic moduli are

consistently lower for air-cured specimens. In both cases, the 28-day moduli for air-cured specimens are lower than the 7-day ones.

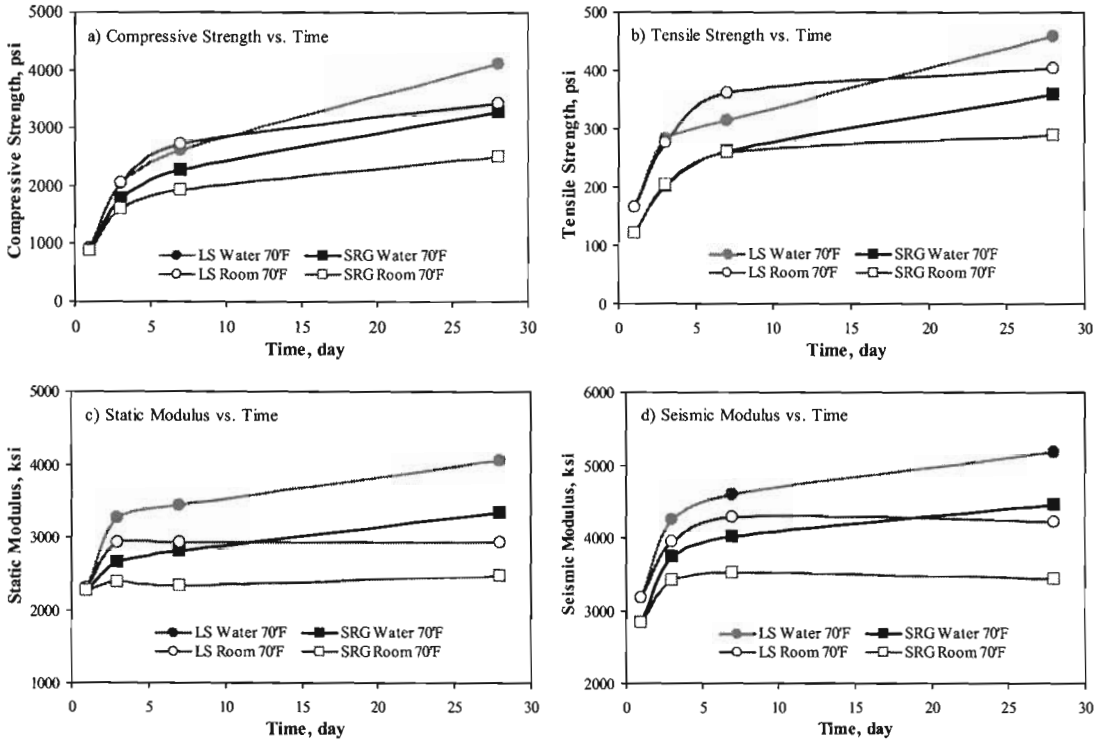

Figure 4.12 – Impact of Curing Humidity on Strengths and Moduli at Temperature of 70°F.

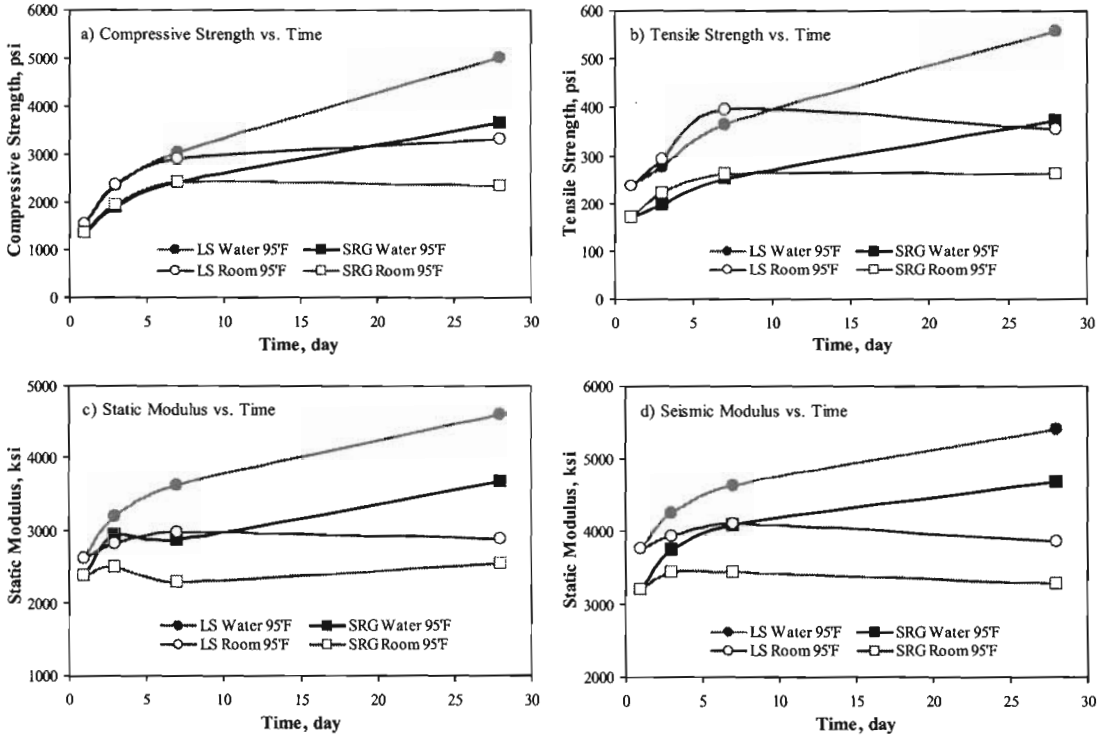

Figure 4.13 – Impact of Curing Humidity on Strengths and Moduli at Temperature of 95°F.

Chapter 5

Development of Global Relationships

The next step in this study was to develop appropriate relationships between the strength parameters and static modulus with the seismic modulus. Ideally, it is be desirable to develop a relationship for each particular mix. However, as a first approximation, it may be possible to develop more global relationships. We also attempted to develop more global relationships for the maturity concept. Since that aspect of the study was outside the scope of this report, the results are included in the appendices and not discussed any further here.

The development of the global relationships is followed through an example. We initiate the example by representing a typical calibration process for a mix. The variations in strength parameters and static modulus with respect to seismic modulus are shown in Figure 5.1 for a mixture made with limestone aggregates, fly ash and cured in a water tank at 70°F (21°C). As indicated in Chapters 2 and 3 (see Figure 3.7), the compressive strength, tensile strength and static modulus correlate well with seismic modulus. One obvious observation from these correlations is that the relationship between the compressive or tensile strength with seismic modulus is not linear. The relationship is somewhat bi-linear. At the very early ages (up to about 3 days) the increase in modulus is greater than the increase in strength; after which, the rate of increase in strength is greater than that of the modulus. For mathematical convenience we utilized a power equation instead of a bi-linear one. However, the relationship between the static and seismic modulus seems to be linear.

To extend the relationships further, the results from the specimens prepared with the same mix but when cured at 95°F (35°C) under water were combined with those cured under standard curing condition shown in Figure 5.1. The relationships obtained from this combination are exhibit in Figure 5.2. Once again, strong relationships can be detected between the three static mechanical properties and seismic modulus. The practical implication of such relationships is that the variation in curing temperature does not significantly impact the relationships developed for the standard-cured (100% humidity or so) specimens.

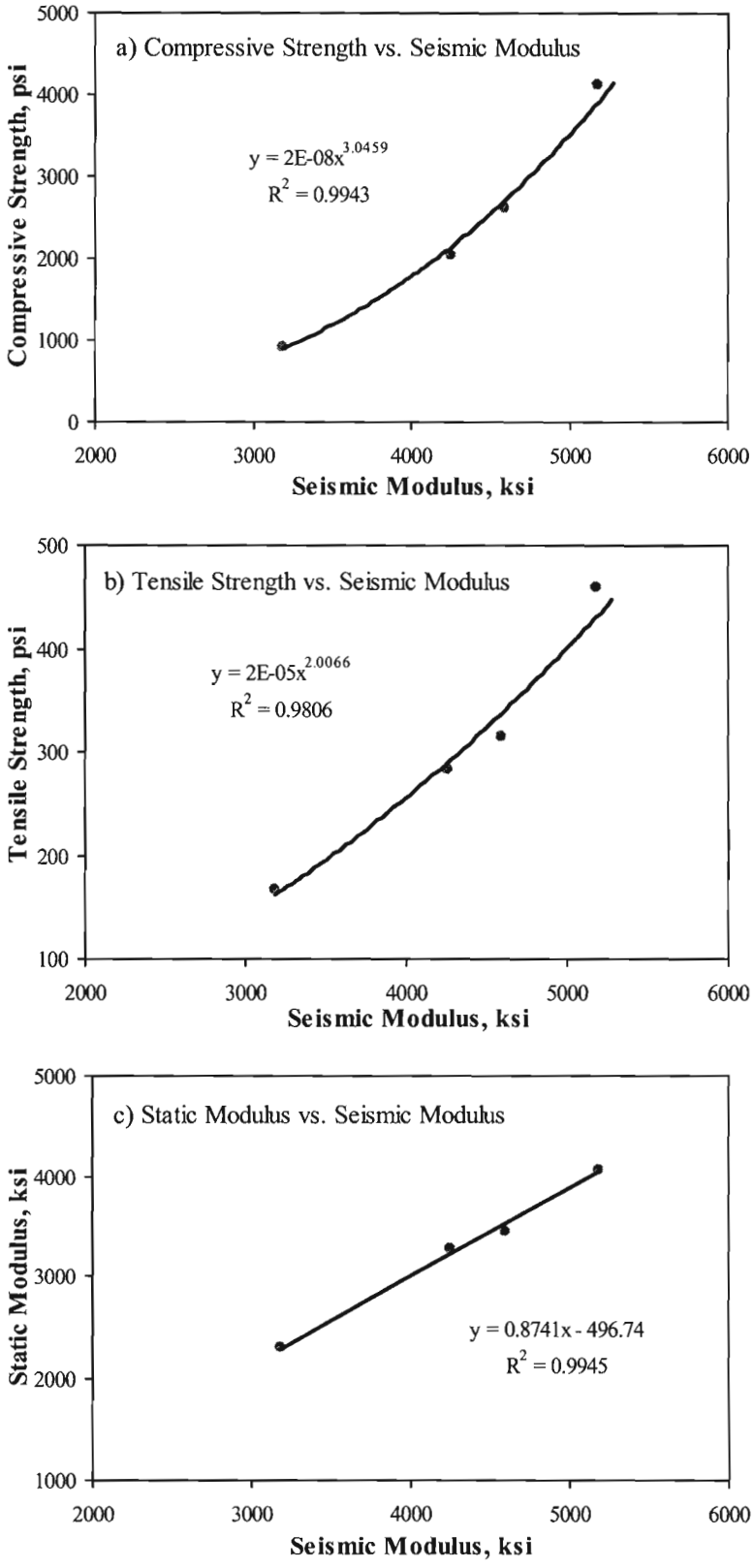

Figure 5.1 – Variations in Strength Parameters and Static Modulus with Seismic Modulus for a Standard LS Mix under Standard Curing Condition (70°F)

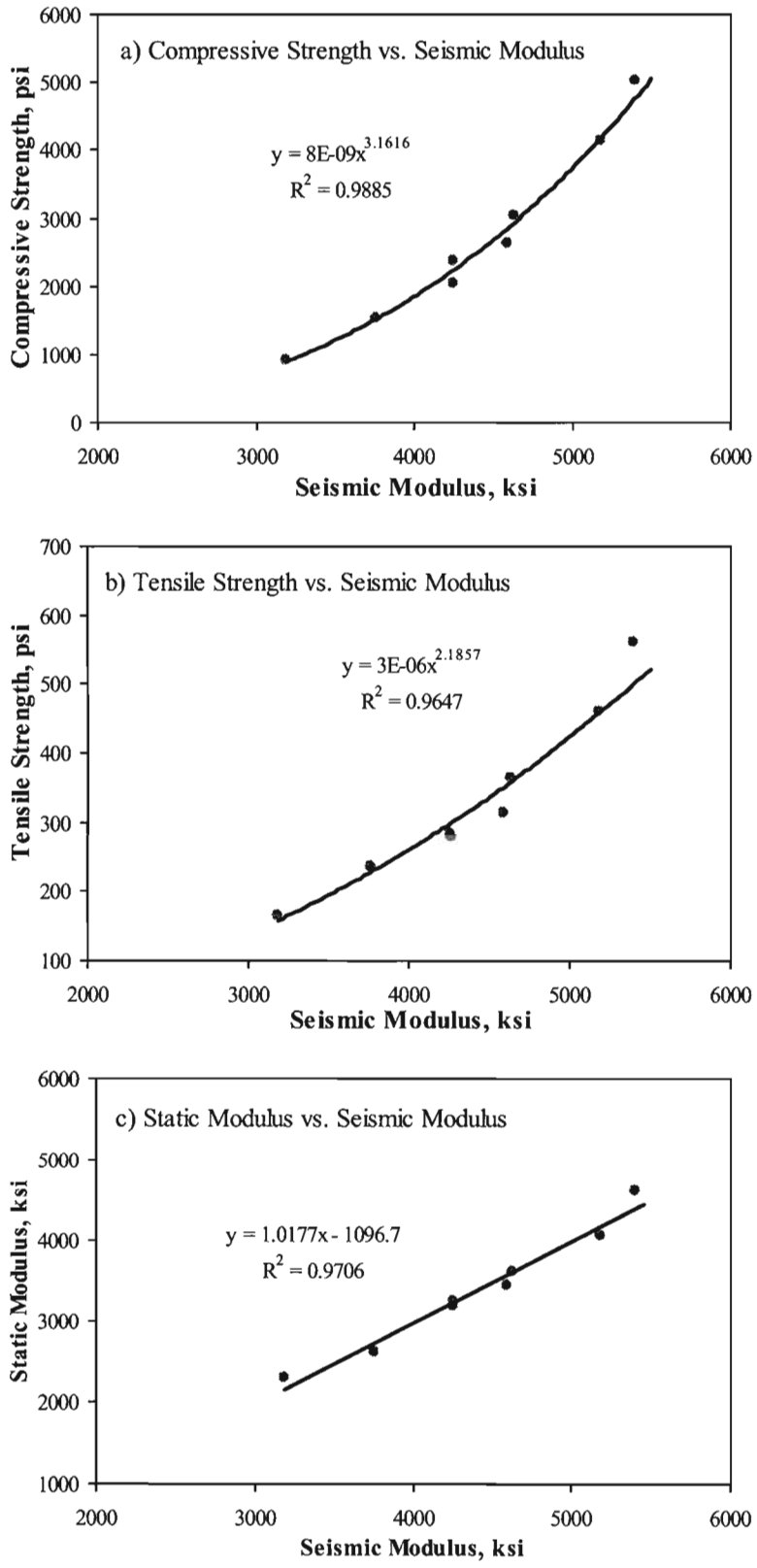

Figure 5.2 – Variations in Strength Parameters and Static Modulus with Seismic Modulus for a Standard LS Mix Water-Cured at 70°F and 95°F

To further expand the relationships, results from specimens of the same mix but cured outside in a sand bed were added to the data. These specimens were covered with a thick layer of curing compound before they were buried in the sand bed. As shown in Figure 5.3, the results are still consistent by comparing the fitting equations with those provided in Figure 5.2. This means that the daily temperature fluctuations encountered during actual field projects do not significantly impact the static mechanical properties vs. seismic modulus relationships developed under the standard curing condition.

In the next step we combined the results from two limestone mixes, the standard, which has 30% by weight of fly ash and one with pure cement. The results from these combinations are shown in Figure 5.4. A visual comparison of Figures 5.3 and 5.4 indicates that there are some differences in the trends between the mixes with and without fly ash. The differences also result in considerable drops of the R^2 values for the combined relationships for two strength parameters. The practical implication of this finding is that fly ash may somewhat impact the validity of the calibration curves developed from the lab-cured specimens of the standard mix for LS coarse aggregates.

Since ensuring clean aggregates throughout a job site is difficult, the impact of combining the mixes with the dirty and clean aggregates on the developed relationships was studied. The results from all mixes made with clean and dirty aggregates, with and without fly ash, cured in water at different temperatures and cured in the field conditions are combined in Figure 5.5. As shown in Figure 4.6, clay coating on the coarse aggregates reduces the compressive and tensile strengths as well as the static and seismic moduli. However, the relationships between the compressive strength with seismic modulus, tensile strength with seismic modulus and static modulus with seismic modulus do not significantly deviate from the corresponding relationships developed for the standard mix cured under the standard condition. Comparing the best fit equations for the two strength parameters shown in Figure 5.5 with those shown in Figures 5.3 and 5.4 indicates that the combined relationships deviate from the standard ones. In other words, it may require a different lab-calibration curve or an adjusting factor for the mixes with dirty LS coarse aggregates.

Finally, we have tried to develop global relationships using all data collected on the four mixes with the limestone aggregates and cured in different environments. When the data from the specimens cured under conditions without adequate humidity levels (room or dry-cured) were considered, the relationships between two strength parameters and seismic modulus became much less prominent (see Figure 5.6). As indicated before, under the dry-cured condition, as soon as the specimens became water starved, the gain in strength and modulus seized. Significant scatter in the data was also observed that can partially be described by the repeatability inherent in each test method.

The relationships between the compressive strength and seismic modulus for the five different scenarios demonstrated in Figures 5.2a to 5.6a are compared in Figure 5.7. Also shown in the figure is the most appropriate global relationship that should be used in the absence of a mixed-specific calibration for this coarse aggregate type. The mix with pure cement, water-cured at 70^{O}F, seems to be the best representative of the compressive strength-seismic modulus relationships. This representative relationship seems to be a reasonable representation of all mixes above a seismic modulus of 4500 ksi as all relationships are bound by the 10% error band. Below a seismic modulus of 4500 ksi, the data from the dry curing condition, especially from the dirty aggregates, seem to yield higher strengths that predicted by the recommended global relationships. On the

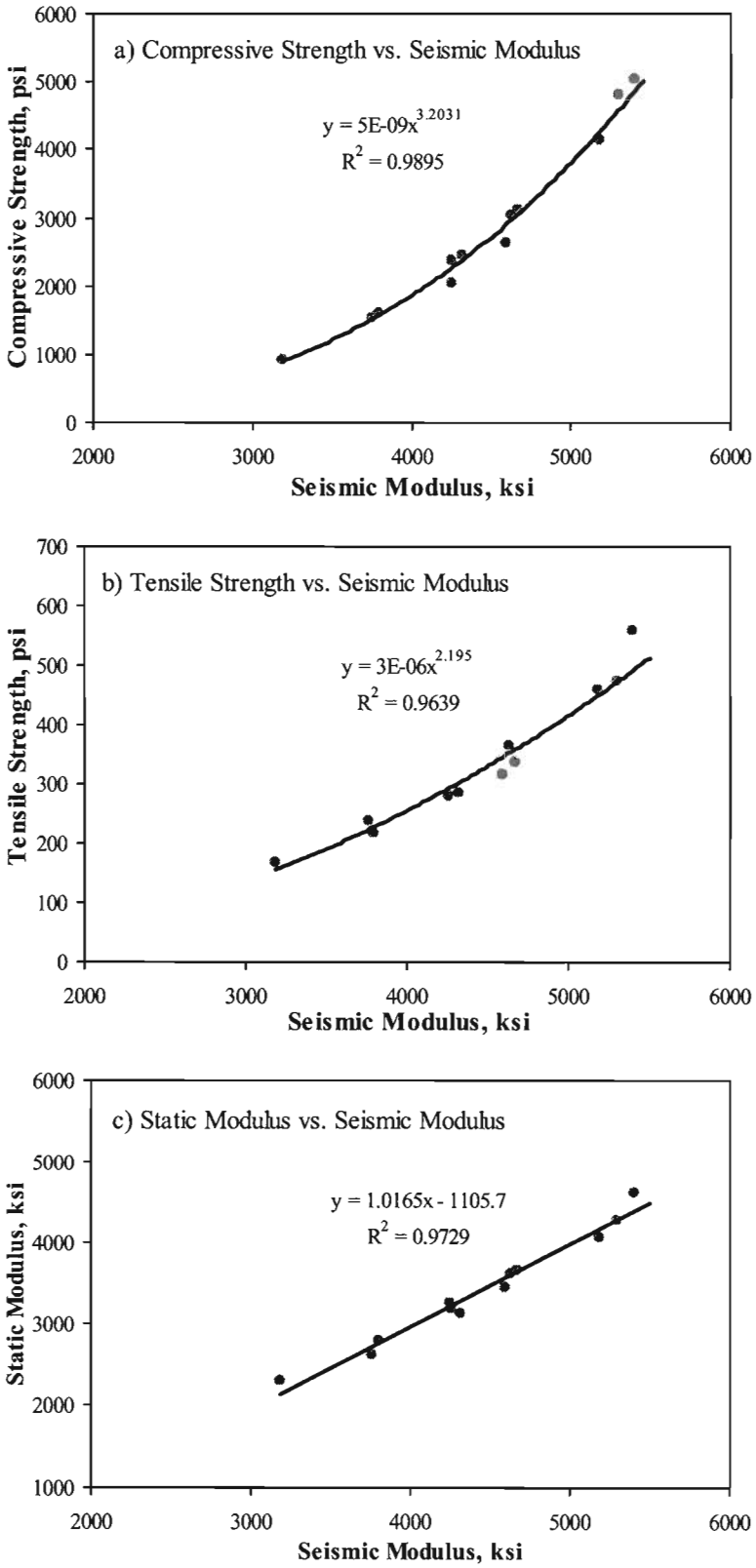

Figure 5.3 – Variations in Strength Parameters and Static Modulus with Seismic Modulus for a Standard LS Mix Water-Cured at 70°F and 95°F and Field-Cured

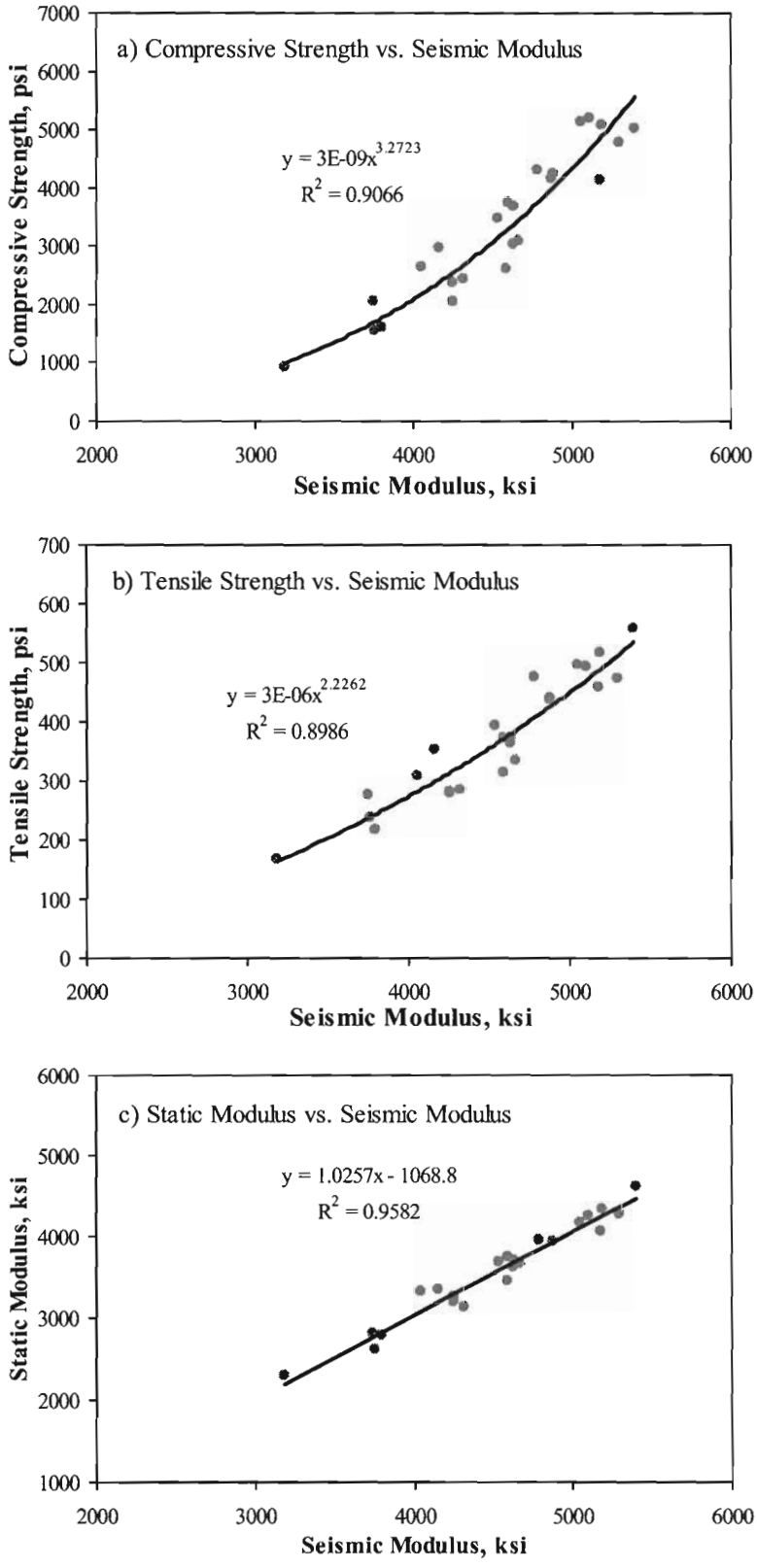

Figure 5.4 – Variations in Strength Parameters and Static Modulus with Seismic Modulus for LS Mixes with and without Fly Ash, Water-Cured at 70°F and 95°F and Field-Cured

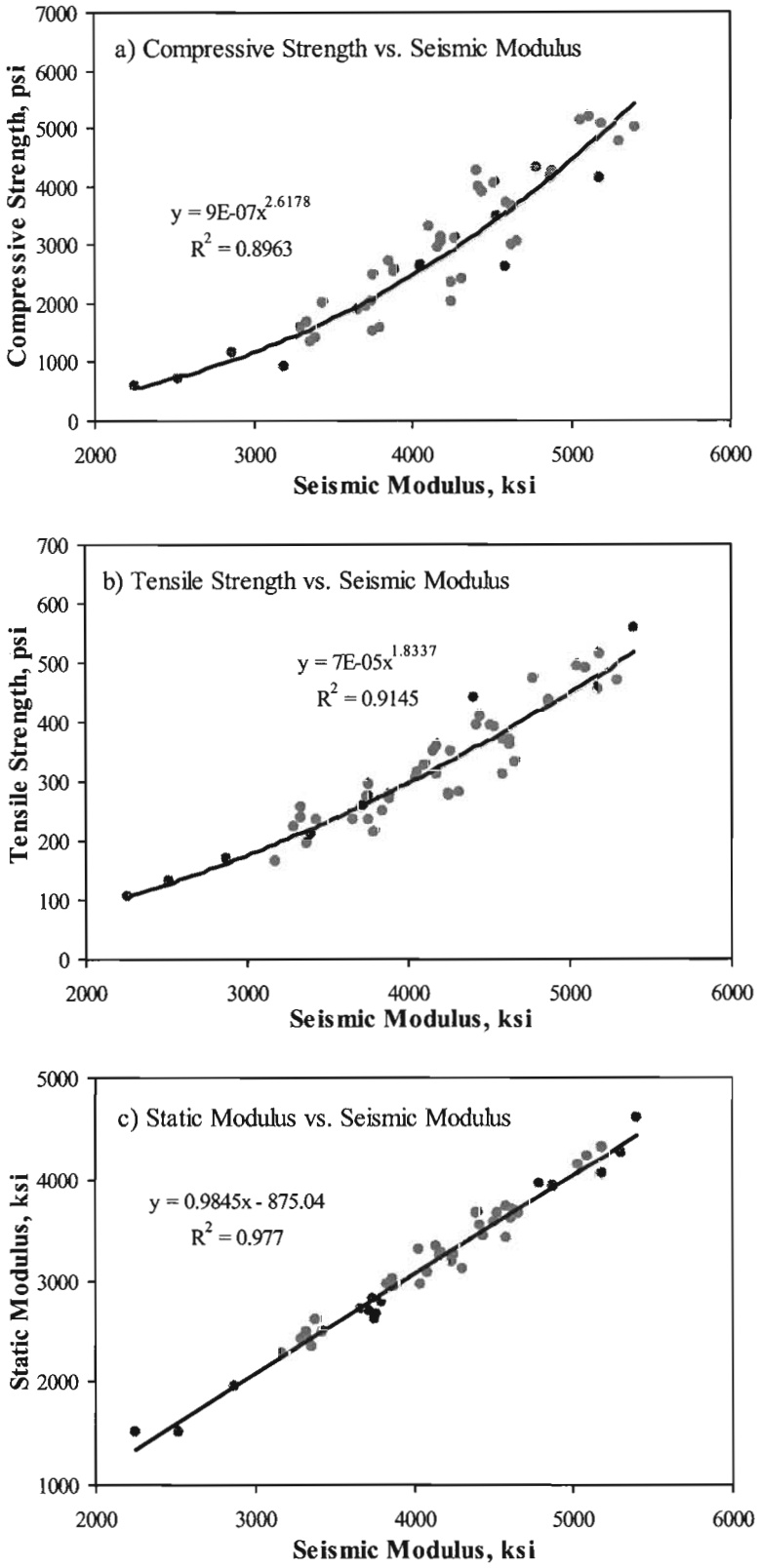

Figure 5.5 – Variations in Strength Parameters and Static Modulus with Seismic Modulus for all LS Mixes Water-Cured at 70°F and 95°F and Field-Cured

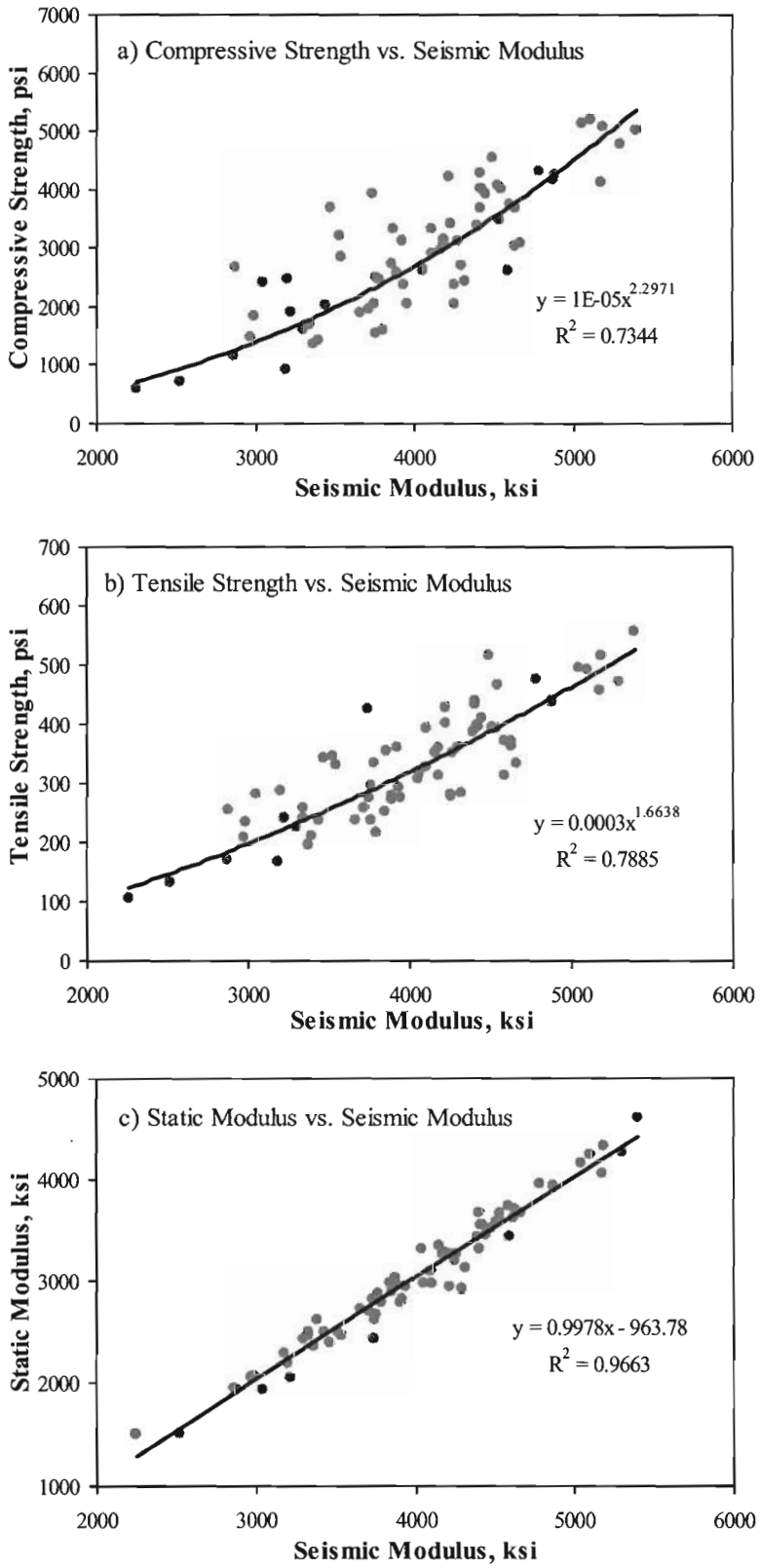

Figure 5.6 – Variations in Strength Parameters and Static Modulus with Seismic Modulus for all LS Mixes and all Curing Conditions

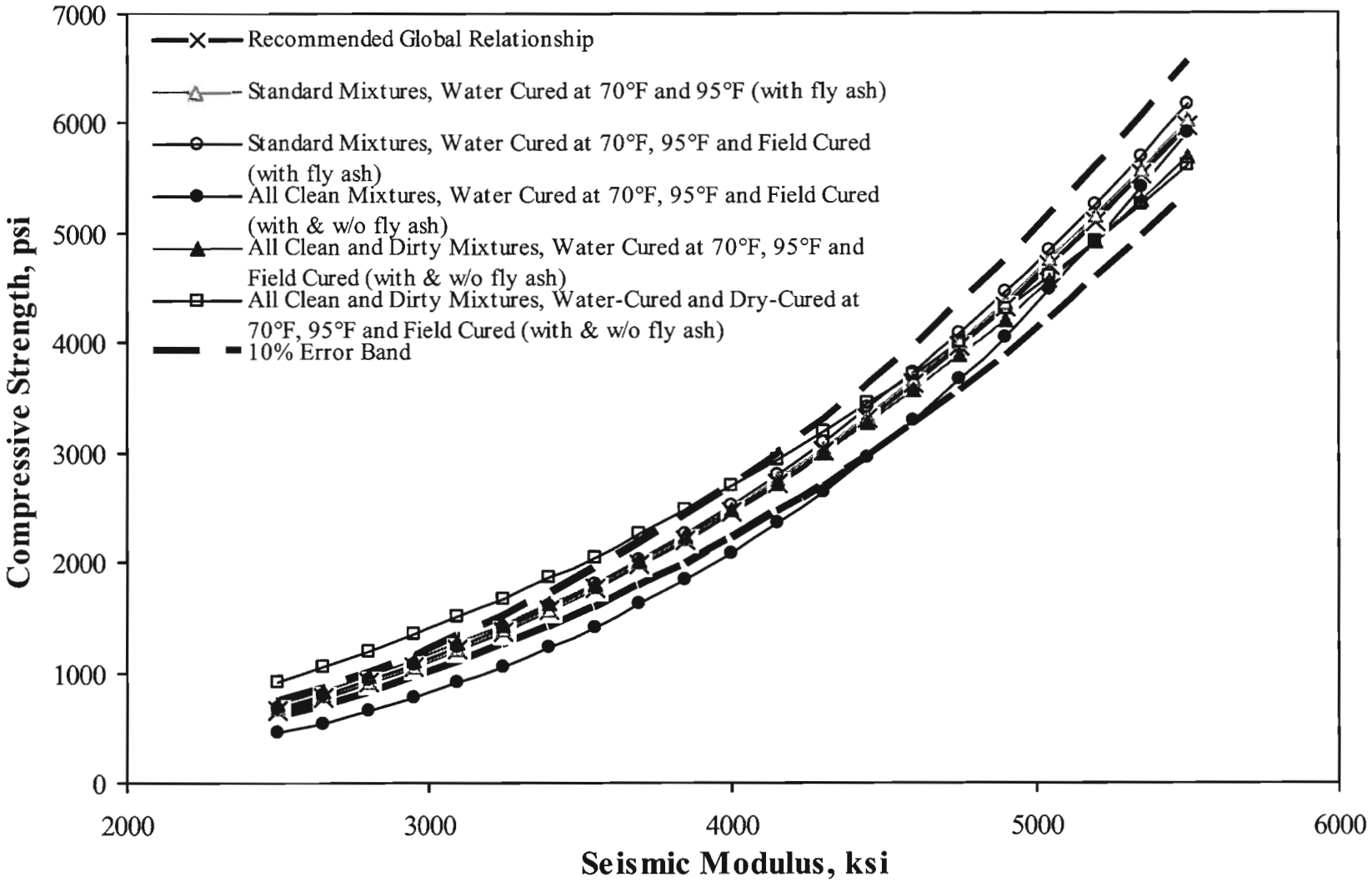

Figure 5.7 – Comparison of all Relationships Developed between Compressive Strength and Seismic Modulus for Different LS Mixes and Different Curing Regimens

other hand, when the mixes with and without fly ash are combined and the wet curing at 95 ^{O}F are considered, the prediction of the strength from the recommended global curve is unconservative at early ages (below a modulus of 4500 ksi).

The relationships between the tensile strength and the seismic modulus for the five different scenarios demonstrated in Figures 5.2b to 5.6b are compared with the recommended global relationships developed from the mix with pure cement, cured under the standard condition, in Figure 5.8. Again, the recommended global relationship appears to be a reasonable representation of all mixtures considered. In consonance with the situation for compressive strength, for a given seismic modulus, the mix with dirty aggregates, dry-cured, demonstrates a higher tensile strength than that with the clean aggregates, and the relationship from mixes with and without fly ash and wet cured at 95^{O}F are unconservative at early ages.

The relationships between the static modulus and the seismic modulus for the five different scenarios demonstrated in Figures 5.2c to 5.6c are compared with the recommended global relationship in Figure 5.9. When compared to the relationships between the seismic modulus and two strength parameters, the relationship for the static modulus vs. the seismic modulus is a strong representation of all five conditions.

We continue by developing a separate global relationship representing a more complex calibration process that will adjust for variables such as the coarse aggregate factor, water reducer amount and using ground-granulated blast furnace slag for mixes with the siliceous river gravel aggregates

The variations in strength parameters and static modulus with respect to seismic modulus are shown in Figure 5.10 for a mix made with the SRG aggregates and 30% fly ash cured in a water tank at 70^{o}F (21°C). As with the LS aggregates, all three relationships are well correlated.

For the sake of brevity, the other individual relationships for the SRG aggregates are not shown here since they are similar to those from the LS aggregate and included in Appendix C. The relationships for all SRG specimens prepared with clean and dirty aggregates, with and without fly ash and cured in water at different temperatures as well as under field conditions are included in Figure 5.11. As with the LS mixes, these global relationships seem to be good approximations for the mix at hand. As emphasized in Chapter 4, even though the trends for the mixes with SRG aggregates and with LS aggregates are similar, the two global relationships are different. The type of coarse aggregate seems to be the most influential factor in developing the global relationships.

When all five different curing conditions (water-curing and dry-curing at two temperatures as well as field-curing) are considered (see Figure 5.12), the results demonstrate more scatter and the relationships between the compressive or tensile strength and seismic modulus are not as strong as when dry-curing was excluded. These trends are similar to those from the LS aggregates specimens (see Figure 5.6).

.

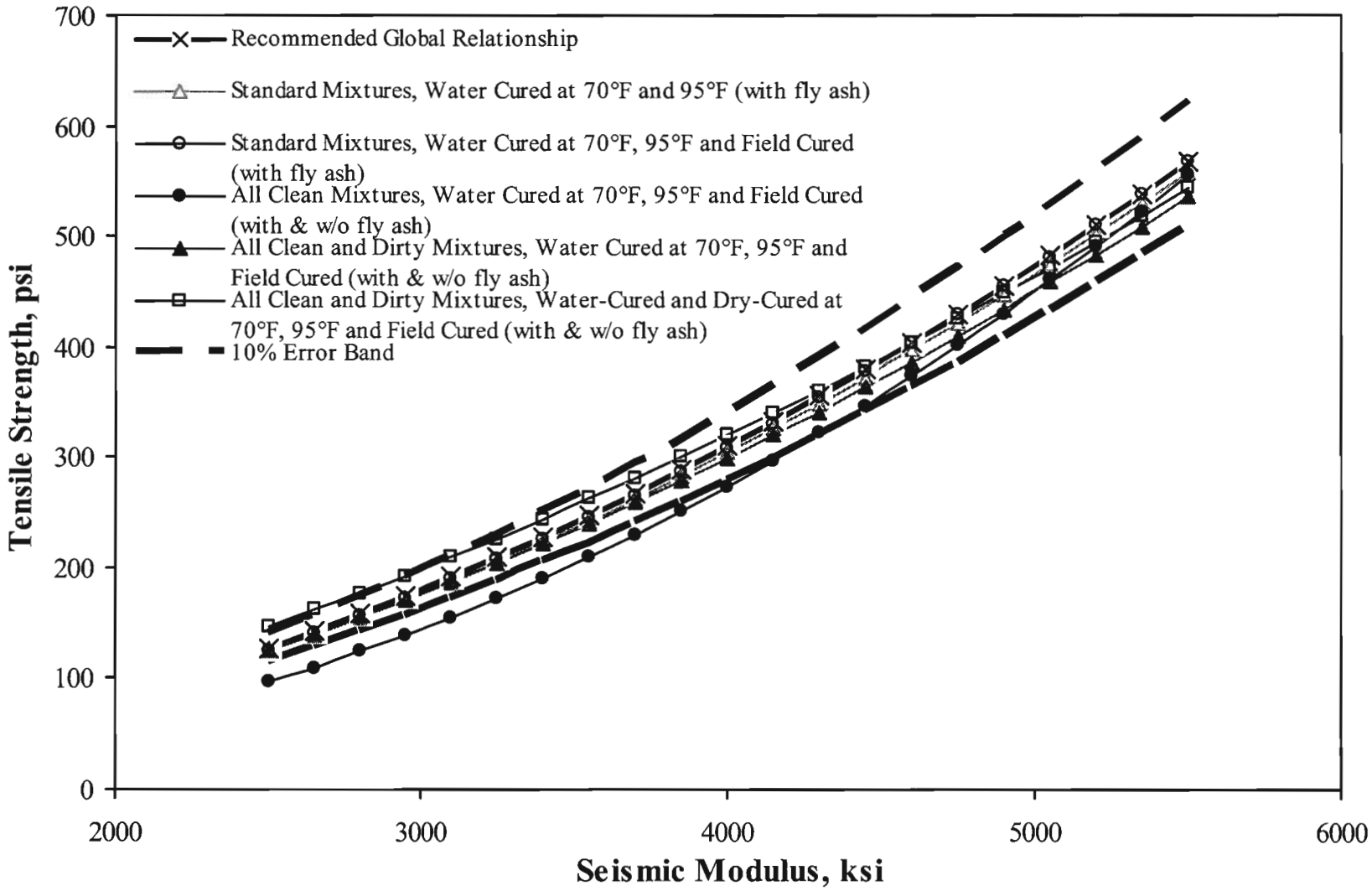

Figure 5.8 – Comparison of all Relationships Developed between Tensile Strength and Seismic Modulus for Different LS Mixes and Different Curing Regimens

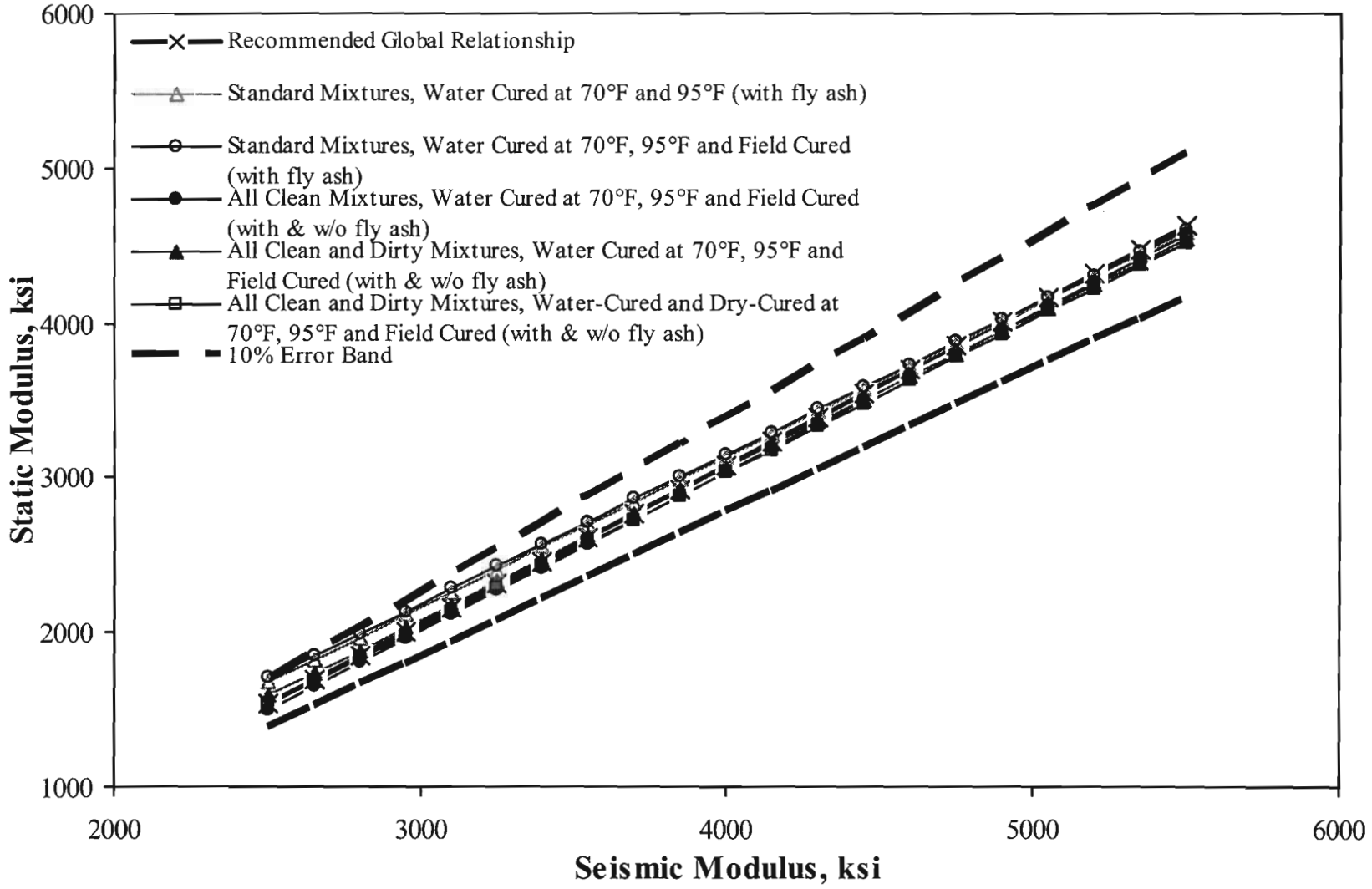

Figure 5.9 – Comparison of all Relationships Developed between Static Modulus and Seismic Modulus for Different LS Mixes and Different Curing Regimens

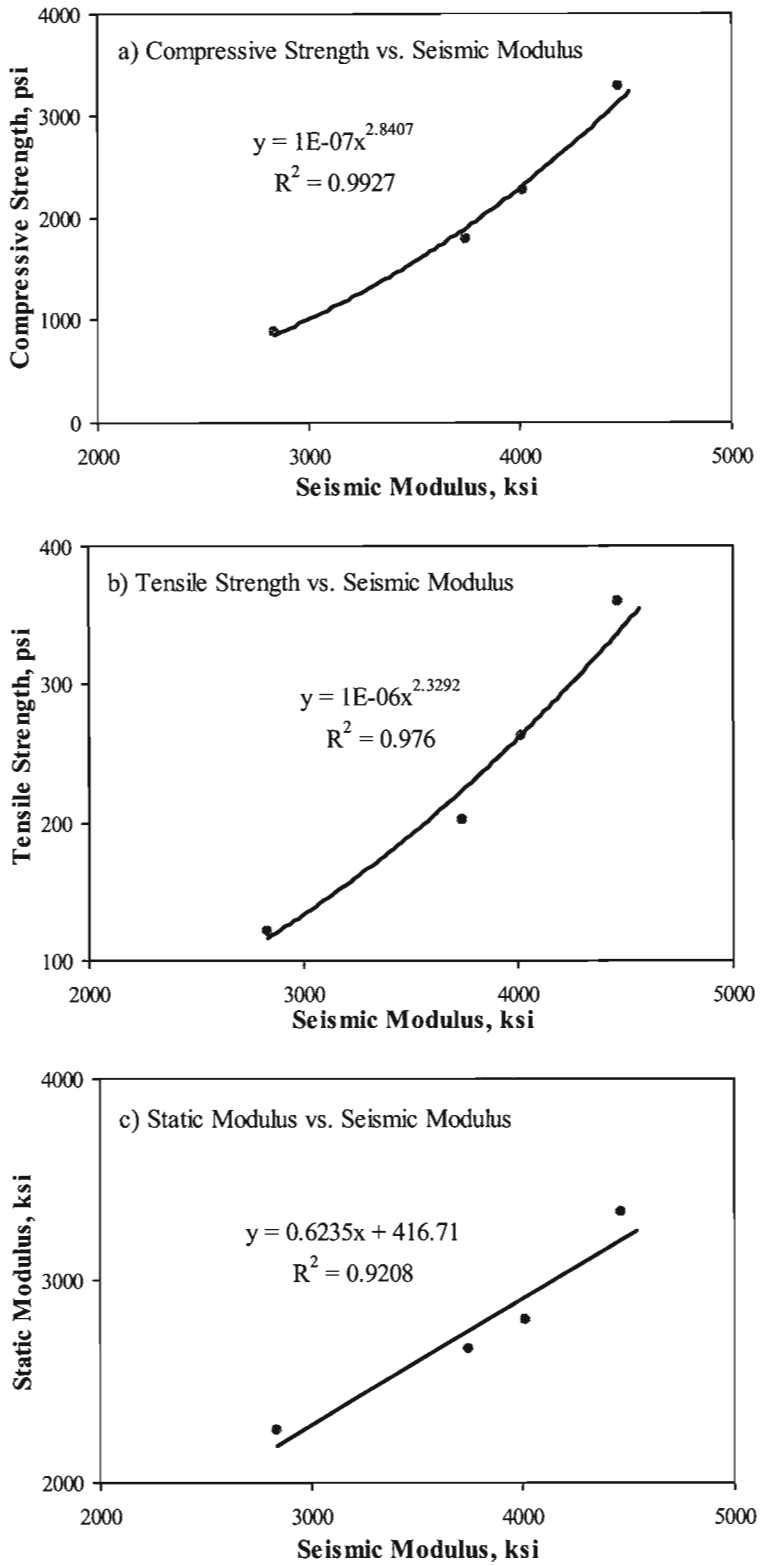

Figure 5.10 – Variations in Strength Parameters and Static Modulus with Seismic Modulus for a Standard SRG Mix Cured under Standard Condition (70°F)

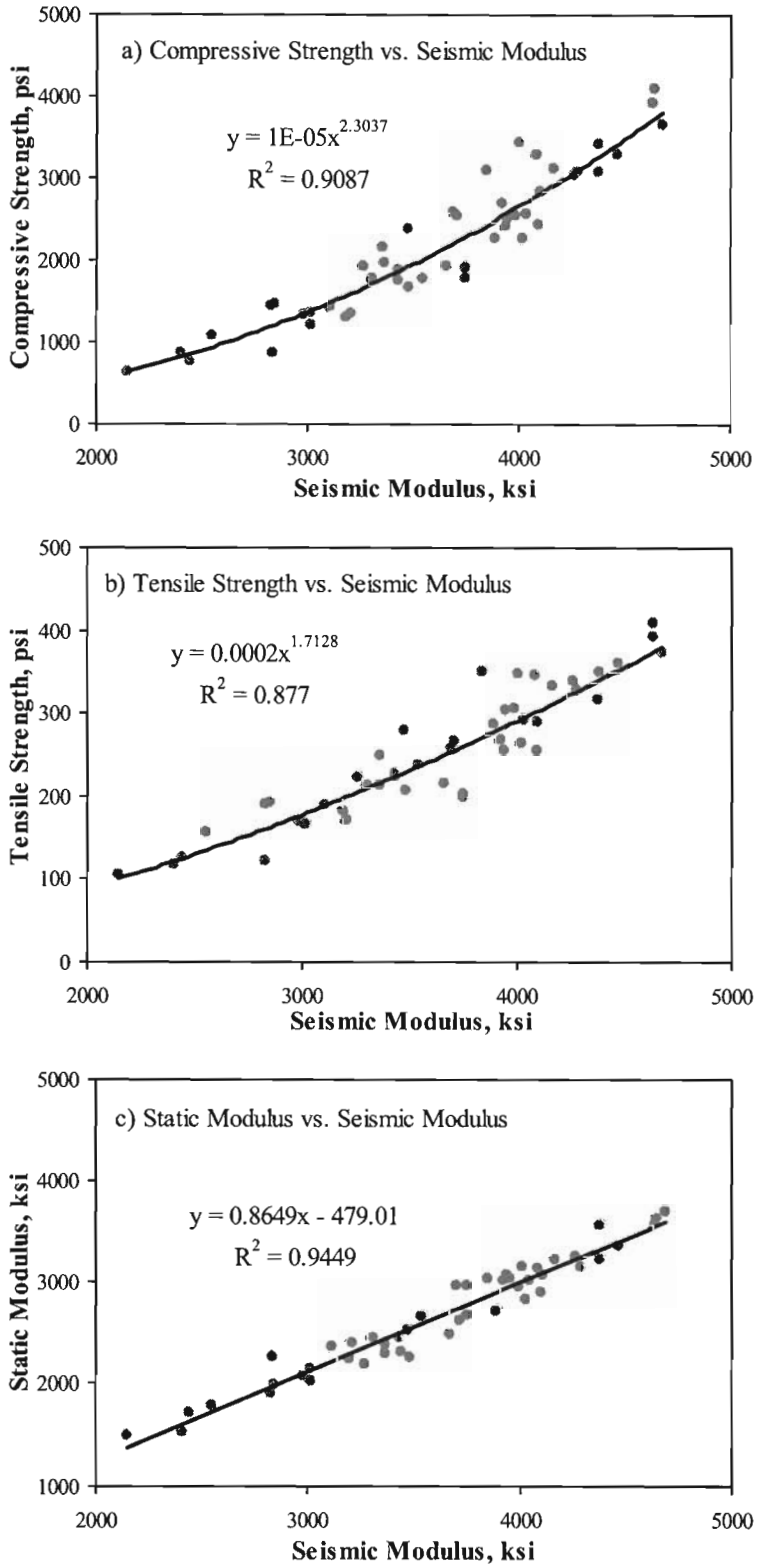

Figure 5.11 – Variations in Strength Parameters and Static Modulus with Seismic Modulus for all Phase-I SRG Mixes Water-Cured in at 70°F, 95°F and Field-Cured

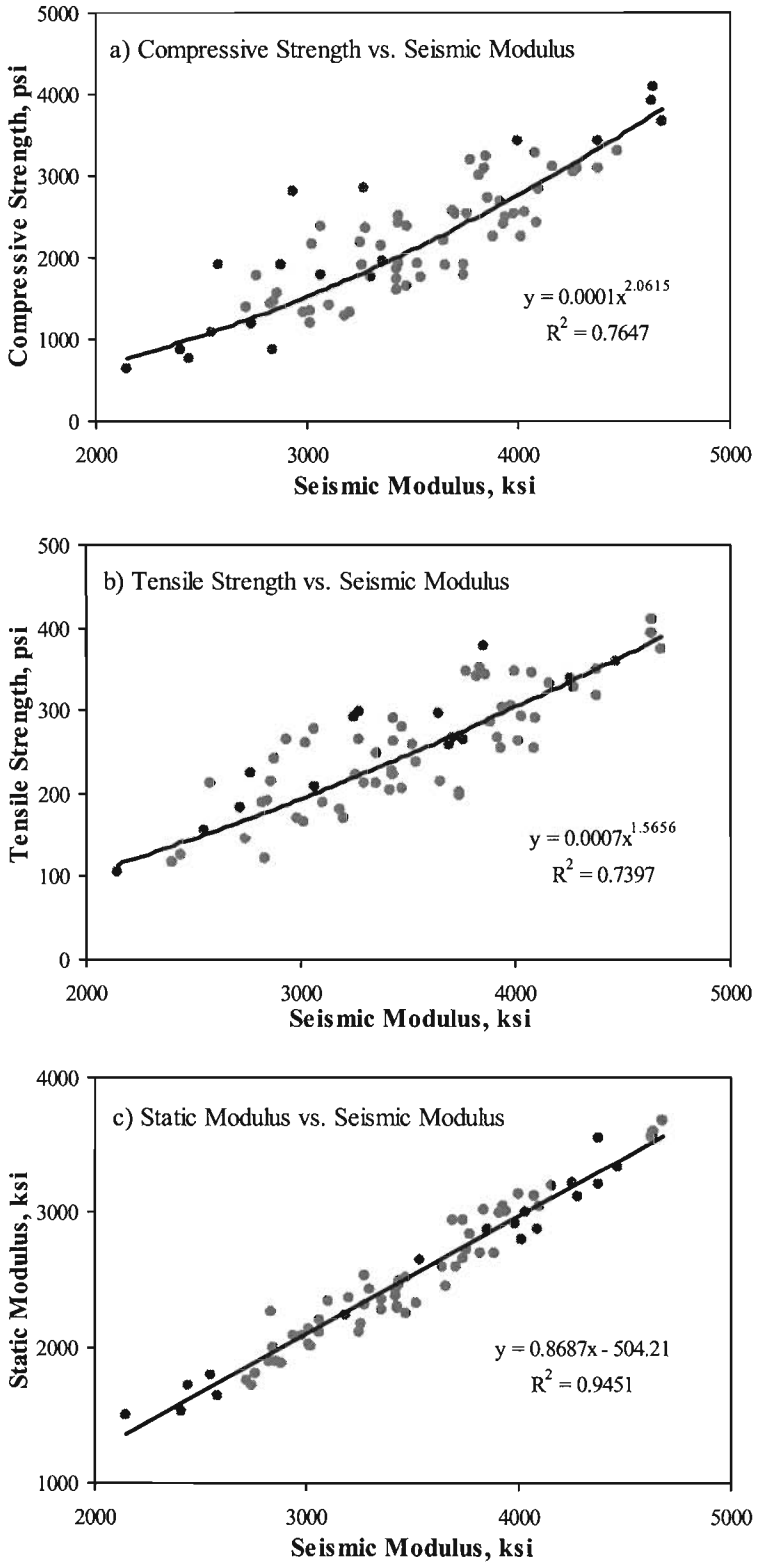

Figure 5.12 – Variations in Strength Parameters and Static Modulus with Seismic Modulus for all Phase-I SRG Mixes and all Curing Conditions

The coarse aggregate factor, water reducing admixtures and ground-granulated blast furnace slag were the variables studied in Phase II. When the results from these parameters are added to the global relationships shown in Figure 5.11, the relationships as shown in Figure 5.13 are obtained. The relationships for the compressive strength, tensile strength and static modulus with seismic modulus remain virtually the same as those shown in Figure 5.11 for the results from the Phase-I study.

The relationships between the compressive strength and seismic modulus for different scenarios are compared with the recommended global relationship in Figure 5.14. Once again, the mixture with pure cement, water-cured at 70°F, is recommended to represent the global relationship. The global relationship seems to be a reasonable representation of all mixtures. Once again, the mix with dirty aggregates, dry-cured, demonstrates a higher strength than that with the clean aggregates, and the relationship from mixes with and without fly ash and wet cured at 95°F are unconservative at early ages. However, these differences are less pronounced when compared to the LS mixtures (Figure 5.7).

The relationships between the tensile strength to seismic modulus for different scenarios are compared with the recommended global relationship in Figure 5.15. Again, the standard relationship appears to be a reasonable representation of all other conditions with the dirty mixes at lower seismic moduli demonstrating higher strengths than the recommended global relationship.

The relationships between the static modulus and seismic modulus for the different scenarios are compared with the recommended global relationship in Figure 5.16. The recommended global relationship seems to be a reasonable representation of all other conditions as judged by almost all relationships falling between the 10% error bands.

Statistical Analysis on the Different Test Parameters

The coefficient of variation (COV) is a statistical and dimensionless representation of measurement scattering (random error) and thus a good tool to evaluate the precision of a particular test performed on concrete specimens. The uncertainty in the measured parameters being correlated directly impacts the uncertainty of the relationships developed between these parameters. The precision with which a parameter (say tensile strength) is estimated from another parameter (say seismic modulus) cannot be better than the lower one in precision of the measurements on either parameter.

In this study, the average COV's obtained from all replicate tests performed to obtain the strengths and moduli for different coarse aggregates are shown in Figure 5.17. The COV's shown in the figure are the averages of all tests performed after 1 day, 3 days, 7 days and 28 days. The most precise test is the seismic test with an average COV of 1.5%. The static modulus and compressive strength tests yield similar COV's of about 3%. The least uncertain test is the splitting tensile with an average COV of about 6%. It should be mentioned that all mechanical tests were performed with an advanced Instron-Satec System.

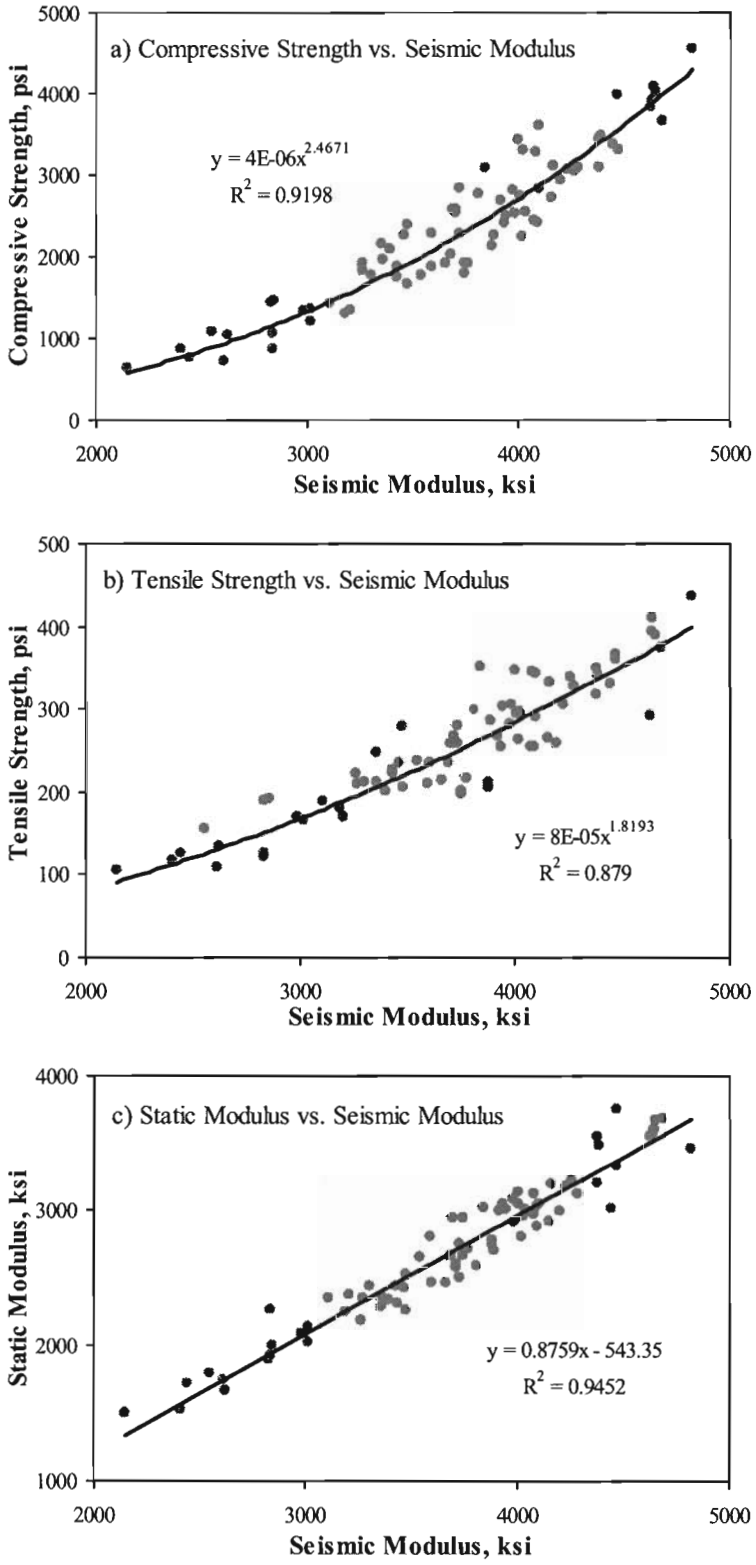

Figure 5.13 – Variations in Strength Parameters and Static Modulus with Seismic Modulus for all SRG Mixes Water-Cured at 70°F, 95°F and Field-Cured

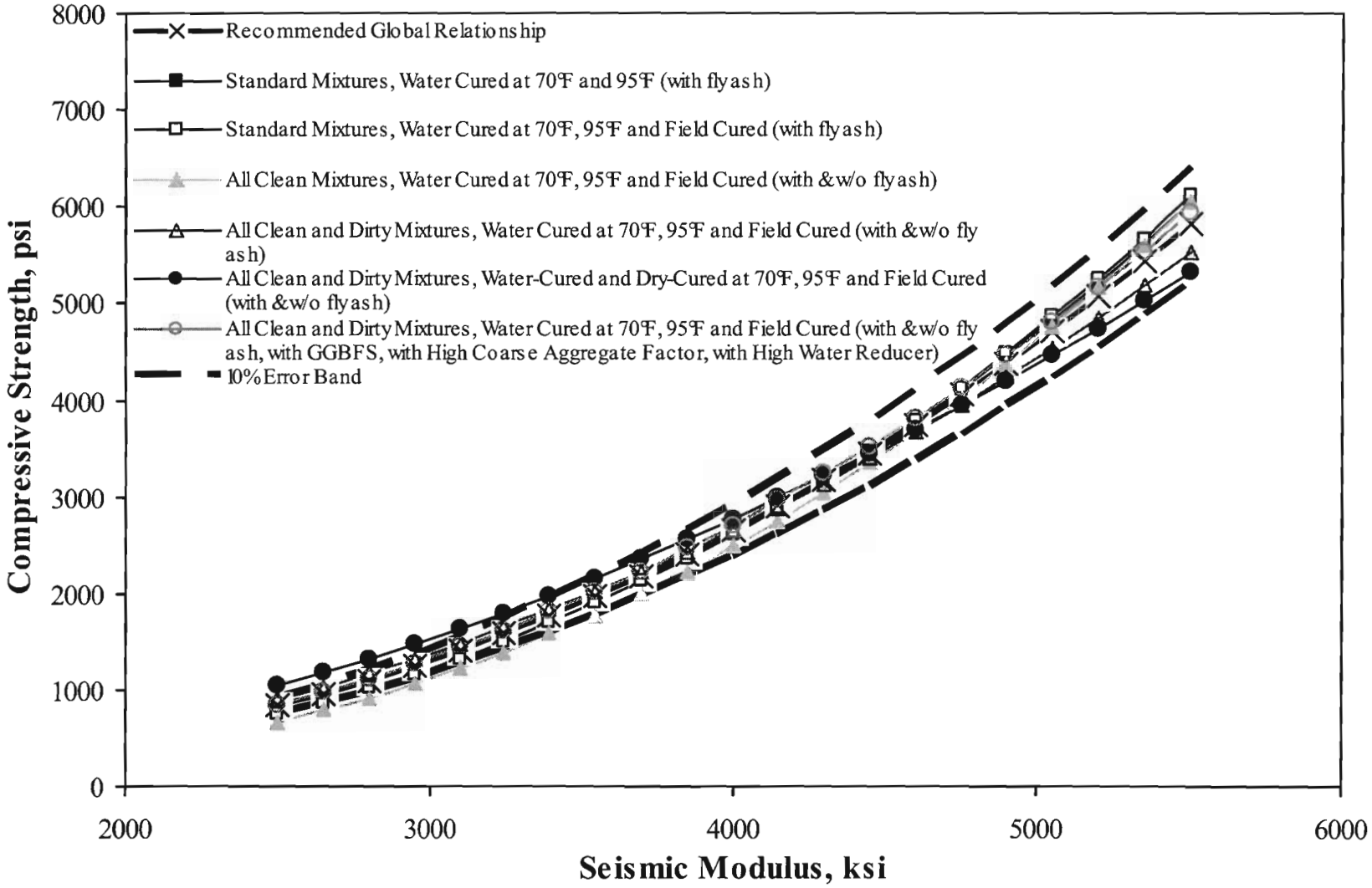

Figure 5.14 – Comparison of all Relationships Developed between Compressive Strength and Seismic Modulus for Different SRG Mixes and Different Curing Regimens

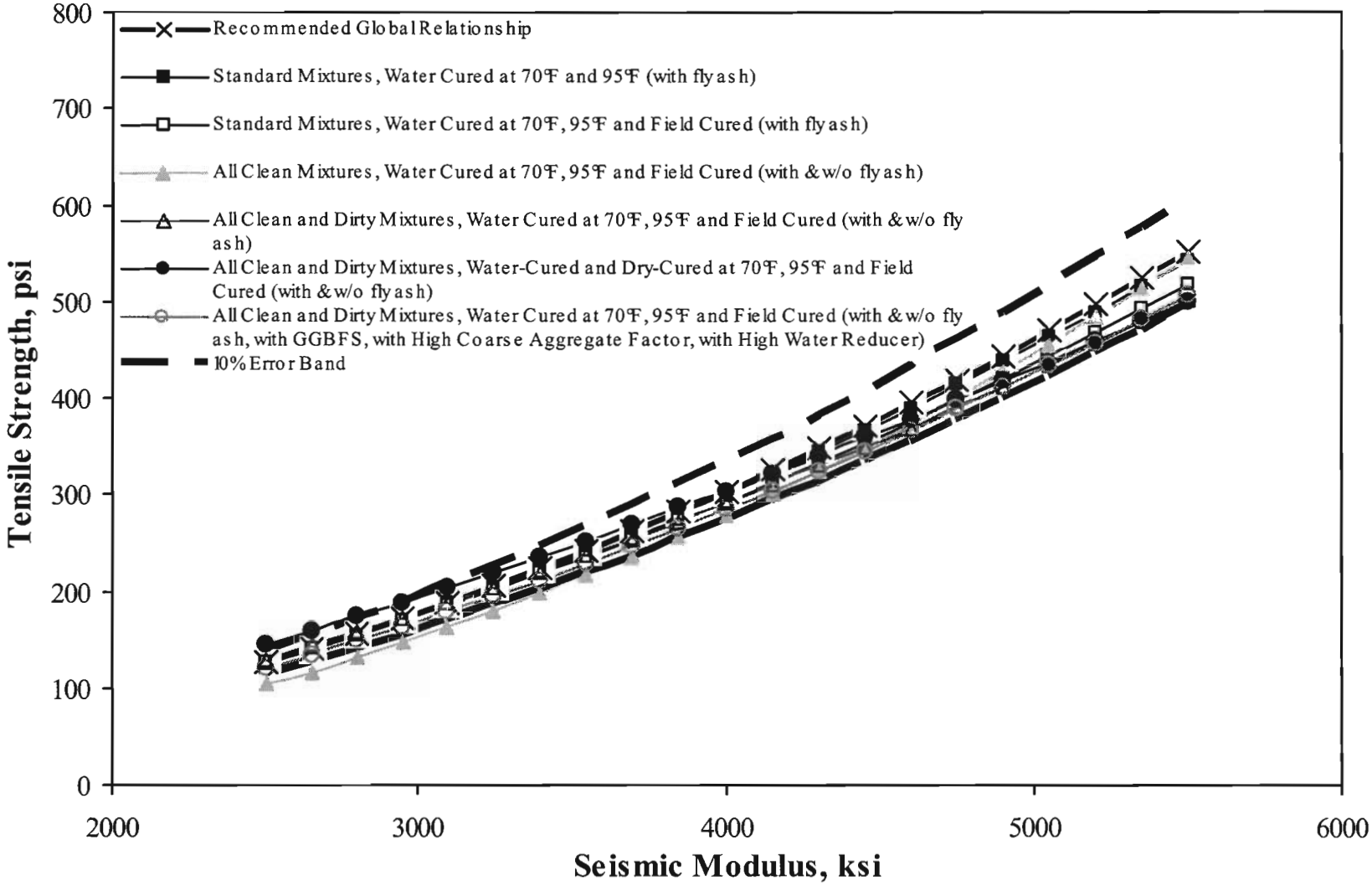

Figure 5.15 – Comparison of all Relationships Developed between Tensile Strength and Seismic Modulus for Different SRG Mixes and Different Curing Regimens

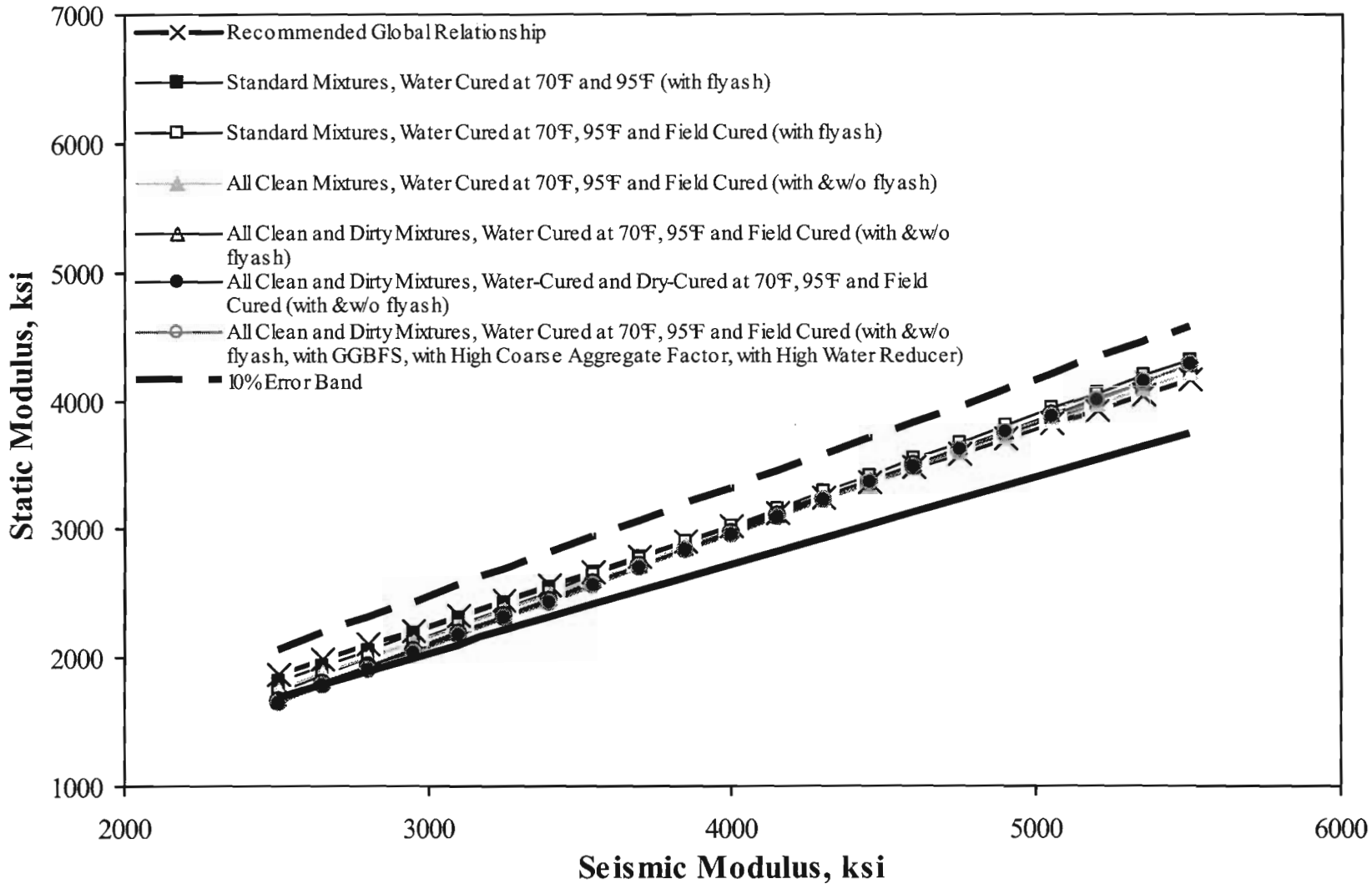

Figure 5.16 – Comparison of all Relationships Developed between Static Modulus and Seismic Modulus for Different SRG Mixes and Different Curing Regimens

A more comprehensive means of describing the uncertainty is the cumulative distribution of the COV's. Figure 5.18 contains such information from this study. For seismic modulus, static modulus, compressive strength and tensile strength, the COV's are 90% of the time less than 2%, 8%, 6% and 12%, respectively. Based on these values, it is not a surprise that the compressive strength vs. seismic modulus is better correlated than the tensile strength vs. seismic modulus. This matter should be considered when the acceptance levels are set on the basis of a particular parameter.

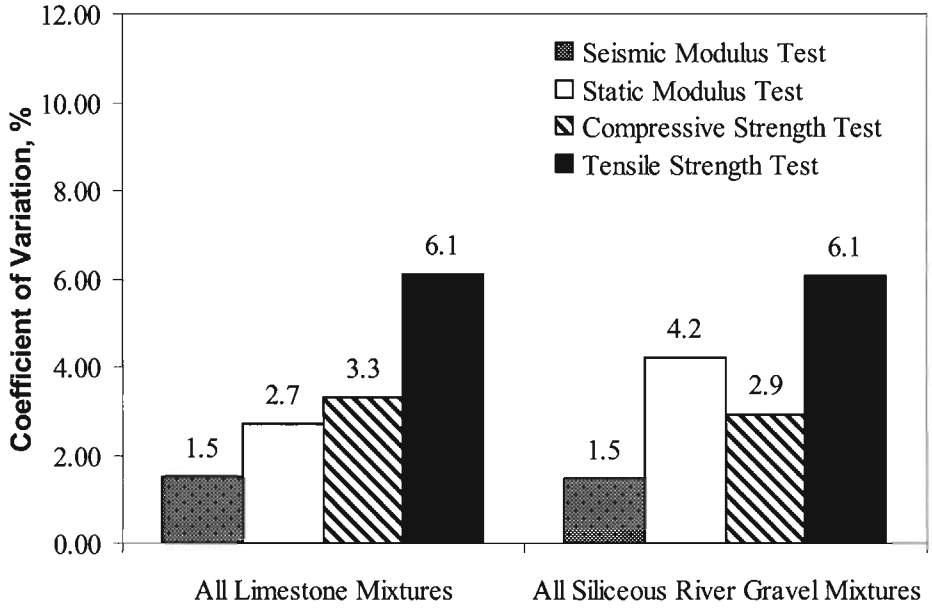

Figure 5.17 – Coefficients of Variation of Tests Performed on all Specimens

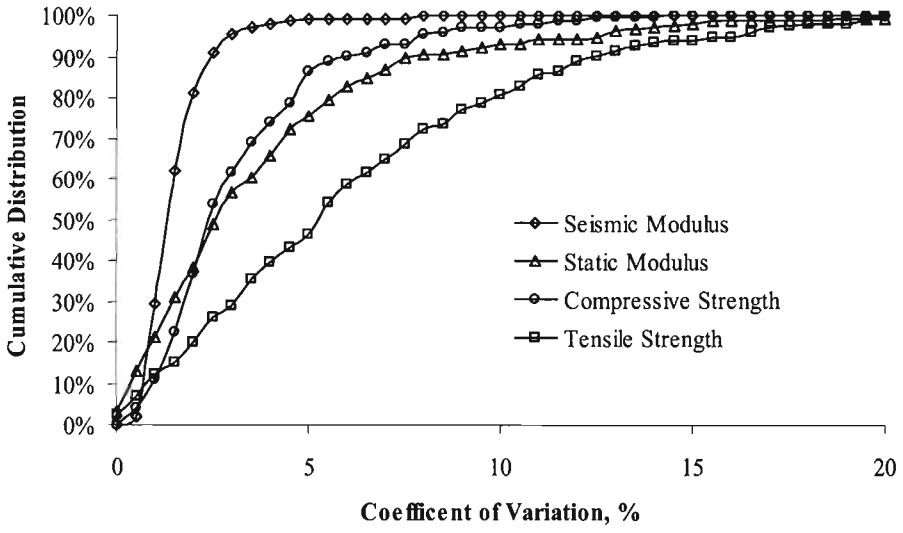

Figure 5.18 – Distribution of Coefficients of Variation for Tests Performed on all Specimens

Chapter 6

Case Study

As a part of this project, a section of US 59, north of Houston, TX was tested. The results from this case study are presented herein.

Location of Site

The site tested was located near Cleveland, TX on the northbound lane of US 59. The project consisted of about 13 in. (280 mm) of continuously reinforced concrete pavement (CRCP). The work was carried out on the outside lane of the highway between Stations 41+00 and 61+00. The concrete approximately between Stations 60+00 and 61+00 was poured on July 19, 2004. The remainder of work was carried out on July 20, 2004.

The mix design for this project is summarized in Table 6.1. The nominal 7-day design flexural strength was 555 psi.

Table 6.1 – Mixture Proportions Used in US 59 Case Study

Material	Amount
Type I-II Cement (lb/yd^3)	362
Sand (lb/yd^3)	1265
Coarse Aggregate (lb/yd^3)	1848
Type Fly Ash (lb/yd^3)	131
Water (gal/yd^3)	215
Air Content (%)	5

Strength-Modulus Calibration

It would have been desirable to carry out the calibration activities before the day of field testing. However, because of time limitations, the calibration was carried out concurrent with the field testing. This task was graciously carried out by the staff of CTR in cooperation with TxDOT personnel from the Materials and Pavements Section of the Construction Division.

About 4 dozen 4 in. by 8 in. (100 mm by 200 mm) cylinders were molded at the site using the material delivered in the ready-mix trucks. The specimens were transported from the site to Austin after 24 hours for curing and testing. At each of nominal times from pouring of 1 day, 3 days, 7 days, 14 days, 21 days and 28 days, six specimens were tested with the free-free resonant column device. Three specimens were then tested in compression and three in split tensile modes to obtain the respective strength values. The variation in the two strengths and seismic modulus with time are shown in Figure 6.1. The seismic modulus and compressive strength demonstrate a pattern of gradual increase with time. Even though the tensile strength also increases with time, the 21-day strength is smaller than those of the 14 and 28 days. This can be attributed to experimental error or high coefficient of variation associated with the tensile strength. Overall, the coefficients of variations associated with seismic modulus, compressive strength and tensile strength were 1.4%, 2.6% and greater than 10%, respectively.

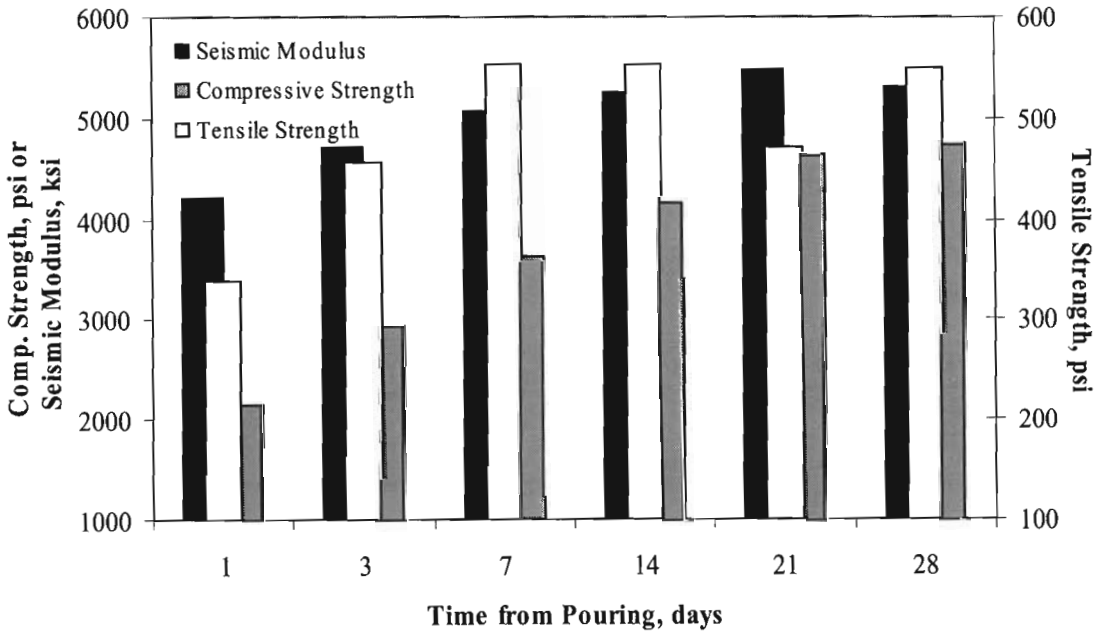

Figure 6.1 – Variations in Compressive Strength, Tensile Strength and Seismic Modulus with Time

The laboratory calibration curve for the compressive strength is shown in Figure 6.2. The best-fit curve describes the data very well, indicated by an R^2 value of 0.98.

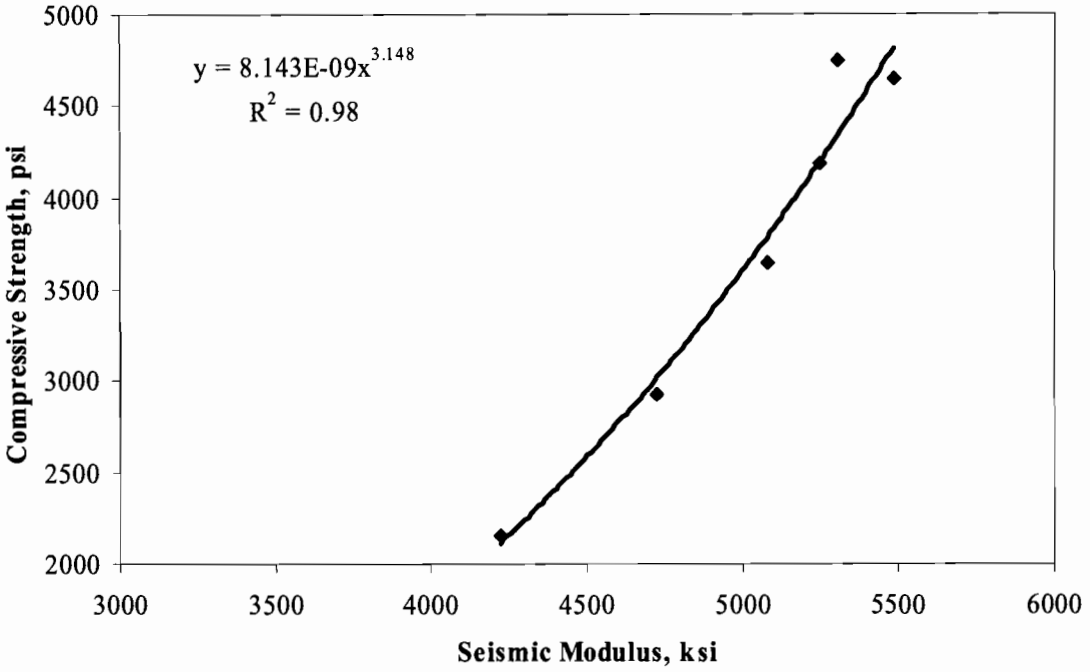

Figure 6.2 – Laboratory Calibration of Compressive Strength with Seismic Modulus

Similarly, the laboratory calibration with regards to the tensile strength is shown in Figure 6.3. Ignoring one outlier related to lower than the anticipated value in tensile strength at 21 days, the tensile strength and seismic modulus are well correlated as well.

Field Testing with PSPA

The next step in this study was to carry out field tests to determine the modulus of the slab and to estimate the related strength parameters. The procedure used to carry out the seismic measurements with the Portable Seismic Pavement Analyzer (PSPA) is included in Appendix D.

Several studies were also carried out in this stage. These studies include: (1) determination of set points of fresh concrete, (2) determination of variation in modulus with time and (3) determination of effectiveness of several curing compounds. These studies are described below.

Determination of Set Points of Fresh Concrete

Hourly measurements were carried out at one point of the slab for the first 24 hours to determine the set point of concrete from the modulus stand point.

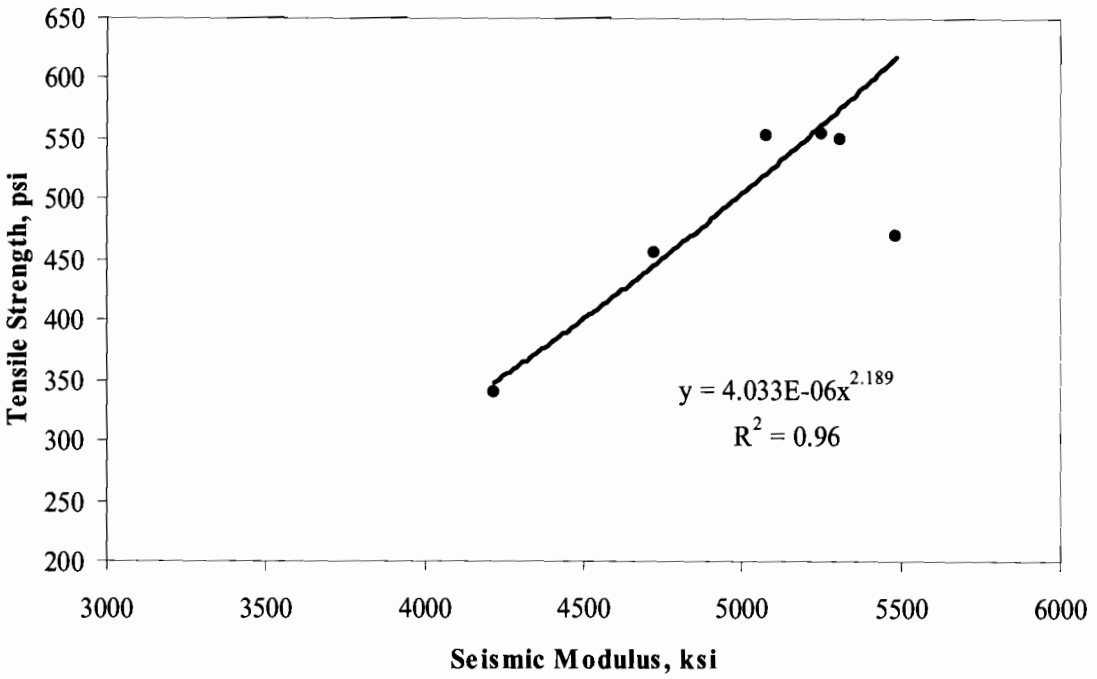

Figure 6.3 – Laboratory Calibration of Tensile Strength and Seismic Modulus

The variation in seismic modulus with time from about 3 hours after pouring to 7 days is shown in Figure 6.4. The first reading was feasible after 3.5 hours. Before this time, the concrete was too soft for coupling of seismic energy. Three distinct regions are apparent in this figure. Up to about 5 hours after pouring (marked as A), the concrete is in its semi-liquid state. As such, the gain in modulus is very minimal. Between points A and B, the concrete solidifies and stiffens very rapidly. At point B (after about 16 hours), the concrete reaches its solid state. Past Point B, the gain in stiffness is more gradual since most of the free moisture inside concrete has been consumed. Practically speaking, the most desirable time for saw-cutting concrete is between Points A and B, perhaps, closer to Point B. Utilizing the calibration curves shown in Figure 6.3, the compressive and tensile strengths after 24 hrs are about 2300 psi and 370 psi, respectively. Understanding that the extrapolation of the calibration curves to five hours after pouring may not be appropriate, the two strengths at that time is less than 100 psi.

Determination of Variation in Modulus with Time

Seismic moduli at 21 points, approximately corresponding to the paving operation associated with July 19 and 20, 2004 at the site, were tested after different times for 28 days. The points where the PSPA tests were carried out, which closely corresponds to the survey stations marked at the side, were about 100 ft (30 m) apart.

The variation in modulus with distance for the tests carried out around 8:00 AM on July 21, 2004 is shown in Figure 6.5. At that time, the concrete ages were between 48 hours (at Station 61+00) to 14 hours (at Station 41+00).

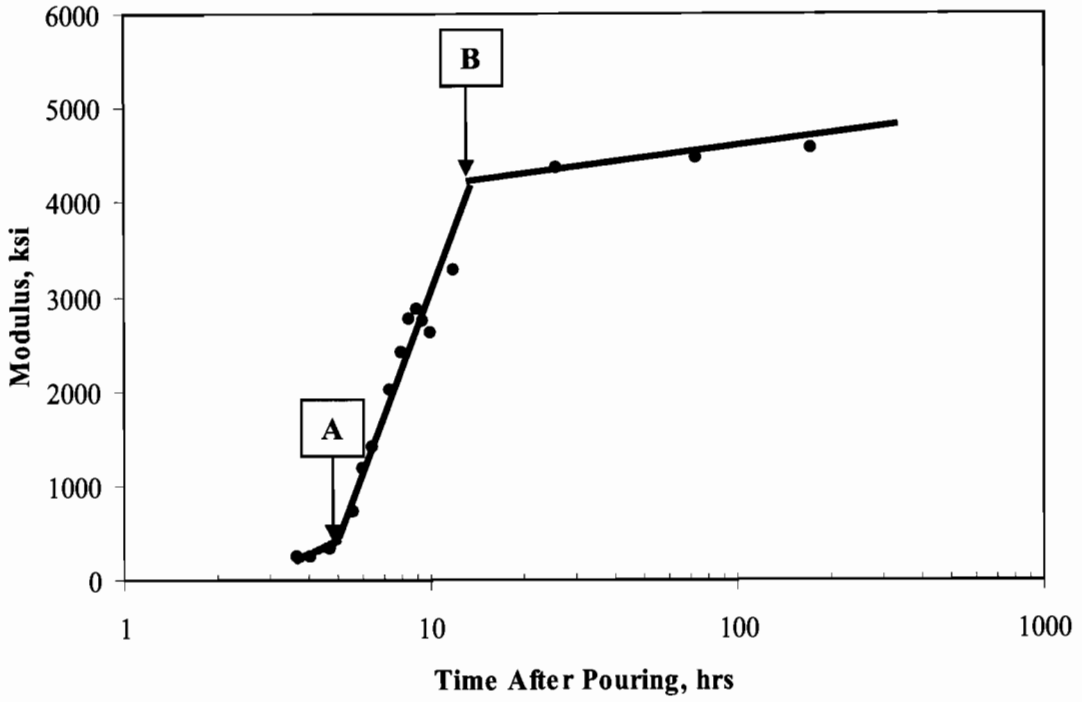

Figure 6.4 – Early-Age Seismic Modulus of PCC with Time

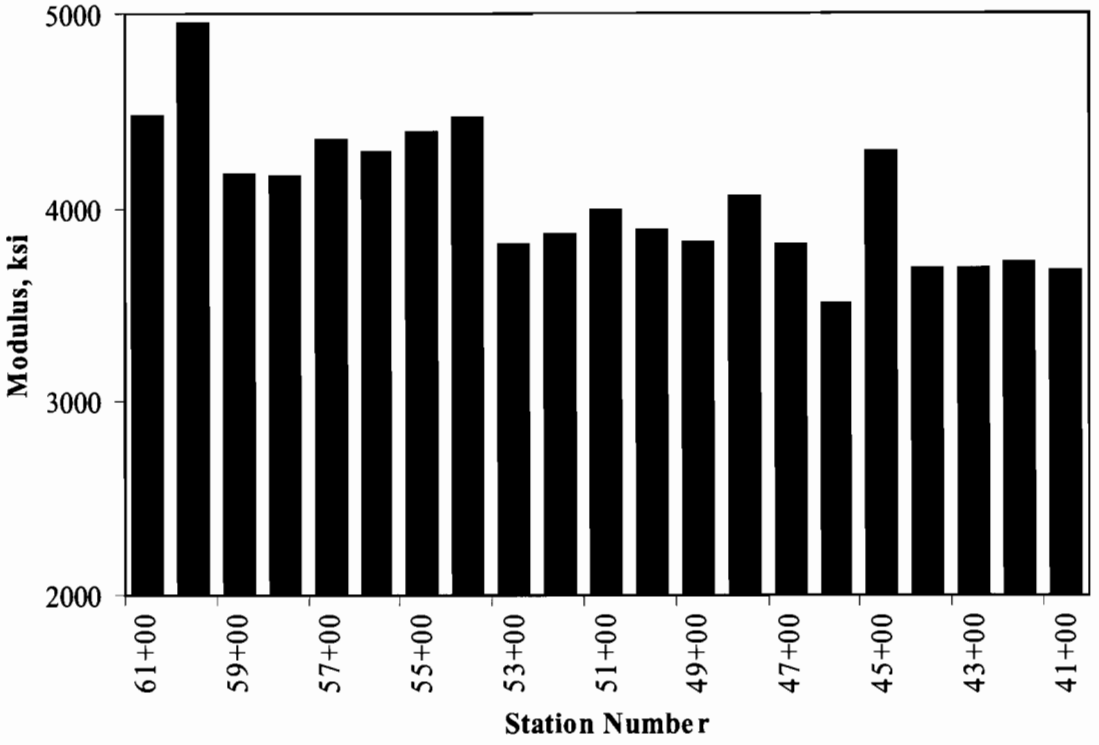

Figure 6.5 –Seismic Moduli Measured from 14 to 48 hours after Pouring

The moduli for the first two stations are greater than the rest of the site because the concrete at these stations were two days old. Also a trend towards lower moduli is observed as the station numbers decrease. This trend is reasonable given about 10 hours age difference between Stations 59+00 and 41+00.

Similar results but from the 28 day tests are shown in Figure 6.6. The modulus varies from about 5000 psi to 6000 psi with the afternoon production yielding higher moduli. Two major factors aside from the quality of construction and environmental parameters can contribute to this variability.

The first item is the variability of the material delivered to the job site. It would have been desirable to check the slump and air content of the mix as delivered. A recent study by Nazarian et al. (2004) demonstrated that for an ordinary paving operation by a qualified contractor, the slump of the ready mix concrete varied between 2 in. and 3.5 in. for a design slump of 3 in and the air content varied between 6% and 8.5% for a design air content of 6% among about thirty consecutive truck loads. The second item is the variability in seismic measurement with the PSPA. Nazarian et al. (2004) also studied this matter. They found that when the same point is repeatedly tested without moving the PSPA, the COV is less than 2%. However, when the device was moved around about the point, the COV increased to about 7%.

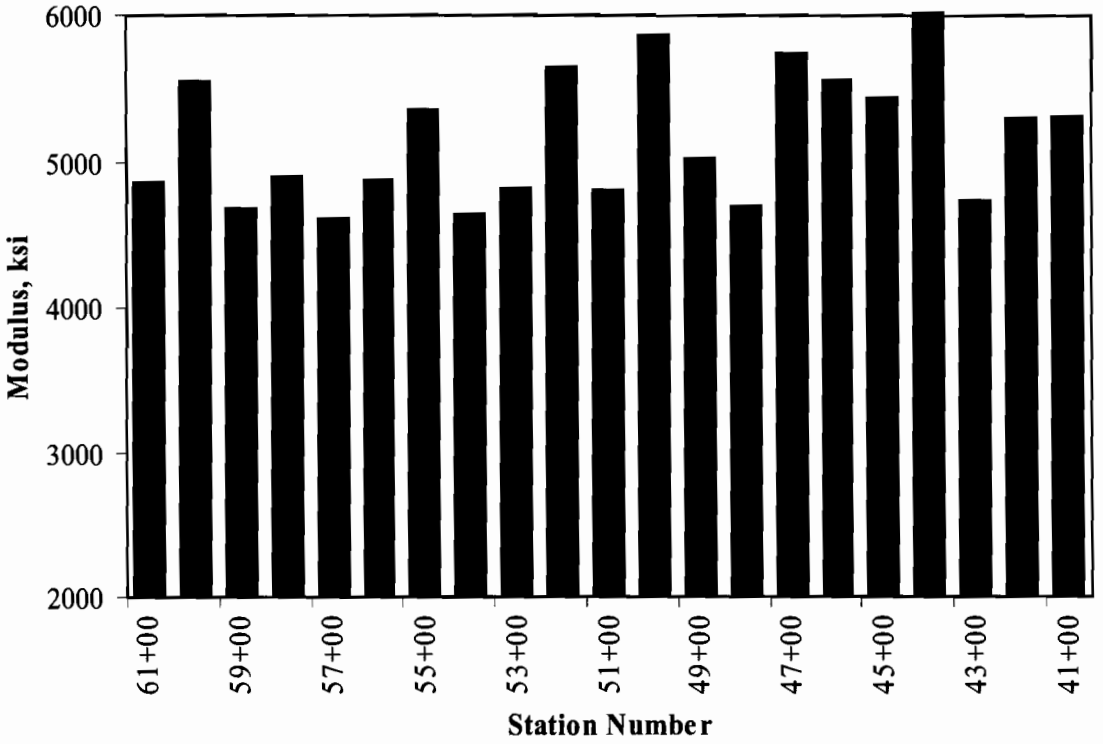

Figure 6.6 – Seismic Moduli Measured 28 Days after Pouring

The averages of seismic moduli and the related coefficients of variation for the entire projects are summarized in Table 6.2. The coefficient of variation is about 11% to 13% for all test periods The average modulus steadily increases with time. The amount of precipitation experienced at the site is also included. It is interesting that the average modulus measured with the PSPA increases more rapidly between 7 days and 14 days. The reason for this matter, aside from experimental error, can be attributed to the significant rainfall of 0.4 in. that was recorded between 7 days and 14 days. If this increase is modulus is related to the precipitation recorded, it may be an indication that the curing method may not be as effective in preventing the evaporation of moisture from the concrete as anticipated. This matter should be investigated in the future studies.

The seismic moduli measured on the slab with the PSPA and on the lab-cured with the free-free resonant column device are compared in Table 6.2 as well. As reflected in Appendix D, the lab modulus and the field modulus are theoretically related through the following relationship:

$$E_{field} / E_{lab} = (1 + \nu) (1 - 2\nu) / (1 - \nu) \qquad (6.1)$$

where ν is the Poisson's ratio. There is about 6% to 8% difference between the two for well-cured concrete with the field modulus smaller than the lab one.

Table 6.2 – Variation in Average Modulus with Time

Time after Pouring, day	Seismic Modulus from PSPA		Cumulative Precipitation, in	Seismic Modulus from Cores	
	Average, ksi	COV, %		Average, ksi	Difference
1	4221	12.0	0.1	3908	8.0%
3	4545	11.3	0.3	4375	3.9%
7	4654	10.4	0.3	4700	1.0%
14	5226	13.1	0.7	4860	7.5%
28	5190	11.2	0.7	4914	5.6%

The variations in modulus with time at the locations of the six i-buttons placed at the site are shown in Figure 6.7. Once again, the modulus tends to increase by the time of placement. For the first day, the moduli measured at the points where the i-buttons placed later in the day are lower simply because of the shorter period between pouring and testing.

Determination of Effectiveness of Several Curing Compounds

Finally, the assessment of variations in modulus with time at five areas treated with different curing compounds was carried out. The results are shown in Figure 6.8. The five treatments that were used consisted of:

- A new highly-reflective compound (labeled New)
- No treatment (labeled None)
- A typical curing compound used in Houston District (labeled Regular, Sun)
- A typical curing compound used in Houston District protected from sun (labeled Regular, Shade)
- A black paint (labeled Black)

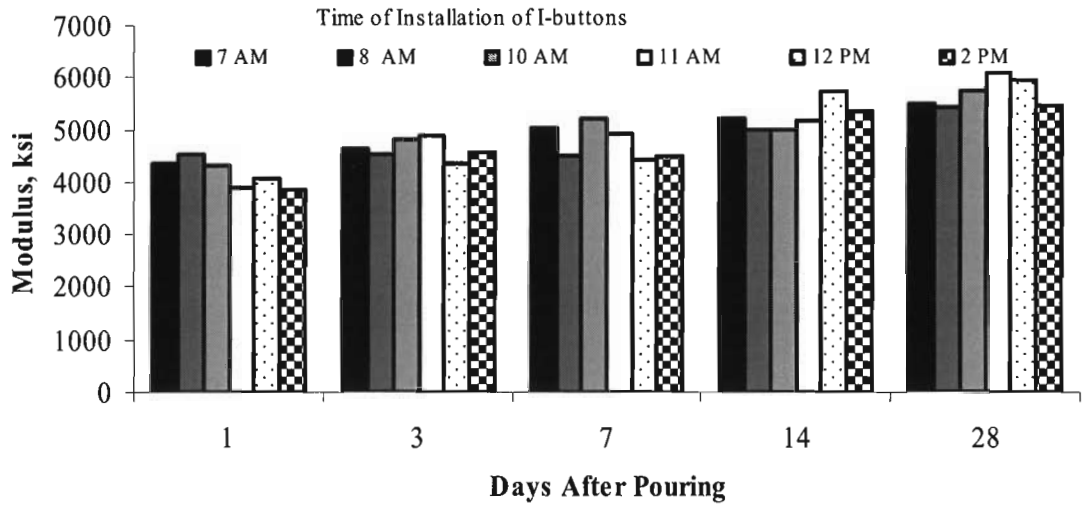

Figure 6.7 – Variation in Seismic Modulus with Time at the I-button Locations

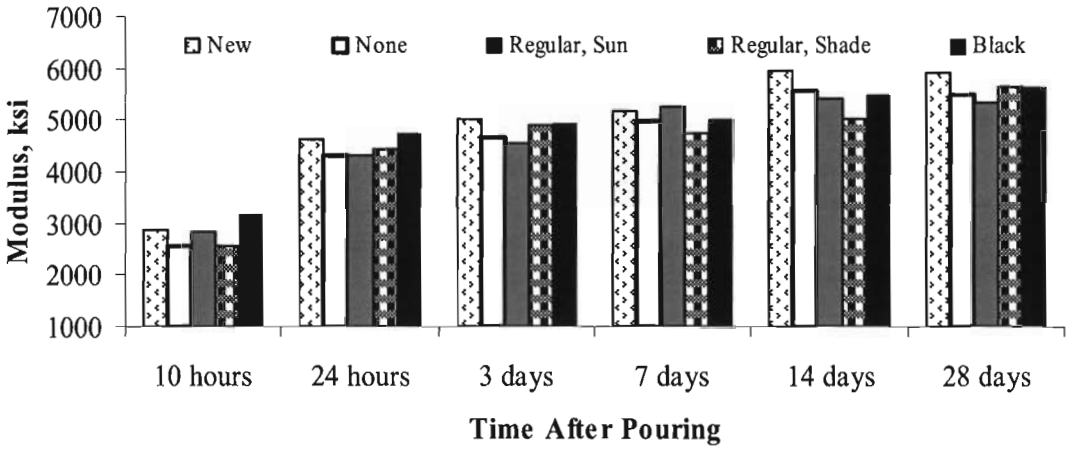

Figure 6.8 – Variation in Seismic Modulus with Time in Areas with Different Treatments

The highly-reflective curing compound seems to be quite effective in terms of providing stiffer concrete. However, as expected, for the first 24 hours, the black paint resulted in the highest stiffness. Providing shade may impact the temperature of the concrete during curing, but it does not seem to impact the gain in strength and stiffness after 24 hours or so. The regular curing compound is only slightly effective in providing the concrete of adequate properties in the field condition.

Chapter 7

Summary and Conclusions

Results from previous TxDOT research efforts and other literature have demonstrated that there are significant differences between the development rate in modulus and that in either tensile or compressive strength with curing time. This is potentially problematic, as it leads to increased stresses in the concrete and may be an underlying cause of excessive horizontal cracking observed in some PCC pavements across the state.

To investigate this problem, an extensive laboratory experiment to characterize the development in both strength and modulus with time under controlled conditions was carried out. The measured parameters were splitting tensile strength, compressive strength and static modulus as well as seismic modulus. In all instances, the maturity of the concrete as a function of time and temperature (time-temperature factor) was measured.

The laboratory experiment consisted of two phases. In Phase I, standard cylinders were made from eight different mixes and cured in five different conditions. The impacts of mix design and curing environment on the development of both strength and modulus parameters of concrete were investigated. Preliminary relationships between the seismic modulus and the compressive strength, tensile strength and static modulus are proposed in the basis of the type of coarse aggregates. The focus of the second phase of this study was toward the impacts of chemical additives and gradation on the relationships developed in Phase I.

Unlike a strength-maturity relationship that is usually very specific to a particular mix under a particular curing condition, a seismic modulus-based relationship is mainly affected by the nature of the coarse aggregate and, to a lesser extent, by other parameters such as curing condition, mineral admixture chemical additives and water-cement ratio.

Findings from this study would be useful in the following two ways:

1. ***Improving Rigid Pavement Design:*** The developed relationships can be incorporated in the design codes such as CRCP-11 to improve the assumptions with regards to the

relationships between the strength and modulus of the concrete in early ages. In that manner, the models used in predicting several distress types can yield more realistic results.

2. ***Construction Quality Management***: It was found that the strength and the seismic modulus for laboratory-cured specimens are highly correlated. Also it was demonstrated that such relationships are not significantly impacted by the environmental-related and most material-related parameters. Furthermore, it was demonstrated that the seismic moduli obtained from field testing are well-related to the seismic moduli obtained from laboratory testing. Therefore, seismic nondestructive testing (NDT) devices can be utilized for quality control of in situ concrete to minimize coring. The relationships between seismic modulus and strength parameters as well as static modulus developed through this laboratory experiment are more robust than those from the maturity method. As such, frequent calibration may not be needed and thus the seismic methods can consider the construction-related problem that is not possible with the maturity method.

References

- ACI Committee 363 (1984). "State of the Art Report on High Strength Concrete." American Concrete Institute Journal, 81(4), 364-411.

- Alexander, D. R. (1996), "In Situ Strength Measurements with Seismic Methods," Report from US Army Engineer Waterways Experiment Station, Vicksburg, Mississippi for the US Air Force Civil Engineering Support Agency, Tyndall AFB, Florida.

- Al-Manaseer, A. and Nasser, K.W. (1987), "New Non-destructive Test for Removal of Concrete Forms," Concrete International, ACI, 9(1), 41.

- Ansari, F.; Maher, A.; Luke, A. (1999), "Development of Maturity Protocol for Construction of NJDOT Concrete Structures," Report No. FHWA NJ 2001-017, Rutgers University, Center for Advanced Infrastructure and Transportation, Piscataway, NJ, 38 p.

- Barton, J.P. (1976), "Neutron Radiography – An Overview," Practical Applications of Neutron Radiography and Gaging, ASTM STP 586, Berger, H., Ed., American Society for Testing and Materials, Philadelphia, 5.

- Bartos, M. J. (1979), "Testing Concrete in Place," Civil Engineering, American Society of Civil Engineers, Vol 66.

- Bickley, J. A. (1993), "Field Manual for Maturity and Pullout Testing on Highway Structures," Report SHRP-C-376, Strategic Highway Research Program, Washington DC.

- Bickley, J.A. (1982), "The Variability of Pullout Tests and In-place Concrete Strength," Concrete International, 4(4), 44.

- Cantor, T.R. (1970), "Status Report on the Windsor Probe Test System," presented to Highway Research Board Committee A2-03, Mechanical Properties of Concrete, at 1970 Annual Meeting, Washington DC.

- Carette, G.G. and Malhotra V.M. (1984) "In-Situ Tests: Variability and Strength Prediction of Concrete at Early Ages," Malhotra, V.M., Ed., American Concrete Institute, Spec Publ. SP-82, 111.

- Carino, N.J. (1981), "Temperature Effects on Strength-Maturity Relation of Mortar," NBSIR 81-2244, U.S. National Bureau of Standards.

- Carino, N.J., Lew, H.S., and Volz, C.K. (1983), "Early Age Temperature Effects on Concrete Strength Prediction by the Maturity Method," Journal of the American Concrete Institute, Vol. 80, No. 2, March-April, pp. 93- 101.

- Carino, N. J. (1984), "Closure to Discussion of Reference 32," Journal of American Concrete Institute, 81(1), 98.

- Chin, F. K. (1971), "Relation between Strength and Maturity of Concrete," Journal of American Concrete Institute, 68(3), 196.

- Chung, H.W. (1978), "Effect of Embedded Steel Bars upon Ultrasonic Testing of Concrete," Magazine of Concrete Research, London, 30(102), 19.

- Clemena, G.G. (1987),"Determining Water Content of Fresh Concrete by Microwave Reflection or Transmission Measurement," Report VTRC-88-R3, Virginia Transportation Research Council, Charlottesville, VA.

- Clemena, G.G. and Steele, R.E. (1988), "Inspection of the Thickness of In-Place Concrete with Microwave Reflection Measurements," Report VTRC-88-R16, Virginia Transportation Research Council, Charlottesville, VA.

- Clemena, G.G. (1983), "Microwave Reflection Measurements of the Dielectric Properties of Concrete," Report VTRC-84-R10, Virginia Transportation Research Council, Charlottesville, VA.

- Freiesleben, H. P. and Pederson, E.J. (1985), "Curing of Concrete Structures," CEB Information Bulletin 166.

- Freiesleben, H. P. and Pederson, E.J. (1977), "Maturity Computer for Controlled Curing and Hardening of Concrete," Nordisk Betong, 1, 19.

- Forster, S.W. (1997), "Concrete Materials and Mix Design for Assuring Durable Pavements," Sixth International Purdue Conference on Concrete Pavement Design and Materials for High Performance, Vol. 1, pp. 111-118.

- Greene, G. W. (1954), "Test Hammer Provides New Method of Evaluating Hardened Concrete," ACI Journal, 51(3), 249.

- Green, W.J., Carrasquillo, R.L., and McCullough, B.F. (1987), "Coarse Aggregate for PCC--Pilot Study Evaluation," Research Report 422-1, Center for Transportation Research, The University of Texas at Austin.

- Hammond, E. and Robson, T.D. (1955), "Comparison of Electrical Properties of Various Cements and Concretes," The Engineer, 199,78 and 115.

- Hansen, W., Jensen, E. A. and Mohr, P. (2001), "The Effect of High Strength and Associated Concrete Properties on Pavement Performance," Publication No. FHWA-RD-00-161, McLean, VA.

- Huang, Y.H. (1993), "Pavement Analysis and Design," Prentice Hall, Kentucky.

- Jensen, B.C. and Braestrup, M.W. (1976), "Lok-tests Determine the Compressive Strength of Concrete," Nordisk Betong, No. 2, 9.

- Johansen, R. (1976), "A New Method for Determination for In-Place Concrete Strength of Form Removal," 1st European Colloquium on Construction Quality Control, Madrid, Spain.

- Jones, R. (1954), "Testing of Concrete by an Ultrasonic Pulse Technique", RILEM International Symposium On Nondestructive Testing of Materials and Structures," Paris, Vol 1, Paper no. A-17, 137. RILEM Bull. No. 19, 2nd part, November.

- Jones, R. and Facaoaru, I. (1969), "Recommendations for Testing Concrete by the Ultrasonic Pulse Method," Materials and Structures Research and Testing (Paris), 2(19), 275.

- Khaloo, A. R. and Kim, N., "Effect of Curing Condition on Strength and Elastic Modulus of Lightweight High-Strength Concrete", ACI Materials Journal, V. 96, No. 4, July 1999, pp. 485-490

- Kolek, J. (1958), "An Appreciation of Schmidt Rebound Hammer," Magazine Concrete Research, London, 10(28, 27).

- Kolek J. (1969), "Non-destructive Testing of Concrete by Hardness Methods," Proceedings of Symposium On Non-destructive Testing of Concrete and Timber, Institution of Civil Engineers, London, 15.

- Kusenberger, F.N. and Barton, J.R. (1981), "Detection of Flaws in Reinforcing Steel in Prestressed Concrete Bridge Members," Report No. FHWA/AD-81/087, Federal Highway Administration, Washington, D.C.

- McCullough, B.F., Zollinger, D.G. and Dossey, T.E. (1995), "Effect of Aggregates on Pavement Performance," Research Report 1244-13F, Center for Transportation Research, The University of Texas at Austin.

- McCullough, B.F., Zollinger, D.G. and Dossey, T.E. (1998), "Evaluation of the Performance of Texas Pavements Made with Different Coarse Aggregates," Research Report 3925-1, Center for Transportation Research, The University of Texas at Austin.

- Malhotra, V.M. (1974), "Evaluation of the Windsor Probe Test for Estimating Compressive Strength of Concrete," RILEM Materials and Structures, Paris; 7:37:3-15.

- Malhotra, V.M. (1976), "Testing Hardened Concrete: Nondestructive Methods," ACI Monogram No. 9, American Concrete Institute, Detroit, 109.

- Malhotra, V.M., Carino, N.J. (1991), "Handbook on Nondestructive Testing of Concrete," CRC Press, Baco Rotan, FL.

- Matzkanin, G.A., De Los Santos, A., and Whiting, D.A. (1982), "Determination of Moisture Levels in Structural Concrete Using Pulsed NMR (Final Report)," Southwest Research Institute, San Antonio, Texas, Federal Highway Administration, Washington, D.C., Report No. FHWA/RD-82-008.

- Mesbah, H. A., Lachemi, M., and Aïtcin C., "Determination of Elastic Properties of High-Performance Concrete at Early Ages", ACI Materials Journal, V. 99, No. 1, Jan. 2002, pp. 37-41

- Mindess, Sidney, J. Francis Young, and David Darwin, "Concrete," Second Edition Prentice-Hall, Inc., Englewood Cliffs, 2003.

- Mitchell, L.J. and Hoagland, G.G. (1961), "Investigation of the Impact Tube Concrete Test Hammer," Bulletin No. 305, Highway Research Board, 14.

- Myers, J.J., (1999), "How to Achive a Higher Modulus of Elasticity," Publication – HPC Bridge Views, FHWA Sponsored NCBC Co-Sponsored Newsletter, Issue No. 5, Sept/Oct 1999

- Neville, A.M. "Properties of Concrete," Fourth Edition John Wiley & Sons, Inc., New York, 1996.

- Nykanen, A. (1956), "Hardening of Concrete at Different Temperatures, Especially Below the Freezing Point," Proceedings, RILEM Symposium on Winter Concreting (Copenhagen, 1956), Danish Institute for Building Research Copenhagen, Session BII.

- Oh, B. H., "Behavior of Concrete under Dynamic Tensile Loads", ACI Material Journal, V. 84, No. 1, Jan. 1987, pp. 8-13

- Okamoto, P.A., Wu C. L., Tarr, S.M., Darter, M.I., Smith, K.D. (1993) "Performance-Related Specifications for Concrete Pavements," Volume 3-Development of a Prototype Performance Related Specification, Report FHWA-RD-93-044, FHWA, U.S. Department of Transportation.

- Oluokun, F. A., Burdette, E. G. and Deatherage, J. H., "Splitting Tensile Strength and Compressive Strength Relationship at Early Ages", ACI Materials Journal, V. 88, No. 2, March 1991, pp. 115-121.

- Oluokun, F. A., "Prediction of Concrete Tensile Strength from Its Compressive Strength: Evaluation of Existing Relations for Normal Weight Concrete", ACI Materials Journal, V. 88, No. 3, May 1991, pp. 302-309.

- Plowman, J.M. (1956), "Maturity and Strength of Concrete," Magazine of Concrete Research, 8(22), 13.

- Popovics, S. "Analysis of the Concrete Strength versus Water-Cement Ratio Relationship", ACI Materials Journal, V. 87, No. 5, Sep. 1990, pp. 517-529.

- Ramaiah, S., Dossey, T., McCullough, B.F. (2001), "Estimating In Situ Strength of Concrete Pavements Under Various Field Conditions," Research Report 1700-1, Center for Transportation Research, The University of Texas at Austin.

- Rebut, P. (1962) "Non-destructive Apparatus for Testing Reinforced Concrete: Checking Reinforcement with the Pachometer (in French)," Rev. Malenaux (Paris), 556, 31.

- Rezansoff, T. and Corbett J. R., "Influence of Accelerating Admixtures on Strength Development of Concrete under Wet and Dry Curing", ACI Materials Journal, V. 85, No. 6, Nov. 1988, pp. 519-528.

- Richart, Jr., F.E., Woods, R. D., Hall Jr., J.R. (1970), Vibrations of Soils and Foundations, Prentice-Hall, Inc., Englewood Cliffs, New Jersey.

- Saul A.G.A. (1951), "Principles Underlying the Steam Curing of Concrete at Atmospheric Pressure," Magazine of Concrete Research, 2(6), 127.

- Schmidt, E. (1950), "The Concrete Test Hammer (Der Beton-Prufhammer)," Schweiz. Bauz. (Zurich), 68(28), 378.

- Setunge, S., Attard, M. M., and Darvall P. L., "Ultimate Strength of Confined Very High-Strength Concretes", ACI Structural Journal, V. 90, No. 6, Nov. 1993, pp. 632-641

- Shilstone, J. M. (2000), "Performance-Based Specifications for Concrete Portion of Concrete Pavements," Presented in TRB Annual Meeting, Washington D.C.

- Tachibana, D., Imai Y., Kawai T., and Inada Y., (1981) High Strength Concrete Incorporating Several Admixtures, ACI SP-121, ed. W.T. Hester, American Concrete Institute, Farmington Hills, Michigan. et al., 1981

- Vassie, P.R. (1978), "Evaluation of Techniques for Investigating the Corrosion of Steel in Concrete," Department of the Environment, Department of Transport, TRRL Report SR397, Crowthorne.

- Weaver, J. and Sandgrove, B.M. (1971), "Striking Times of Formwork Tables of Curing Periods to Achieve Given Strengths," Construction Industry Research and Information Association, Rep. 36.

- Yuan, D., Nazarian S., and Zhang D. (2003)," "Use of Stress Wave Technique to Monitor and Predict Concrete Stress Development of," Airfield Pavement: Challenges and New Technologies, Proceedings of the Specialty Conference, Edited by Moses Karakouzian, ASCE, 2004, pp. 409-423.

- Zia, P.,Ahmad, S., Leming, M.,(1994), "High-Performance Concretes" Report FHWA-RD-97-030, FHWA, U.S. Department of Transportation.

List of ASTM Standards

- ASTM C-31 "Standard Test Method.

- ASTM C-39 "Standard Test Method for Compressive Strength of Cylindrical Specimens," Annual Book of ASTM Standards, Vol 04.02.

- ASTM C-78 "Standard Test Method for Flexural Strength of Concrete (Using Simple Beam with Third-Point Loading)," Annual Book of ASTM Standards, Vol 04.02.

- ASTM C-192 "Standard Test Method

- ASTM C-215 "Standard Test Method for Fundamental Transverse, Longitudinal, and Torsional Frequencies of Concrete Specimens," Vol 04.02.

- ASTM C-293 "Standard Test Method for Flexural Strength of Concrete (Using Simple Beam with Center-Point Loading)," Annual Book of ASTM Standards, Vol 04.02.

- ASTM C-469 "Standard Test Method for Static Modulus of Elasticity and Poisson's Ratio of Concrete in Compression," Annual Book of ASTM Standards, Vol 04.02.

- ASTM C-496 "Standard Test Method for Splitting Tensile Strength of Cylindrical Concrete Specimens," Annual Book of ASTM Standards, Vol 04.02.

- ASTM C-597-83 "Standard Test Method for Pulse Velocity through Concrete," Annual Book of ASTM Standards, Vol 04.02, Philadelphia.

- ASTM C-900 "Standard Test Method for Pullout Strength of Concrete," Annual Book of ASTM Standards, Vol 04.02.

- ASTM C-1074 "Standard Practice for Estimating Concrete Strength by the Maturity Method," Annual Book of ASTM Standards, Vol 04.02, Concrete and Aggregates.

Appendix A

Lab Seismic Testing Method and Device

FREE-FREE RESONANT COLUMN (FFRC) TESTING

The free-free resonant column test is a simple laboratory test for determining the modulus and possibly Poisson's ratio of pavement materials. The modulus measured with this method is the low-strain seismic modulus. The method is applicable to specimens of Portland cement concrete, asphalt concrete, stabilized base and subgrade, compacted subgrade and granular base provided the length is greater than the diameter. A length-to-diameter of 2 is strongly recommended. Since the seismic tests are nondestructive, a membrane can be placed around the specimen so that the specimen can be tested later for strength or stiffness (resilient modulus).

Performing this test on pavement materials will allow districts to develop a database that can be used to smoothly unify the design procedures and construction quality control. As in any other quality management program, acceptance criteria for quality control should be developed. The proposed acceptance criteria can be based on free-free resonant column testing of specimens prepared in the lab. The specimens used for this purpose are similar to those used for determining the optimum moisture/maximum dry density tests for base and subgrade.

When a cylindrical specimen is subjected to an impulse load at one end, seismic energy over a large range of frequencies will propagate within the specimen. Depending on the dimensions and the stiffness of the specimen, energy associated with one or more frequencies are trapped and magnified (resonate) as they propagate within the specimen. The goal with this test is to determine these resonant frequencies. Since the dimensions of the specimen are known, if one can determine the frequencies that are resonating (i.e. the resonant frequencies), one can readily determine the modulus of the specimen using principles of wave propagation in a solid rod (see Richart et al., 1970 for the theoretical background).

A schematic of the test set-up is shown in the figure. An accelerometer is securely placed on one end of the specimen, and the other end is impacted with a hammer instrumented with a load cell. The signals from the accelerometer and load cell are used to determine the resonant frequencies.

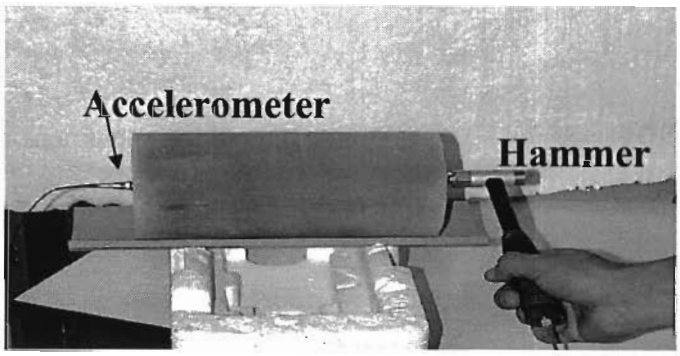

Results from an ideal condition are shown here. Resonant frequencies appear as peaks in a so-called amplitude spectrum. Two peaks are evident, one corresponding to the longitudinal propagation of waves in the specimen, and the other corresponding to the shear mode of vibration. It is simple to distinguish the two peaks. The longitudinal resonance always occurs at a higher frequency than the shear resonance.

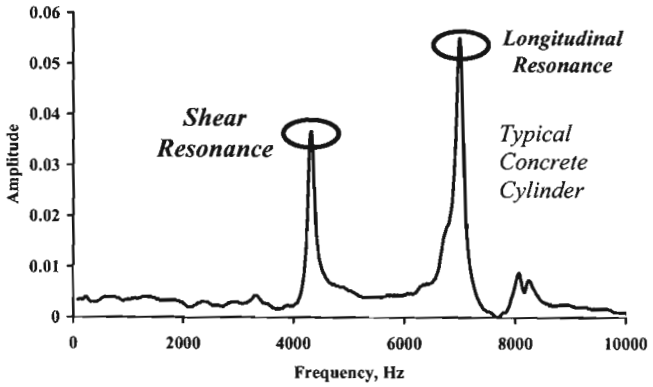

For our application, the longitudinal resonance is essential but the shear resonance is a nicety. As we will see later, the longitudinal resonance that provides the modulus, and the ratio of the longitudinal to shear resonant frequencies, provides the Poisson's ratio. For specimens with length-to-diameter of about 2, the frequency ratio cannot be less than 1.4.

Even though the resonant frequencies are not sensitive to the locations of the accelerometer and to the impact on the specimen ends, the amplitude associated with each resonance varies with these two parameters. Fortunately, the amplitudes are not important at all. Only the frequencies at which the peak amplitudes (resonant frequencies) occur are significant.

If the accelerometer is placed exactly at the center of one end, and the other end is impacted exactly at the center, the shear resonance totally disappears. The best compromise for getting adequate energy for both resonant frequencies is to place the accelerometer about 1/3 to 1/2 the radius from the center and impact the other end in the center.

How "sharp" (narrow and tall) a resonant peak is depends on the material being tested. The softer and the more absorbent (having higher damping properties) the material is, the less sharp the peak will be.

Once the longitudinal resonant frequency, f_L, and the length of the specimen, L, are known, Young's modulus, E, can be found from the following relation:

$$E = \rho \ (2 f_L L)^2. \qquad \text{(A-1)}$$

where ρ is mass density. The mass density is calculated from:

$$\rho = M / L A_s \qquad \text{(A-2)}$$

where A_s is the cross-sectional area of the specimen. Poisson's ratio, ν, is determined from

$$\nu = (0.5 \alpha - 1) / (\alpha - 1) \qquad \text{(A-3)}$$

where

$$\alpha = (f_L / f_S)^2 C_{L/D} \qquad \text{(A-4)}$$

with $C_{L/D}$ being a correction factor when the length-to-diameter ratio differs from 2. These equations are implemented in an excel worksheet shown below. The yellow zone contains data input by the operator during testing. The green zone contains the results that are concern to the user. The white zone contains intermediate results for advanced and expert users. The turquoise zone contains the summary results.

Test No.	ID No.	Age	TTF	Diamater	Length	Mass	Compress. Frequency	Shear Frequency	Mass Density	Young's Modulus	Poisson's Ratio	Strength	√Strength
		days	°C°hr	mm	mm	kg	Hz	Hz	Kg/m³	MPa		lbs/in²	√lbs/in²
1	Sample1	1	0	152.40	304.80	13.344	6265.32	3750.00	2400	35009.6	0.23		
2	Sample2	1	0	152.40	304.80	13.344	6259.61	3750.00	2400	34945.9	0.23		
3													
4													
5													
6													
7													
8													
9													
10													
11													
12													
13													
14													
15													
16													
17													
18													
19													
20													
Average									2400	34978	0.23	N/A	N/A
Standard Deviation									0	45.1	0.00	N/A	N/A
Coeff. Of Variation									0.0%	0.1%	0.2%	N/A	N/A

Appendix B

Typical Relationships Developed in Phase I

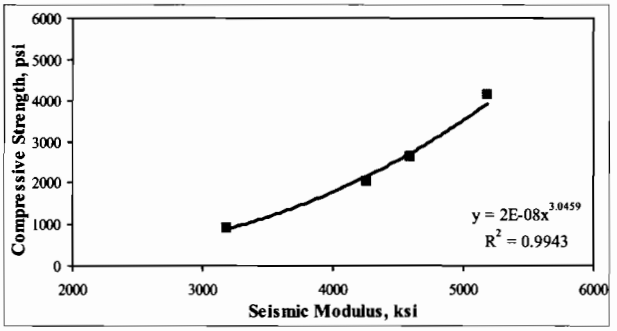

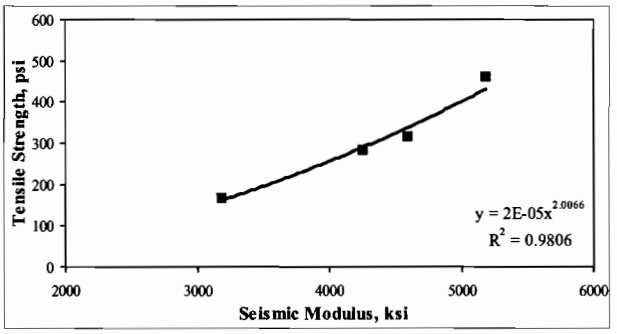

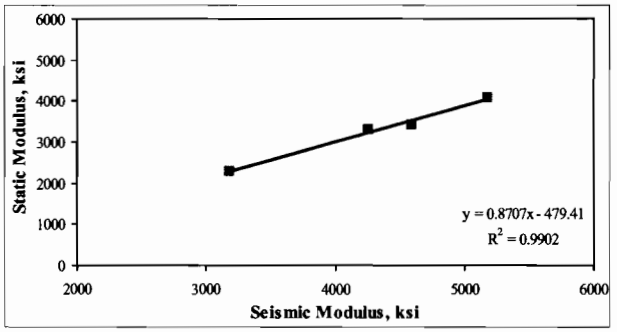

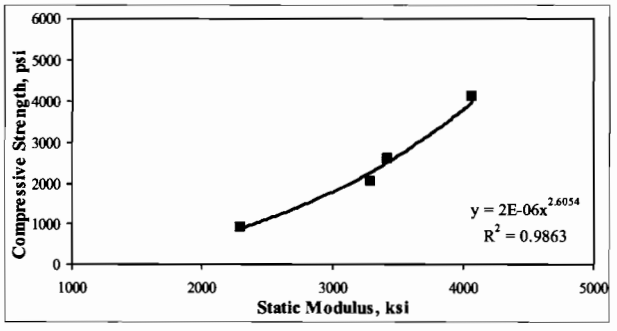

Figure B.1a - Typical relationships developed for a clean limestone with fly ash mix cured in water at 70°F.

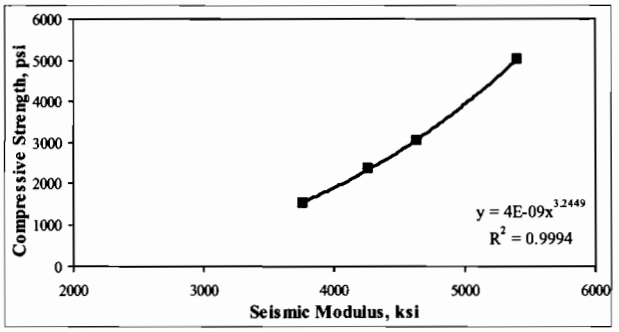

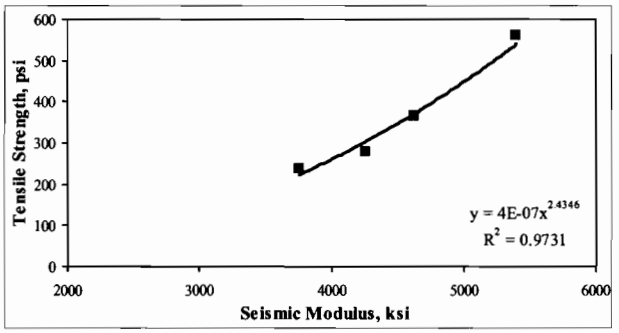

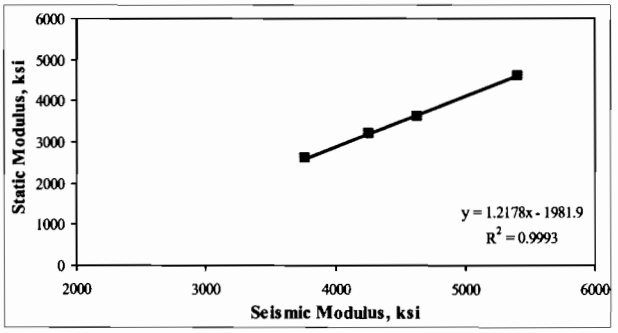

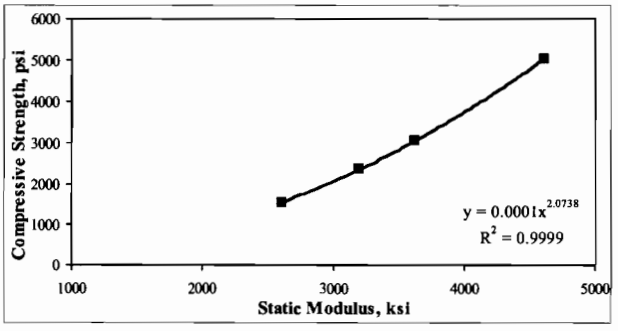

Figure B.1b - Typical relationships developed for a clean limestone with fly ash mix cured in water at 95°F.

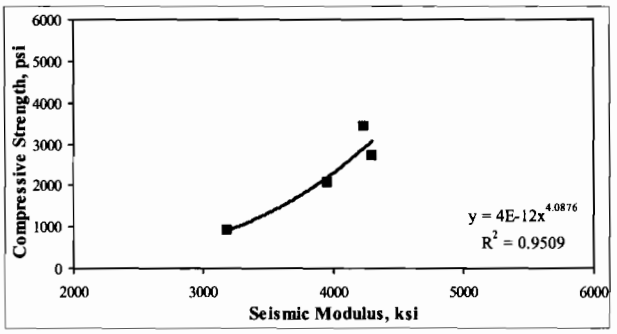

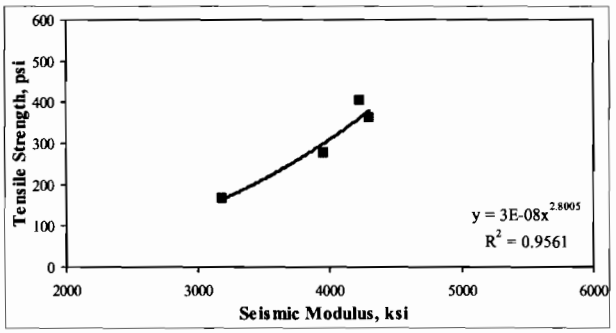

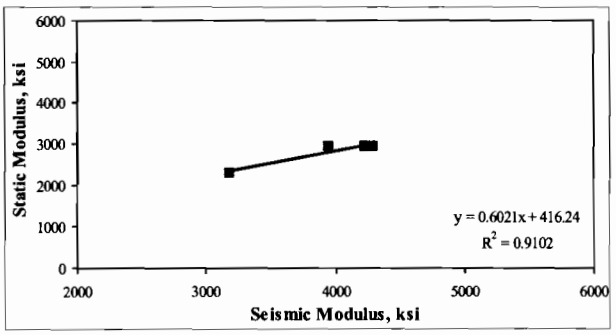

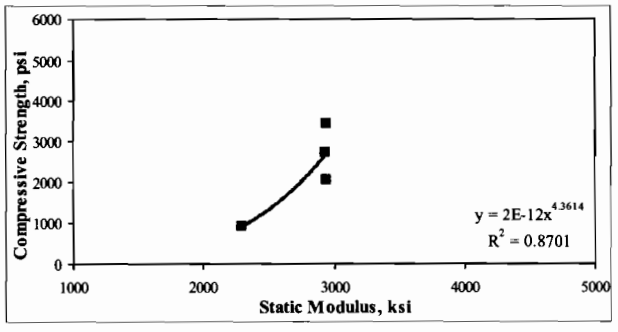

Figure B.1c - Typical relationships developed for a clean limestone with fly ash mix cured in a room at 70°F.

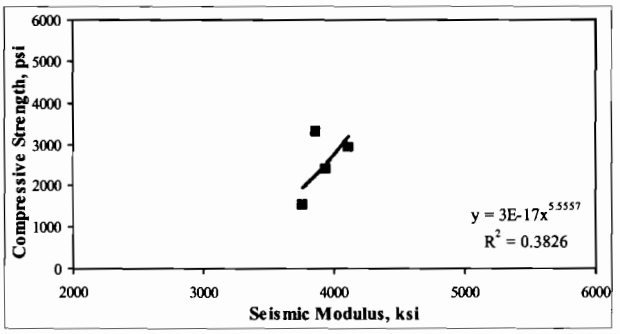

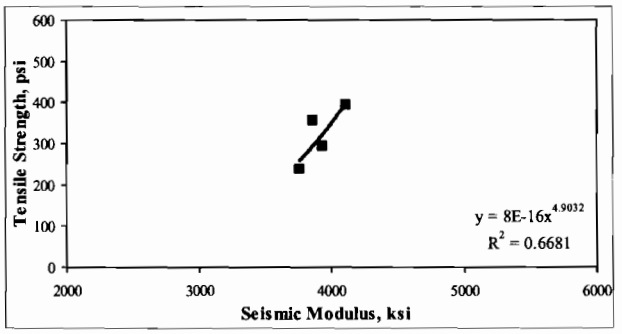

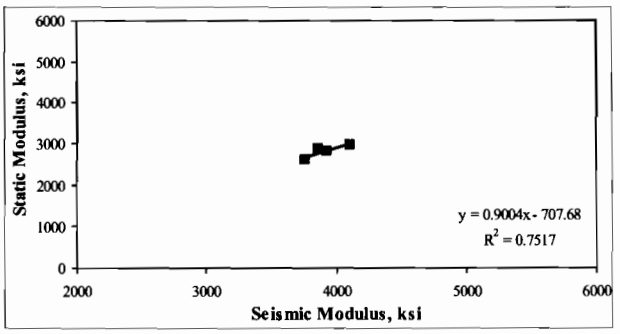

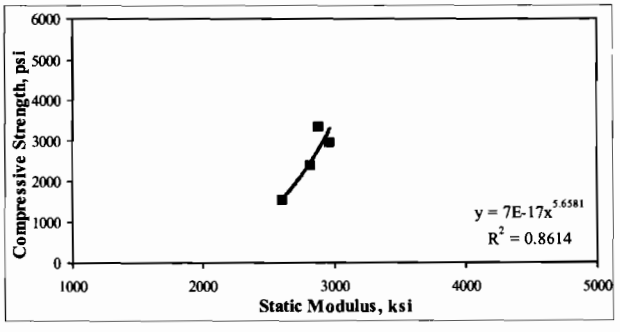

Figure B.1d - Typical relationships developed for a clean limestone with fly ash mix cured in a room at 95°F.

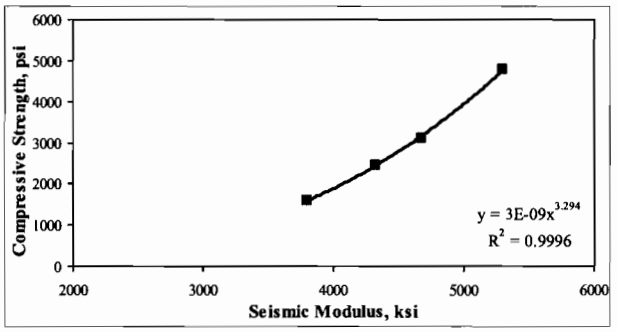

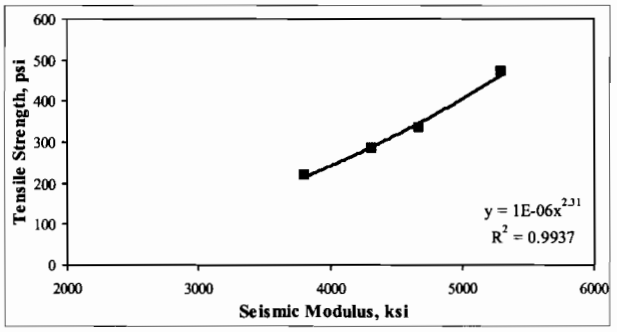

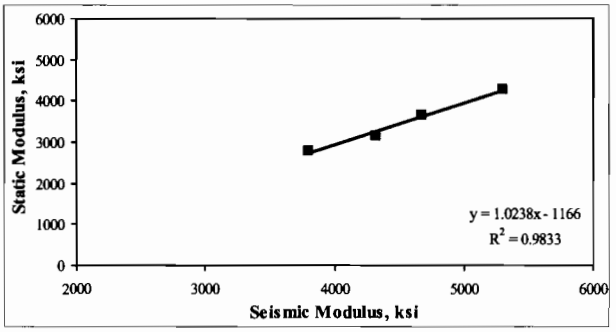

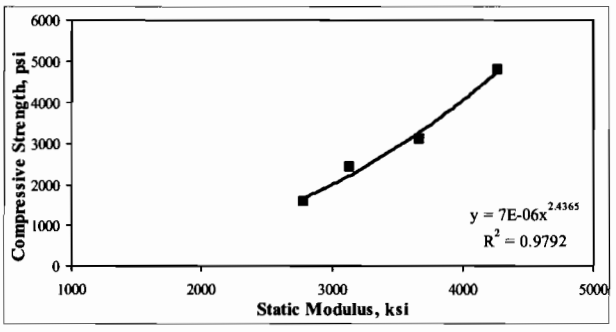

Figure B.1e - Typical relationships developed for a clean limestone with fly ash mix cured in the field.

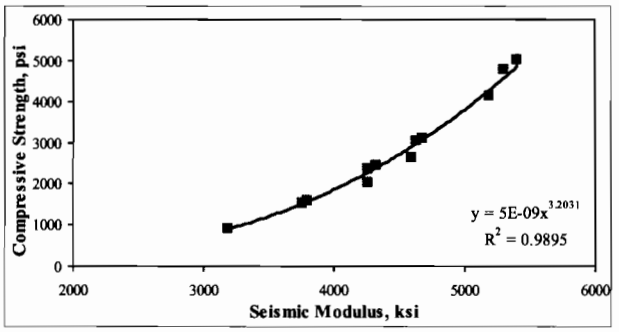

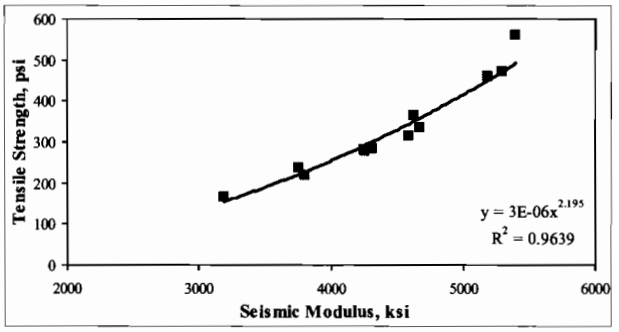

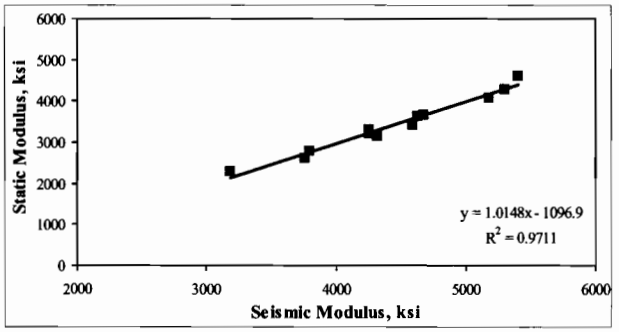

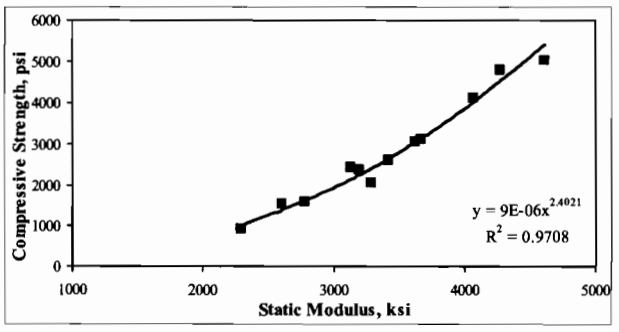

Figure B.1f - Typical relationships developed for a clean limestone with fly ash mix, when water 70°F, 95°F and field curing are combined together.

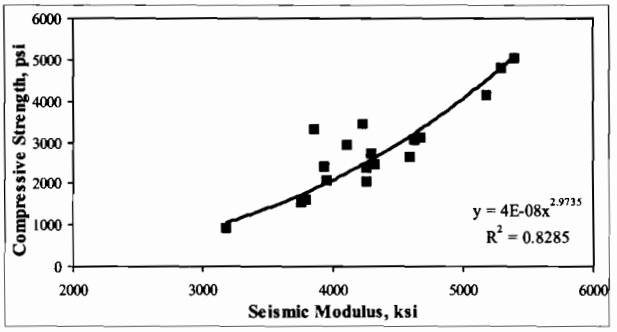

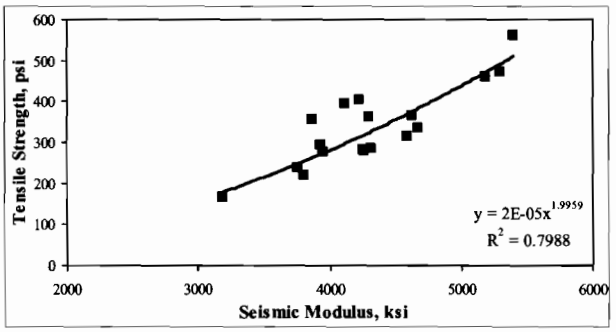

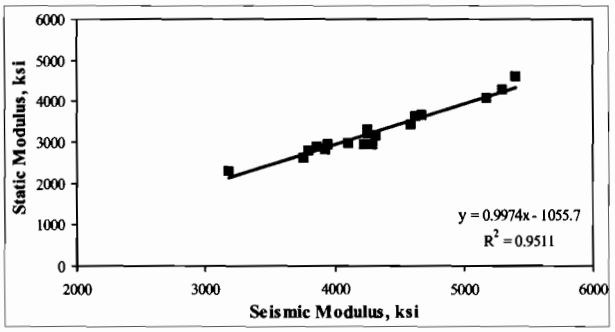

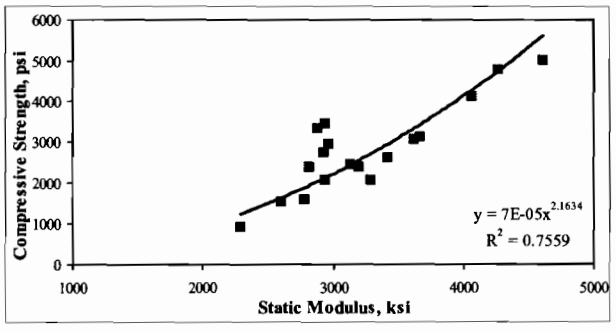

Figure B.1g - Typical relationships developed for a clean limestone with fly ash mix, when water 70°F, water 95°F, room 70°F, room 95°F and field curing are combined together.

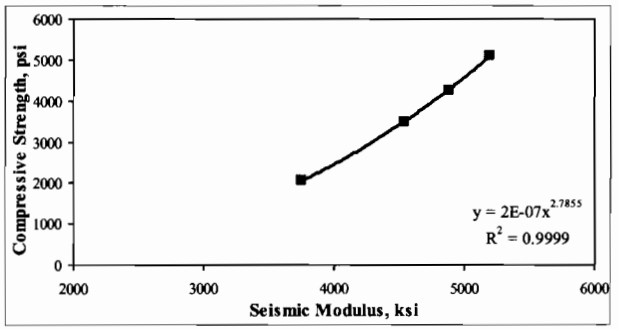

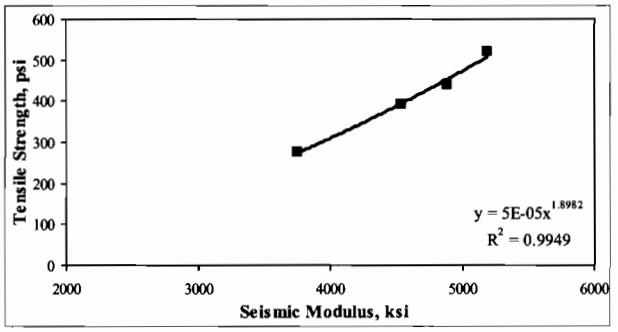

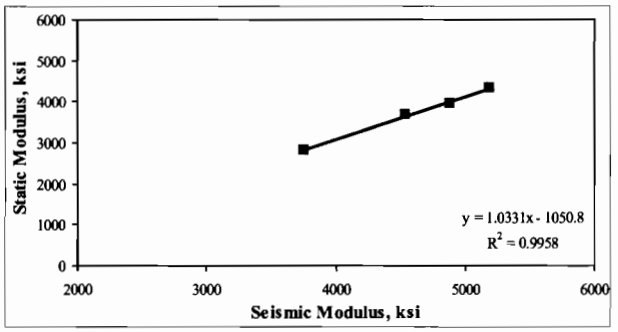

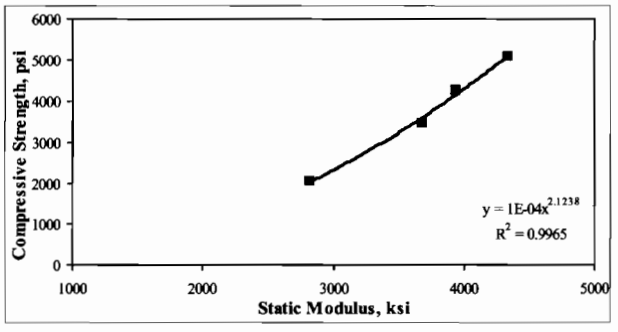

Figure B.2a - Typical relationships developed for a clean limestone without fly ash mix cured in water at 70°F.

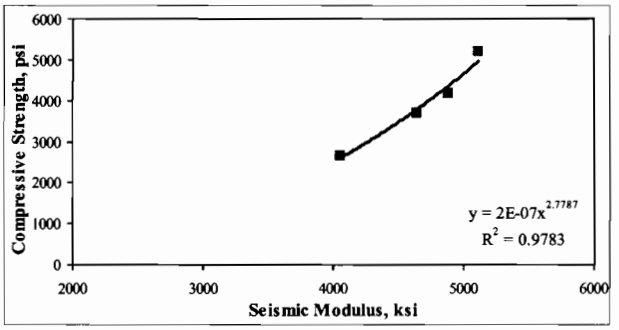

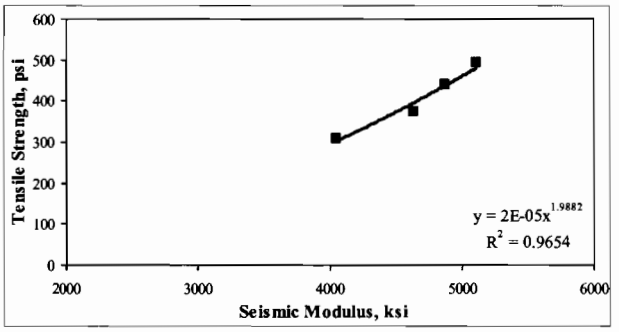

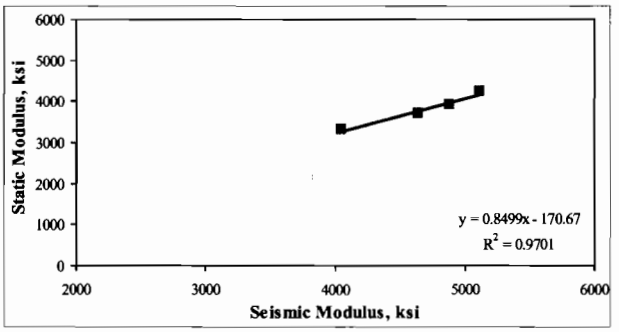

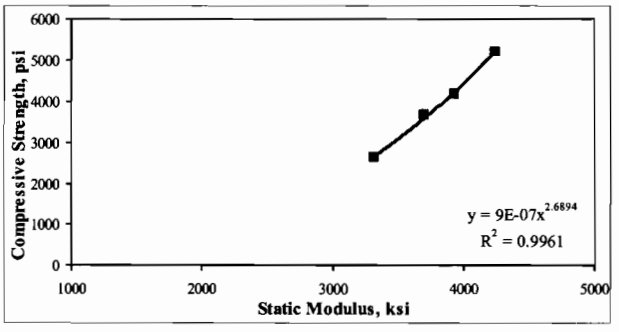

Figure B.2b - Typical relationships developed for a clean limestone without fly ash mix cured in water at 95°F.

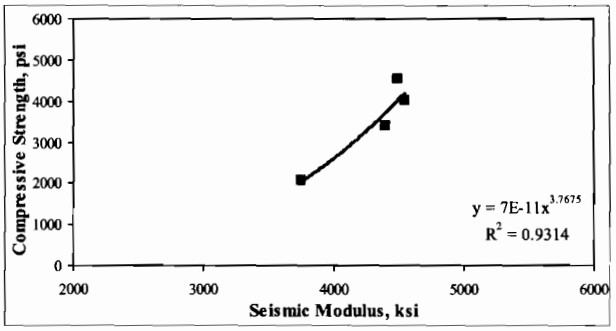

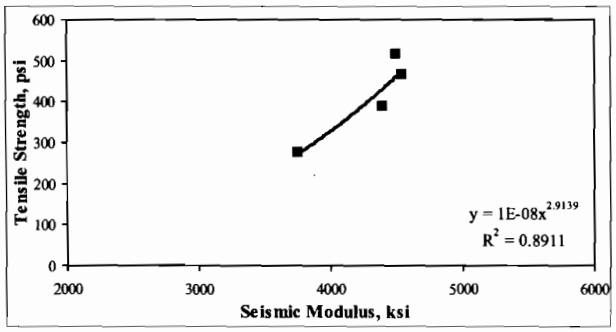

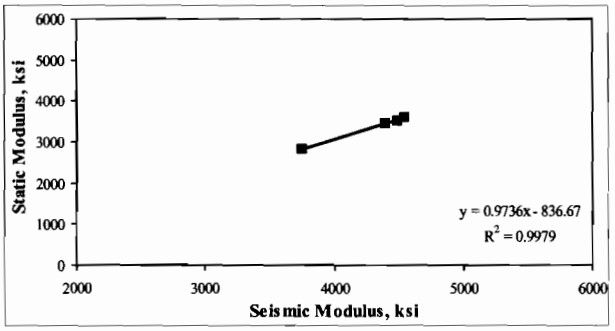

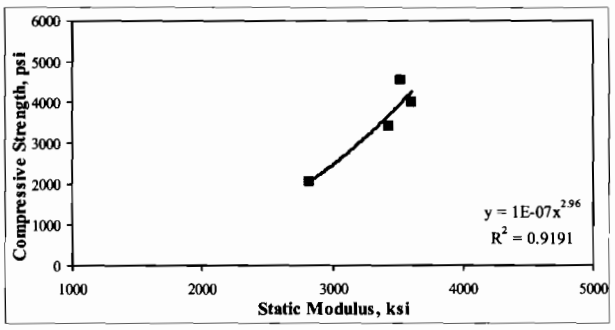

Figure B.2c - Typical relationships developed for a clean limestone without fly ash mix cured in a room at 70°F.

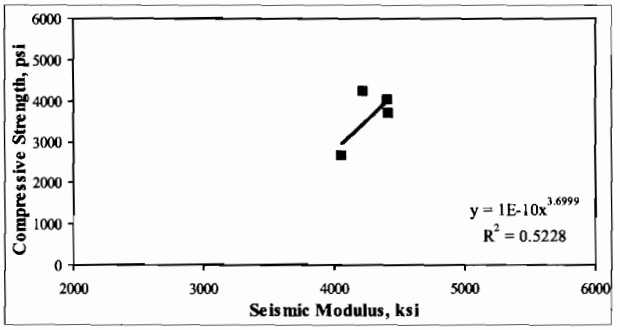

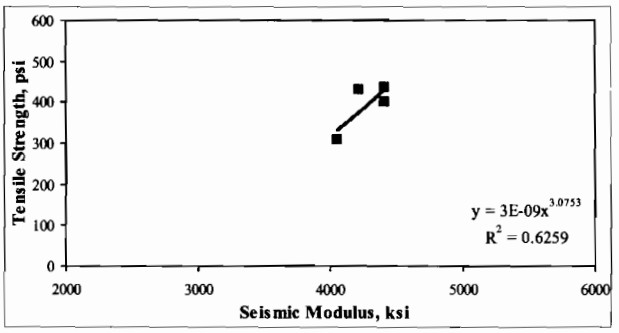

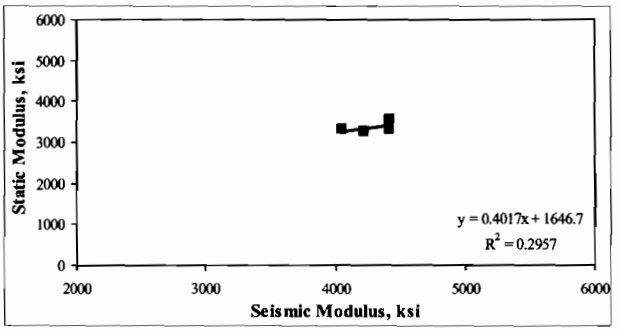

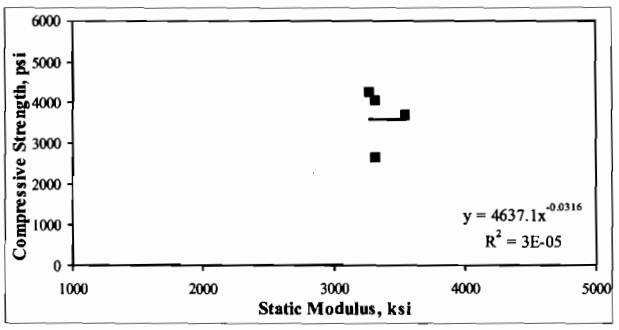

Figure B.2d - Typical relationships developed for a clean limestone without fly ash mix cured in a room at 95°F.

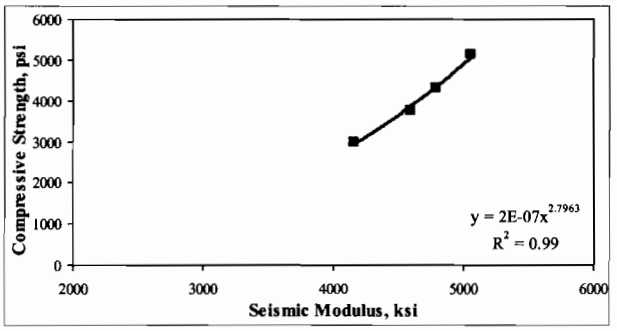

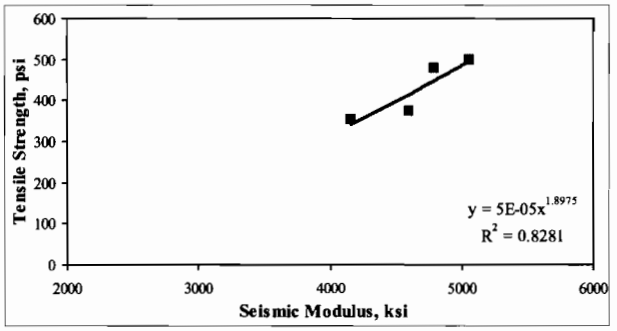

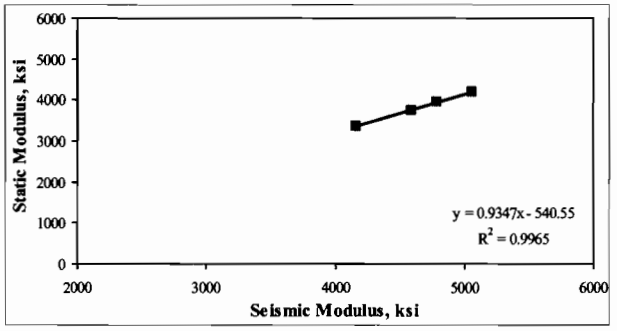

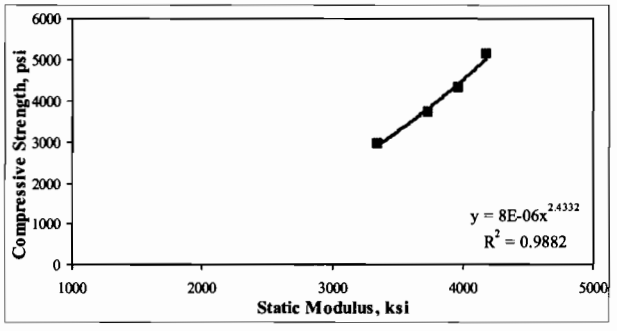

Figure B.2e - Typical relationships developed for a clean limestone without fly ash mix cured in the field.

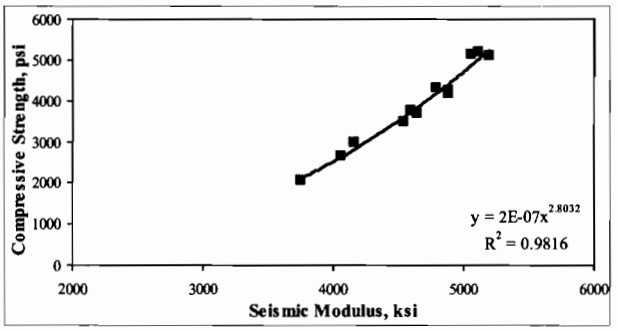

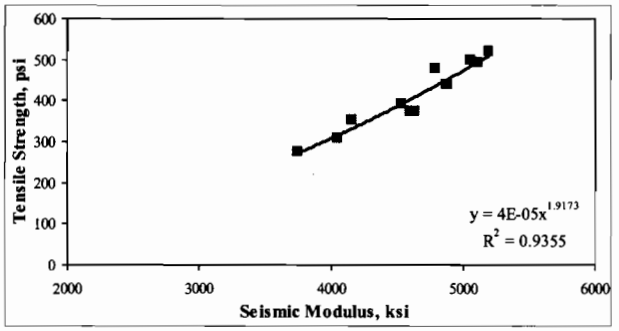

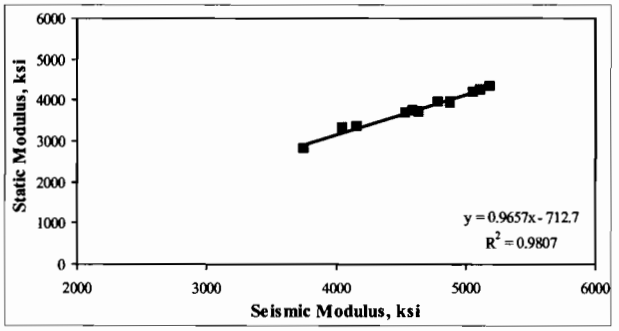

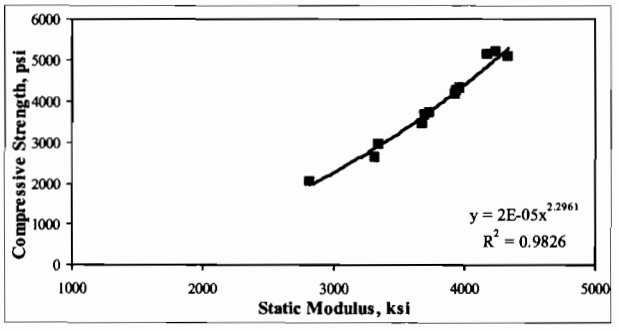

Figure B.2f - Typical relationships developed for a clean limestone without fly ash mix, when water 70°F, water 95°F and field curing are combined together.

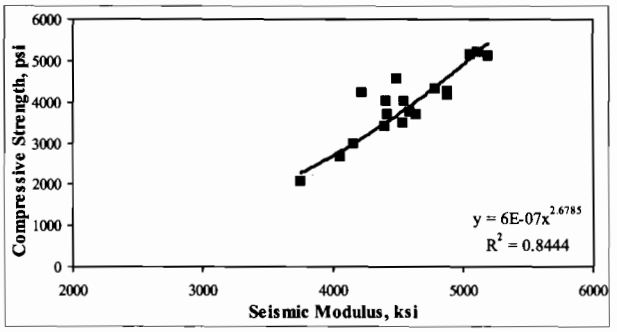

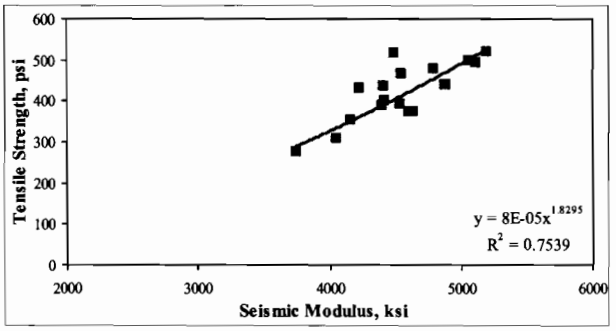

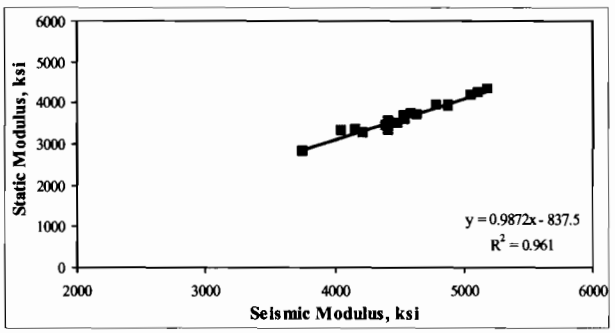

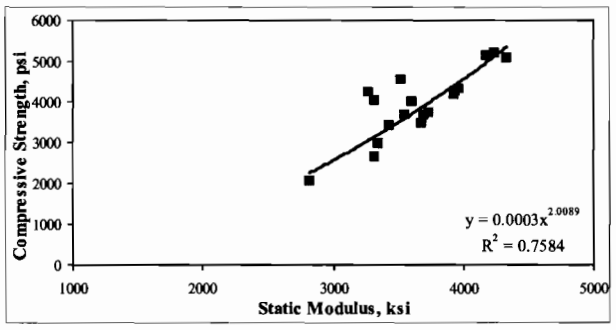

Figure B.2g - Typical relationships developed for a clean limestone without fly ash mix, when water 70°F, water 95°F, room 70°F, room 95°F and field curing are combined together.

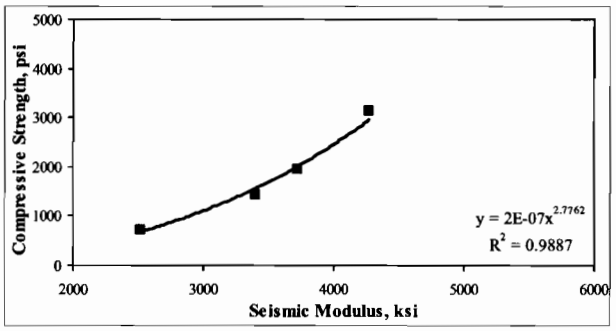

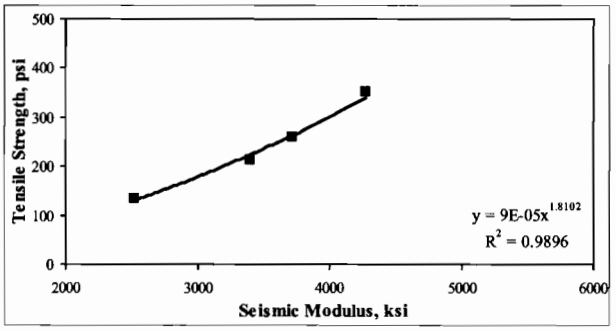

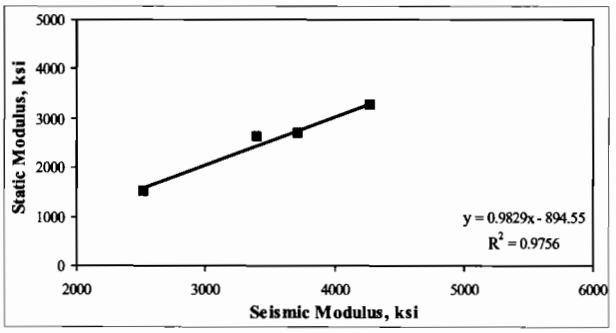

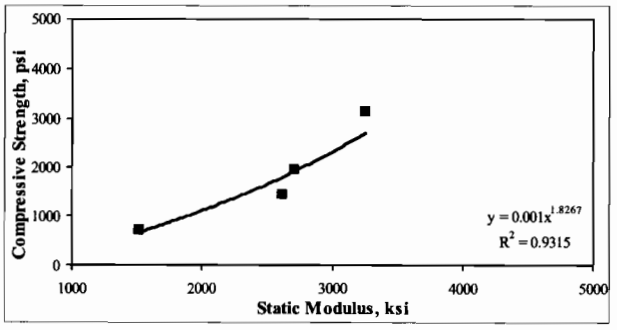

Figure B.3a - Typical relationships developed for a dirty limestone with fly ash mix cured in water at 70°F.

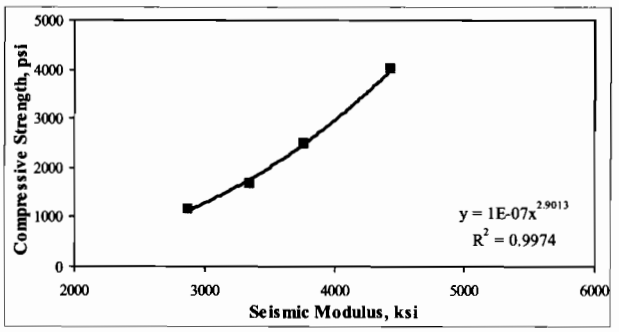

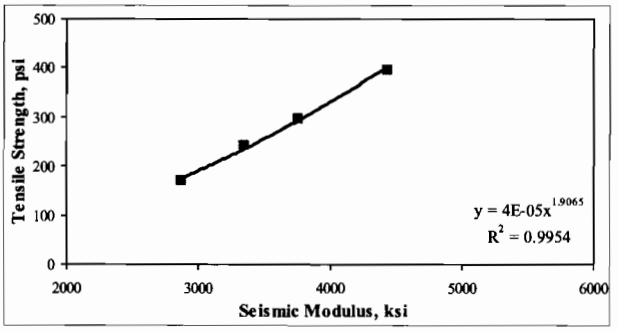

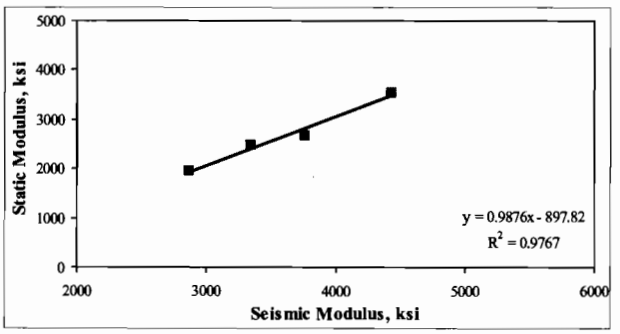

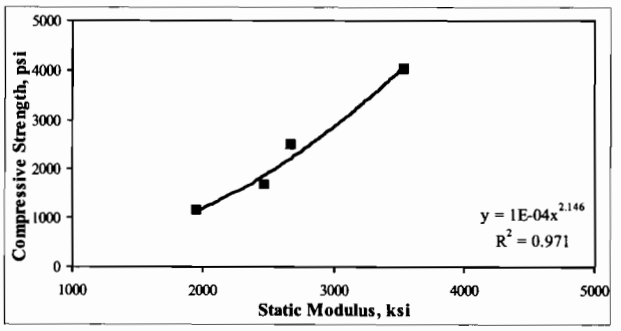

Figure B.3b - Typical relationships developed for a dirty limestone with fly ash mix cured in water at 95°F.

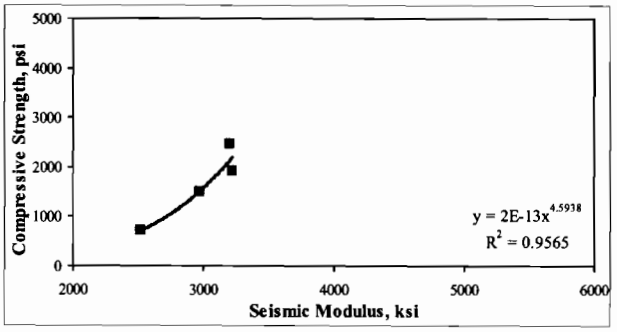

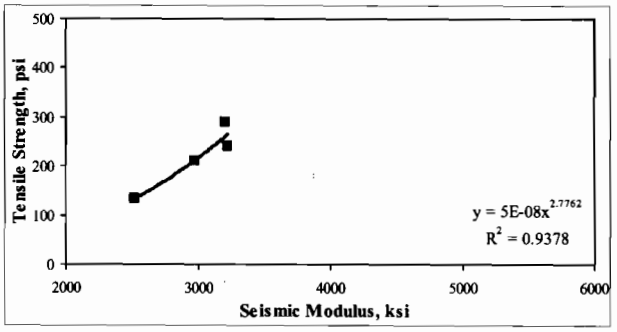

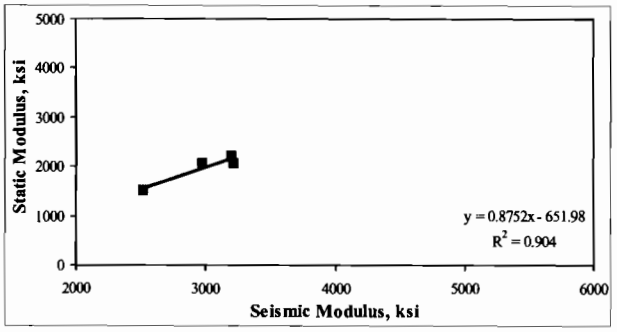

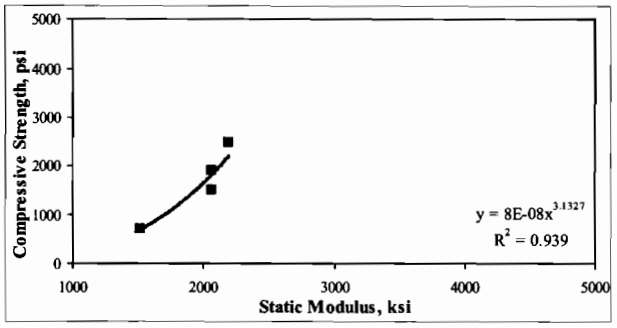

Figure B.3c - Typical relationships developed for a dirty limestone with fly ash mix cured in a room at 70°F.

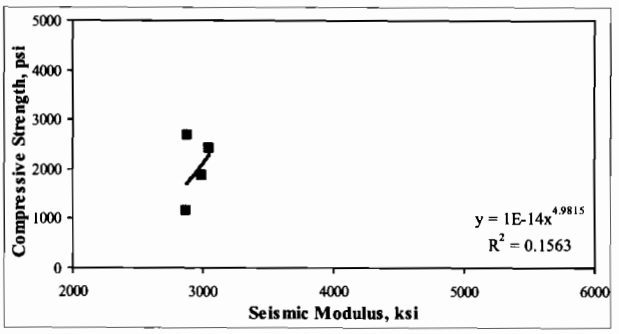

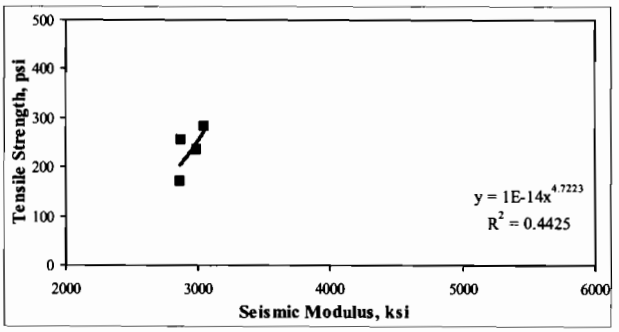

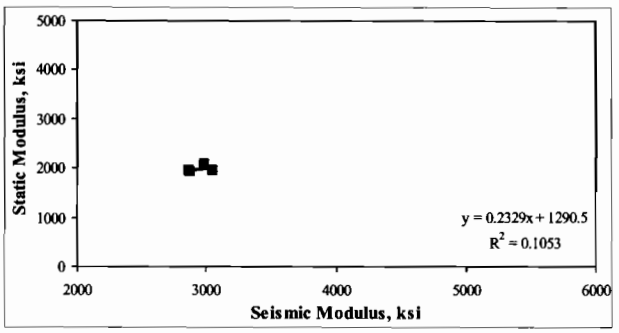

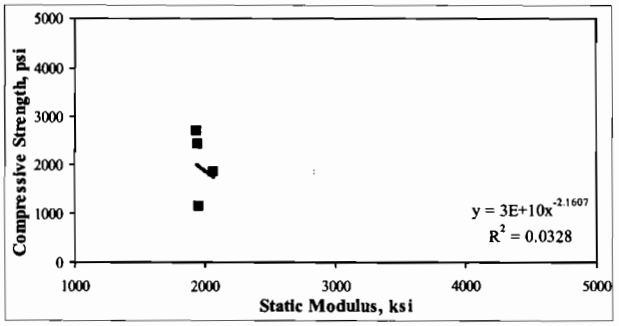

Figure B.3d - Typical relationships developed for a dirty limestone with fly ash mix cured in a room at 95°F.

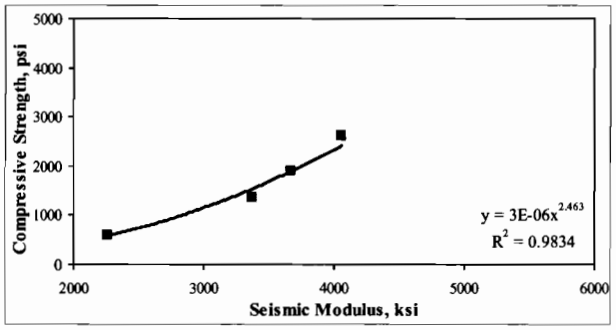

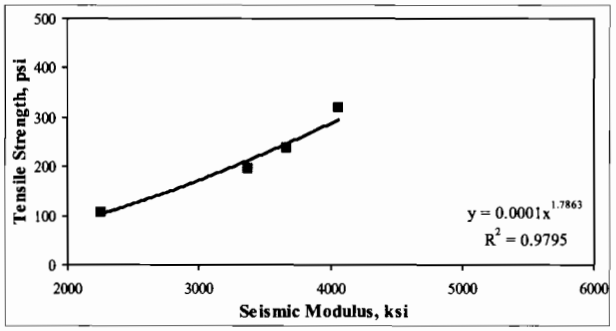

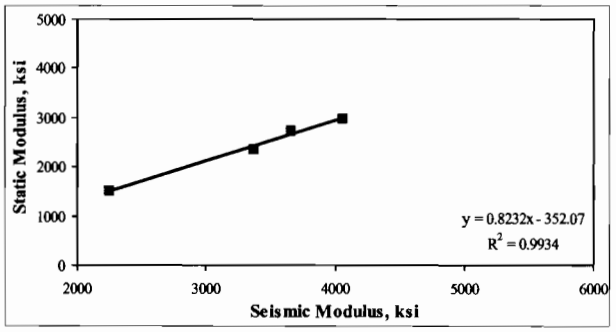

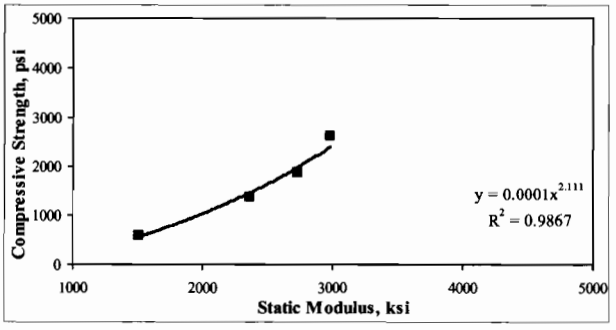

Figure B.3e - Typical relationships developed for a dirty limestone with fly ash mix cured in the field.

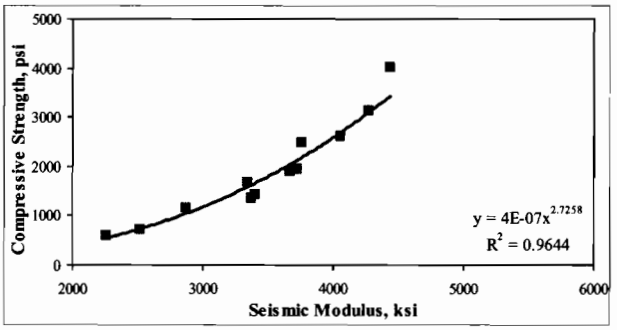

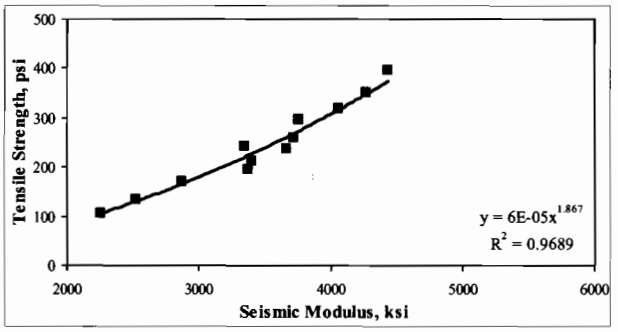

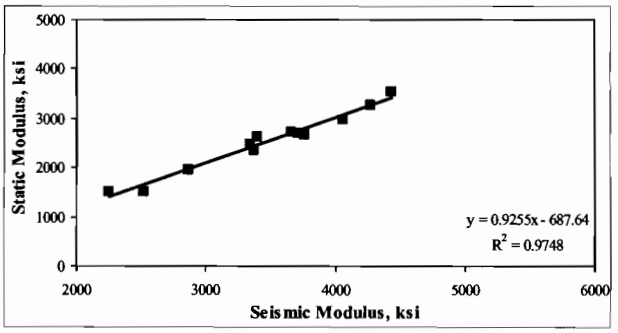

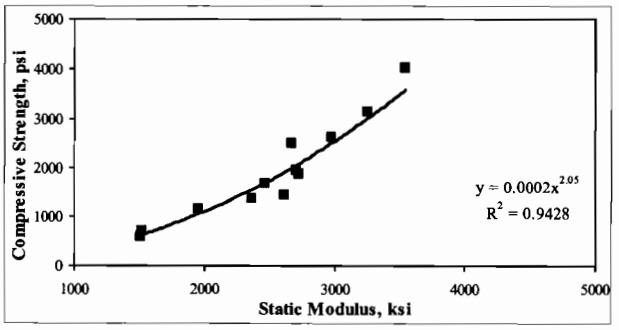

Figure B.3f - Typical relationships developed for a dirty limestone with fly ash mix, when water 70°F, 95°F and field curing are combined together.

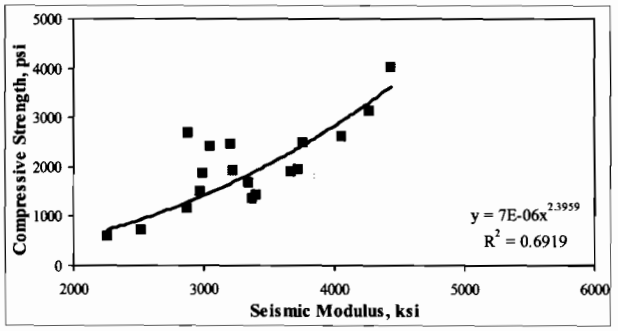

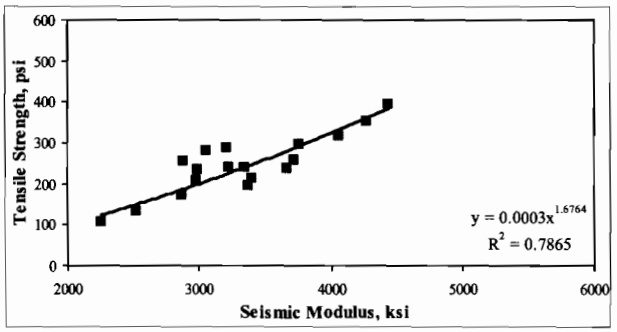

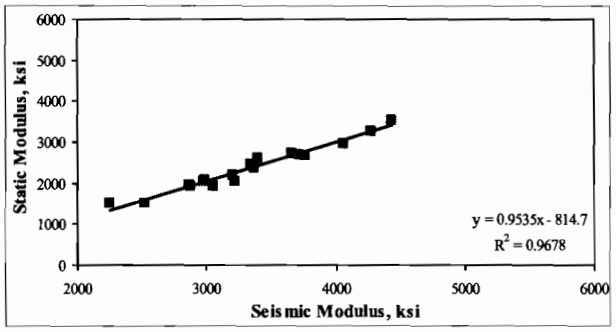

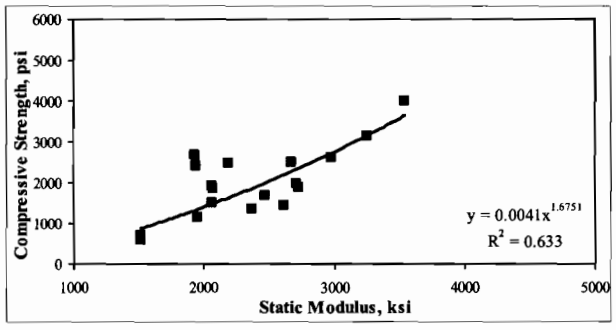

Figure B.3g - Typical relationships developed for a dirty limestone with fly ash mix, when water 70°F, water 95°F, room 70°F, room 95°F and field curing are combined together.

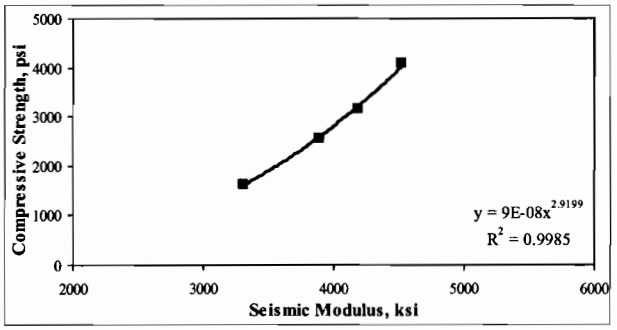

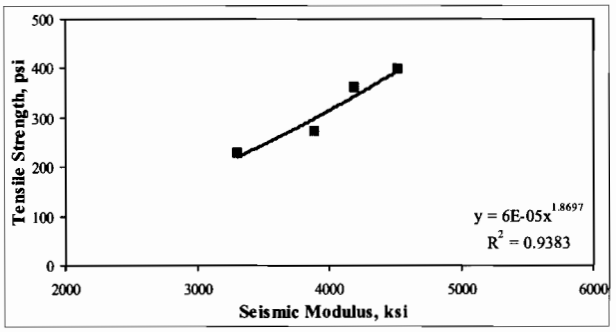

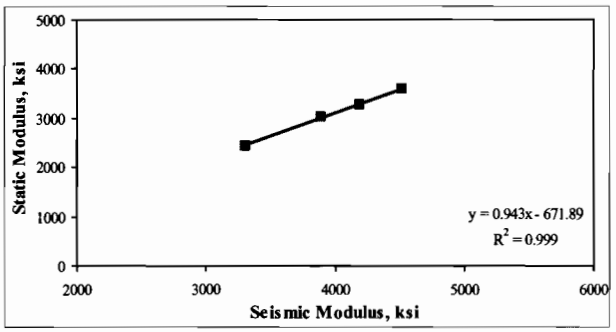

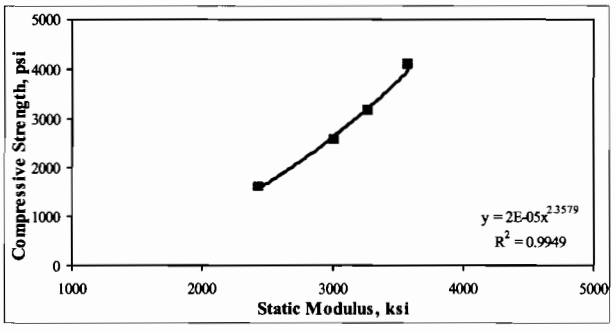

Figure B.4a - Typical relationships developed for a dirty limestone without fly ash mix cured in water at 70°F.

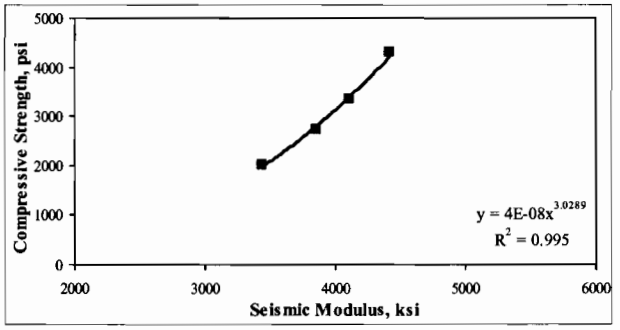

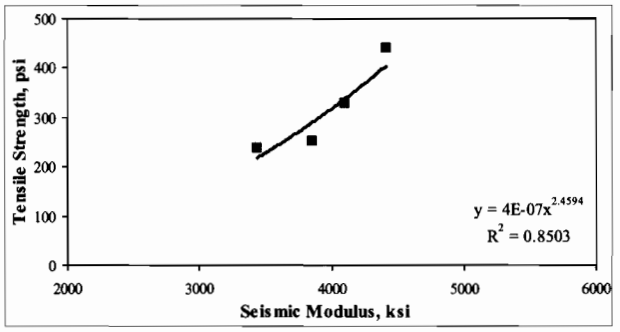

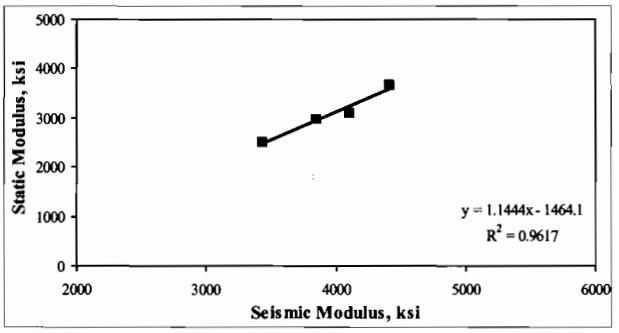

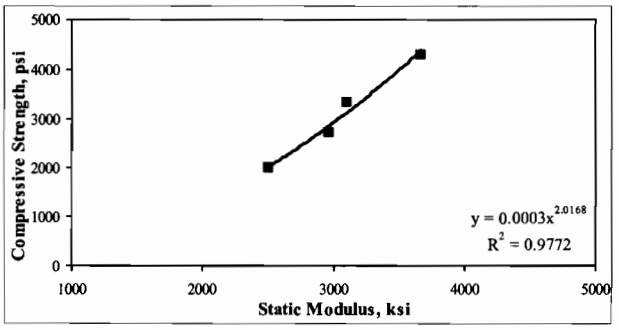

Figure B.4b - Typical relationships developed for a dirty limestone without fly ash mix cured in water at 95°F.

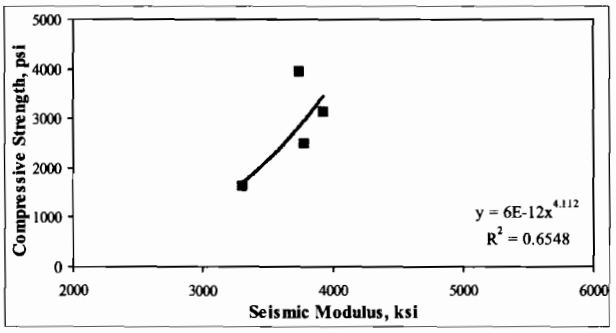

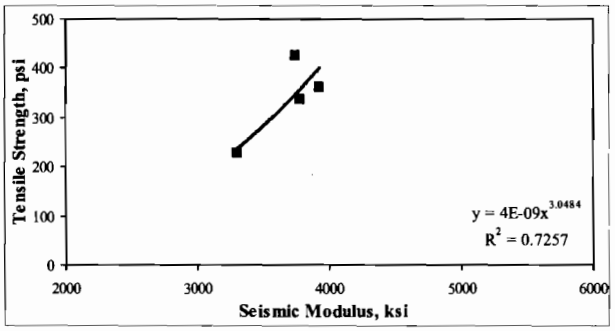

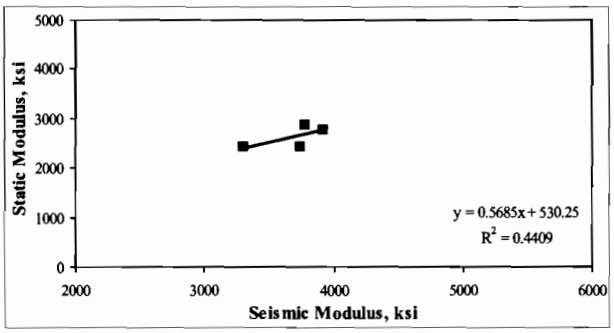

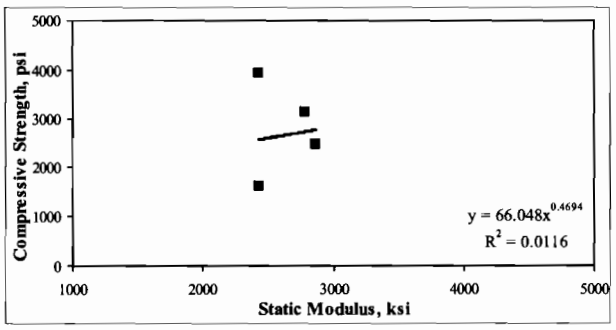

Figure B.4c - Typical relationships developed for a dirty limestone without fly ash mix cured in a room at 70°F.

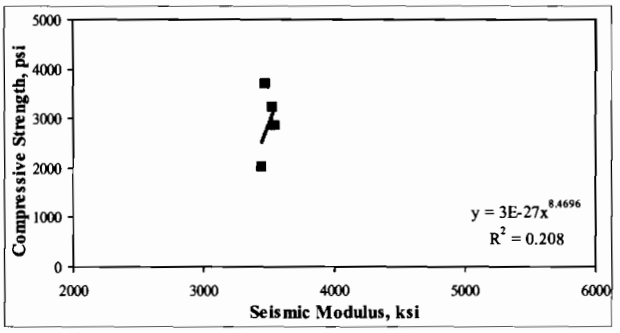

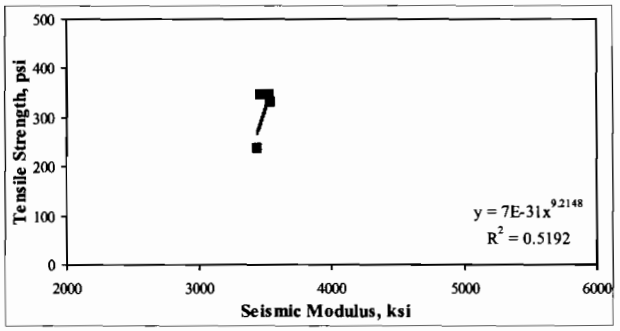

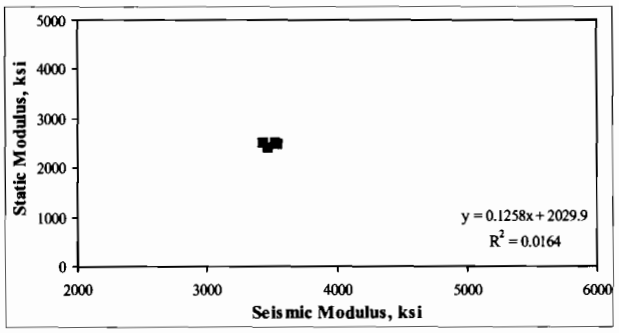

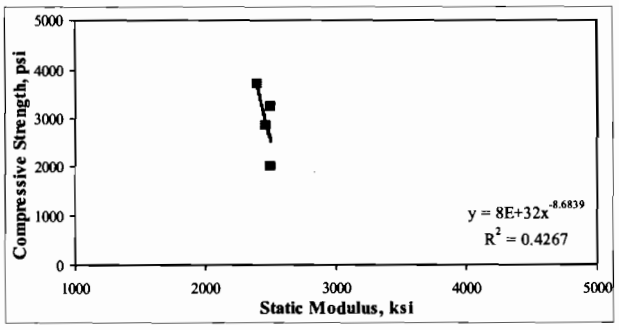

Figure B.4d - Typical relationships developed for a dirty limestone without fly ash mix cured in a room at 95°F.

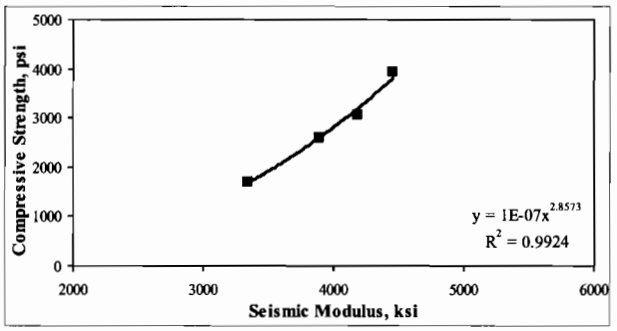

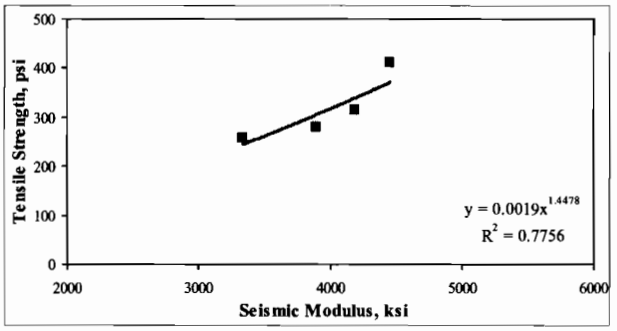

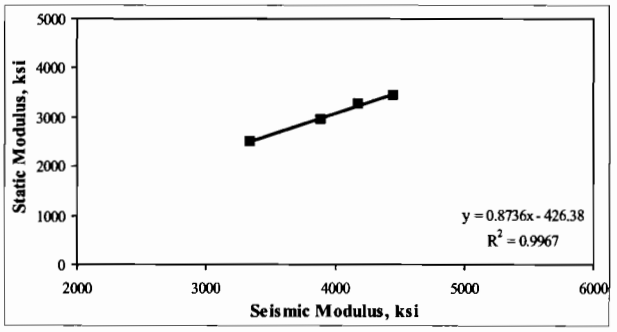

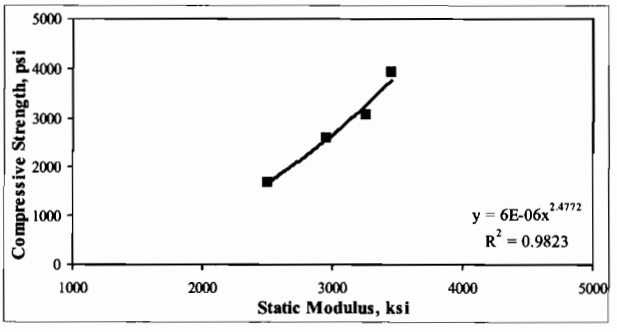

Figure B.4e - Typical relationships developed for a dirty limestone without fly ash mix cured in the field.

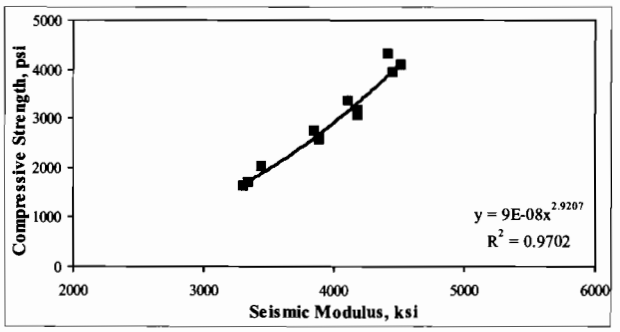

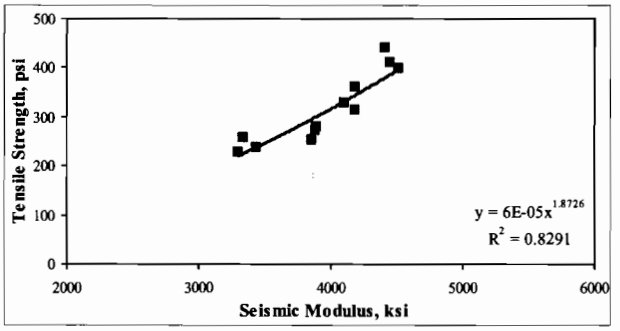

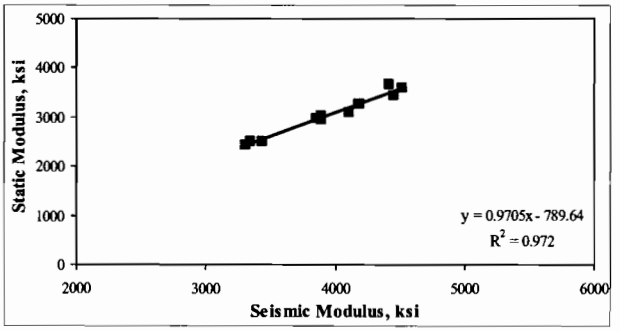

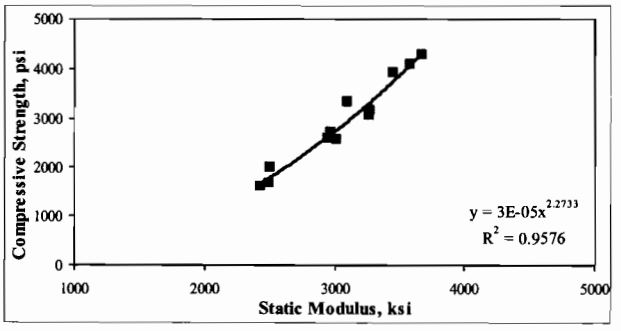

Figure B.4f - Typical relationships developed for a dirty limestone without fly ash mix, when water 70°F, water 95°F and field curing are combined together.

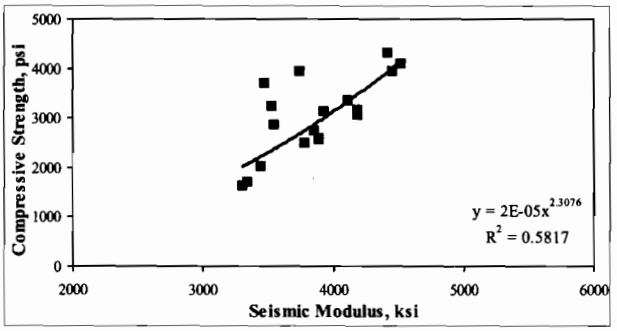

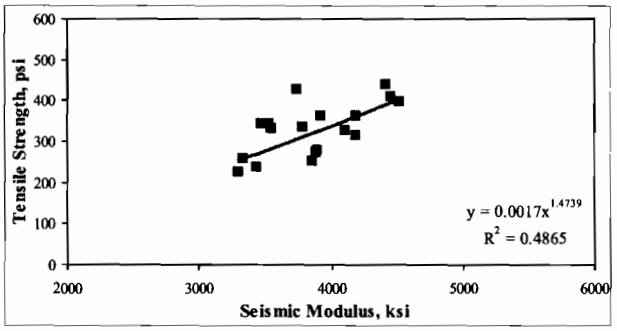

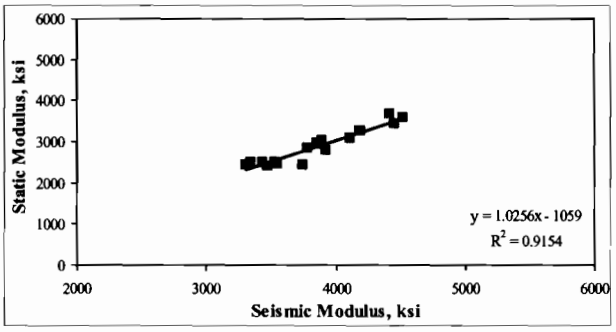

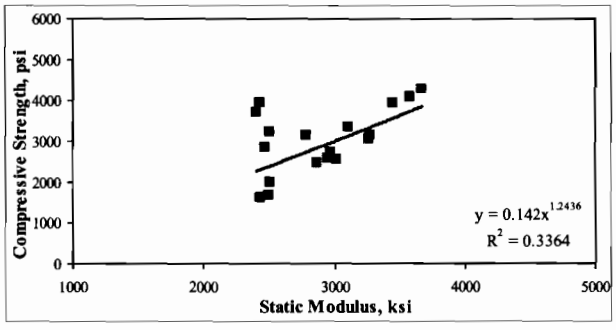

Figure B.4g - Typical relationships developed for a clean limestone without fly ash mix, when water 70°F, water 95°F, room 70°F, room 95°F and field curing are combined together.

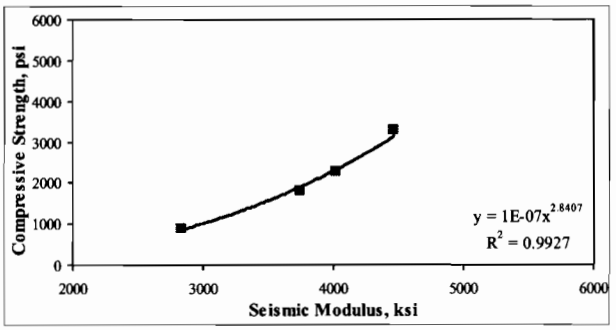

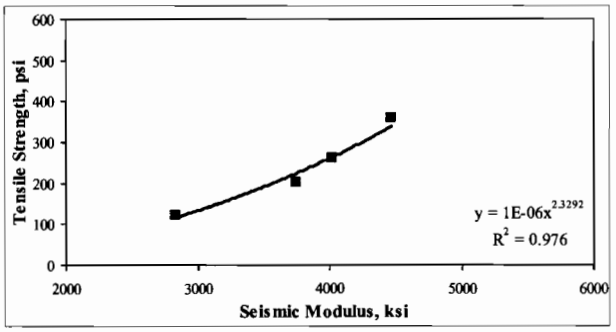

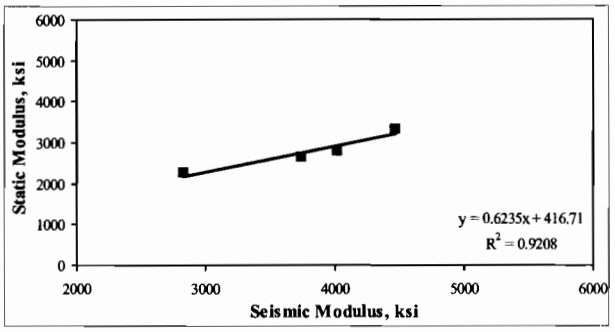

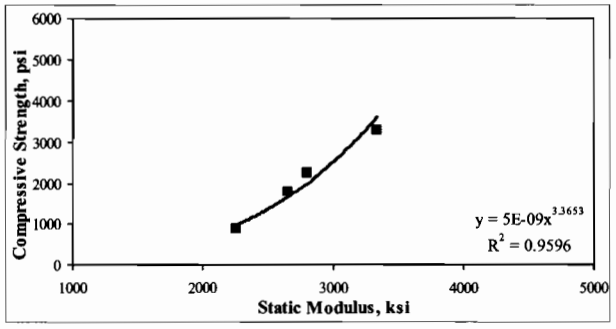

Figure B.5a - Typical relationships developed for a clean siliceous river gravel with fly ash mix cured in water at 70°F.

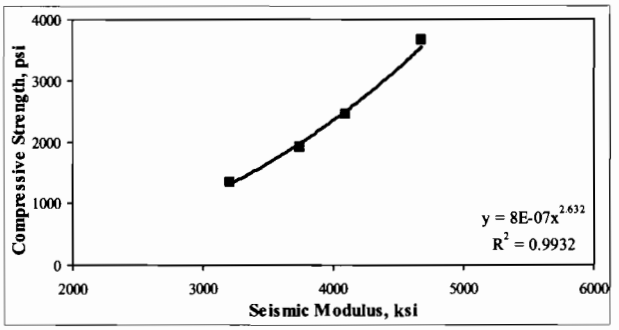

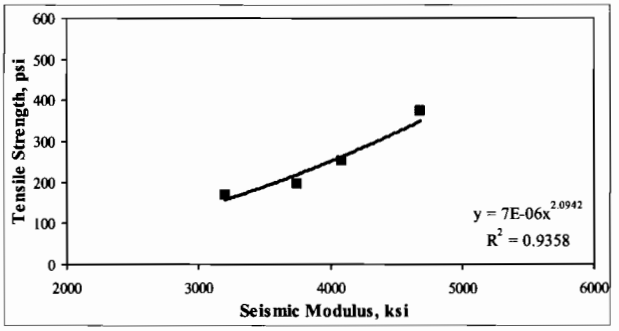

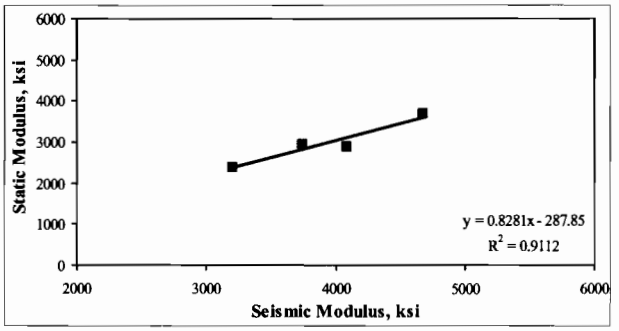

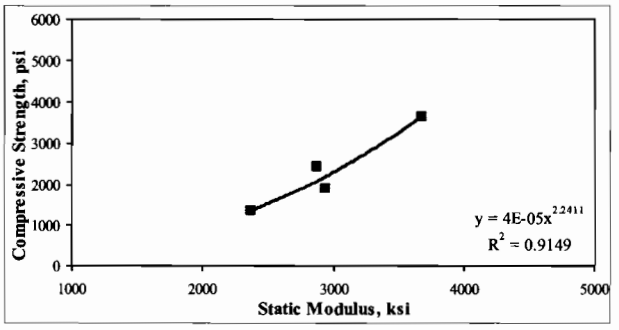

Figure B.5b - Typical relationships developed for a clean siliceous river gravel with fly ash mix cured in water at 95°F.

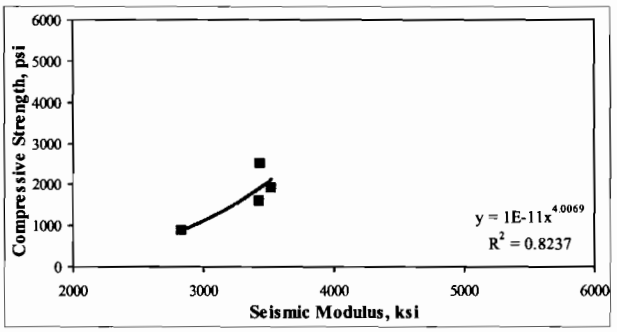

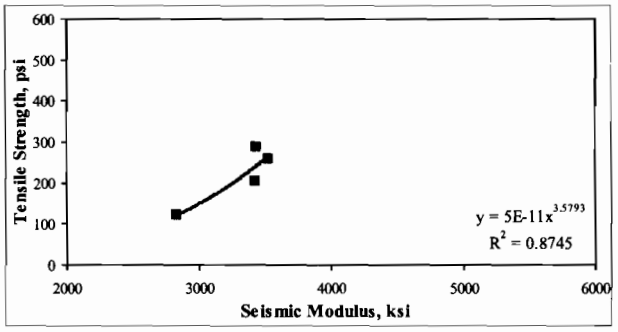

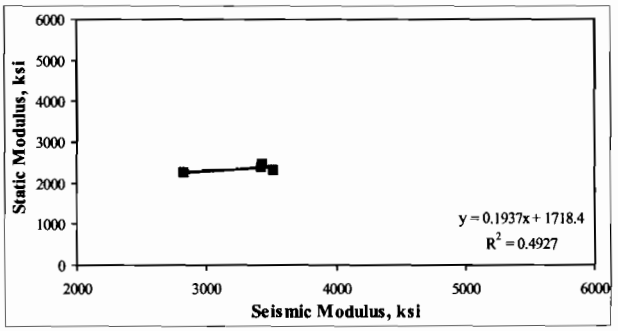

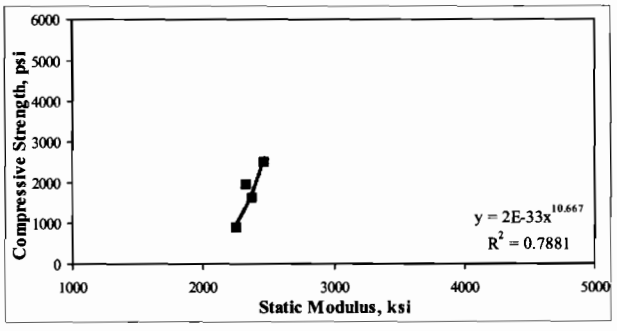

Figure B.5c - Typical relationships developed for a clean siliceous river gravel with fly ash mix cured in a room at 70°F.

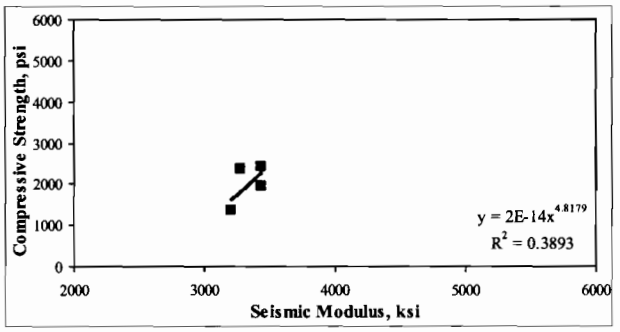

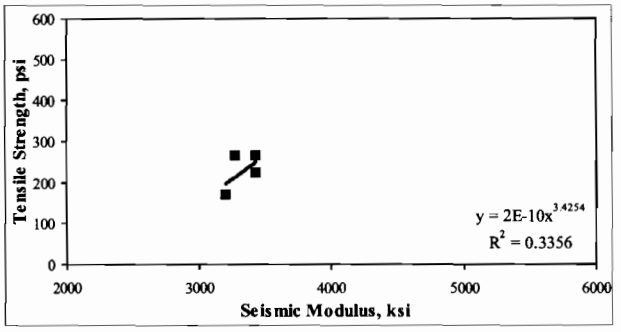

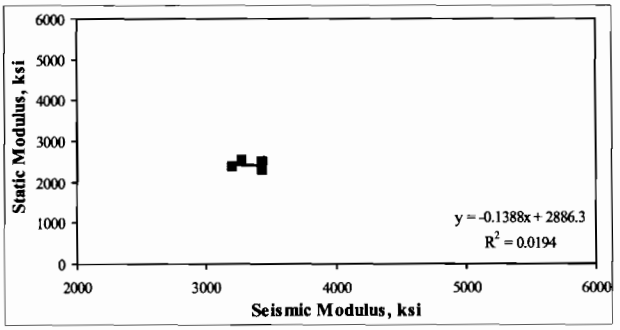

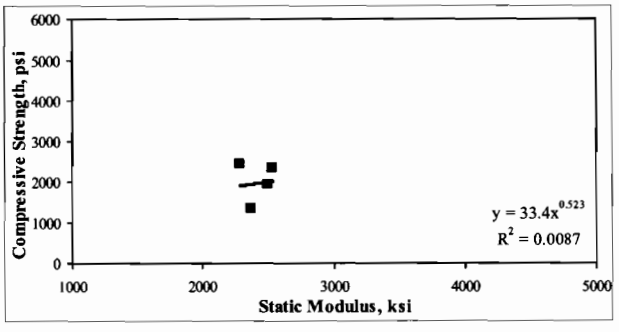

Figure B.5d - Typical relationships developed for a clean siliceous river gravel with fly ash mix cured in a room at 95°F.

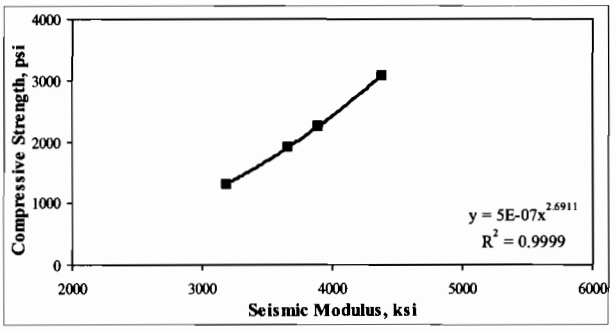

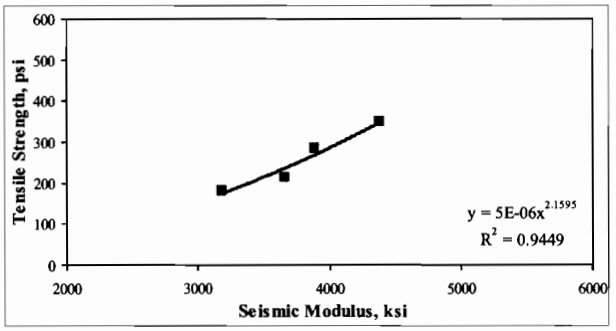

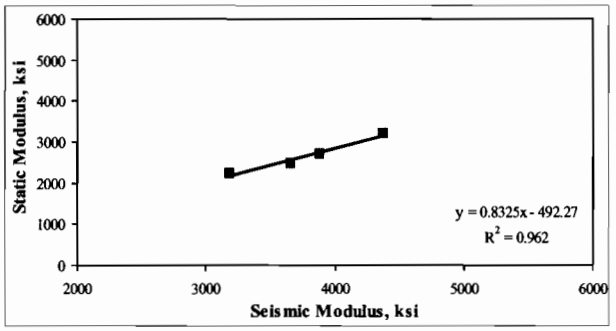

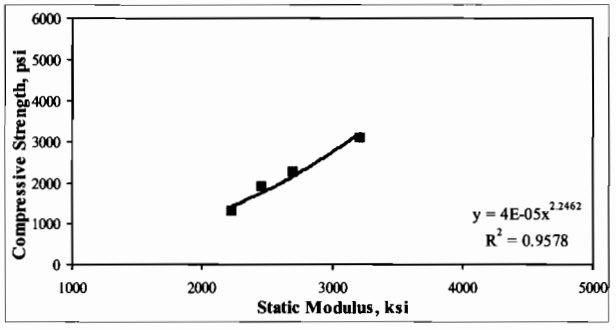

Figure B.5e - Typical relationships developed for a clean siliceous river gravel with fly ash mix cured in the field.

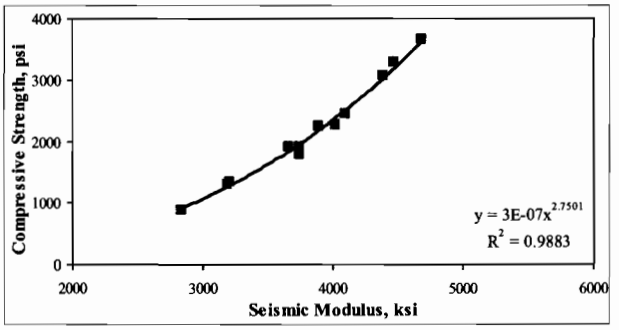

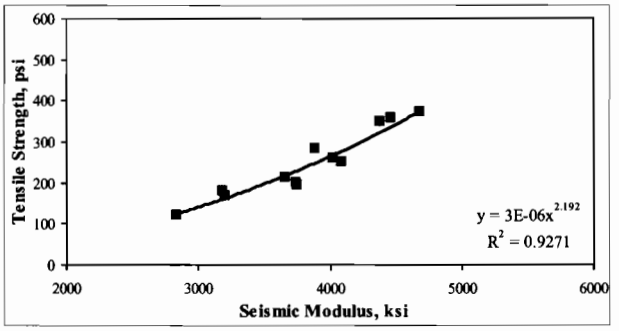

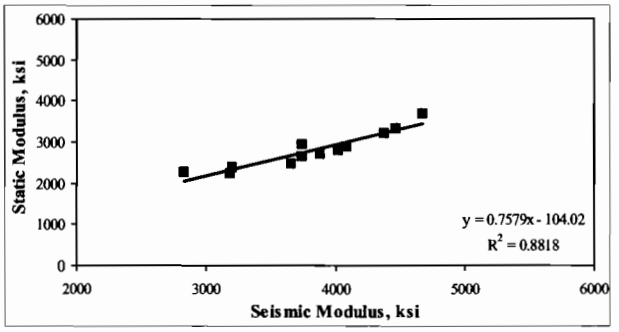

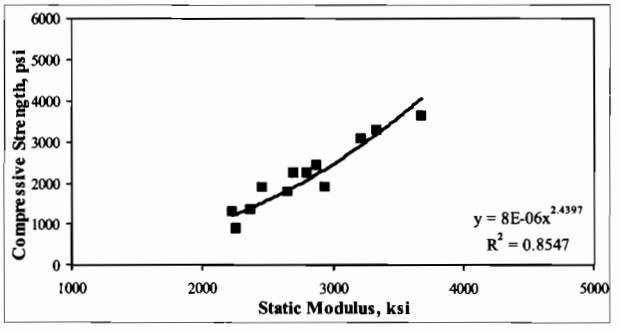

Figure B.5f - Typical relationships developed for a clean siliceous river gravel with fly ash mix, when water 70°F, 95°F and field curing are combined together.

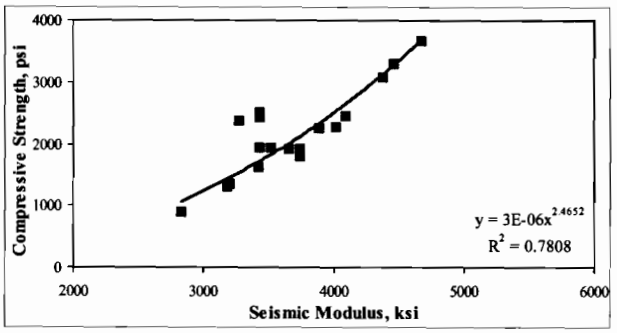

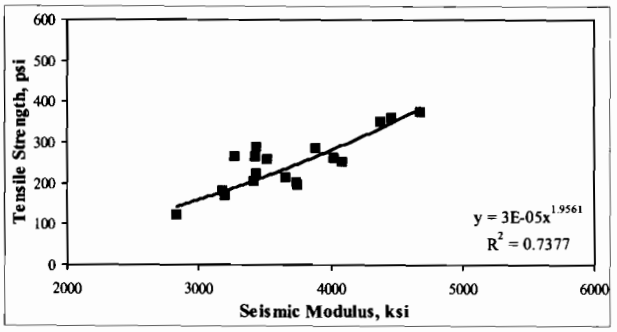

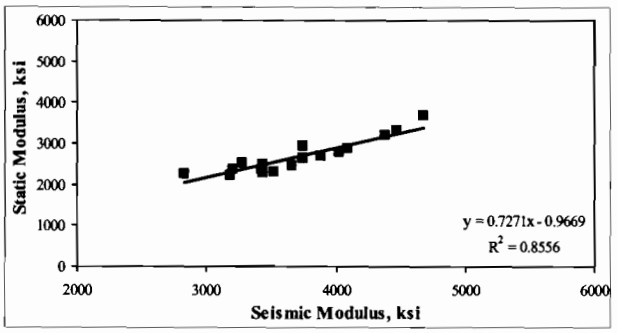

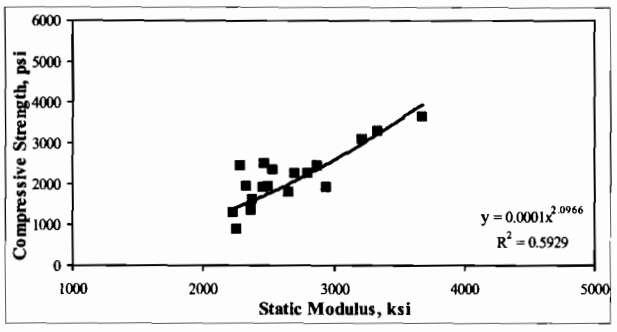

Figure B.5g - Typical relationships developed for a clean siliceous river gravel with fly ash mix, when water 70°F, water 95°F, room 70°F, room 95°F and field curing are combined together.

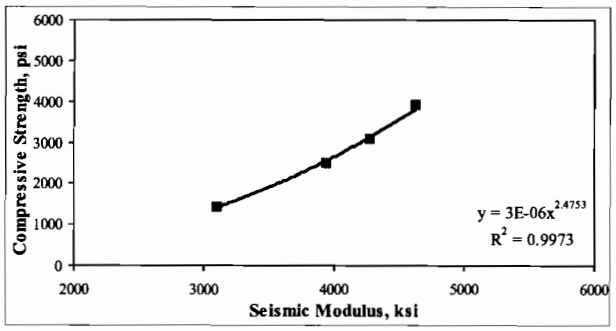

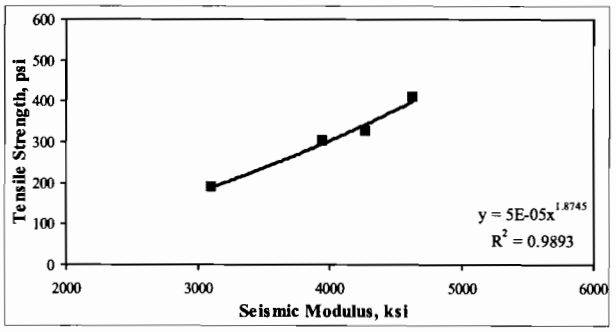

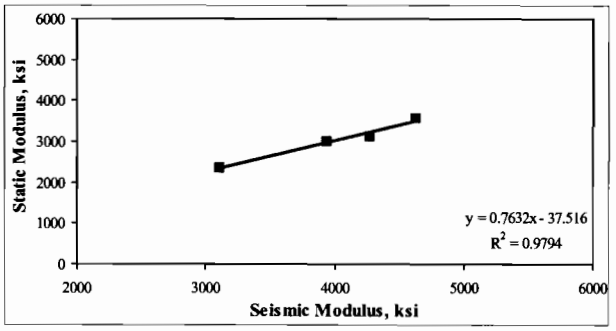

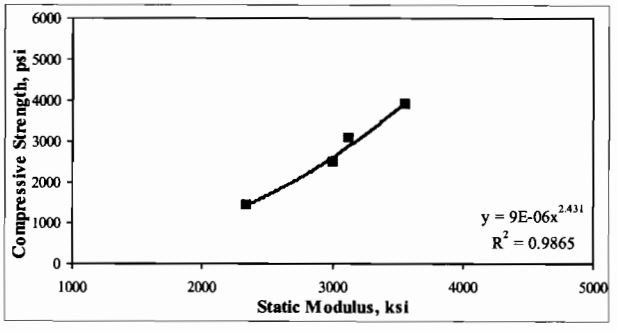

Figure B.6a - Typical relationships developed for a clean siliceous river gravel without fly ash mix cured in water at 70°F.

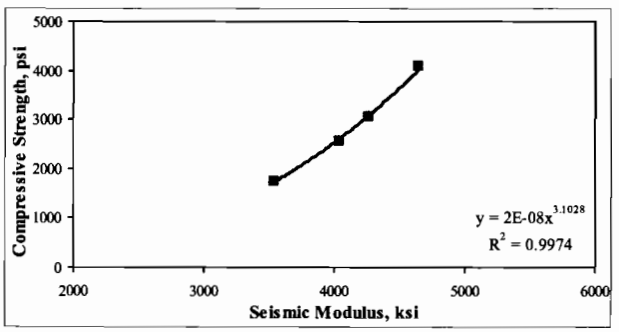

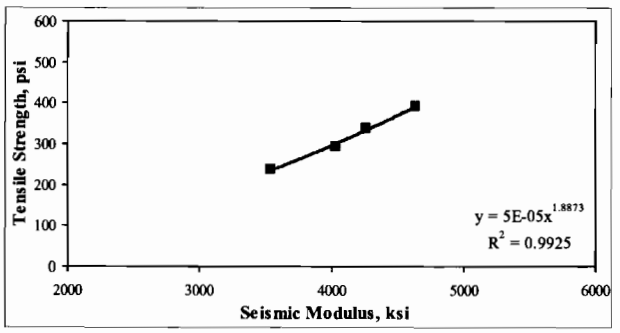

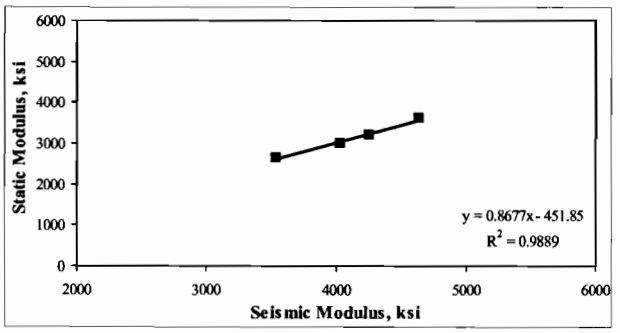

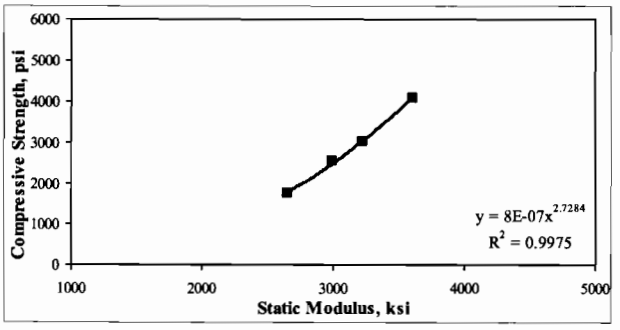

Figure B.6b - Typical relationships developed for a clean siliceous river gravel without fly ash mix cured in water at 95°F.

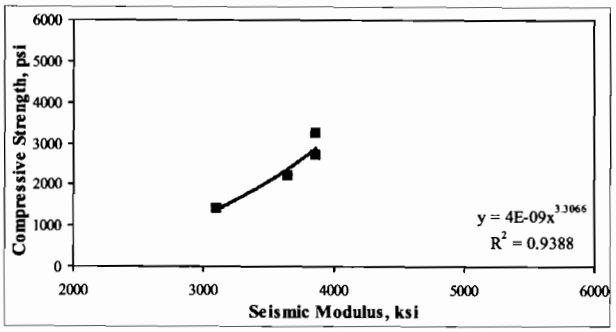

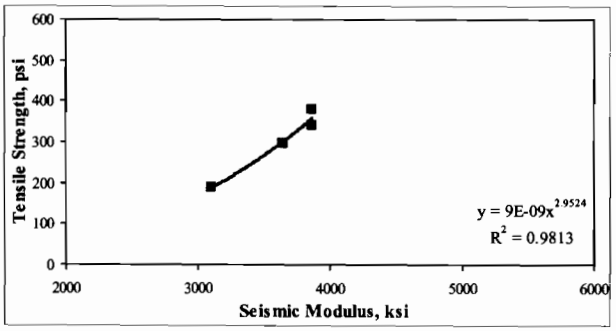

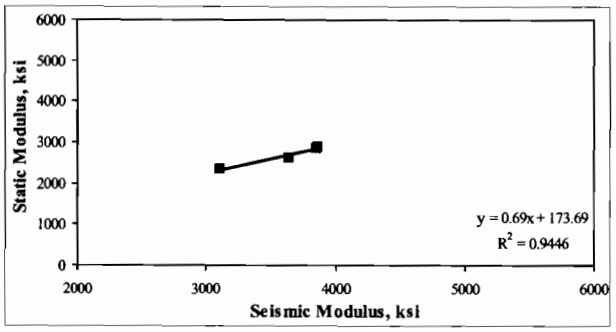

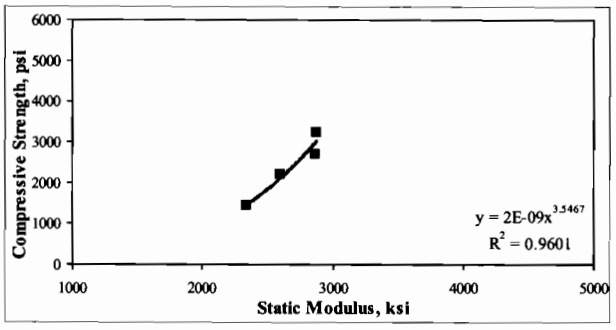

Figure B.6c - Typical relationships developed for a clean siliceous river gravel without fly ash mix cured in a room at 70°F.

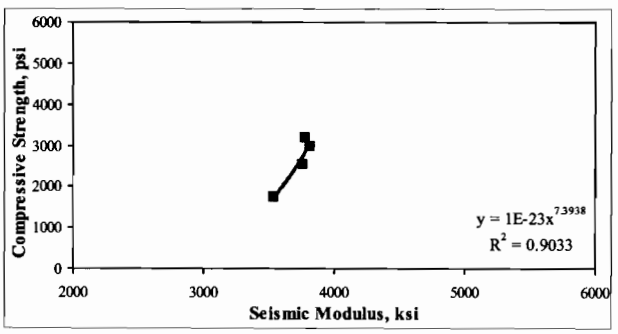

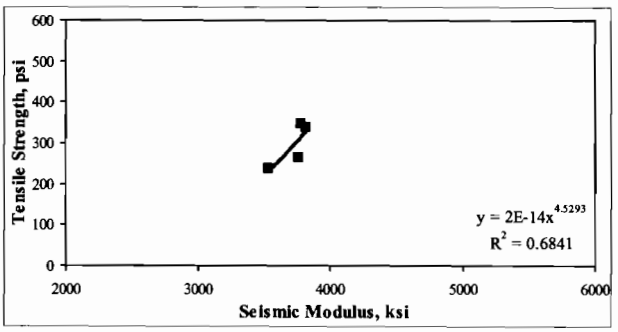

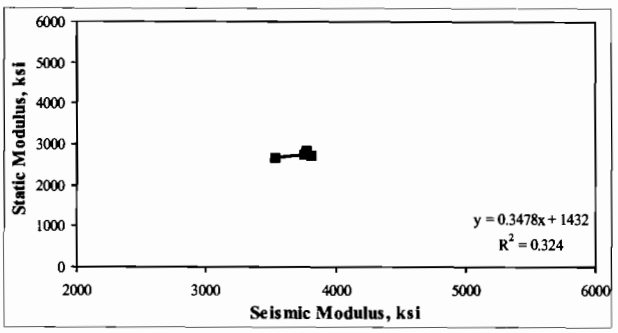

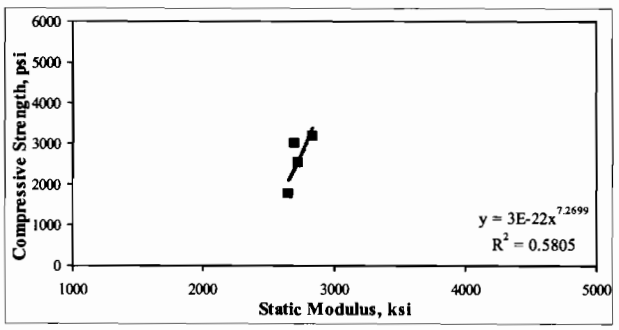

Figure B.6d - Typical relationships developed for a clean siliceous river gravel without fly ash mix cured in a room at 95°F.

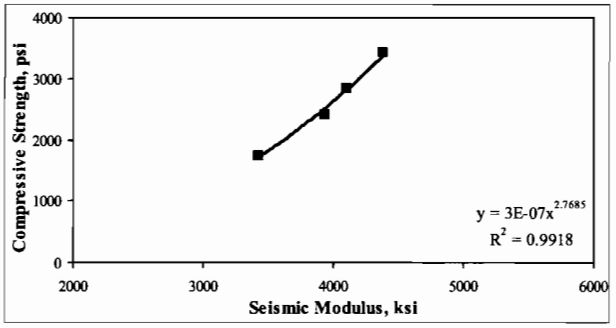

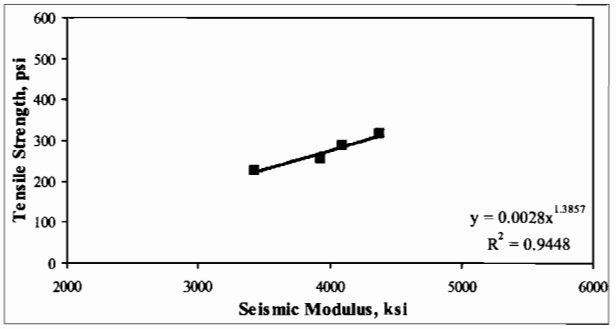

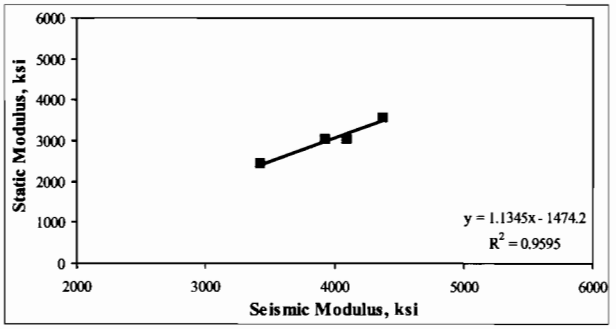

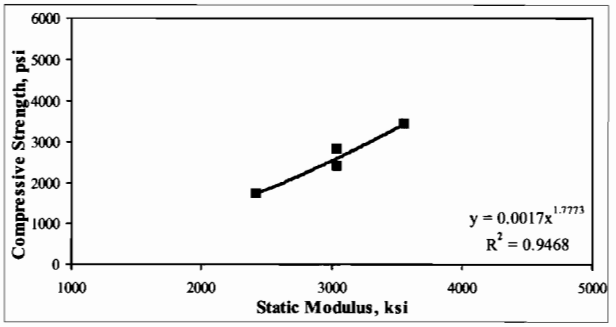

Figure B.6e - Typical relationships developed for a clean siliceous river gravel without fly ash mix cured in the field.

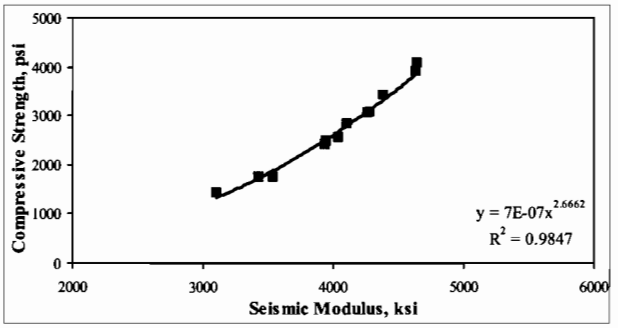

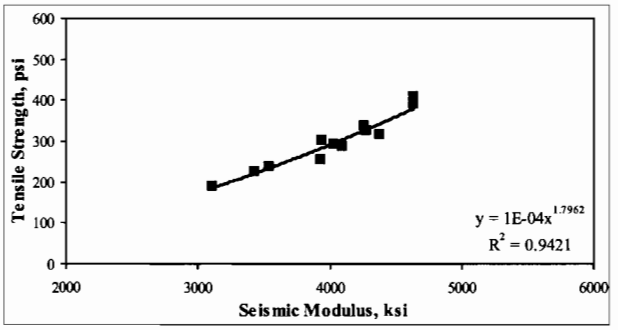

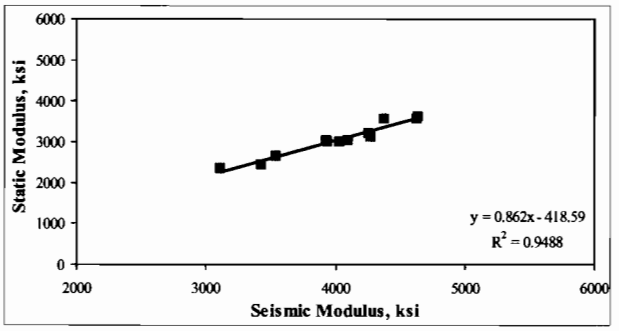

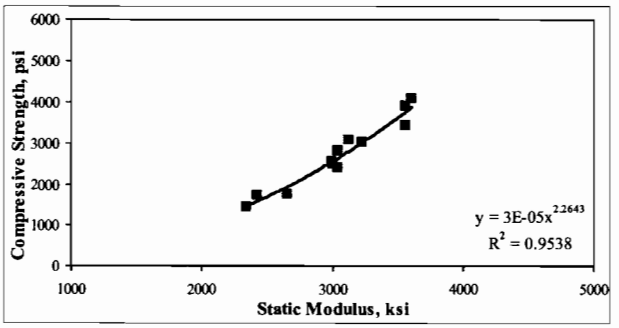

Figure B.6f - Typical relationships developed for a clean siliceous river gravel without fly ash mix, when water 70°F, 95°F and field curing are combined together.

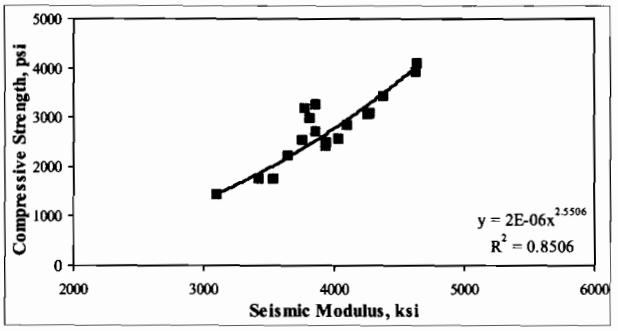

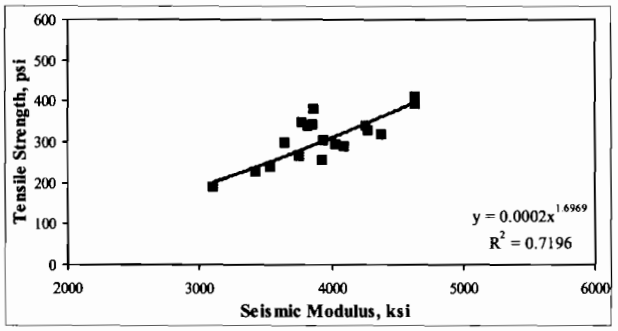

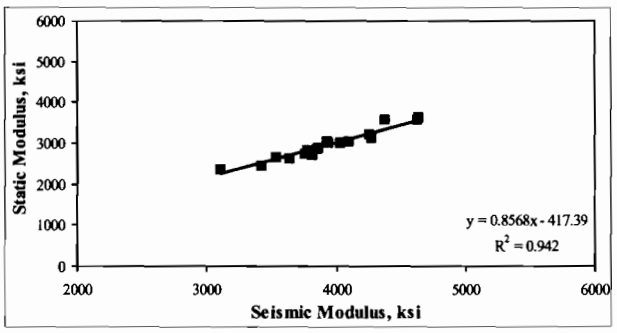

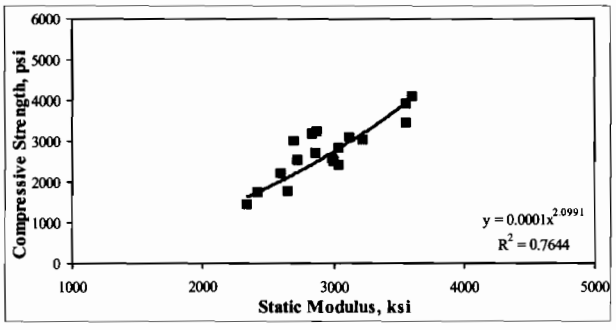

Figure B.6g - Typical relationships developed for a clean siliceous river gravel without fly ash mix, when water 70°F, water 95°F, room 70°F, room 95°F and field curing are combined together.

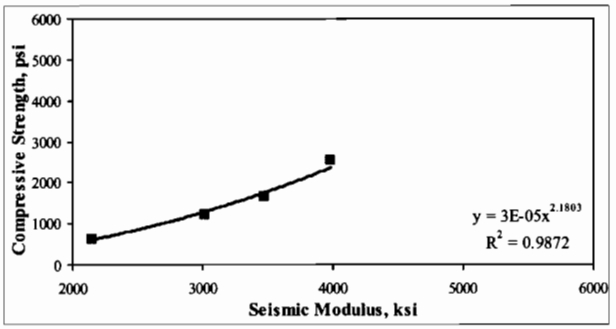

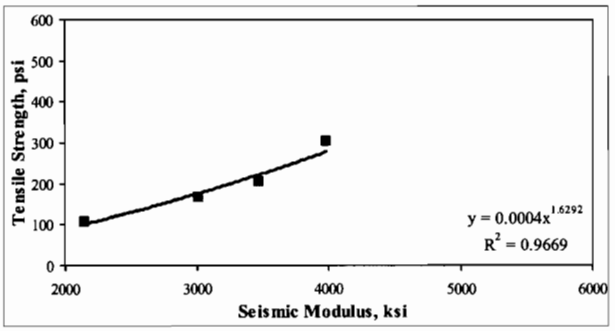

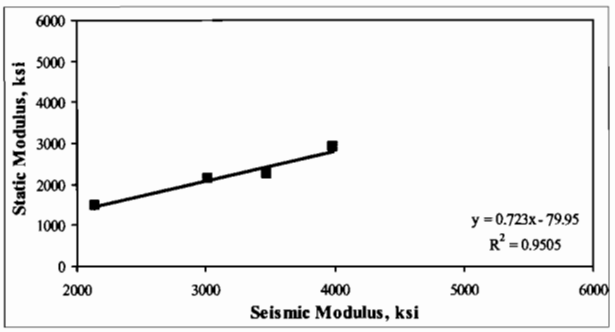

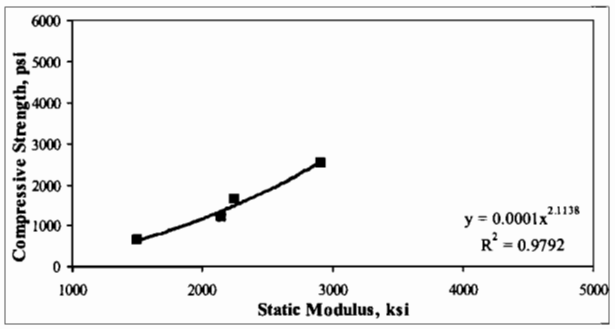

Figure B.7a - Typical relationships developed for a dirty siliceous river gravel with fly ash mix cured in water at 70°F.

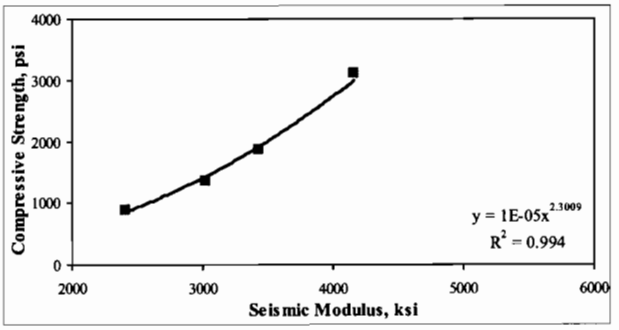

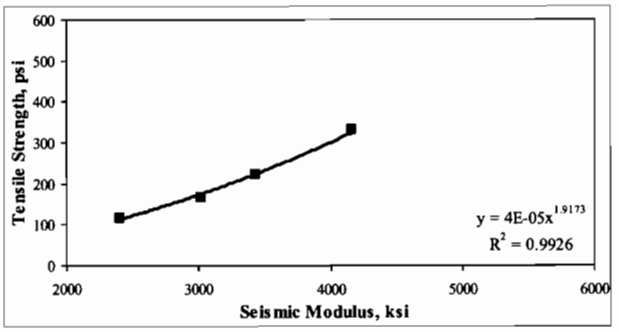

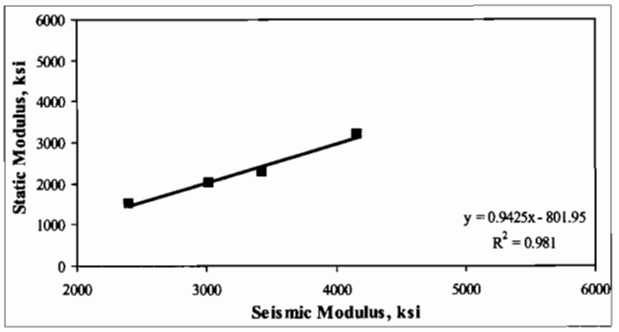

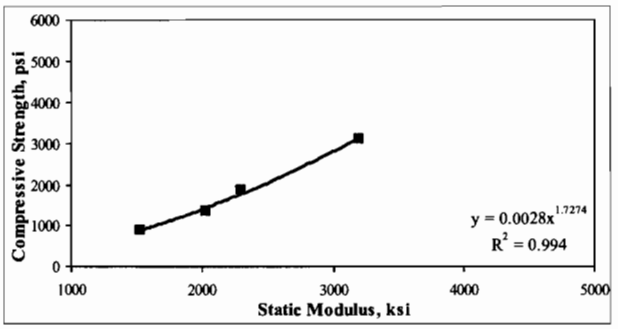

Figure B.7b - Typical relationships developed for a dirty siliceous river gravel with fly ash mix cured in water at 95°F.

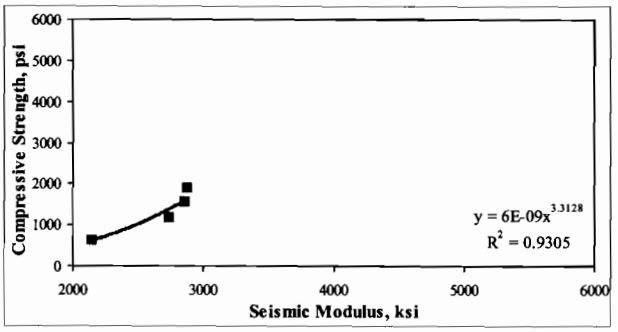

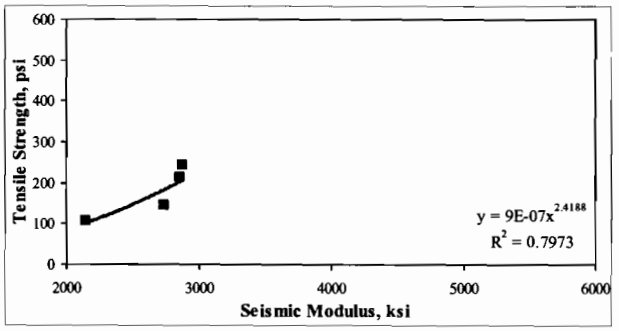

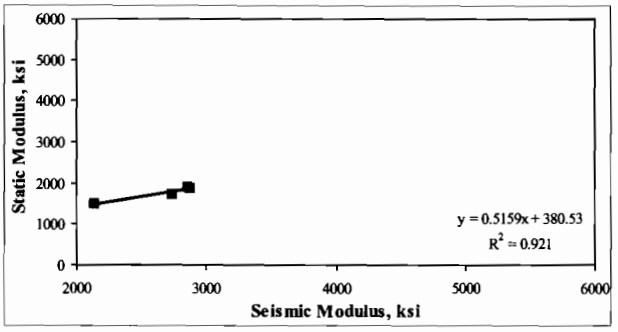

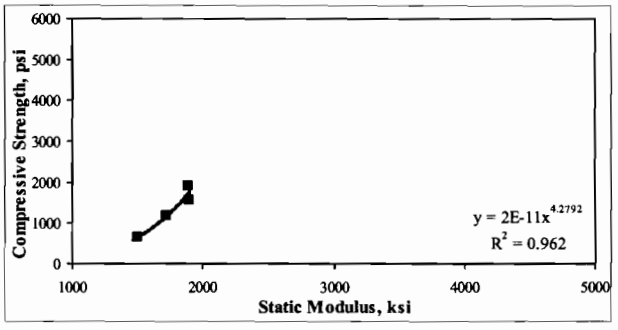

Figure B.7c - Typical relationships developed for a dirty siliceous river gravel with fly ash mix cured in a room at 70°F.

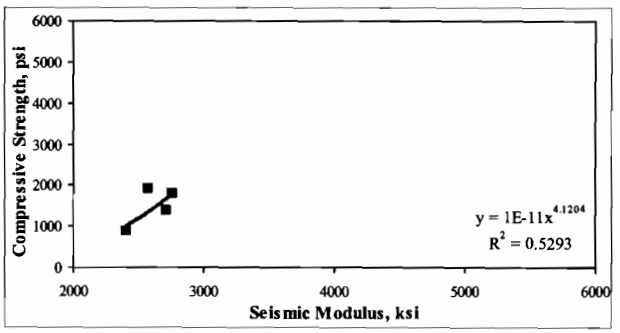

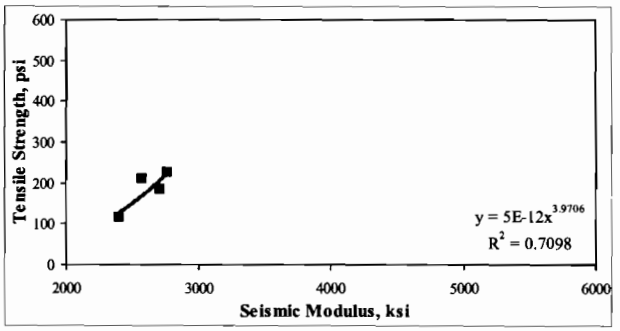

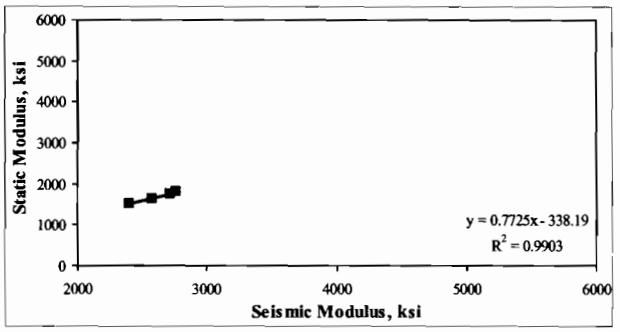

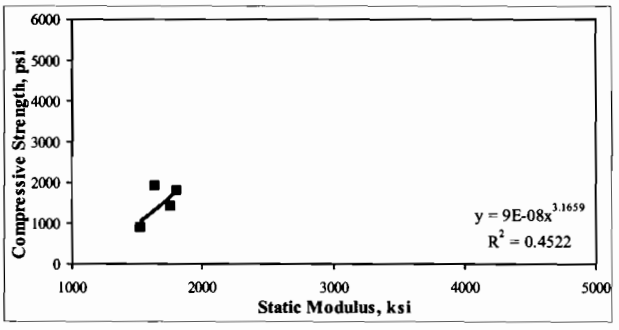

Figure B.7d - Typical relationships developed for a dirty siliceous river gravel with fly ash mix cured in a room at 95°F.

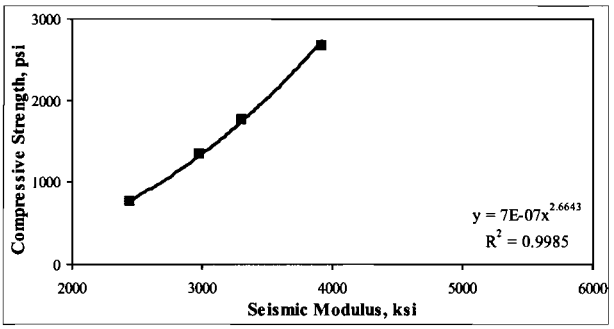

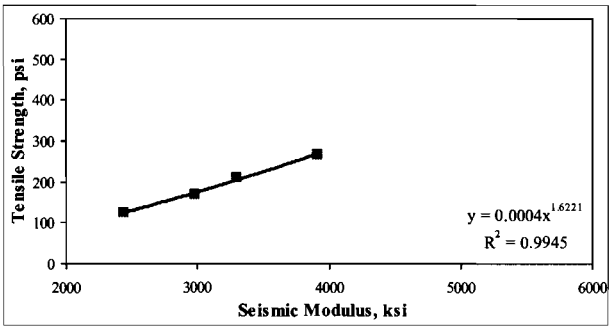

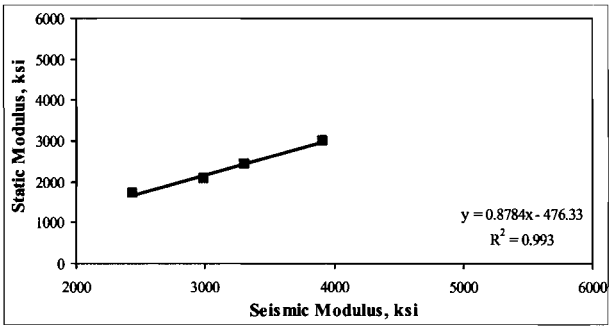

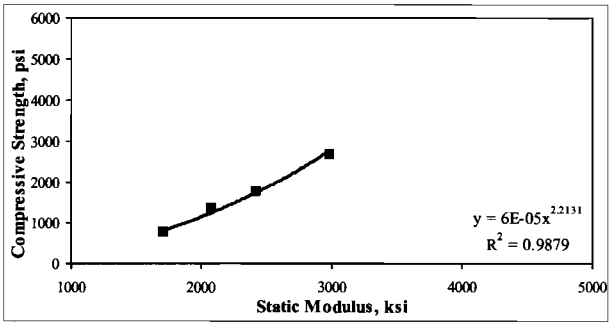

Figure B.7e - Typical relationships developed for a dirty siliceous river gravel without fly ash mix cured in the field.

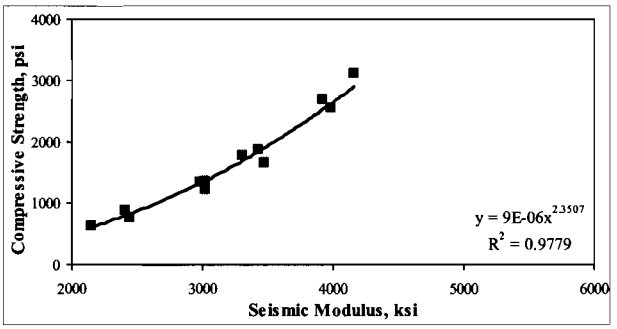

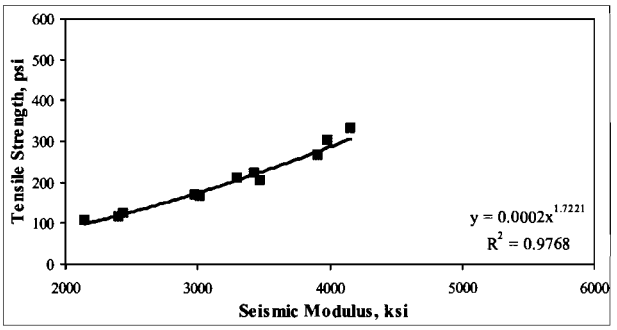

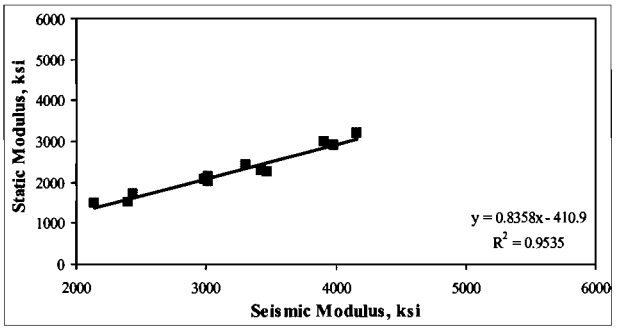

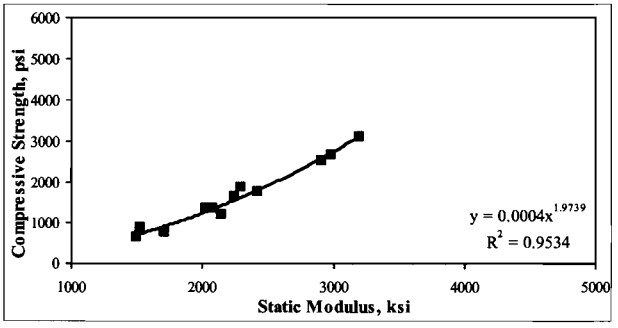

Figure B.7f - Typical relationships developed for a dirty siliceous river gravel with fly ash mix, when water 70°F, 95°F and field curing are combined together.

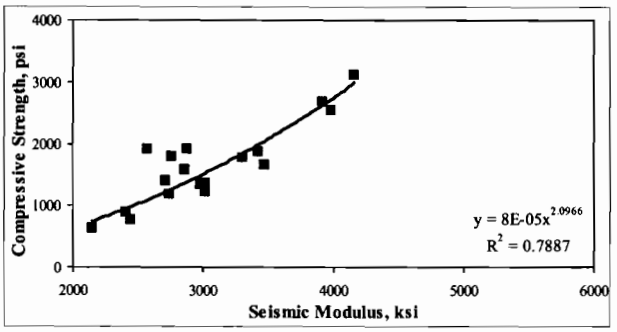

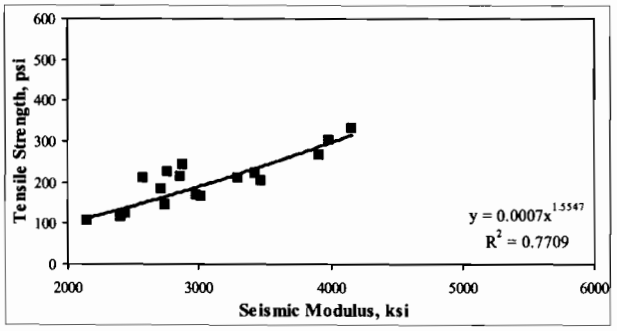

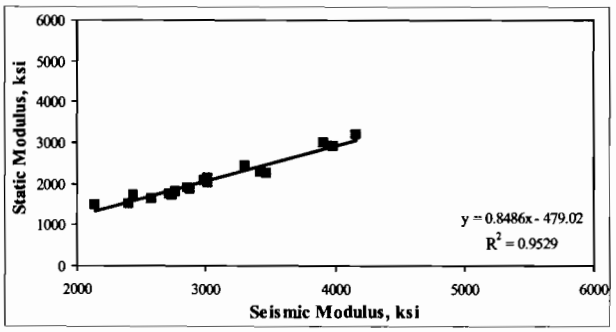

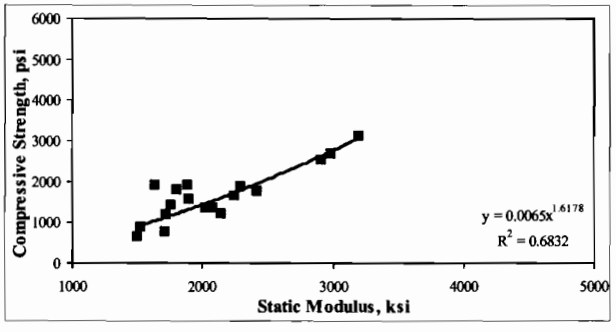

Figure B.7g - Typical relationships developed for a dirty siliceous river gravel with fly ash mix, when water 70°F, water 95°F, room 70°F, room 95°F and field curing are combined together.

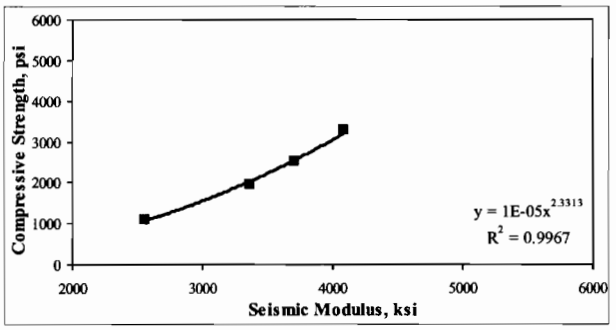

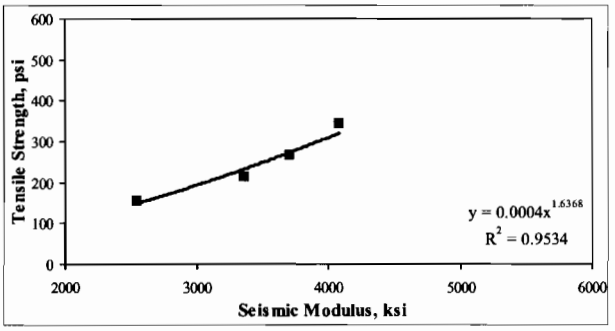

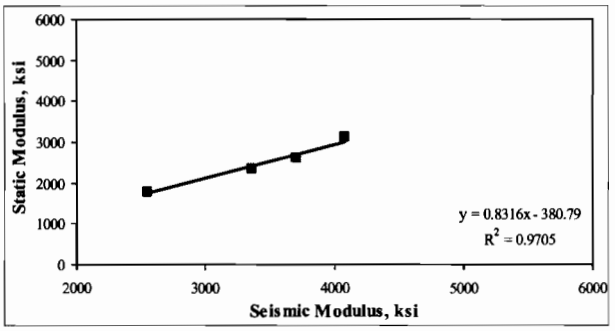

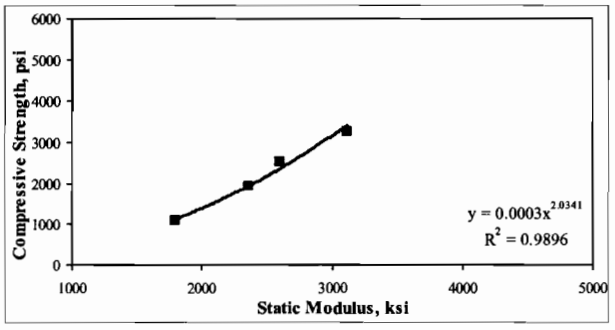

Figure B.8a - Typical relationships developed for a dirty siliceous river gravel without fly ash mix cured in water at 70°F.

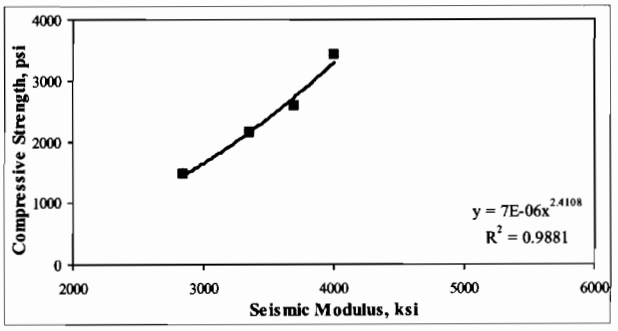

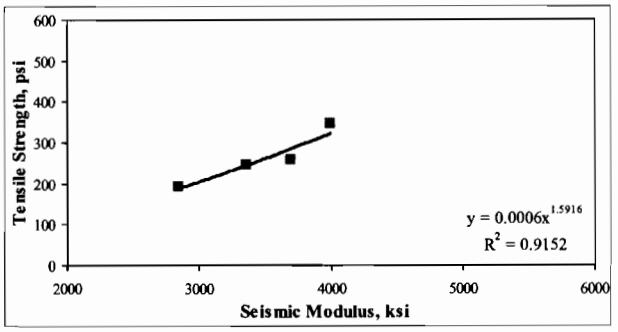

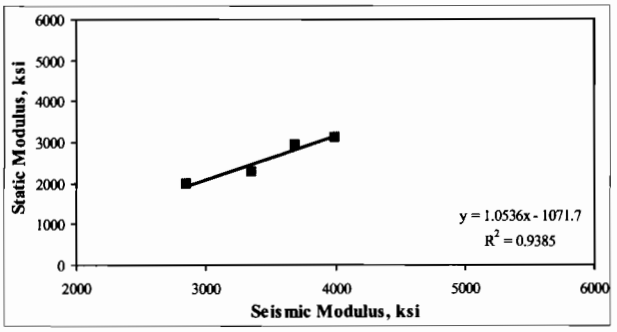

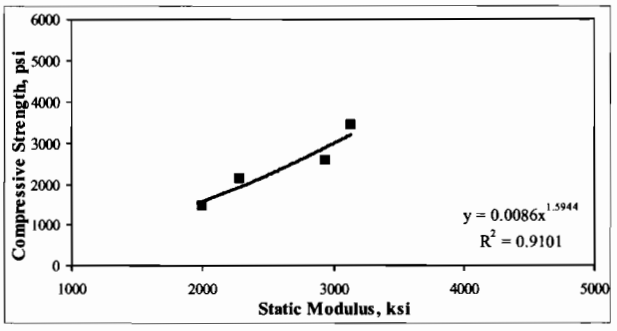

Figure B.8b - Typical relationships developed for a dirty siliceous river gravel without fly ash mix cured in water at 95°F.

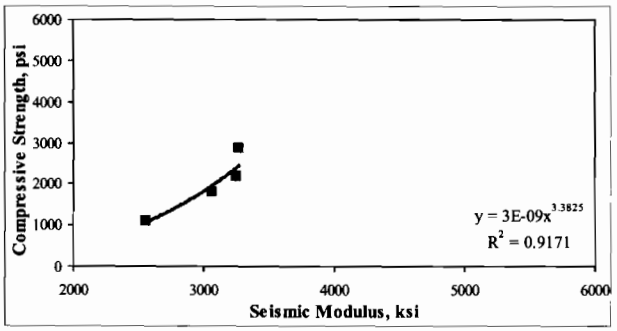

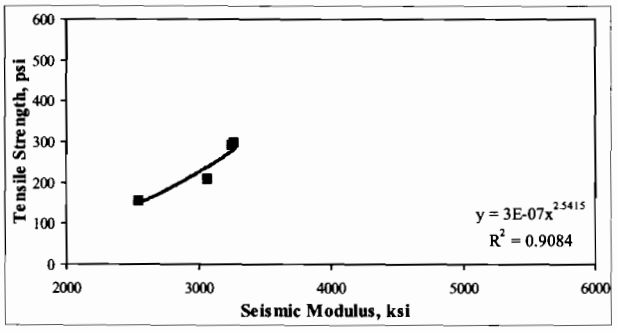

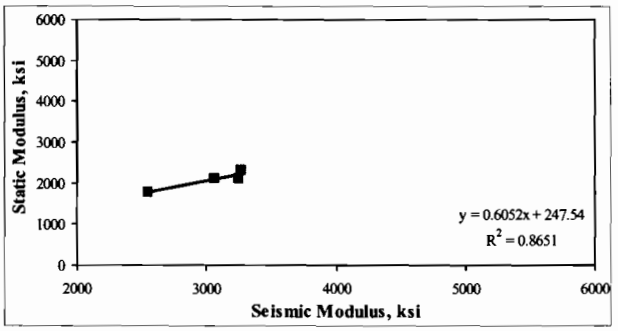

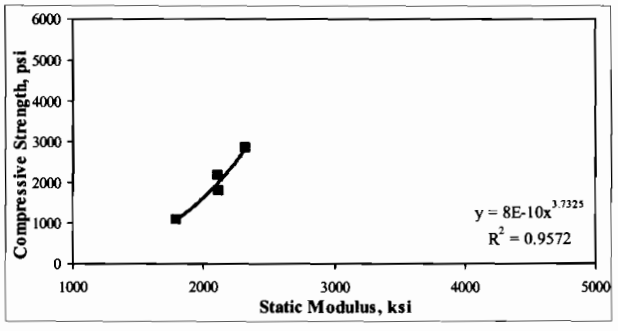

Figure B.8c - Typical relationships developed for a dirty siliceous river gravel without fly ash mix cured in a room at 70°F.

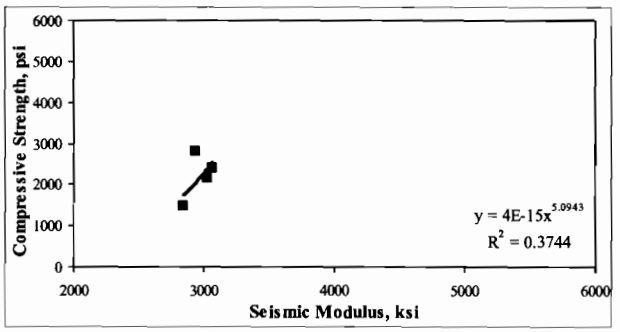

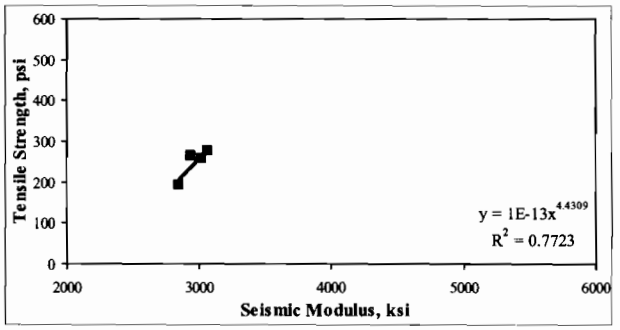

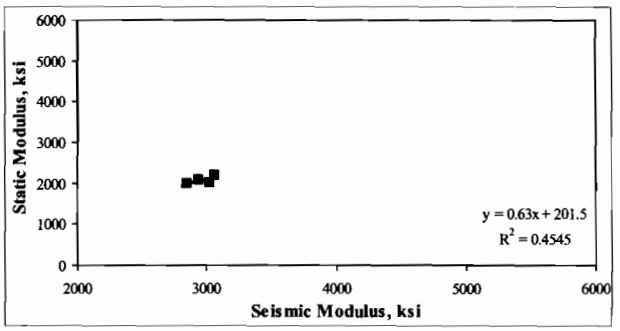

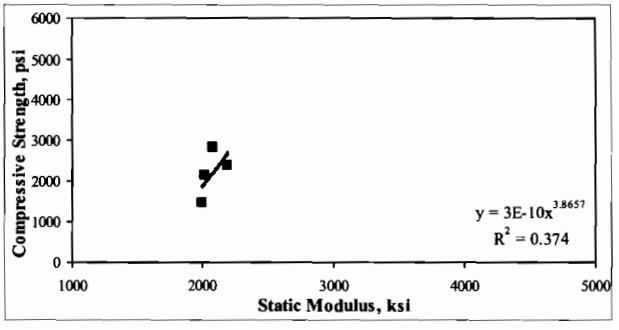

Figure B.8d - Typical relationships developed for a dirty siliceous river gravel without fly ash mix cured in a room at 95°F.

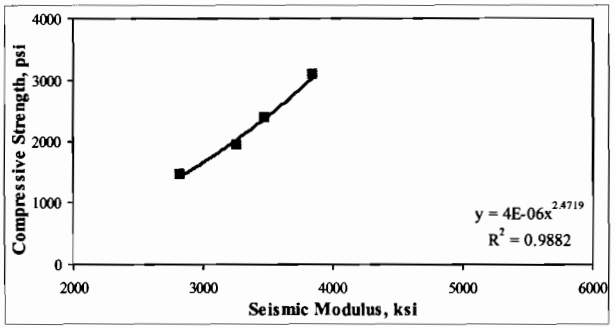

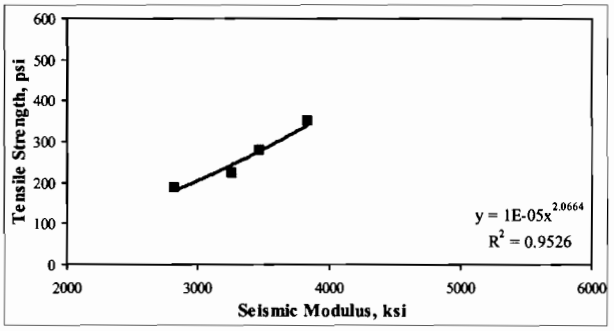

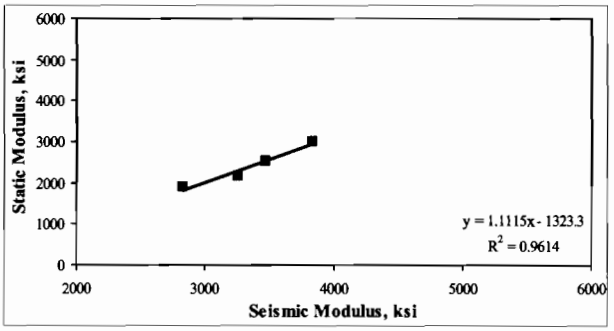

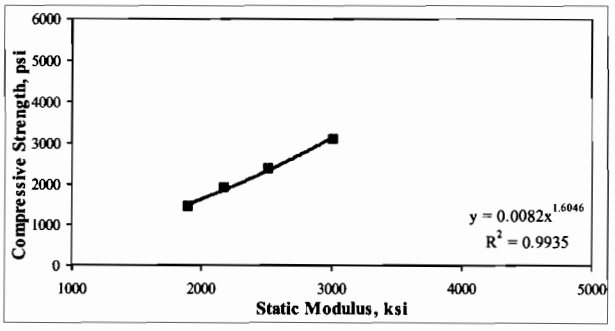

Figure B.8e - Typical relationships developed for a dirty siliceous river gravel without fly ash mix cured in the field.

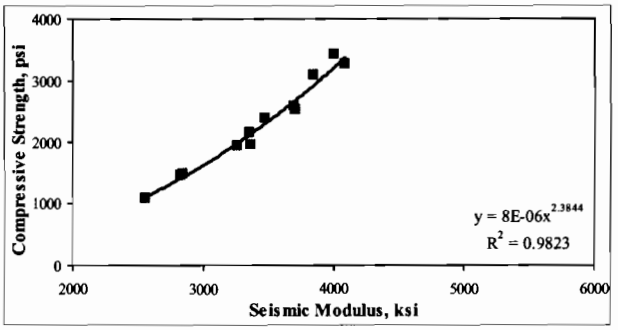

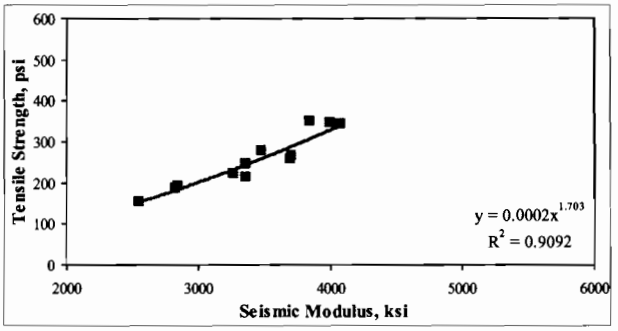

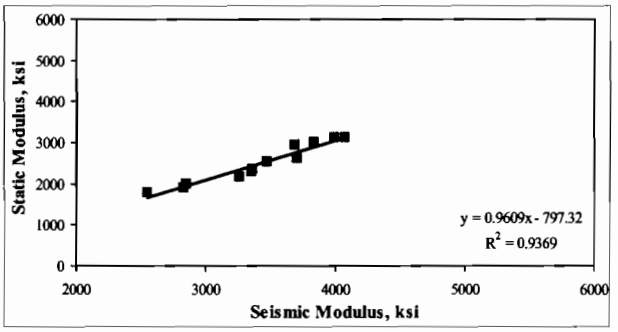

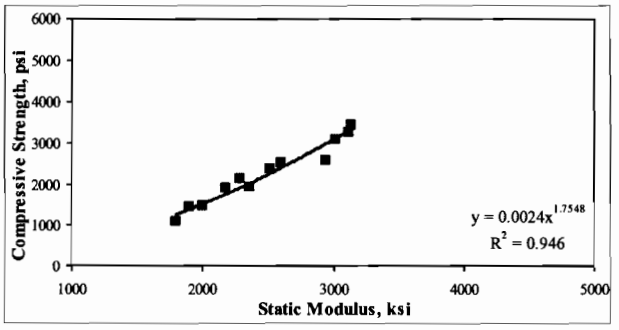

Figure B.8f - Typical relationships developed for a clean siliceous river gravel without fly ash mix, when water 70°F, 95°F and field curing are combined together.

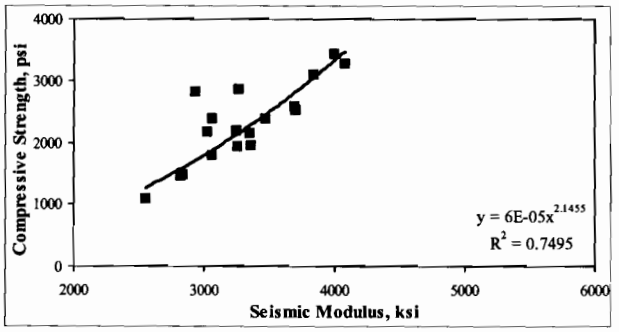

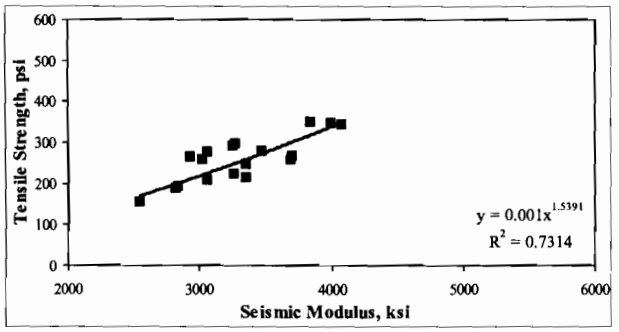

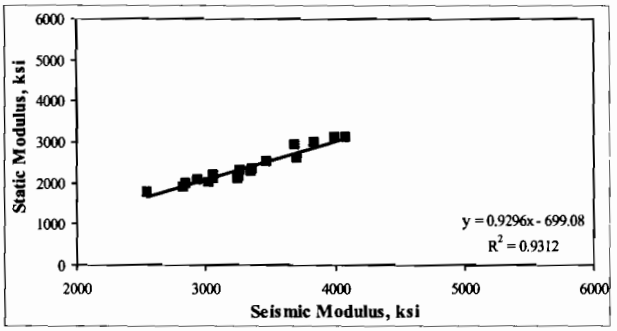

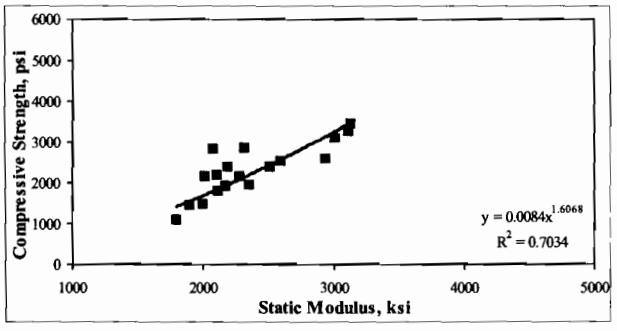

Figure B.8g - Typical relationships developed for a dirty siliceous river gravel without fly ash mix, when water 70°F, water 95°F, room 70°F, room 95°F and field curing are combined together.

Appendix C

Typical Relationships Developed in Phase II

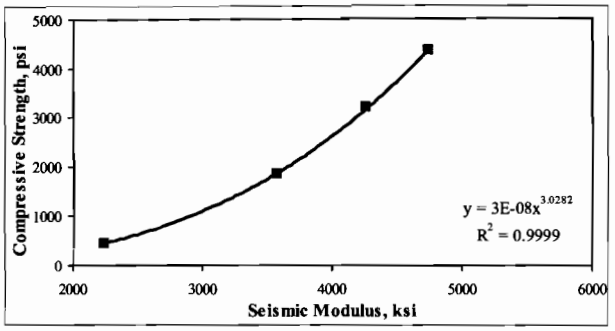

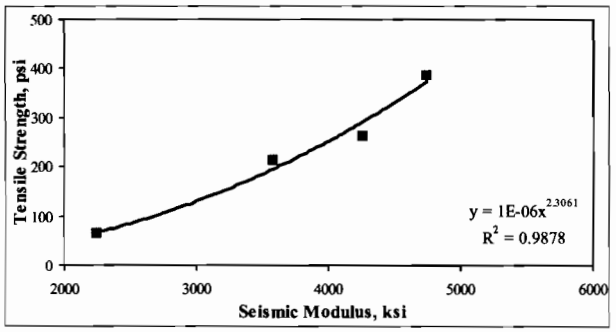

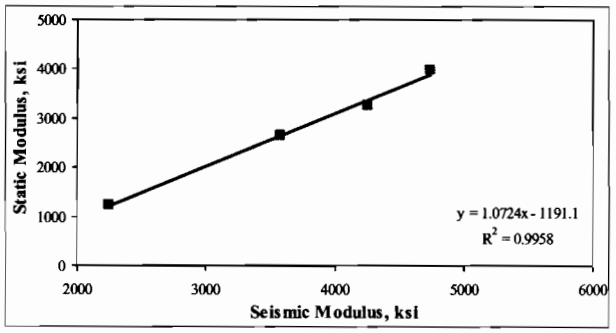

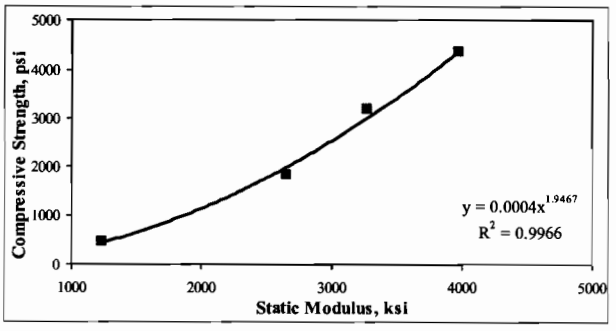

Figure C.1a - Typical relationships developed for a clean SRG, low CAF, low WR and with GGBFS mix cured in water at 70°F.

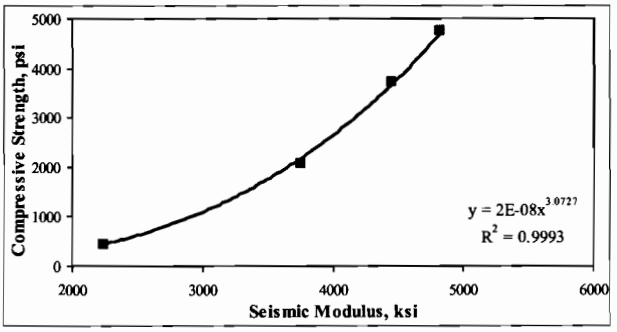

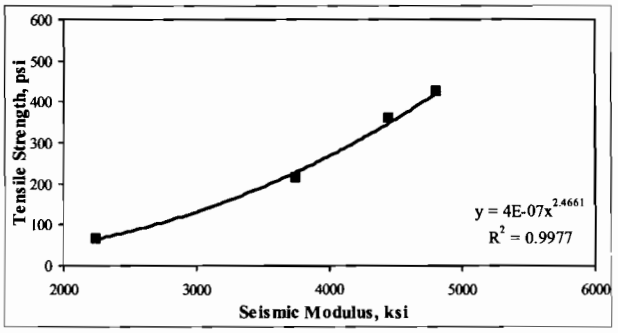

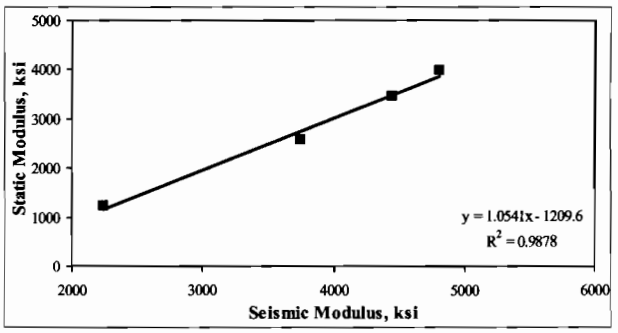

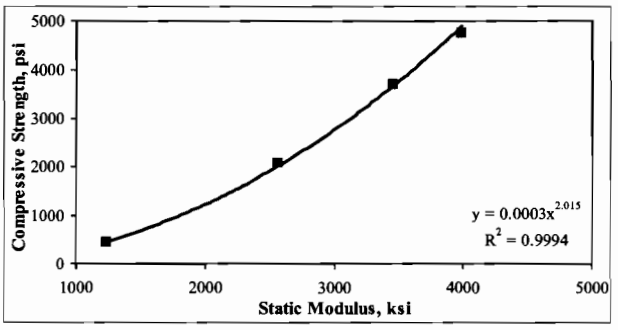

Figure C.1b - Typical relationships developed for a clean SRG, low CAF, low WR and with GGBFS mix cured in water at 95°F.

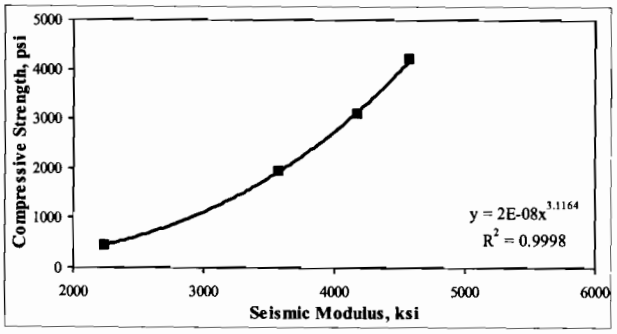

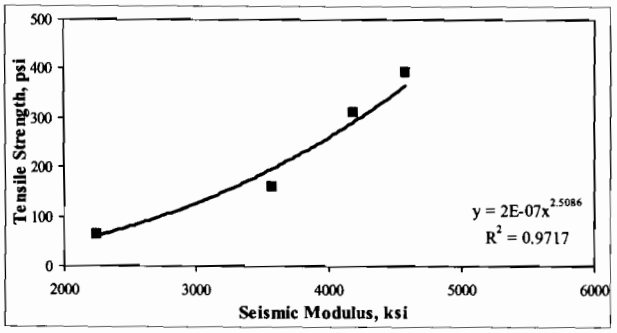

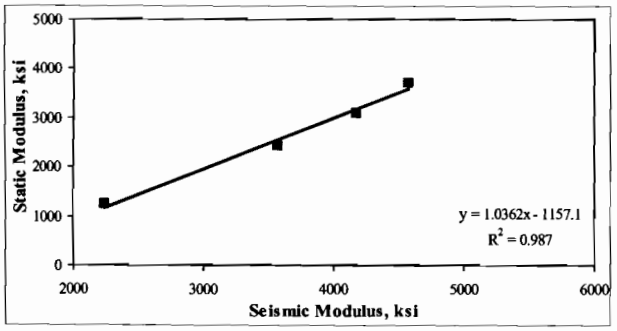

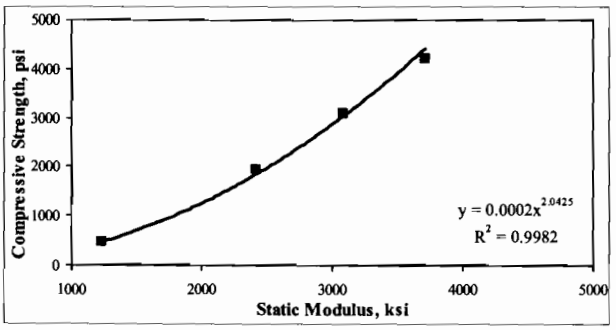

Figure C.1c - Typical relationships developed for a clean SRG, low CAF, low WR and with GGBFS mix cured in the field.

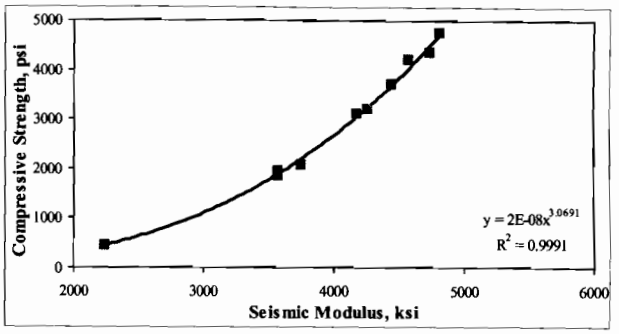

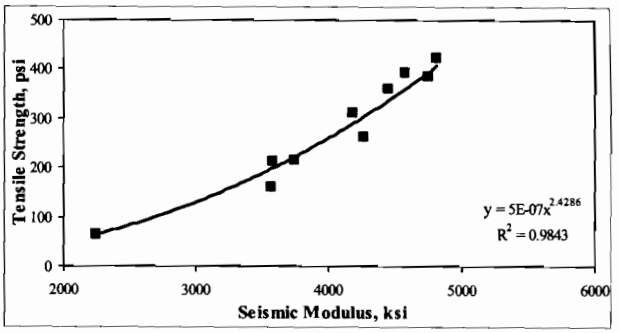

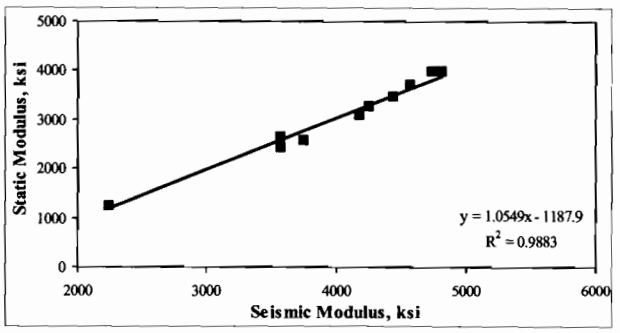

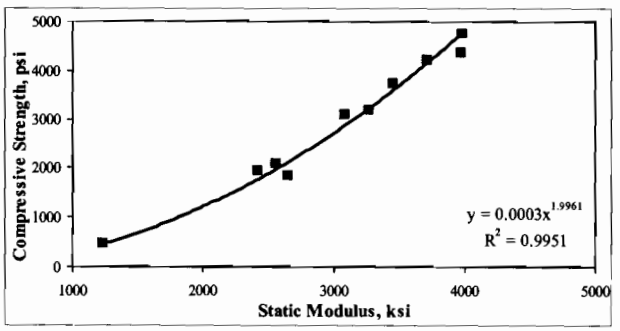

Figure C.1d - Typical relationships developed for a clean SRG, low CAF, low WR and with GGBFS mix; when water 70°F, water 95°F, and field curing are combined together.

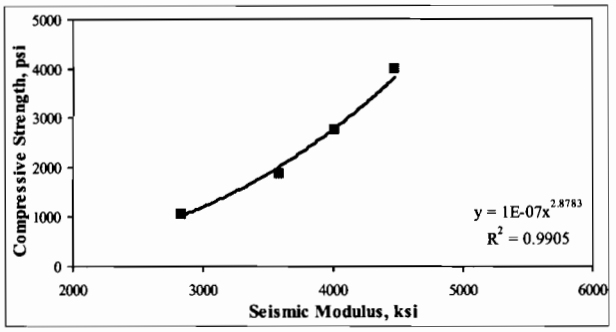

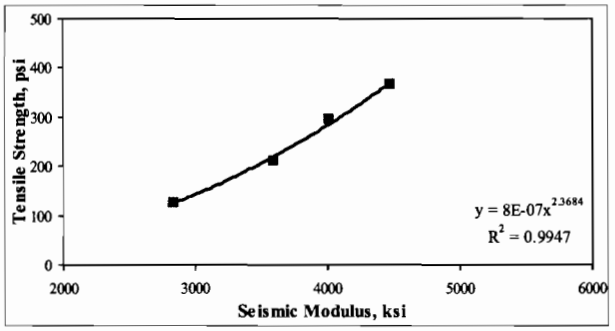

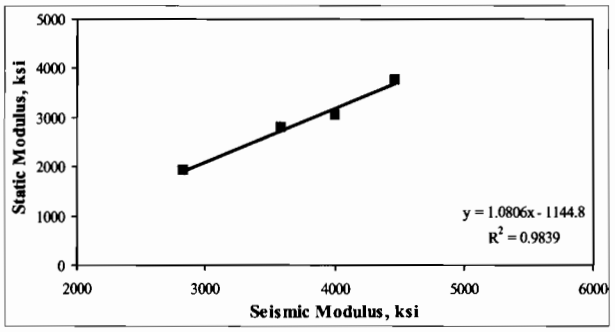

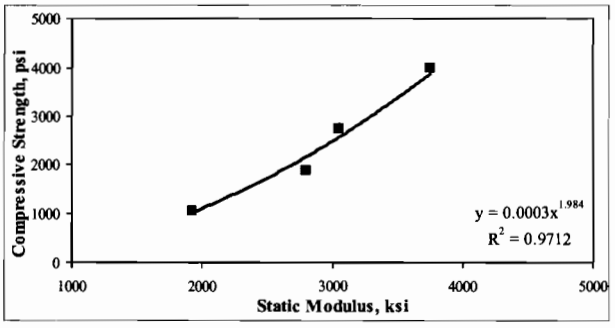

Figure C.2a - Typical relationships developed for a clean SRG, low CAF, high WR and with GGBFS mix cured in water at 70°F.

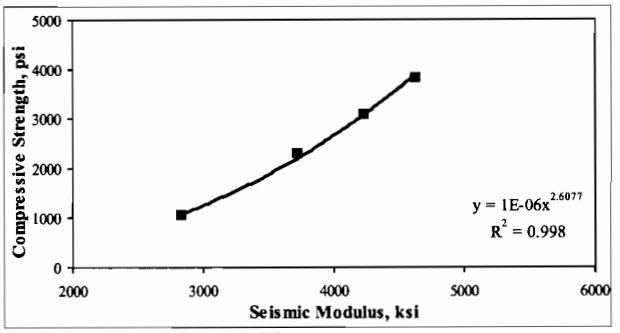

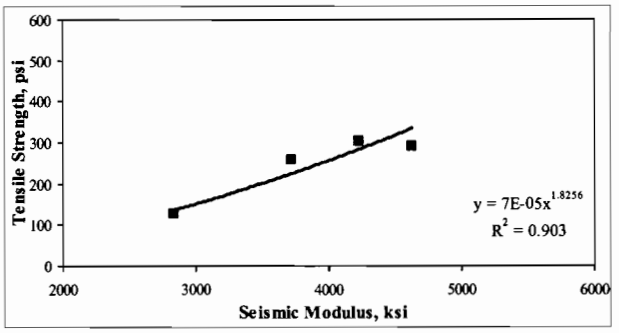

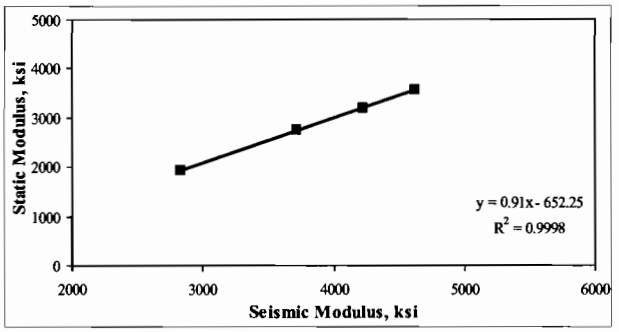

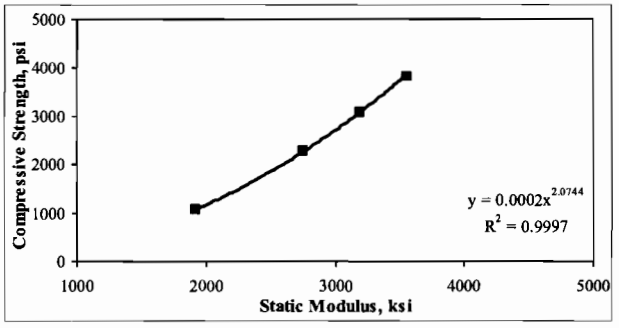

Figure C.2b - Typical relationships developed for a clean SRG, low CAF, high WR and with GGBFS mix cured in water at 95°F.

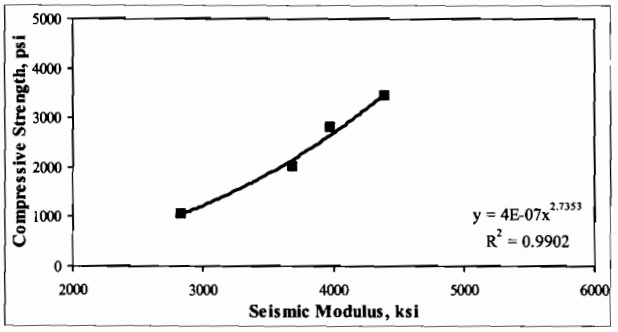

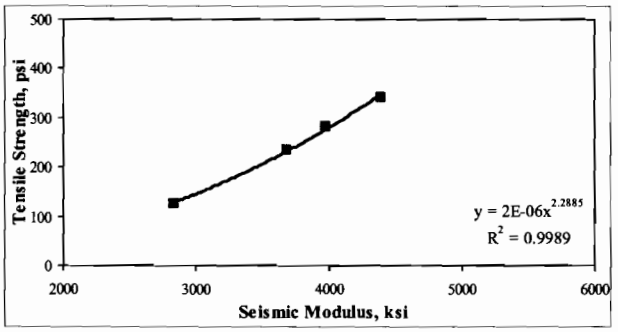

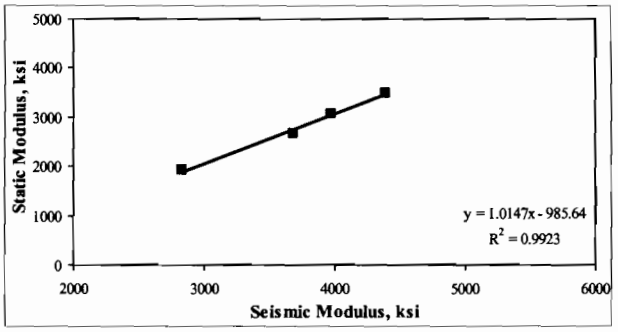

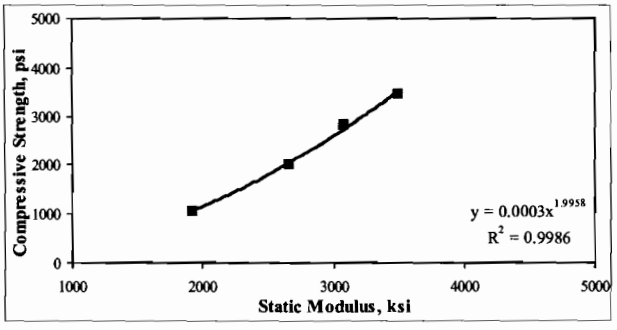

Figure C.2c - Typical relationships developed for a clean SRG, low CAF, high WR and with GGBFS mix cured in the field.

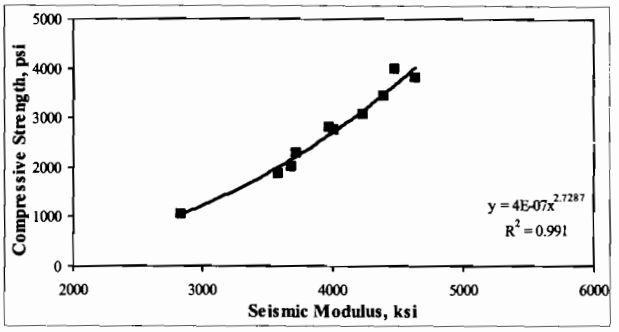

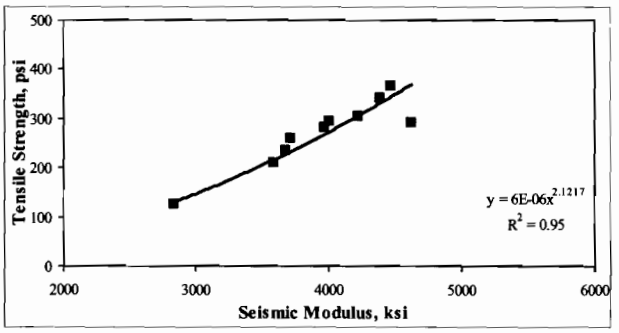

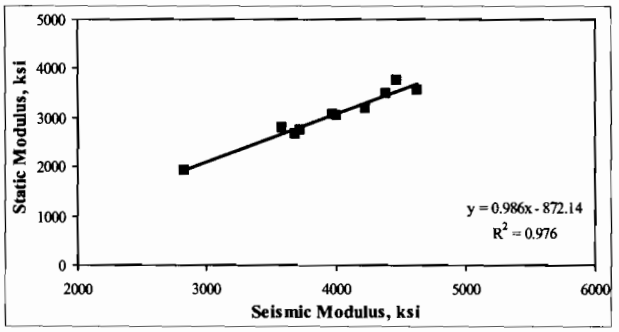

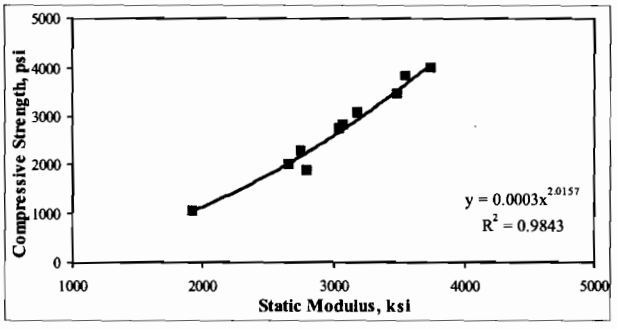

Figure C.2d - Typical relationships developed for a clean SRG, low CAF, high WR and with GGBFS mix; when water 70°F, water 95°F, and field curing are combined together.

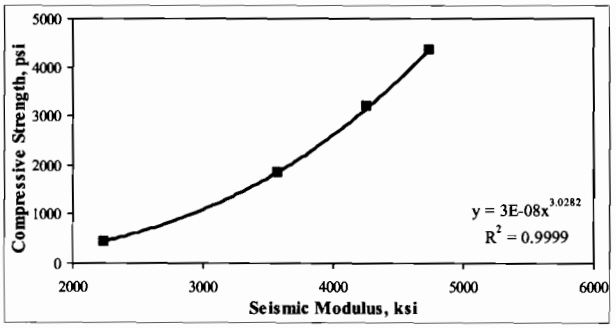

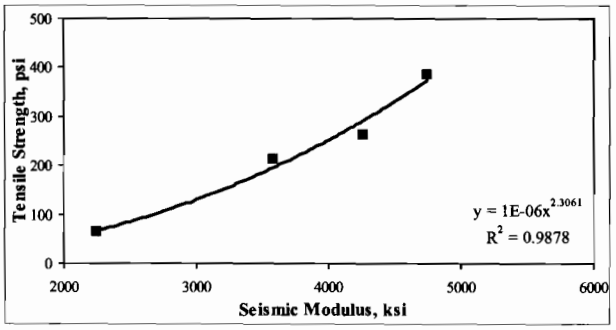

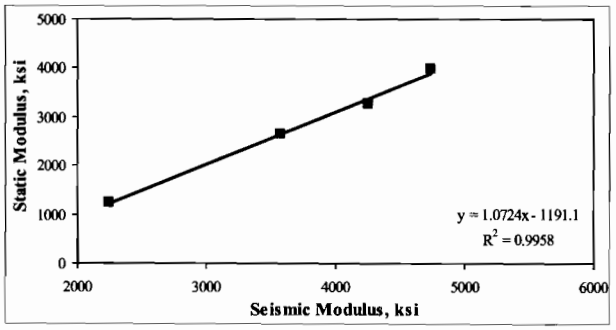

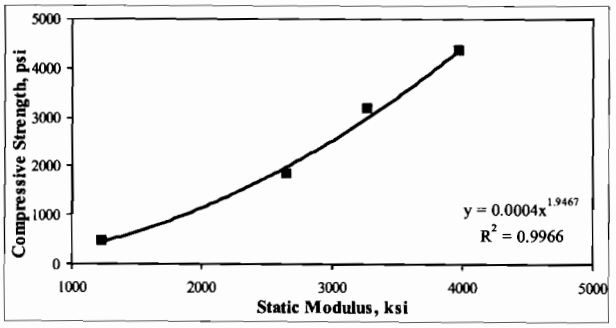

Figure C.3a - Typical relationships developed for a clean SRG, low CAF, high WR and with fly ash mix cured in water at 70°F.

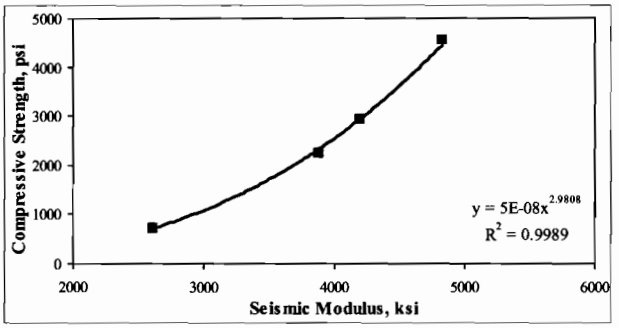

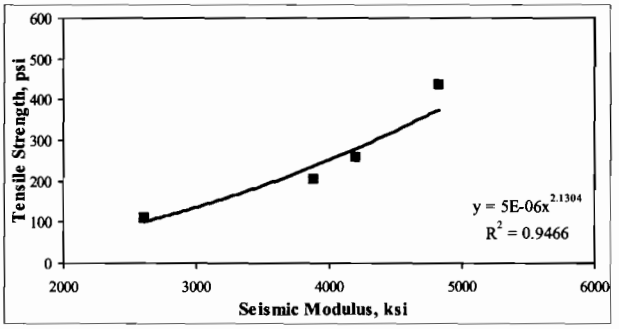

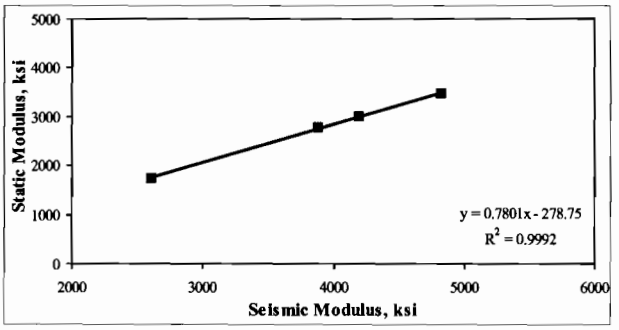

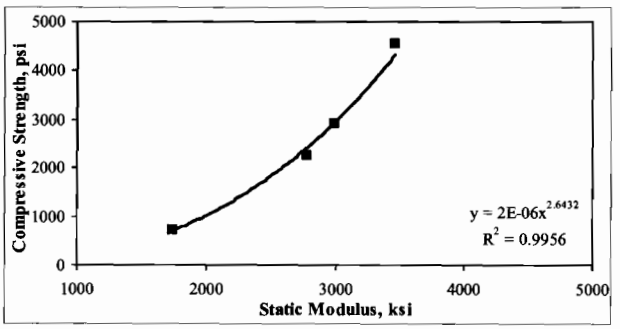

Figure C.3b - Typical relationships developed for a clean SRG, low CAF, high WR and with fly ash mix cured in water at 95°F.

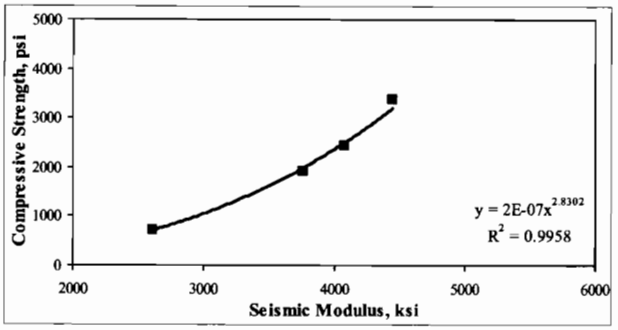

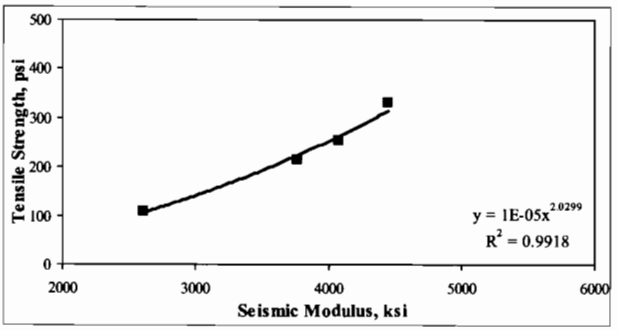

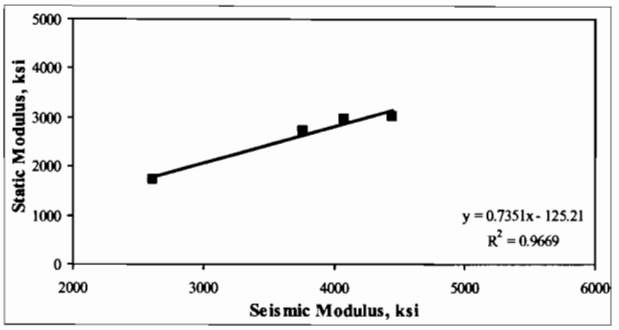

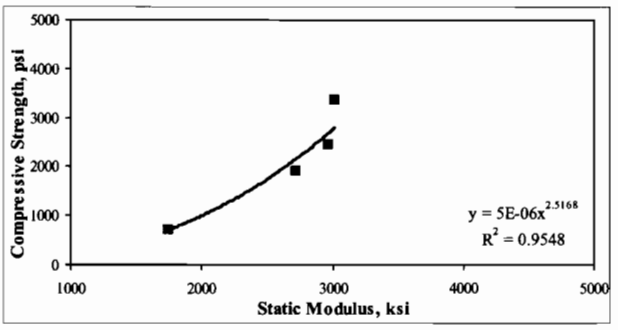

Figure C.3c - Typical relationships developed for a clean SRG, low CAF, high WR and with fly ash mix cured in the field.

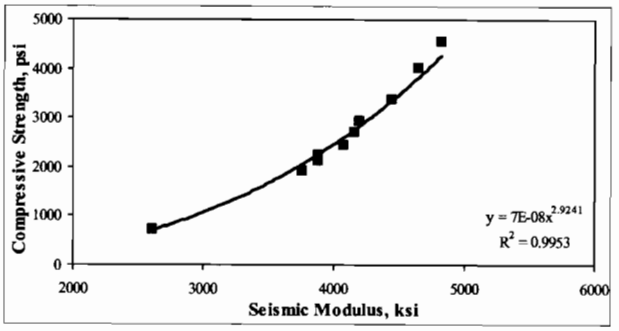

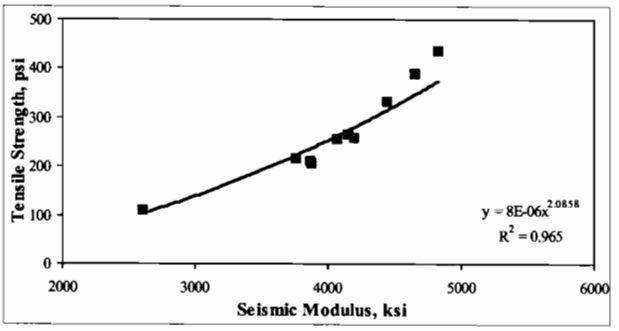

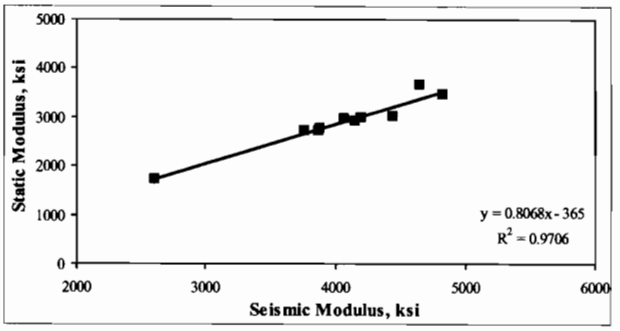

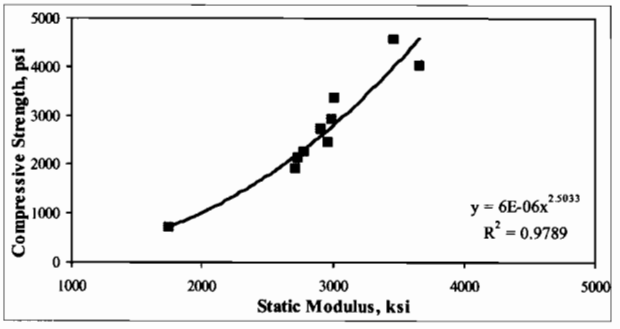

Figure C.3d - Typical relationships developed for a clean SRG, low CAF, high WR and with fly ash mix; when water 70°F, water 95°F, and field curing are combined together.

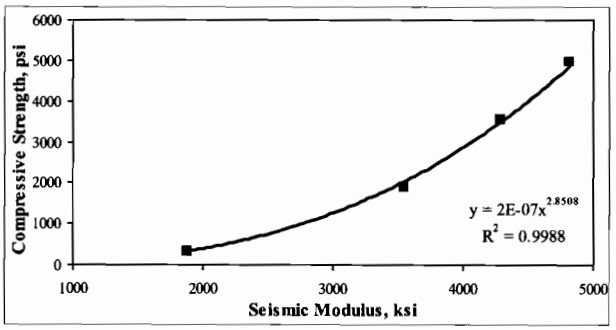

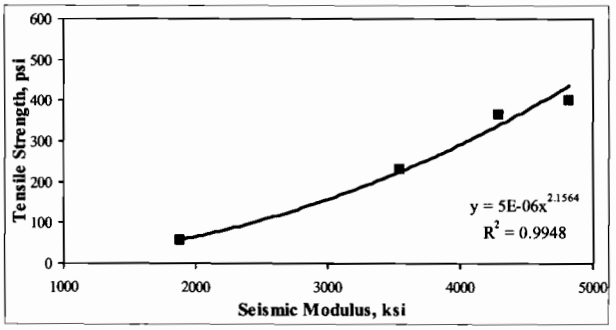

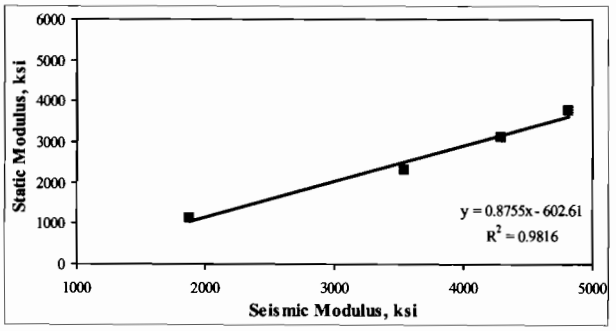

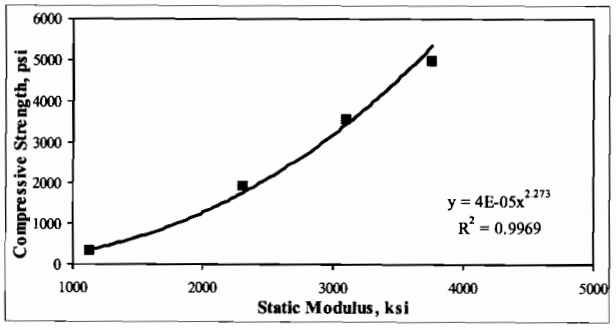

Figure C.4a - Typical relationships developed for a clean SRG, high CAF, low WR and with GGBFS mix cured in water at 70°F.

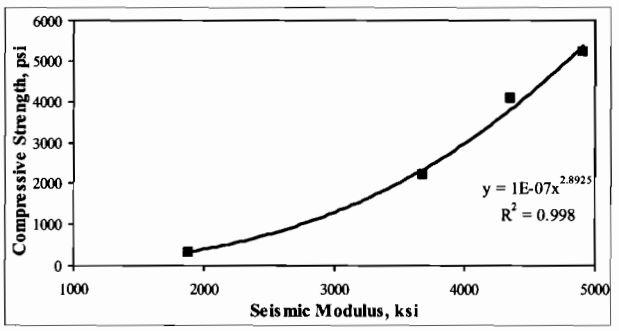

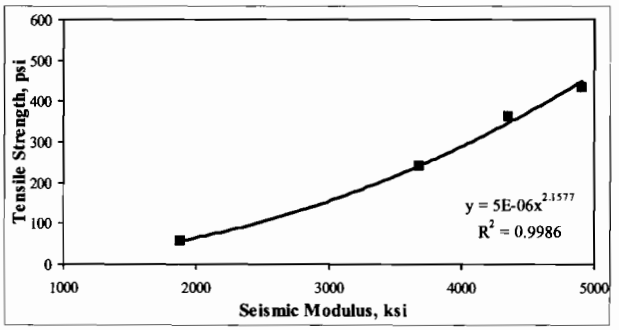

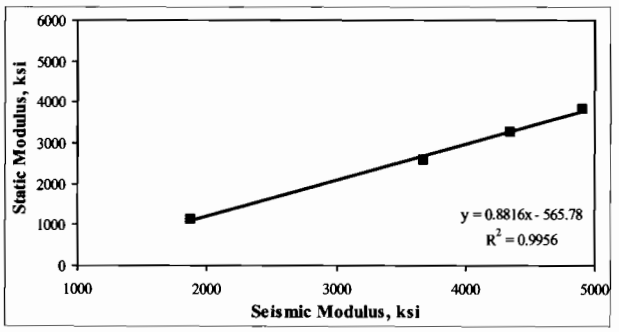

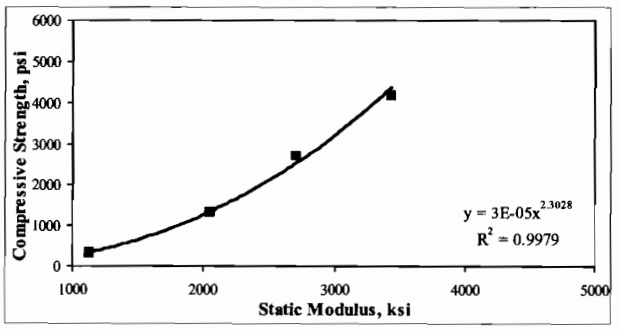

Figure C.4b - Typical relationships developed for a clean SRG, high CAF, low WR and with GGBFS mix cured in water at 95°F.

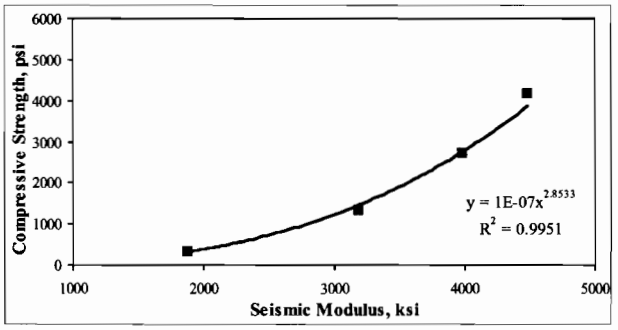

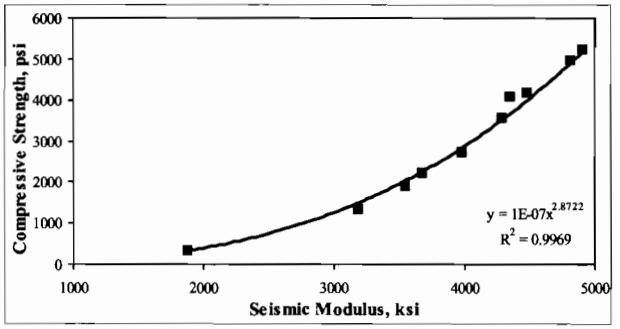

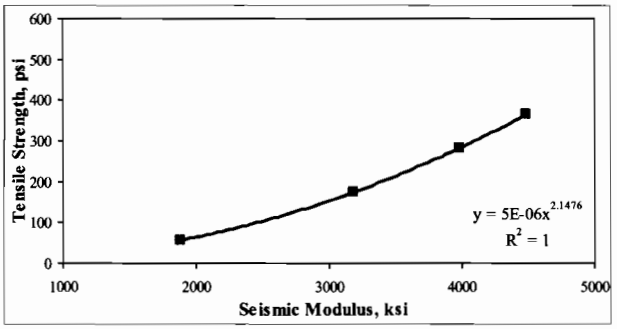

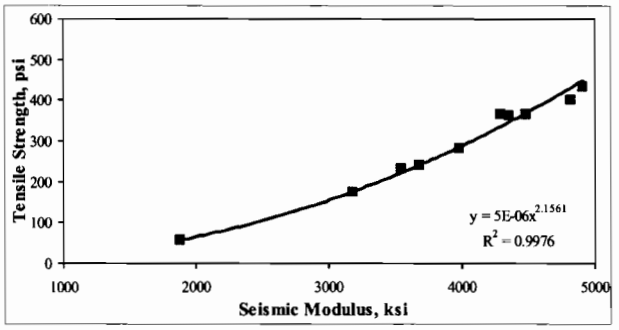

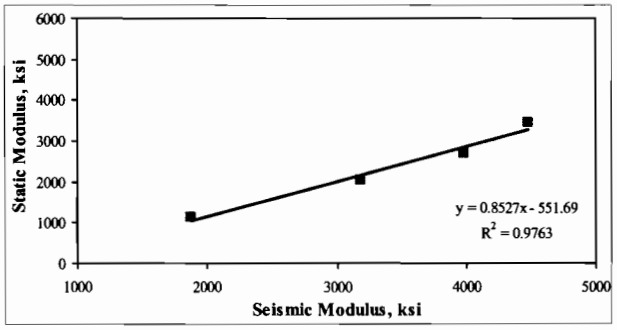

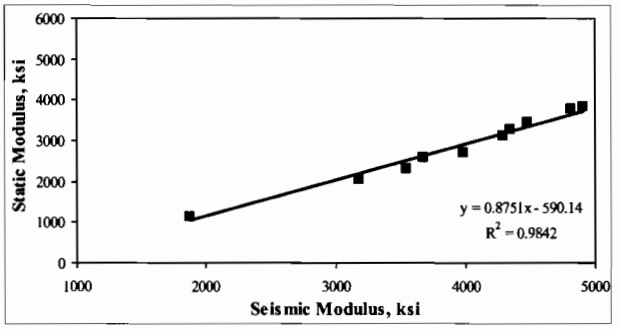

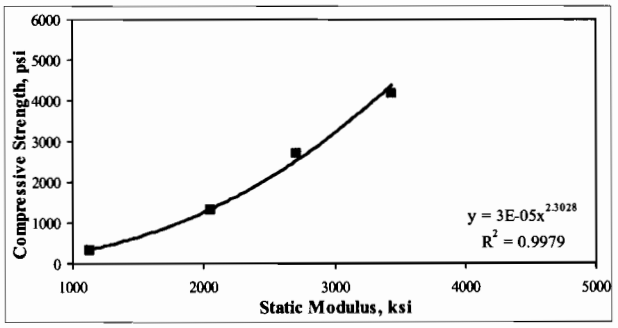

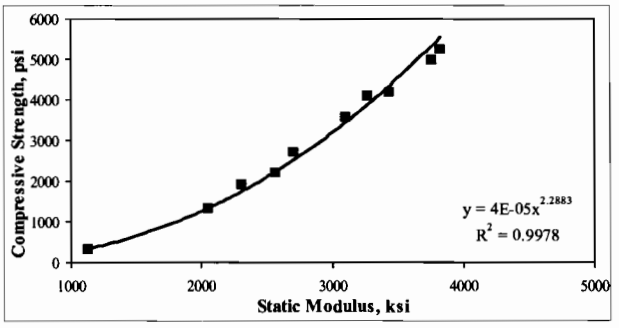

Figure C.4c - Typical relationships developed for a clean SRG, high CAF, low WR and with GGBFS mix cured in the field.

Figure C.4d - Typical relationships developed for a clean SRG, high CAF, low WR and with GGBFS mix; when water 70°F, water 95°F, and field curing are combined together.

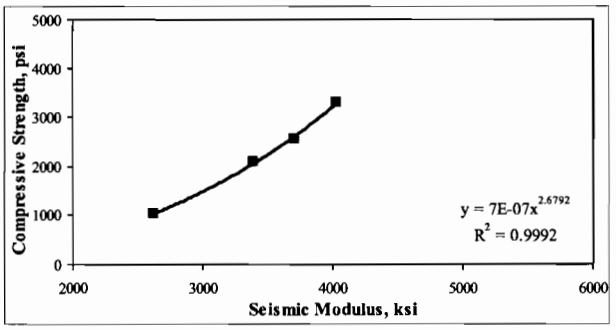

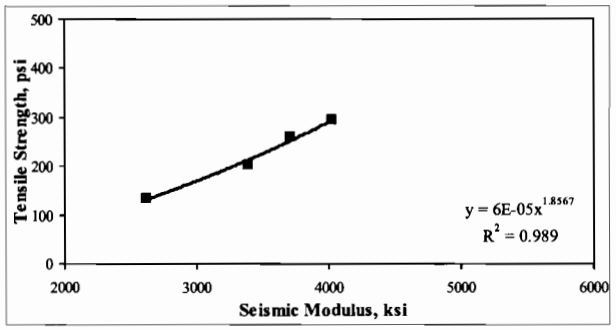

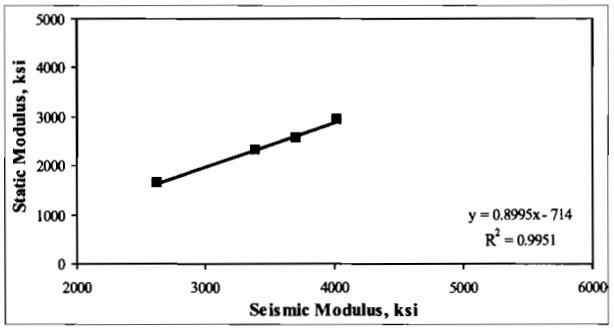

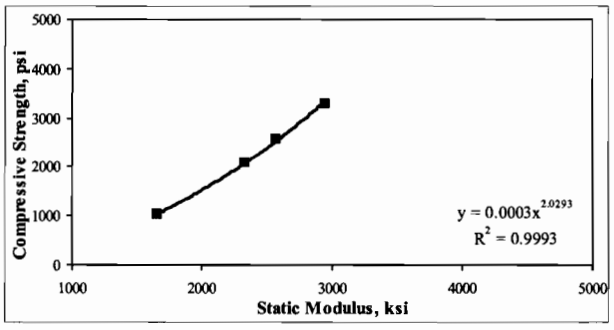

Figure C.5a - Typical relationships developed for a clean SRG, high CAF, low WR and with fly ash mix cured in water at 70°F.

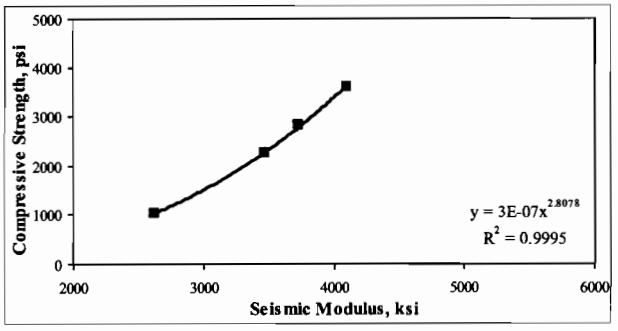

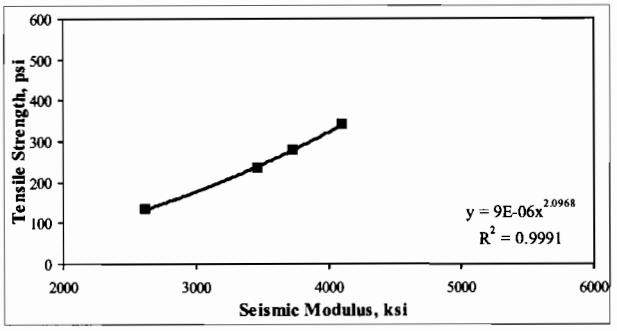

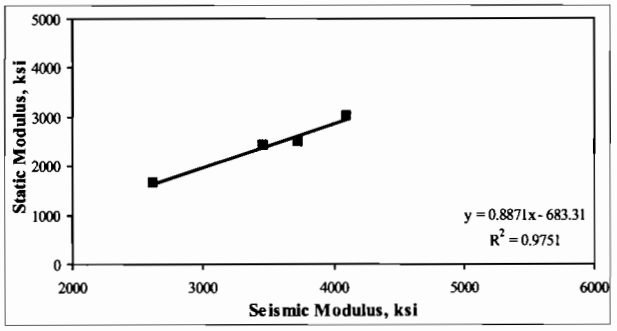

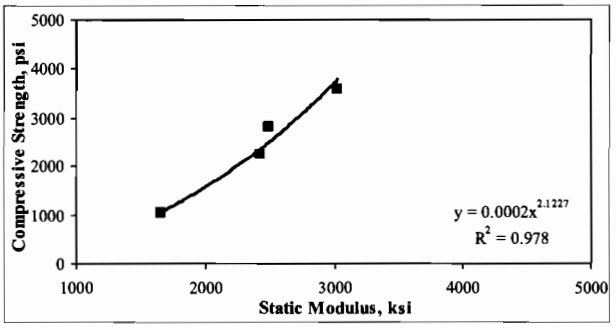

Figure C.5b - Typical relationships developed for a clean SRG, high CAF, low WR and with fly ash mix cured in water at 95°F.

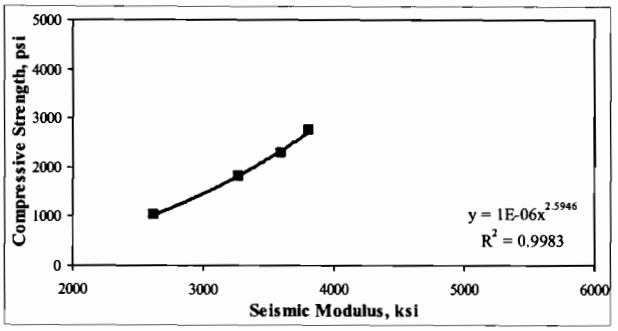

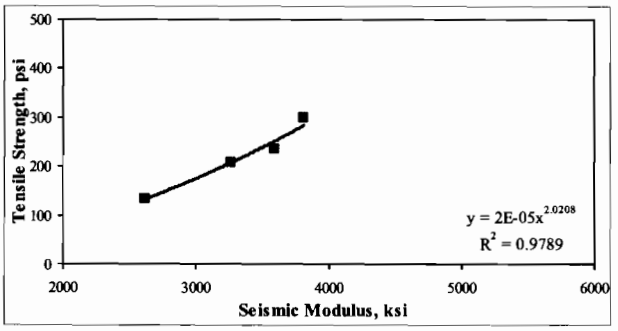

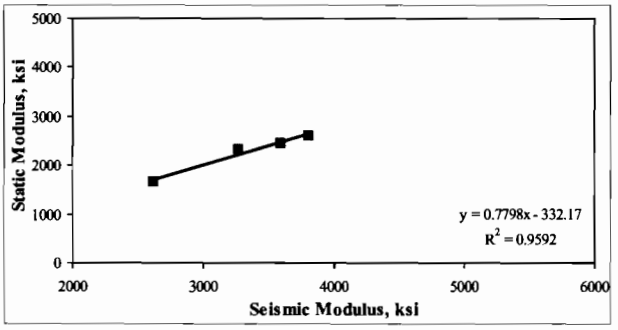

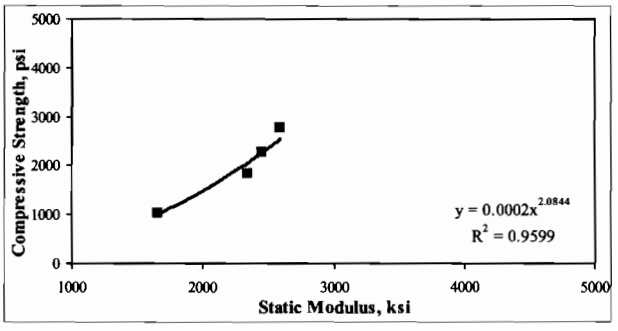

Figure C.5c - Typical relationships developed for a clean SRG, high CAF, low WR and with fly ash mix cured in the field.

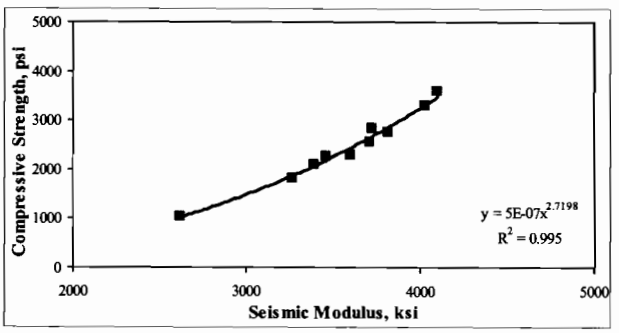

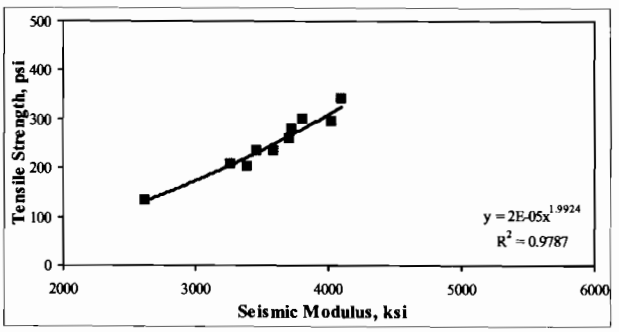

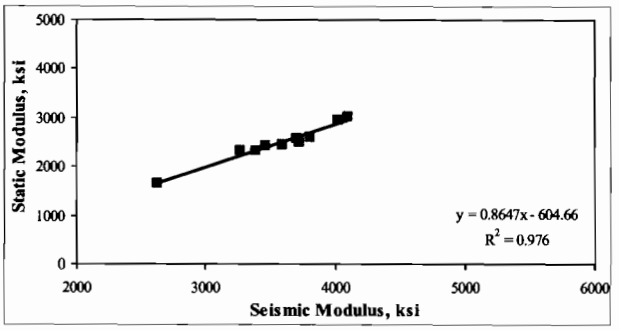

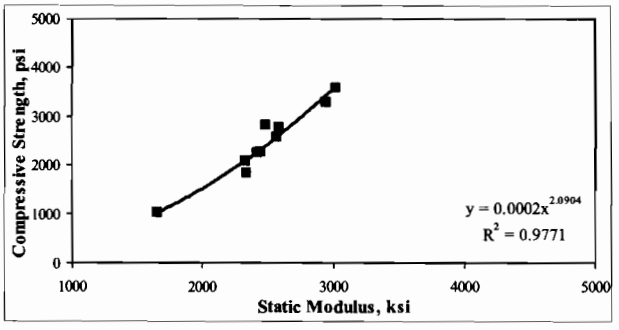

Figure C.5d - Typical relationships developed for a clean SRG, high CAF, low WR and with fly ash mix; when water 70°F, water 95°F, and field curing are combined together.

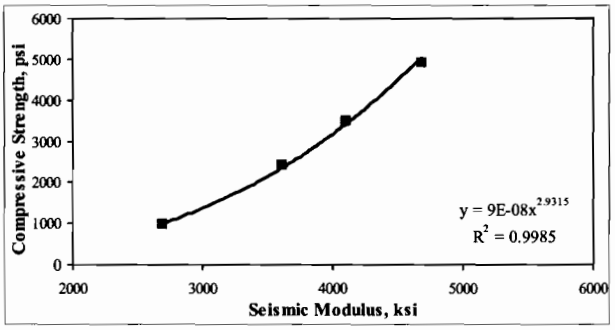

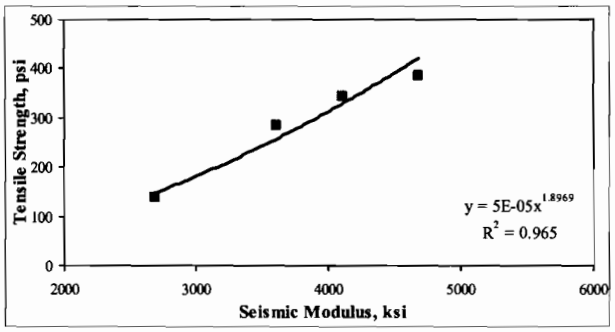

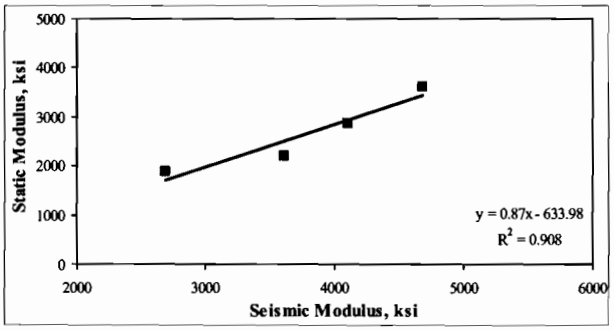

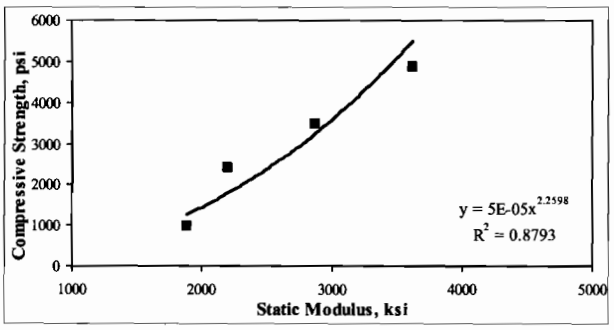

Figure C.6a - Typical relationships developed for a clean SRG, high CAF, high WR and with GGBFS mix cured in water at 70°F.

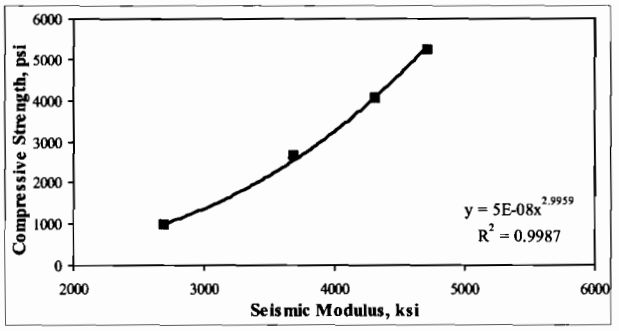

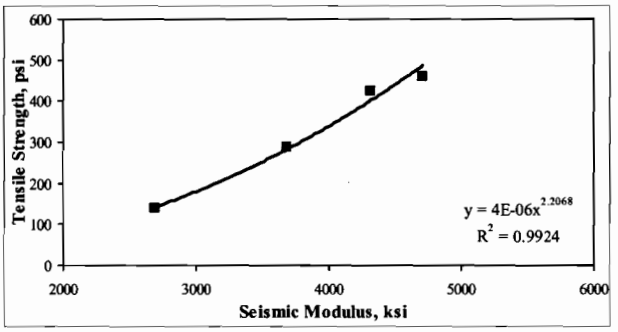

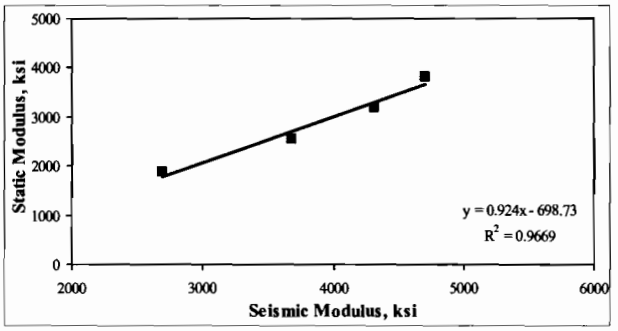

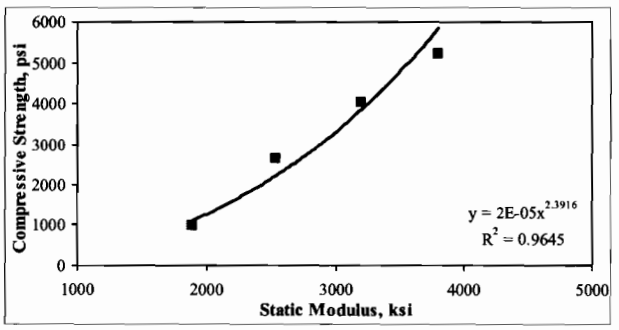

Figure C.6b - Typical relationships developed for a clean SRG, high CAF, high WR and with GGBFS mix cured in water at 95°F.

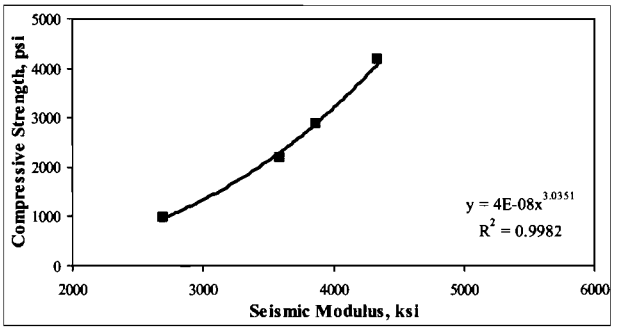

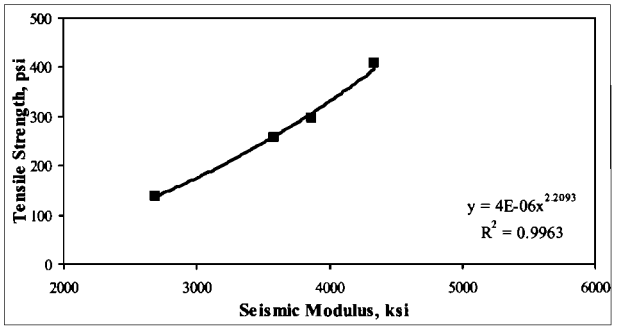

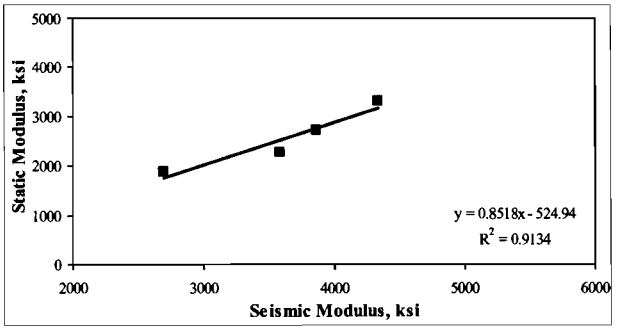

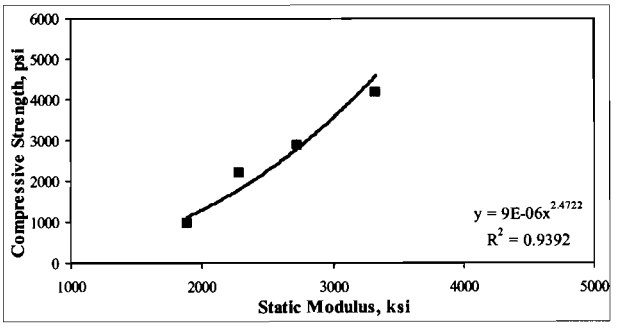

Figure C.6c - Typical relationships developed for a clean SRG, high CAF, high WR and with GGBFS mix cured in the field.

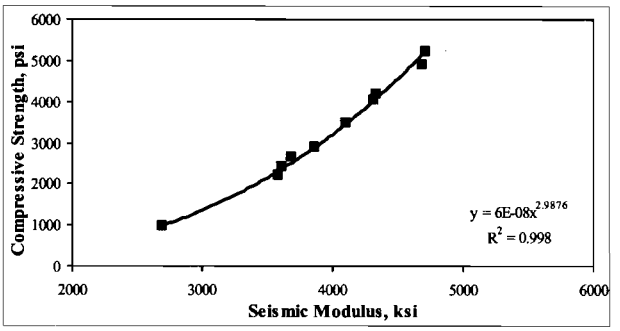

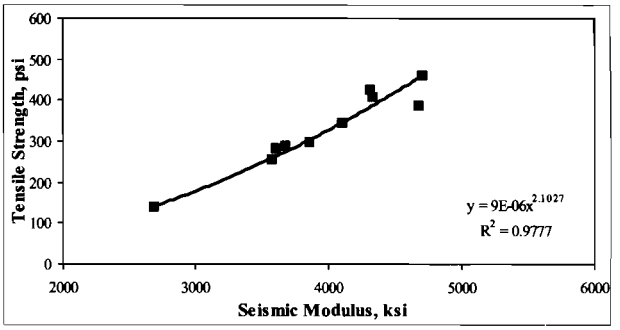

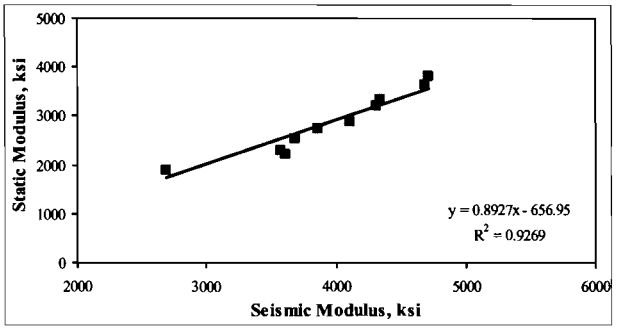

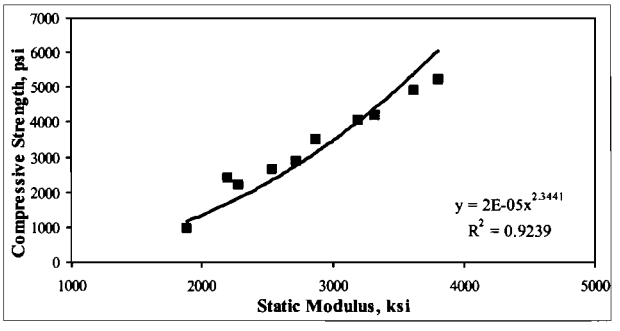

Figure C.6d - Typical relationships developed for a clean SRG, high CAF, high WR and with GGBFS mix; when water 70°F, water 95°F, and field curing are combined together.

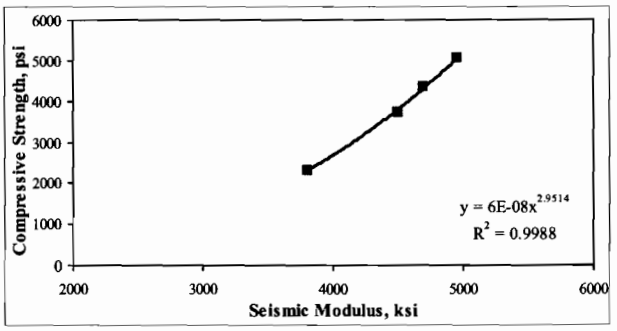

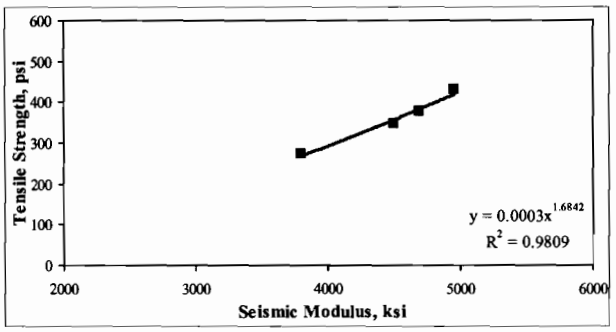

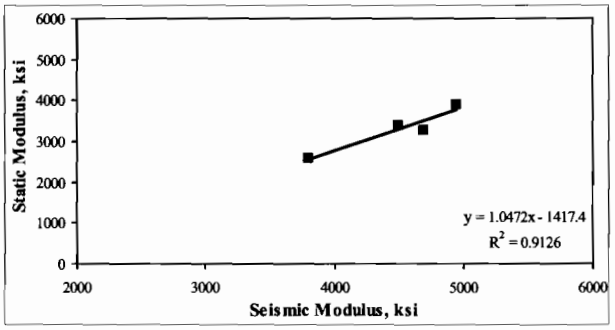

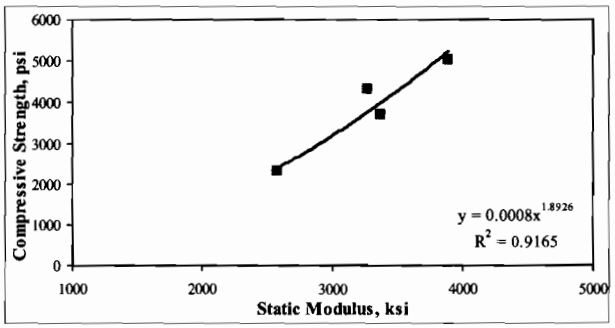

Figure C.7a - Typical relationships developed for a clean SRG, high CAF, high WR and with fly ash mix cured in water at 70°F.

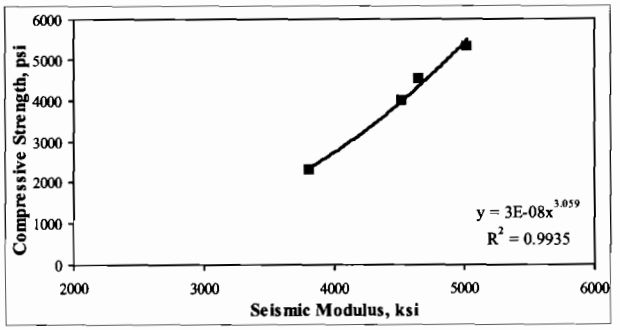

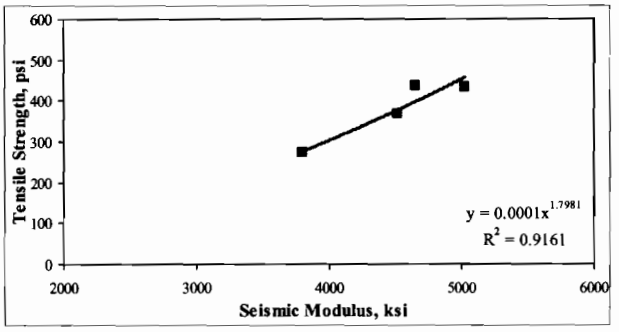

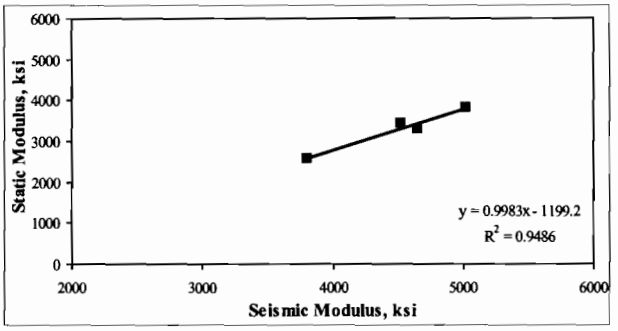

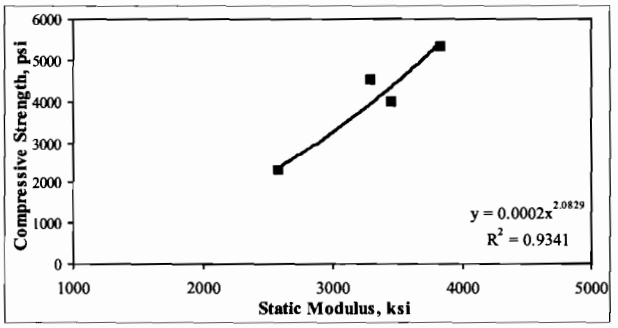

Figure C.7b - Typical relationships developed for a clean SRG, high CAF, high WR and with fly ash mix cured in water at 95°F.

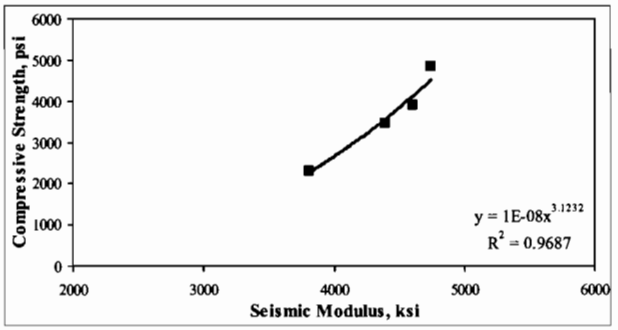

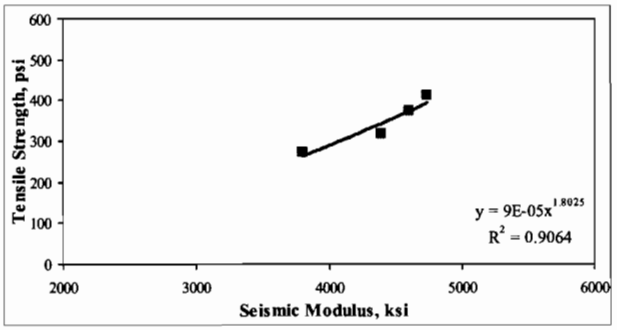

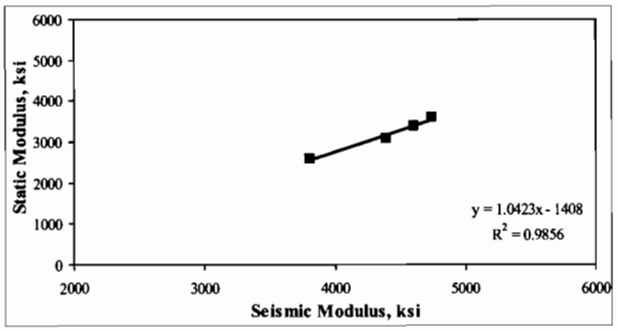

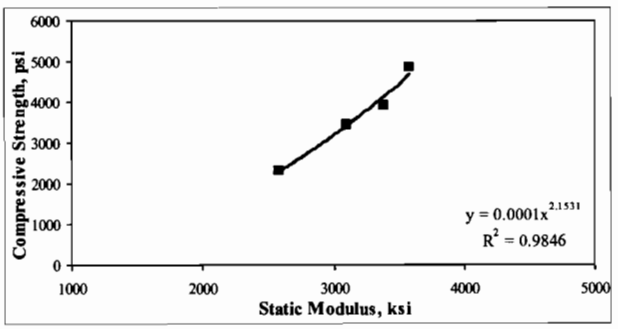

Figure C.7c - Typical relationships developed for a clean SRG, high CAF, high WR and with fly ash mix cured in the field.

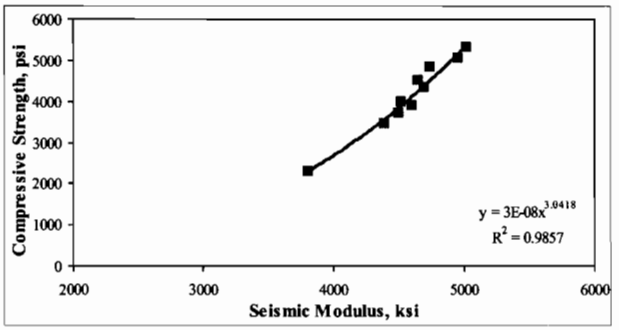

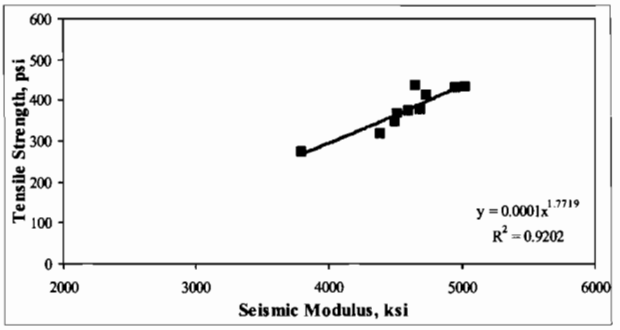

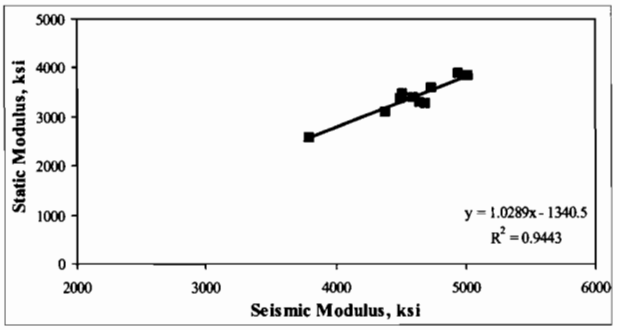

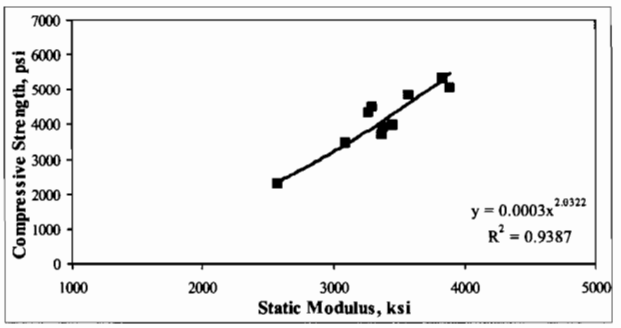

Figure C.7d - Typical relationships developed for a clean SRG, high CAF, high WR and with fly ash mix; when water 70°F, water 95°F, and field curing are combined together.

Appendix D

Field Seismic Testing Method and Device

ESTIMATING MODULUS OF PORTLAND CEMENT CONCRETE WITH PORTABLE SEISMIC PAVEMENT ANALYZER (PSPA)

The Portable Seismic Pavement Analyzer (PSPA) is a suitable device for estimating seismic modulus of concrete. The seismic modulus can be related to other concrete properties such as compressive strength and modulus of rupture. Testing with the PSPA is very rapid, with the collection and preliminary reduction of data at one point taking less than 15 seconds.

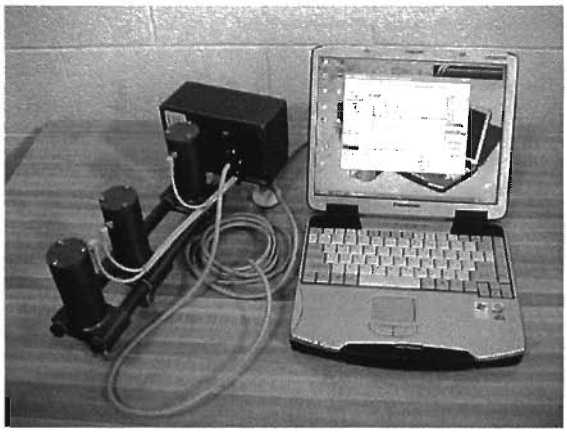

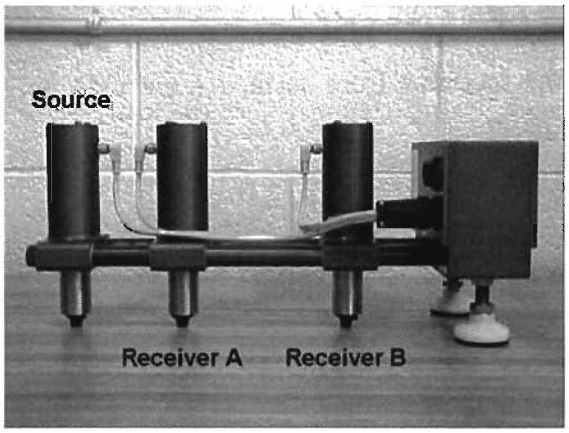

The PSPA consists of a source and two receivers. The source is a computer-controlled impactor that it is capable of generating stress waves at both the sonic and ultrasonic ends of the frequency spectrum. The two receivers are used to monitor the sonic waves generated by the impactor. The ultrasonic surface wave (USW) method is used to determine the modulus as described below.

When the surface of a material, such as PCC, is impacted with a point source, several types of waves propagate in that material. These waves can be categorized into two broad groups: body waves and surface waves. Body waves, typically called compression waves (a.k.a. P-waves) or shear waves (a.k.a. S-waves) propagate along a spherical front within the material. In the contrary, surface waves (a.k.a. Rayleigh waves, R-waves) propagate along a spherical front. Surface waves contain about two-thirds of the seismic energy generated within a layer as such the analysis is more robust. Also since surface waves propagate along a cylindrical front, the depth of inspection can be readily controlled as will be described shortly.

The goal with seismic methods is to measure the propagation velocity of waves within a medium. The propagation velocity is theoretically related to the linear elastic modulus of a material. The relationship between velocity, V, traveltime, Δt, and receiver spacing, ΔX, can be written in the following form:

$$V = \frac{\Delta X}{\Delta t} \tag{D.1}$$

In this equation, V can be the propagation velocity of any of seismic waves [i.e. compression wave, V_P; shear wave, V_S; or surface (Rayleigh) wave, V_R]. Knowing any one wave velocity, the modulus can be determined, using appropriate transformations. Shear velocity, V_S can be used to determine shear modulus, G, using:

$$G = \frac{\gamma}{g} V_s^2 \tag{D.2}$$

Young's modulus, E, which is the primary parameter of interest to pavement engineers, can be determined from shear modulus, through the Poisson's ratio, ν, using:

$$E = 2(1+\nu) G \tag{D.3}$$

To obtain the modulus from surface wave velocity, V_R is first converted to shear wave velocity using:

$$V_S = V_R (1.13 - 0.16\nu) \tag{D.4}$$

Young's modulus is then determined by using Equations C.2 and C.3.

Surface waves (or Rayleigh, R-waves) contain about two-thirds of the seismic energy. Accordingly, the most dominant arrivals are related to the surface waves making them the easiest to measure. The Ultrasonic Surface Wave (USW) method is an offshoot of the SASW method is used to obtain the modulus of the PCC. The major distinction between these two methods is that in the USW method the modulus of the top pavement layer can be directly determined without an inversion (backcalculation) algorithm.

As sketched in the figure below, at wavelengths less than or equal to the thickness of the uppermost layer, the velocity of propagation is independent of wavelength. Therefore, if one simply generates high-frequency (short-wavelength) waves and if one assumes that the properties of the uppermost layer are uniform, the shear wave velocity of the upper layer, V_s, can be determined from

$$V_s = (1.13 - 0.16\nu) V_{ph} \tag{D.5}$$

The modulus of the top layer, E_{field}, can be determined from

$$E_{field} = 2 \rho V_s^2 (1 + \nu). \tag{D.6}$$

where V_{ph} = phase velocity of surface waves, ρ = mass density, and ν = Poisson's ratio.